

SYNTHESIS OF PLANAR FOUR-LINK MECHANISMS FOR FORCE GENERATION

by

Robert Randall Soper

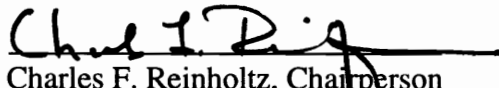
Thesis submitted to the Faculty of the
Virginia Polytechnic Institute and State University
in partial fulfillment of the requirements for the degree of


MASTER OF SCIENCE


in

MECHANICAL ENGINEERING

APPROVED:


Charles F. Reinholtz, Chairperson
Mechanical Engineering, VPI&SU


Harry H. Robertshaw
Mechanical Engineering, VPI&SU


Scott L. Hendricks
Engineering Science and Mechanics,
VPI&SU

August, 1995
Blacksburg, Virginia

Key Words: Synthesis, Force-Generation, Linkage, Burmester, closed-form

Synthesis of Planar Four-Link Mechanisms for Force Generation

by
Robert Randall Soper

Charles F. Reinholtz (chairperson)

Mechanical Engineering

Abstract

This thesis presents a technique for synthesizing weighted four-bar linkages to produce a specified resisting force or torque.

Historically, mechanism force synthesis has assumed that output positions must always be associated with prescribed forces. This results in the loss of design parameters. Applications which do not require a specified output position benefit from the design method presented in this thesis.

This thesis presents two significant contributions to the field of kinematics. First, it contains a full development and demonstration of the use of integrated force constraints to develop position constraints for linkages. Second, it presents the development and use of inverse-mechanical-advantage sensitivity as an evaluation and design tool.

The mathematical derivation of a novel synthesis technique is presented in full detail. Also presented is a complete and robust design method for force-generating linkages that has been implemented in software, tested in hardware design, and adopted by industry. The closed-form-equation-based synthesis technique developed herein provides the designer with a graphical representation of an infinite solution set to the force generation problem. Associated sensitivity, static and dynamic analyses allow the designer to quickly evaluate each solution.

This work is loving dedicated to the memory of
Mary Nancy Hull (June 5, 1914 - January 28, 1994).

She is proud of me.

Acknowledgments

Many people made this work possible. I am indebted to them all.

Charles Reinholtz is the chairman of my committee. He was intimately involved with all aspects of this project. Our success was guaranteed by his tireless devotion, deep insight, grounded experience, and fatherly guidance. His healthy skepticism kept me out of trouble. There is much to admire about this man. Most of all, I respect his policy of inviting students into his office and his home and industry into his classroom and his laboratory. He has been my mentor and my friend, and I hope that our association continues for many years to come.

It is no accident that the three members of my committee are the best *teachers* in the College of Engineering. Harry Robertshaw taught me the importance of writing in engineering and academics. His guidance of the senior laboratory course brought out the best in all of his GTA employees. Scott Hendricks teaches the most difficult and stimulating courses at this university. All of his students agree, you have to work hard in Hendricks's courses. But no one works harder than Dr. Hendricks. Thank you both.

I am also extremely indebted to Dr. Sanjay G. Dhande, Dept. Head of the Mechanical Engineering Department, Indian Institute of Technology, Kanpur. He assumed responsibility for my research and the rest of the Nautilus team during the absence of Dr. Reinholtz in the summer of 1994. He was the first to suggest an investigation of the sensitivity of force-generating linkages. He strongly suggested an investigation of force-generating linkage synthesis by optimization techniques. It has been an honor to have worked directly for two men so well admired in the field of kinematics.

Nautilus International, Inc. and the Virginia Center for Innovative Technology both provided funding which made my research possible. Nautilus's involvement with this project went much farther than simple funding, however. Nautilus's interest and enthusiasm provided excitement, direction and practicality for this research. Our frequent

interaction gave the research a momentum it would have surely lacked otherwise. I would like to thank many members of the Nautilus organization for their interest: Greg Webb (Vice President, Engineering), Danny Stanton (President), Cindy Scar (Vice President, Marketing), and all of the Engineering Staff, in particular, Buddy Halsey, Brian Billings and Gary Mitchell.

One member of Nuatilus's Engineering Staff has been the strongest advocate that any research group could ever ask for. His dedication to his company and his Alma Mater are unparalleled. He has tested, critiqued and enthusiastically applied all of our methods and code. Thank you Mike Lo Presti, you're quite a friend.

Two graduate students, Michael T. Scardina and Paul H. Tidwell, have been deeply involved in this research and the associated publications and programming. Mike, in particular, has been my sounding board and my codesigner. Thanks to both of you!

Many students have helped me along the way. They have made graduate school both exciting and fun. Thanks to all of Charlie's students, all of Harry's students, all of Harley's students, and all of the Nautilus undergraduate students. Thanks in particular to my friends and cohorts: Dave "D. R. Schmiely" Schmiel, Mike Scardina, Jon Hill, Chris Fannon, and, of course, Toni "ask Mr. Science Guy" Ganino.

Anita Lynne Soper, my dearest wife, thank you for all you always do.

Finally, thanks to Heidi Claire, man's best friend, who bravely resisted all temptation to eat this manuscript. Good Girl!

Contents

1 Introduction	1
1.1 Background and Motivation	1
1.2 Linkages Versus Cams, Advantages and Disadvantages	4
1.3 General Tools Required for Kinematic Force Synthesis	9
1.3.1 Position Analysis of Planar Four-Bar Linkages	9
1.3.2 Inversion	14
1.3.3 Burmester Point Pairs	15
1.3.4 D'Alembert's Principle (Virtual Work)	17
1.3.5 Transmission Angle	19
1.4 Review of Literature	20
2 Problem Definition and Constraints	28
2.1 Kinematic Model and Variable Definitions	28
2.1.1 Four-Link Weighted-Grounded-Link Case	29
2.1.2 Four-Link Weighted-Coupler-Link Case	33
2.1.3 Strength Data Issues	34
2.2 Number of Mathematical Solutions	36
2.2.1 Four-Link Weighted-Grounded-Link Case	36
2.2.2 Four-Link Weighted-Coupler-Link Case	39
2.3 Design Constraints	41
3 Weighted-Grounded-Link Synthesis Method	45
3.1 Massless Links and Static Force Transfer	45
3.2 Integrating Force Constraints	46
3.2.1 The General Problem -- Constant Torque Resistance	47
3.2.2 The Linear Torsion Spring Problem	49
3.2.3 The Load Weight Problem	50
3.3 Transformation to Body-Guidance Space by Inversion	54

3.4 Four Position Body-Guidance Synthesis (Burmester Theory)	55
3.4.1 Matrix Formulation of Loop Closure	56
3.4.2 Solving the Quasi-Loop-Closure Equation	58
3.5 Transformation to Non-Inverted Solution Space	60
3.6 Solution Interpretation and Analysis	61
3.6.1 Solution Defects and Rectification	62
3.6.2 Analysis of Resistance Curve	64
3.6.3 Analysis of Coupler and Bearing Stress	65
3.7 Design Tactics and Example Problem	66
3.7.1 Choosing Precision Points	66
3.7.2 Choosing the Weight Start Angle and Arm Length	67
3.7.3 Choosing the Solution Range	68
3.7.4 Avoiding Defective Regions	69
3.7.5 Alternatives for Difficult Problems	70
3.7.6 Example -- Synthesis of a Compound Rowing Machine	71
4 Weighted Coupler Link Synthesis Method	77
4.1 How This Problem Differs	77
4.2 Integrating Force Constraints	78
4.2.1 The Track-Mounted Linear Tension-Compression Spring Problem	78
4.2.2 The Load Weight Problem	81
4.3 Four Position Body-Guidance Synthesis (Burmester Theory)	85
4.4 Solution Interpretation and Analysis	86
4.4.1 Analysis of the Resistance Curve	87
4.4.2 Analysis of Grounded-Link and Bearing Stress	88
4.5 Example Problem	90
5 Post Processing: Sensitivity and Force Analysis	96
5.1 Applications of Sensitivity	96
5.2 Extended Force Analysis	101

5.2.1 Static Effect of Massed Links	101
5.2.2 Dynamic Effects and Trajectory Selection	104
6 Other Synthesis Cases	110
6.1 Enumeration of Cases	110
6.1.1 Four-Link Mechanism with Multiple Weight Locations	110
6.1.2 Four-Link Mechanism with Multiple Resistance Types	114
6.1.3 Two Degree-of-Freedom Five-Bar Under Gravity Load	115
6.2 A Special Case -- The Watt Six-Bar Linkage	117
6.2.1 As A Series Body Guidance, Mechanical Advantage Generator	118
6.2.2 As a Double Force Generator	120
6.3 Ground Work for Optimization	123
6.3.1 Development of a Cost Function	123
6.3.2 Penalty Functions	124
6.3.3 Convergence Methods	126
7 Conclusions and Recommendations	128
7.1 Summary	128
7.2 Further Research	129
References	131
Appendix A, Weighted-Grounded-Link Synthesis Program	135
Appendix B, Weighted-Coupler Synthesis Program	151
Appendix C, Derivation of Influence Coefficients	167
Appendix D, Sensitivity Analysis, Weighted-Grounded-Link Case	179
Appendix E, Sensitivity Analysis, Weighted-Coupler Case	193
Appendix F, Post-Processing: Analysis Programs	207
Vita	219

List of Figures

1-1	How a Tailored Resistance Curve Increases Work	2
1-2	Wrapping Cam Mechanism	4
1-3	The Nautilus “Power Plus” Linkage Concept	5
1-4	Standard Four-Link Mechanism	10
1-5	Standard and Inverted Frames of Reference	14
1-6	Burmester Point Pairs	16
1-7	Transmission Angle	19
2-1	Standard Weighted-Grounded-Link Model	29
2-2	Horizontal Applied Force	30
2-3	Equivalent Rotations and Scalings	31
2-4	Standard Weighted-Coupler Model	34
3-1	Constant Torque Resistance	47
3-2	Linear Torsional Spring Resistance	50
3-3	Standard Weighted-Grounded-Link Model	51
3-4	Function Generator	53
3-5	Inverted Function Generator	54
3-6	Body Guidance Solution Dyad	56
3-7	Burmester Curves	74
3-8	Solution Linkage	75
3-9	Resistance Curve of the Solution	75
3-10	Internal Coupler Force	76
3-11	Bearing Forces	76
4-1	Track-Mounted Linear Spring Resistance	79
4-2	Standard Weighted-Coupler Model	82
4-3	Resulting Body-Guidance Problem	84
4-4	Burmester Curves	93

4-5	Solution Linkage	94
4-6	Resistance Curve of the Solution	94
4-7	Internal Grounded Link Force	95
4-8	Bearing Forces	95
5-1	Free Body Diagram	100
6-1	Triple-Weighted Four-Bar Linkage	111
6-2	Four-Bar Linkage with Multiple Resistance Types	113
6-3	Double-Weighted Five-Bar Linkage	116
6-4	Watt Six-Bar Body Guidance, Mechanical Advantage Generator	118
6-5	Watt Six-Bar Double Mechanical Advantage Generator	122
6-6	Watt Six-Bar Mechanical Advantage Generator, Weighted Coupler	122

List of Tables

2.1	Number of Possible Solutions for the Weighted-Grounded-Link Case	38
2.2	Number of Possible Solutions for the Weighted-Coupler-Link Case	40
3.1	Strength Data, Compound Row	72
3.2	Precision Points	73
3.3	Body Motion	73
3.4	Quasi-Loop-Closure Coefficients	73
3.5	Solution Design Parameters	73
4.1	Relationships Between Force Generating Synthesis and Standard Synthesis Problems	78
4.2	Solution Pivot Locations in the Real-Imaginary Plane	86
4.3	Strength Data	91
4.4	Precision Points	92
4.5	Body Motion	92
4.6	Quasi-Loop-Closure Coefficients	92
4.7	Solution Design Parameters	92
6.1	Change of Variables for Synthesis	120

Nomenclature

a	Acceleration
A_R	Area under the resistance curve
\underline{b}	Least squares coefficients (vector)
B	Bearing force (nondimensional)
c	Constraint violation
\bar{D}_n	Location of the body at precision point n
f	Number of temporal divisions
F	Force
h	Track height
i	$\sqrt{-1}$; Index
I	Mass moment of inertia
k	Spring constant
k_T	Spring constant, torsional
l_{in}	Input handle length
l_n	Length of link n
l_o	Unstretched length
l_w	Weight arm length
L_n	Length of link n (nondimensional)
m	Index
\bar{M}	Grounded solution link
n	Precision point; Link; Index
P	Penalty function
$\bar{P}_{1,2}$	Burmester points
q	Design parameter
\bar{r}_{nm}	Vector that locates m^{th} pivot with respect to the n^{th} center of mass

R	Resistance curve (nondimensional)
s	Displacement
S	Strength curve (nondimensional)
t	Parametric variable; Time
t_c	Stroke duration
T	Torque
U	Statistical uncertainty
v	Velocity
V	Cost function
W	Load weight
\tilde{W}	Load weight (nondimensional)
\underline{x}	Least squares abscissa data points (vector)
X	Least squares abscissa matrix
\underline{y}	Least squares ordinate data points (vector)
\bar{Z}	Moving solution vector
α	Angular acceleration; Orientation of the body
β	User input angle
Γ_n	Angular velocity of link n (nondimensional)
$\bar{\delta}_n$	Displacement of the body at precision point n
$\bar{\Delta}_n$	Quasi-loop-closure coefficient
ε	Geometric reduction factor
θ_n	Angle of link n
θ_{in}	Input offset angle
θ_w	Weight arm offset angle
κ	Influence coefficient
μ	Mechanical advantage

ξ	Four-bar closure, +1 or -1
Ξ	Unstretched angle, torsional spring
τ	Transmission angle
Φ	Output angle
χ	Ground link (gravitational) orientation
ψ_n	Orientation of the grounded solution link at precision point n
ω	Angular velocity

Chapter 1, Introduction

1.1 Background and Motivation

The focus of this research is the synthesis of planar four-link mechanisms to satisfy specified input torque curves. The research was performed under a contract with Nautilus with the specific intent of providing algorithms and software to assist designers in developing linkages suitable for exercise equipment. I chose not to divorce Nautilus from the content of this thesis because the direction and goals presented herein are more easily understood in that context. The techniques developed for synthesis and analysis presented are not reduced in importance or general applicability because of the specific application. The synthesis techniques developed within this thesis have applications in process machinery, including mixers, presses and engaging mechanisms, and in nonlinear control actuation, as well as in exercise equipment. In particular, current research includes an examination of the feasibility of replacing the variable mechanical advantage cams employed in compound bows with linkages or other mechanisms.

Nautilus exercise equipment is noteworthy in its design. In addition to the stringent specifications placed on durability and “feel”, Nautilus equipment seeks to provide a more efficient workout by tailoring their designs to the user’s ability to exert force. The *nondimensional strength curve* is a measurement of the user’s ability to exert force over the range of motion of an exercise. Our ability to exert force is dependent on

the strength and geometry of the muscle groups and skeletal structure involved. While the strength of the muscle groups varies widely between individuals, human structural geometry is relatively similar (Lieber, 1992, Thompson, 1973, Schneck, 1990, and Harrison, 1970). If the strength curve of each person is normalized with respect to some reference force (typically the maximum over the range), the resulting nondimensional curve will be approximately the same for the majority of people; this curve is the nondimensional strength curve.

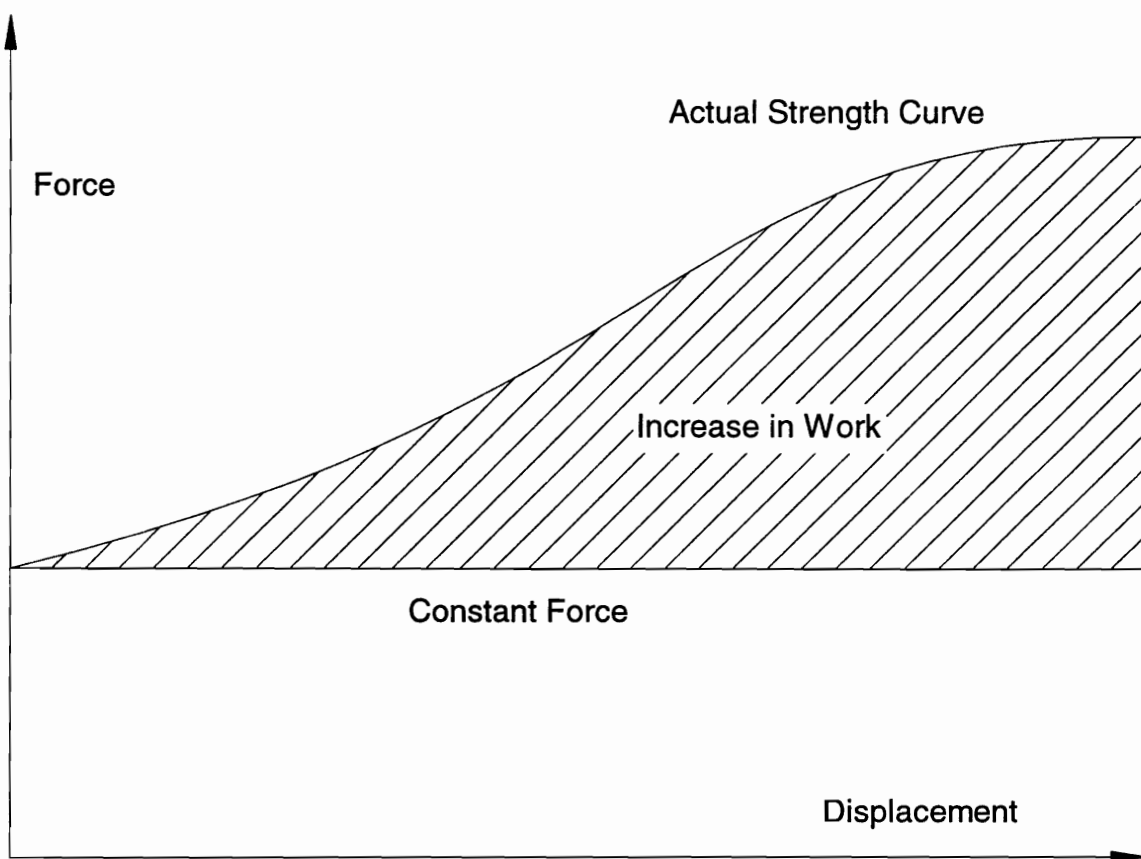


Figure 1-1, How a Tailored Resistance Increases Work

In strength exercise equipment the optimal workout is given by the machine that matches the user's ability to exert force at each position throughout the range of motion. If a constant resistance (e.g. a weight) is used throughout the range of motion, the resistance must be limited to the minimum force the user can exert over the range. In this case less work can be done. Work is the area under a curve relating force and displacement, and the reduction in work is graphically illustrated in Fig. 1-1. The non-dimensional curve of the resisting force of the machine is called the *resistance curve*. The fundamental goal of this research is to design linkage-based exercise machines with resistance curves that closely resemble the non-dimensional strength curves for the exercises.

In nearly all of the original Nautilus equipment the variable resistance curve was provided by a weight lifted by the user through an intermediate *wrapping cam*. A picture of a typical wrapping cam is shown in Fig. 1-2. The concept behind this mechanism is relatively simple; if a constant torque is applied to the cam, then the tension in the chain must vary with the radius of the cam to maintain static equilibrium. Conversely, a constant tension may be applied to the cam through the chain, and a cam-radius-dependent nonlinear torque must be applied to resist it. For more than twenty years the cam-based equipment has been the signature product of Nautilus. It is the shape of the cam, which sometimes resembles a nautilus shell, that gives the company its name.

Until recently, all Nautilus cams were synthesized using graphical techniques. Research contracted by Nautilus from 1992 to 1994 led to an analytical cam synthesis

technique using conjugate geometry. This work is well documented in two papers and a Ph.D. dissertation (Tidwell, et al. 1992, 1994, and Tidwell 1995).

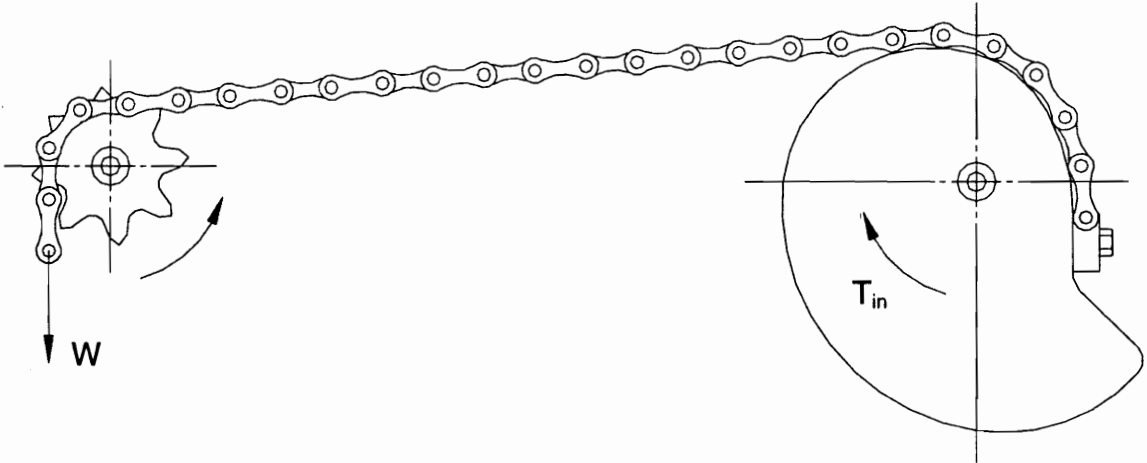


Figure 1-2, Wrapping Cam Mechanism, courtesy Tidwell (1995)

Although Nautilus anticipates continued success with their cam-based, selectorized “Next Generation” line of equipment, they have recently introduced a new line of equipment whose nonlinear mechanical advantage is based on linkages. This new linkage-based equipment line has been given the trade name “Power Plus”.

1.2 Linkages Versus Cams, Advantages and Disadvantages

Linkages have several inherent advantages over cams. This has led Nautilus to venture into this new field. However, the choice of linkages for the new product line is not without disadvantages. In this section, I will enumerate these qualitative differences.

The current Nautilus line, the “Next Generation” line, uses wrapping cams (wrapped by either roller chains or Kevlar reinforced rubber belts) and a *selectorized*

weight-stack. A selectorized weight-stack is made up of a set of rectangular weight plates that ride vertically on a pair of linear bearings. A pin is used to select (hence the term selectorized) the load weight by locking some number of weights above into a single unit. Selectorized weight stacks are common in gym quality strength machines. The selectorized weight stack is an integral part of the machine.

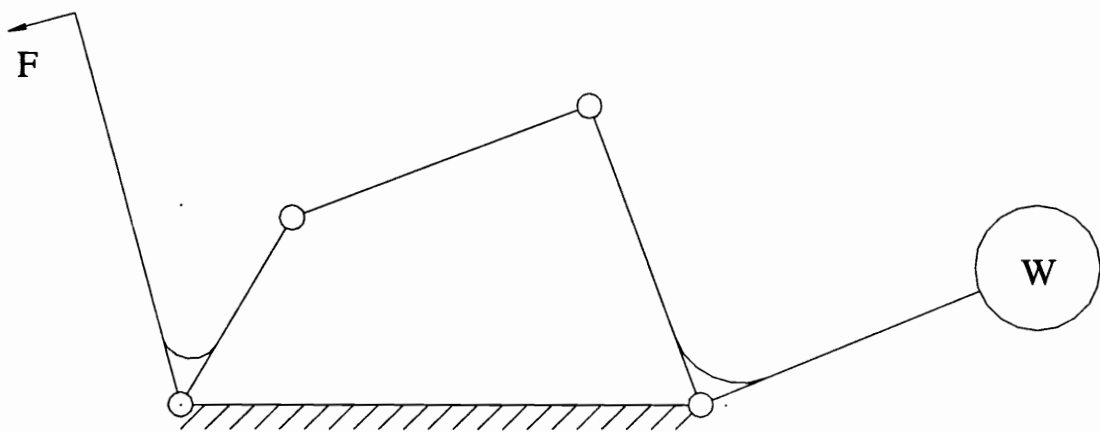


Figure 1-3, The Nautilus “Power Plus” Linkage Concept

In the most recent line of Nautilus strength equipment, the “Power Plus” line, the mechanism which provides a nonlinear mechanical advantage is a four-bar linkage. The general schematic for this mechanism is shown in Fig. 1-3. The Power Plus line is said to be *plate loaded* equipment, rather than selectorized. A horizontal post at the end of the linkage allows barbell-style weight plates to be added for resistance. One advantage of plate loading equipment is that the resistance weights are not integral parts of the machine; one set of weights can be used on many machines.

The linkage-based Power Plus line has two distinct sets of advantages over the cam-based Next Generation line: (1) advantages of linkage-based action over wrapping cams, and (2) advantages of plate-loading equipment over selectorized.

Linkages have certain advantages over cams as force and torque transmitting mechanisms. The most important consideration is a reduction in cost. Manufacture and assembly of linkages is relatively straightforward, requiring only cuts of designed lengths and machining each end to accommodate a bearing or bushing. Cam manufacture requires special NC milling operations with multiple passes -- a relatively expensive proposition in equipment and labor.

Another important issue in choosing between a linkage and a wrapping cam is on-site maintenance. For a cam wrapped by a roller-chain, grease or some other lubricant must be applied periodically, whereas a linkage can use permanently sealed and lubricated bearings or inexpensive self-lubricating bushings. For belt-wrapped cams, slight misalignment within the mechanism can cause the belt to rub against the edge of the cam or the frame of the machine. This rubbing leads to greatly increased belt wear. Such misalignments are frequently caused by deformations due to non-symmetric weight loading. Nautilus believes that the linkage based equipment will be considerably more durable and require much less field maintenance.

Feedback from initial testing of linkage-based designs has confirmed another advantage of linkages over cams -- improved feel. Feel is a subjective variable that is very important in the exercise equipment market. In part, feel is known to be related to

small vibrations in the action of the machine. Linkages have improved feel over chain-wrapped cams because, as the sprocket picks up each chain link, the velocity of the link changes from straight line motion to the circular motion of the sprocket. The result is a discontinuity in the link motion -- an impact. These impacts effect the feel of the machine. Belt-wrapped cams have a different problem. The stiffness of the rubber belts have been improved by Kevlar reinforcing, but, particularly at high loads, the belts undergo a certain amount of deformation at the beginning of each stroke. This results in a "spongy" feel, and, more importantly for our purposes, in a change in the resistance curve of the machine. Linkages can generally be designed to be relatively stiff under the maximum loading, which eliminates much of the elastic feel of the machine.

Linkages are not without their disadvantages. While cams and linkages both produce nonlinear forces, linkages are limited in their ability to match a prespecified resistance curve. A cam can match a desired output curve exactly because its radius can be varied at every design point, giving the designer the ability to match the specified resistance curve at an infinite number of intermediate position in the range of motion.¹ Because linkages only have a finite number of parameters that can be varied, they can only match a generally prescribed output resistance curve at a limited number of points. An examination of mathematical constraints applied to force-generating linkages is included in Chapter 2. This property of linkages means that, in the general case, no

¹ In general, cam designers need to be concerned with discontinuities in the displacement and its derivatives, giving rise to the famous Klopmok and Muffley cam displacement curves (Mabie and Reinholtz, 1987, pp. 79-90), we can be reasonably certain that with a very smooth curve (like a strength curve) discontinuities are not significant.

linkage will ever be a solution to the specified resistance curve over the entire range. By selecting only a limited number of exact points on the curve the designer is able to find a number of linkages that satisfy the prescribed output in an approximate sense.

Another potential disadvantage of linkages is that, given sufficient internal compressive load, the coupler link might buckle. The closed-form linkage synthesis method presented in this thesis does not provide a direct method to ensure that the linkage solution will have a tensile or compressive coupler link. Buckling will only occur in the presence of relatively large internal compressive forces, although the required force decreases as the length of the coupler link increases. We ensure that the linkage is not in danger of a buckling failure by providing an analysis of the internal stress in the coupler link as part of the synthesis package.

A more general discussion of cam verses linkage selection can be found in Shooter (1995). However, the use of linkages is not the only advantage that the Power Plus line has over the Next Generation line. There is also the issue of selectorized verses plate-loading weight resistance.

Surprisingly, the weight stack is one of the most expensive components of the Next Generation equipment. The weights are usually ten or twenty pound steel plates. Each weight plate must have three holes drilled through the top surface, two for the linear bearings and one for the center connector post. An intersecting hole must be drilled on the front surface for the pin. Nautilus paints each weight plate with multiple coats. The raw material, machining, painting, and linear guide rails are all very expensive. By

selling the weights separately, not only is the manufactured cost of the machine reduced considerably, but the shipment weight is reduced, resulting in additional savings.

Selecting the type of mechanism that is correct for the application is the first step to any synthesis. This process is called *type synthesis*. In solving any prescribed nonlinear force or torque problem, the designer must first consider type synthesis. Linkages, cams, noncircular sprockets, nonlinear springs and other devices are all possible solutions. If the choice of a linkage has been made, other issues remain to be resolved. In particular, the choice of the number of links (four-bar or Watt-type six-bar for example) and the synthesis method (closed-form, numerical or optimization) must be made. This thesis presents the closed-form synthesis of a four-bar linkage for force-transmission in detail, with only brief discussion of optimization and synthesis of other linkage types. Before we begin detailed examination of the synthesis method, we will review certain prerequisite topics in standard kinematics.

1.3 General Tools Required for Kinematic Force Synthesis

Certain basic kinematic topics are essential to the synthesis method presented in this thesis. They are reviewed here for completeness.

1.3.1 Position Analysis of Planar Four-Bar Linkages

In general, the position analysis of mechanisms is a nonlinear problem with multiple solutions. The analysis equations are nonlinear because the variables of interest are contained within transcendental terms in the governing relationships. One excellent

method for solving the governing position equations for a four-bar linkage is presented in Mabie and Reinholtz (1987, appendix one). Their method is reproduced here with some variation.

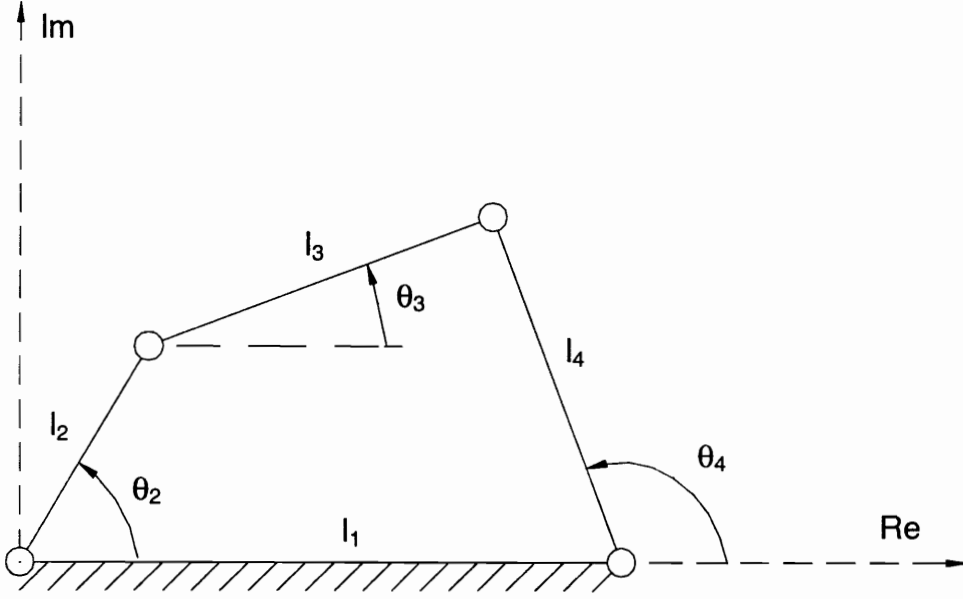


Figure 1-4, Standard Four-Link Mechanism

In this section and throughout this thesis all vectors are represented in the complex plane, thus

$$\vec{l}_n = l_n e^{i\theta_n} . \quad (1.1)$$

A powerful technique for solving closed-loop mechanisms is to sum the vectors which describe the loop, a process called *loop closure*. For the standard four-bar linkage shown in Fig. 1-4, loop closure gives

$$\vec{l}_2 + \vec{l}_3 = \vec{l}_1 + \vec{l}_4 , \quad (1.2)$$

$$l_2 e^{i\theta_2} + l_3 e^{i\theta_3} = l_1 + l_4 e^{i\theta_4} , \quad (1.3)$$

or, employing the Euler identity

$$l_2 \sin(\theta_2) + l_3 \sin(\theta_3) = l_4 \sin(\theta_4) \quad (\text{imaginary part}) \quad (1.4a)$$

$$l_2 \cos(\theta_2) + l_3 \cos(\theta_3) = l_1 + l_4 \cos(\theta_4) \quad (\text{real part}). \quad (1.4b)$$

In the position analysis problem, all of the link lengths are known, and the input angle, θ_2 , is specified. This gives two equations in the two unknowns, θ_3 and θ_4 . Next we isolate the term involving one of the unknown angles on one side of each of Eqs. (1.4). Then we square the equations and add them together. After some manipulation, the result can be shown to be of the form

$$E \sin(\theta) + F \cos(\theta) + G = 0, \quad (1.5)$$

where θ is the other unknown angle (θ_3 if we isolated θ_4 for example). The values for E , F and G for a standard four-bar linkage are

$$E_3 = 2l_2l_3 \sin(\theta_2) \quad (1.6a)$$

$$F_3 = 2l_2l_3 \cos(\theta_2) - 2l_3l_1 \quad (1.6b)$$

$$G_3 = l_2^2 + l_3^2 + l_1^2 - l_4^2 - 2l_1l_2 \cos(\theta_2) \quad (1.6c)$$

$$E_4 = -2l_4l_2 \sin(\theta_2) \quad (1.6d)$$

$$F_4 = 2l_1l_4 - 2l_4l_2 \cos(\theta_2) \quad (1.6e)$$

$$G_4 = l_1^2 + l_4^2 + l_2^2 - l_3^2 - 2l_1l_2 \cos(\theta_2) \quad (1.6f)$$

Equations like (1.5) appear frequently in engineering problems. In many cases a numerical solution is sufficient. In this case, because we have set out to develop closed-

form equations, we must employ a trigonometric identity. One possibility is the tangent half-angle identity, which is given by²:

$$\tan\left(\frac{\theta}{2}\right) = t, \quad (1.7)$$

$$\cos(\theta) = \frac{1-t^2}{1+t^2}, \quad (1.8)$$

$$\sin(\theta) = \frac{2t}{1+t^2}. \quad (1.9)$$

Substituting Eqs. (1.8) and (1.9) into Eq. (1.5) gives

$$E\left(\frac{2t}{1+t^2}\right) + F\left(\frac{1-t^2}{1+t^2}\right) + G = 0,$$

$$\text{or} \quad (G-F)t^2 + 2Et + (G+F) = 0. \quad (1.10)$$

Solving for t using the quadratic equation and applying Eq. (1.7) results in a closed form expression for θ :

$$\theta = 2 \cdot \tan^{-1}\left(\frac{-E \pm \sqrt{E^2 + F^2 - G^2}}{G-F}\right). \quad (1.11)$$

Equation (1.11) provides some interesting insights into four-link mechanisms.

When the term under the radical, the discriminant of the polynomial, is negative, i.e.

$$E^2 + F^2 - G^2 < 0, \quad (1.12)$$

² Most calculus books (Swokosky, 1983, *Calculus with Analytic Geometry*, Prindle, Weber & Schmidt, Boston, for example) give the tangent half-angle identity as

$\tan\left(\frac{\theta}{2}\right) = \frac{1-\cos(\theta)}{\sin(\theta)} = \frac{\sin(\theta)}{1+\cos(\theta)}$ which can be shown to be equivalent. In many cases the parametric form shown is more powerful.

the linkage cannot assemble for this value of θ_2 (the vector loop cannot be closed with the given link lengths). In the case where the discriminant is equal to zero, the mechanism is at a singular or “dead” point (Mabie and Reinholtz, 1987, p. 21). We would expect that the above equation would give four solutions for a given value of θ_2 . Two would arise from the solution of the quadratic equation for t and two would arise from the double-valued inverse tangent function. Only two solutions are physically possible, however, because the equations always give a pair of repeated solutions. The two valid solutions indicate different *closures* or *branches* of the linkage (Mabie and Reinholtz, 1987, pp. 20-29, 572). Another useful point can be made regarding the inverse tangent function. Although computers and calculators will in general return default angles between -180° and $+180^\circ$ for the inverse tangent function (quadrant checking usually requires a more advanced function), the default for the inverse tangent function combined with the two roots the quadratic will capture both solutions. Therefore our solution to the position loop closure equations can be given by:

$$\theta_3 = 2 \cdot \tan^{-1} \left(\frac{-E_3 + \xi \sqrt{E_3^2 + F_3^2 - G_3^2}}{G_3 - F_3} \right), \quad (1.13a)$$

$$\theta_4 = 2 \cdot \tan^{-1} \left(\frac{-E_4 - \xi \sqrt{E_4^2 + F_4^2 - G_4^2}}{G_4 - F_4} \right), \quad (1.13b)$$

where the default inverse tangent is used and $\xi = +1$ or -1 is used to indicate the closure. Note that for the correct closure for both angles, the two expressions must use opposing roots of the quadratic equation.

Once the position analysis of the linkage has been accomplished, linear relationships for the velocities and accelerations can be found by taking derivatives of Eq. (1.3) with respect to time, respectively:

$$i\dot{\theta}_2 l_2 e^{i\theta_2} + i\dot{\theta}_3 l_3 e^{i\theta_3} = i\dot{\theta}_4 l_4 e^{i\theta_4}, \quad (1.14)$$

and
$$-\dot{\theta}_2^2 l_2 e^{i\theta_2} + i\ddot{\theta}_2 l_2 e^{i\theta_2} - \dot{\theta}_3^2 l_3 e^{i\theta_3} + i\ddot{\theta}_3 l_3 e^{i\theta_3} = -\dot{\theta}_4^2 l_4 e^{i\theta_4} + i\ddot{\theta}_4 l_4 e^{i\theta_4}, \quad (1.15)$$

where an over dot indicates differentiation with respect to time.

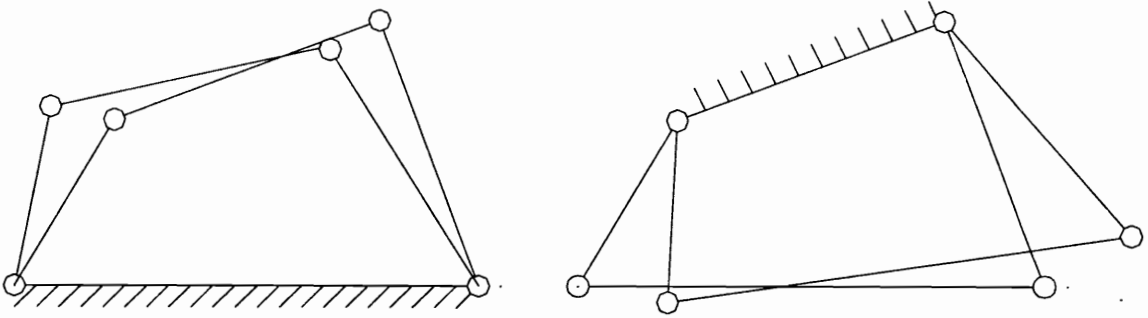


Figure 1-5, Standard and Inverted Frames of Reference

1.3.2 Inversion

In kinematics, relative motion may be equivalently measured in any frame of reference. Valid reference frames can be fixed or moving. This powerful idea is frequently applied through the concept of inversion. Inverting a four-link mechanism involves viewing the mechanism as though either the driving link (input) has changed or the fixed link has changed or both. From a mathematical perspective, a change in the driving link means that some angle other than θ_2 in Eq. (1.3) will be treated as given.

Operations similar to those presented in section 1.3.1 can be used to solve for the remaining unknowns.

The other type of inversion, viewing the mechanism as though one of the moving links is fixed, can be accomplished by establishing a moving reference frame attached to the link. Mathematically, the result is, at each position, the mechanism must be translated and rotated such that the objective link remains fixed with respect to the new reference frame. For example, suppose we wish to examine the mechanism (shown in Fig. 1-5) such that link three remains fixed. Initially we have

$$l_2 e^{i\theta_2} + l_3 e^{i\theta_{30}} = l_1 + l_4 e^{i\theta_4} , \quad (1.16)$$

where θ_{30} denotes the initial angle of the third link. If we allow the linkage to rotate such that link three has rotated by an amount $\Delta\theta_3$, then in the non-inverted frame of reference the loop closure equation is

$$l_2 e^{i\theta_2} + l_3 e^{i(\theta_{30} + \Delta\theta_3)} = l_1 + l_4 e^{i\theta_4} . \quad (1.17)$$

However, in the inverted reference frame link three does not appear to move

$$l_2 e^{i(\theta_2 - \Delta\theta_3)} + l_3 e^{i\theta_{30}} = l_1 e^{i(-\Delta\theta_3)} + l_4 e^{i(\theta_4 - \Delta\theta_3)} . \quad (1.18)$$

This is a case where the power of the complex exponential form becomes very apparent, because rotation operations can be accomplished by simple multiplications.

1.3.3 Burmester Point Pairs

The key to the synthesis method presented in this thesis is the use of *Burmester theory*. Burmester theory is used to solve multiple precision point synthesis problems in

closed form. The actual mathematical operations involved in the application of Burmester theory to our specific application are presented in detail in Chapter 3. A powerful feature of Burmester theory is that it results in a system of equations for the design parameters with an extra unknown. Because the number of unknowns exceeds the number of equations by one, the result is an infinite set of potential solution linkages. By iterating over the unknown variable, a family of solutions can be found in closed form. By displaying this solution set graphically, we are able to give the designer a powerful tool to aid in selecting the best solution.

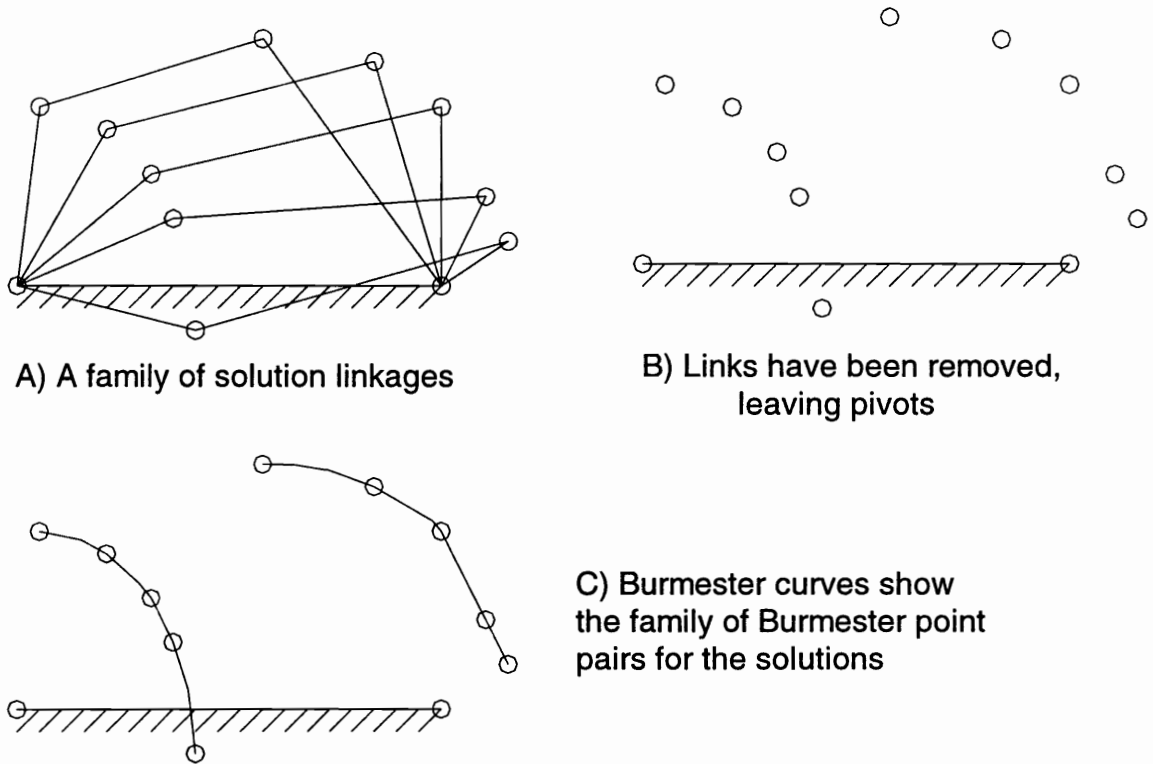


Figure 1-6, Burmester Point Pairs

The graphical result which is used to display the infinite solution set is also part of Burmester theory. First, we imagine that the ground link of each solution has been scaled to the same length and oriented to the same angle. Next, we allow the infinite set of solution linkages to be superimposed over one another. Finally, we erase the links from this image leaving only the revolute joints at the intersection of links two and three and links three and four. The resulting pairs of points are called *Burmester point pairs* (Sandor and Erdman, 1984). Each point in the pair lies on a locus of points which represents the possible pivot locations of a solution to the precision point synthesis problem. By plotting the loci (the Burmester curves) of solution points, the designer is given an excellent perspective on the relative geometry of the solutions. Figure 1-6 demonstrates the graphical Burmester result.

1.3.4 D'Alembert's Principle (Virtual Work)

D'Alembert's principle, or the principle of virtual work, is both simple and powerful. The principle is based on Newton's Third Law, but is derived by allowing a virtual displacement to occur. Virtual displacements are time independent, but they must satisfy all kinematic constraints. The nature of kinematic constraints are such that the vector dot product of the constraint forces with the virtual displacements, summed over the bodies involved, is zero. The simplicity of virtual work, therefore, is based on hiding the constraint forces (Meirovitch, 1970). For a planar mechanism, a method of analysis using virtual work is presented by Mabie and Reinholtz (1987, pp. 421-422).

$$\sum \vec{T}_i \cdot \delta \vec{\theta}_i + \sum \vec{F}_i \cdot \delta \vec{s}_i = \sum m_i \vec{a}_i \cdot \delta \vec{s}_i + \sum I_i \vec{\alpha}_i \cdot \delta \vec{\theta}_i, \quad (1.19)$$

where T and F are external forces and torques, summed over i , the index of bodies. In our particular case, the dynamic forces and the weights of the links are assumed to be negligible with respect to the applied static load weight. Because our analysis is for purely static forces, the virtual displacements given above are the same as true differential displacements. If we take the result and divide by dt , we have

$$\sum \vec{T}_i \cdot \vec{\omega}_i + \sum \vec{F}_i \cdot \vec{v}_i = 0, \quad (1.20)$$

where, because we are considering a static case, the velocities are virtual. They are used because they reflect the kinematic constraints efficiently. Not only is this equation useful in force analysis, it also shows that force generating mechanisms can be synthesized using kinematic velocity constraints. If we further assume that the mechanism in question is a linkage, and that only opposing planar input and output torques are applied to the mechanism then the result is

$$T_{in} \omega_{in} - T_{out} \omega_{out} = 0. \quad (1.21)$$

This is a most useful and interesting result. The *mechanical advantage*, μ , which is usually defined as a force or torque ratio, may sometimes be expressed as velocity ratio, in this case

$$\mu = \frac{T_{out}}{T_{in}} = \frac{\omega_{in}}{\omega_{out}}. \quad (1.22)$$

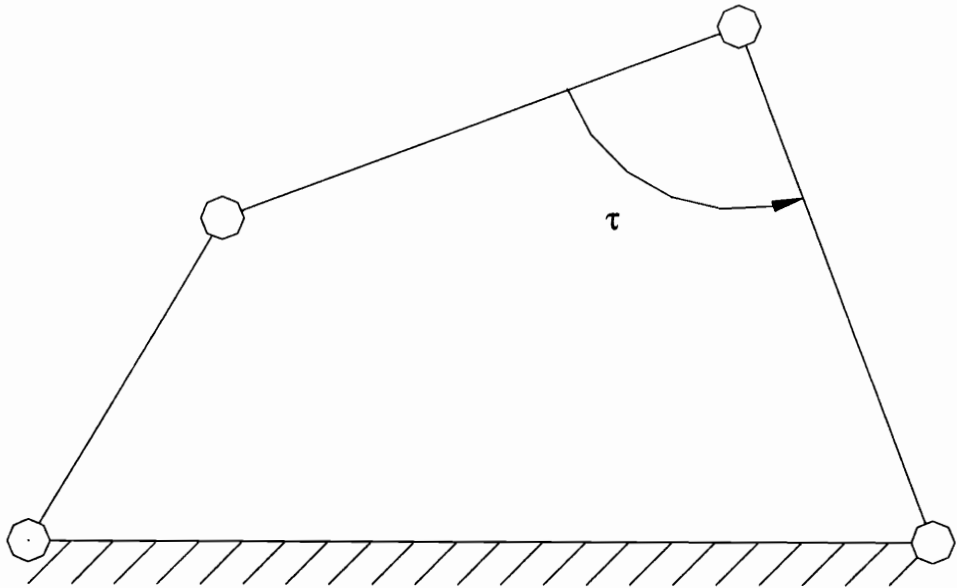


Figure 1-7, Transmission Angle

1.3.5 Transmission Angle

The *transmission angle* of a four-link mechanism is defined as the interior angle between the coupler and the output link. This angle is shown as τ in Fig. 1-7. Transmission angles are generally considered to be a good measure of the ability of the linkage to transmit force (Mabie and Reinholtz, 1987, pp. 21-22). If the mass and inertia of the coupler link are significantly smaller than the magnitude of the transmitted forces, then the coupler can be treated as a two-force member. Internal forces can only be transmitted axially by a two-force member. We can see that for transmission angles near 90° , the force is most efficiently transferred from the coupler link. When the

transmission angle reaches 0 or 180°, the mechanism is unable to transmit force; it is at a dead point (see 1.3.1 above).

In our case, because we are synthesizing for a prescribed force ratio, analysis of transmission angles is redundant. They are mentioned here because previously many works have treated force in a synthesis problem as a constraint of the transmission angle of the solution. In the method we are discussing, however, a poor transmission angle might be desirable, if a large input force is prescribed.

Transmission angles also reflect important information about the internal forces which are developed within the coupler link. Because our approach does not guarantee what is generally considered to be acceptable transmission angles, we must analyze the internal forces in our linkage solutions to ensure that these forces remain within acceptable limits.

1.4 Review of Literature

The kernel of this thesis, the closed-form synthesis method presented in chapter 3, represents a significant divergence from the majority of the work in the area of synthesis of force-generating linkages. However, a number of references are provided in this section in the general area of synthesis for force-generation and related topics in order to provide the reader with an understanding of the current state of the art. In addition, a few influential references are discussed in depth.

We can see from many published applications that designing linkages for force (or torque) transmission is not a new concept. An obelisk at Luxor was lowered using a four-bar linkage for its transport to Paris in 1831. The maximum load during the lowering process was reduced to 43 percent of the obelisk's weight (Hartenburg and Denavit, 1964). Another common example of force generating linkage mechanisms is in toggle linkages, like those shown in Goodman (1965). Midha, et al. (1984) discuss student solutions to the synthesis of a mechanism for a punch. One of the specifications is that the developed mechanisms have acceptable mechanical advantage characteristics at a given output position. Nathan (1985) produces a constant force parallelogram four-bar linkage using a spring actuator. Okada (1986) develops a stretch mechanism using pulleys, springs and a spreading linkage.

Force and velocity are related through the principle of virtual work. Because of this, most of the previous work in linkage synthesis for force is viewed as synthesis for higher-order derivatives of position. This type of synthesis is called *order synthesis* in Sandor and Erdman (1984). Because time is replaced by the time-dependent geometric variable such as input link rotation, kinematitians tend to think of synthesis for velocity as synthesis for two *Infinitesimally Separated Positions* (ISP) of displacement. Similarly, acceleration would be viewed as synthesis for three ISPs. The designation for standard position synthesis is *Finitely Separated Positions* (FSP). In linkage synthesis, only a limited number of positions may be satisfied exactly. Therefore, ISP synthesis for velocity consumes the available precision points at twice the rate of ordinary FSP

synthesis. Of course we can synthesize for a combination of ISP's and FSP's as long as the maximum number of available precision points is not exceeded. Order, or ISP, synthesis has a long history in kinematics. Important works include: Freudenstein (1956), Sandor and Erdman (1984), Brown and Mabie (1971), Urien (1971), and Schaefer and Kramer (1979). The synthesis technique presented within this thesis represents a subtle but significant departure from ISP synthesis; one which is considerably more useful for our application. Like many applications, ours places a constraint on the velocity or force ratio between the input and output links of the mechanism. However, unlike most force-generating linkage solutions, the output position of the linkage is not a specified function of the input. Rather than synthesizing for ISP's, we can integrate the force constraint to form an energy constraint and make direct use of synthesis for FSP's. The result is a synthesis technique that makes more efficient use of the available precision points.

Linkage synthesis accounting for force transmission and dynamics effects on the applied torque and time response of the linkage, is known as *dynamic synthesis*. A summary of the early work in dynamic synthesis is presented in Star (1974). In this work, Star is careful to define dynamic synthesis as being distinct from order synthesis and transmission angle synthesis. Dynamic synthesis does not place any dynamic requirements on the initial kinematic synthesis. After a mechanism has been synthesized to meet kinematic constraints, its dynamic properties are analyzed. If they are found to be insufficient, the designer hopes to find a better solution through another iteration of the kinematic synthesis. This technique relies heavily on the speed of digital computers.

According to Star's definitions, the synthesis technique presented herein falls more correctly under the heading of "synthesis to meet inertialess force transfer properties." More recent work in this area includes Rigelman and Kramer (1988).

Other synthesis work has attempted to address force transmission issues by designing either for transmission angle or for mechanical advantage. Important works include: Shoup and Pelan (1971), Gupta (1977), Midha, et al. (1984), Barker and Shu (1988), and Ogot and Gilmore (1991). None of these works attempt to synthesize linkages for force properties independent of output position.

One way in which input forces for linkages are designed is the process of *equilibration* or *linkage balancing*. This standard technique constrains the synthesis only based on kinematic considerations. Dynamic effects are considered afterward by adding mass to links in order to change their inertia (Ogawa and Funabashi, 1969, Hockey, 1972, and Harmening, 1974), or by designing sub-unit mechanisms, either cams (Benedict et al., 1971) or springs and dampers (Benedict and Tesar, 1970, and Matthew and Tesar, 1977), to eliminate the dynamic effects. Although equilibration has little direct technical similarity to the synthesis technique presented here, it is related to our problem in three distinct ways:

1. Equilibration, particularly by sub-unit mechanisms, represents a significant and popular alternative to our technique.
2. The object of linkage balancing is usually to eliminate fluctuations of the input torque. It is sometimes called input torque balancing. In our case we are designing

for some specific nonlinear input torque; we might say our problem is a type of *input torque unbalancing*.

3. The method we are designing has an application in linkage equilibration. A linkage designed by our techniques could be used in series with an unbalanced linkage in order to smooth the input torque. This is similar to the work of Yong and Zhen (1989). The result would be a Watt type six-link mechanism (see chapter 6).

A few references discussing analytical methods for synthesizing force generating linkages have a more direct relationship to the method presented in this thesis. In his classic work on linkage synthesis, Tao (1964) uses integration of an expression of conservation of energy over the path of action. Tao's work is particularly significant in that it presents a synthesis technique for which force is considered independent of position. Although Tao does not develop a full solution, his presentation of the problem and solution outline follow the same approach adopted here. Hall (1961) poses a similar problem as an exercise in his book. Gustavson (1968) develops analytical tools for synthesizing a four-bar mechanism for torque ratios at two positions by differentiating Fruedenstien's equation.

Extensive work on force system synthesis has been done by Roth and his students. Their work began by examining open loop kinematic chains (manipulators) (Roth, 1989, and Raghavan and Roth, 1989) and continued in closed loop chains (Huang and Roth 1994, 1992, 1990). In particular, Huang and Roth (1990) examine the number of precision points which constrain the design parameters of a closed-loop planar linkage to

a finite number of solutions. Their analysis is unusual in that force constraints can be considered independent from position constraints. A similar analysis is presented in section 2.2 of this work.

It is worth noting that this work is not the first attempt to generate linkages for the specific application of resistance-profiled exercise equipment. Bokelberg and Gilmore (1990) synthesize a four-bar mechanism for variable mechanical advantage with a linear spring as a resistance. However, they formulate their problem such that the number of available design parameters is significantly less than employed here. In addition, and more importantly, rather than employing a closed-form technique, they use numerical techniques. A numerical solution has two advantages over closed-form techniques: (1) the number of precision points can be increased by one, because unlike Burmester theory, numerical analysis can solve the implicit system of equations that has been constrained to a finite number of solutions, and (2) the analytical development is significantly simplified. The drawback of a numerical solution is that it results in only one solution, rather than a family of solutions. This drawback makes finding acceptable designs difficult. The result is that closed-form synthesis is the more robust technique. Burmester theory is used to synthesize for the problem that is not completely mathematically constrained by the selected precision points. This allows Burmester theory to generate an infinite set of possible solutions. If an increase in the number of precision points by one (to a completely constrained problem) seems desirable, we need not turn to numerical methods. The total solution set to a completely constrained

problem can be found by using two Burmester synthesis's whose precision points overlap expect for one. The solution to the totally constrained problem is the intersection of the two solution sets.

Another technique that is often employed in mechanism design is optimization. Optimization is a process of refined iteration. Optimization is powerful because it requires only analysis calculations rather than the typically more complicated synthesis calculations. Designs are compared against one another using a *cost function*, whose definition depends on the characteristics that the designer finds attractive. Works that employ optimization to find force-generating linkage and mechanism design include Benedict and Tesar (1970), Hamid and Soni (1971), Bagci and Rieser (1984), Okada (1986), and Ogot and Gilmore (1991). Some discussion of the development of a solution to this particular design by optimal methods is included in Chapter 6, "Other Synthesis Cases".

Mechanisms other than linkages can be used to provide nonlinear mechanical advantage. In particular certain papers have dealt with the use of cams to provide nonlinear forces, either for mechanical advantage or linkage balancing (Benedict, et al., 1971, Okada, 1986, Yong and Zhen, 1989, Freudenstein and Chen, 1991, Tidwell, et al., 1994 and 1992, and Tidwell, 1995). A series of important and influential works are by Tidwell. Tidwell, et al. (1994, 1992) develop analytical tools for synthesizing wrapping cam mechanisms that generate exact input to output force ratios. Many features of this linkage synthesis technique are analogous to similar features presented in the wrapping

cam synthesis development. Tidwell generates cam profiles by applying integrated force ratio constraints to conjugate geometry equations (the “constitutive” equation for cam action). Similarly, we will apply integrated force ratio constraints to loop closure equations (which govern linkage action). In order to accommodate the two directions of input torque application, counter-clockwise and clock-wise, Tidwell defines two cases for wrapping cam synthesis, open and crossed configurations. If we assume (arbitrarily, but without loss of generality) that the output chain is picked up on the extreme right of the machine, then clock-wise (opposing) rotation of the input is accomplished when the line of the connecting chain crosses the center line between the cam and the sprocket. This case is called a *crossed-chain wrapping cam*. The standard open or uncrossed configuration results in clockwise input rotation. In the analytical synthesis of the cam, the crossed configuration introduces a factor of minus one into the equations. For linkages, we have an analogous effect for a *counter-rotating linkage*, wherein a factor of minus one is introduced with respect to the standard *co-rotating* case.

Although these references establish a basis for our technique, no existing work directly or fully addresses the issues of force synthesis independent of output position. This work has immediate application to the design of exercise equipment, compound bows, balancing devices and other equipment. A novel synthesis technique is developed in the following chapters.

Chapter 2, Problem Definition and Constraints

2.1 Kinematic Model and Variable Definitions

The primary goal of this research is to develop methods for designing weight-loaded linkages to produce specified static resistance curves. The immediate application of this work is to exercise equipment, where the resistance curve produced by the linkage must be a good match to the physiologic strength curve for a given exercise.

In selecting a configuration for the planar linkage, we must recognize that a tradeoff exists between design simplicity and obtaining an accurate resistance curve. Increasing the number of design parameters by increasing the number of links, offset angles, etc., allows the resistance curve to match the strength curve exactly at a greater number of precision points. Unfortunately, increasing the number of design parameters also increases the design complexity, manufacturing cost and the difficulty of developing closed-form synthesis equations. In most cases a four-link mechanisms have been found to yield acceptable resistance curves with reasonable design effort and mechanical complexity. Design methods for more complex linkages can be developed using the general approach outlined in this thesis.

Two cases exist for the synthesis of planar four-link mechanism, namely, a weighted-grounded-link case and a weighted-coupler-link case. The models for these cases are developed in the following subsections.

2.1.1 Four-Link Weighted Ground Link Case

A schematic of the weighted-grounded-link mechanism is shown in Fig. 2-1. The four-bar mechanism transfers a nonlinear load to the input link, l_{in} , from a constant weight at the end of the output link, l_w . The synthesis goal is to match the nondimensional resistance curve of the mechanism, R , to the nondimensional strength curve of the user, S , over the range of motion of the exercise, angle β .

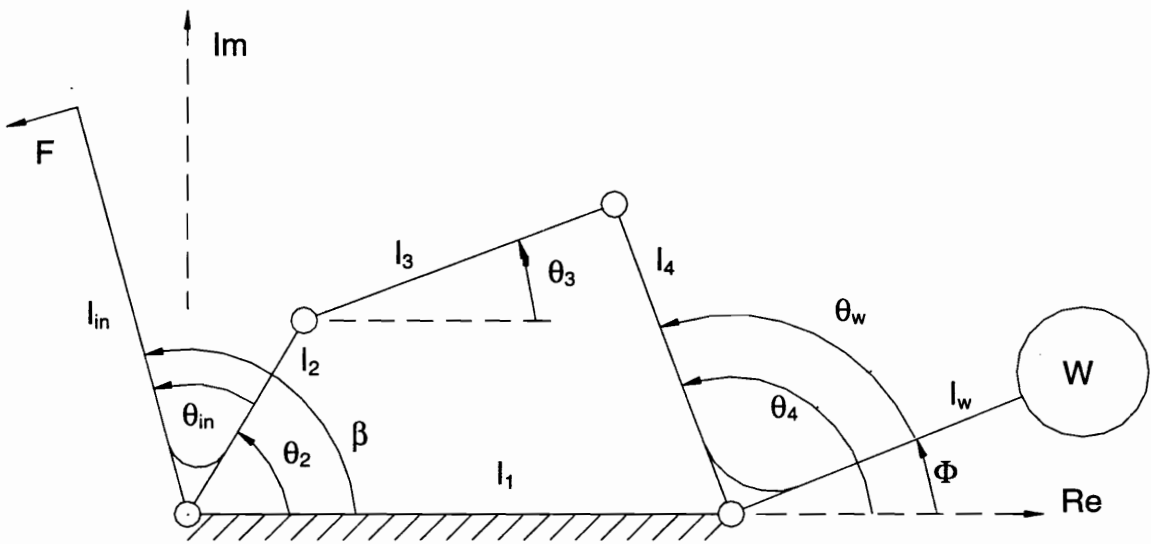


Figure 2-1, Standard Weighted-Grounded-Link Model

The strength curve is determined experimentally and is usually based on measurements of the static force that a user can apply at each angle β . Note that the input link of the four-bar linkage may be direct user input, or it may be driven through a secondary input. A typical situation where this occurs involves the transmission of the applied force through an intermediate linkage used for body guidance purposes. This is

addressed as a subset of Watt six-bar linkage problems in Chapter 6. In either case the functional relationship between S and β must be known before synthesis can begin.

In the derivations in this thesis, we will assume that the measured force is the perpendicular component of the force applied to the input handle. This assumption is based on the way in which the data is typically taken. In some cases the measured force might be horizontal, for example. To deal with such a case, we would simply transform the data through a trigonometric relationship, as shown in Fig. 2-2.

$$F_{\text{perpendicular}}(\beta) = \sin(\beta) \cdot F_{\text{horizontal}}(\beta) \tag{2.1}$$

The strength curve is nondimensionalized with respect to some characteristic force, typically the maximum force encountered over the range of motion. Our goal is to match the nondimensional resistance curve of the mechanism with the nondimensional strength curve. The resistance curve is defined as the inverse of mechanical advantage of the mechanism, that is, the ratio of the perpendicular input force to the weight load

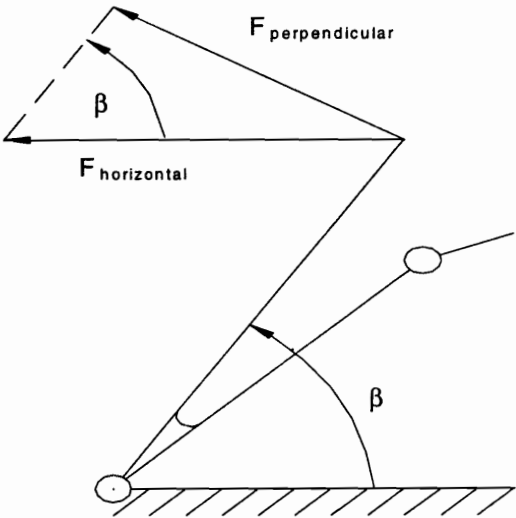


Figure 2-2, Horizontal Applied Force

$$R = \frac{1}{\mu} = \frac{F}{W} = S. \quad (2.2)$$

From this point on, any reference to the strength or resistance curves will be assumed to be to the nondimensional forms.

The strength curve is usually determined by suitable measurements on a specially designed test apparatus. To determine the proper set up for the test apparatus, the range of motion for the input, β , and the length of the input handle, l_{in} , must be selected. These values are determined based on the optimal physiologic motion. In this thesis, it will be assumed that β , $R(\beta)$, and l_{in} are preselected inputs.

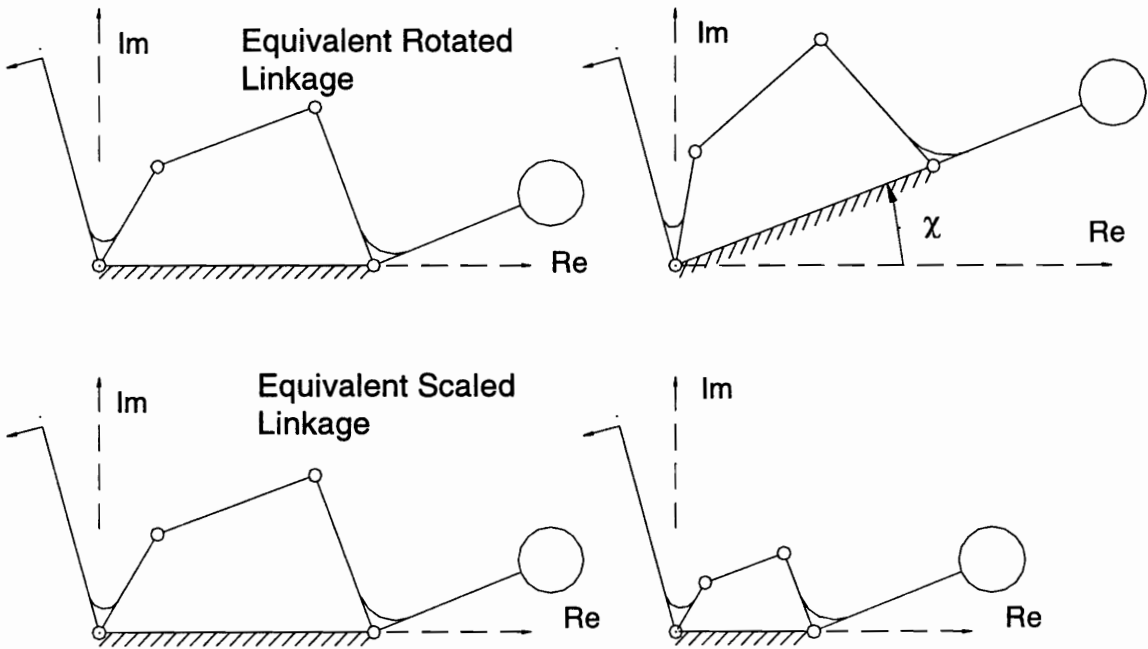


Figure 2-3, Equivalent Rotations and Scalings

Figure 2-1 shows the design parameters for our problem. The input and output offset angles are θ_{in} and θ_w , respectively. The definition of the “input” and “output” of

the model are based on the use of the machine as exercise equipment with the user as the input. In addition to these offset angles, link lengths, l_1 through l_4 and l_w and a ground link orientation angle χ (see Fig. 2-3) are assumed to be the unknown. This gives a total of eight design parameters.

Note that the user input angle, β , is defined to be the sum of the input angle and the input offset, $\theta_2 + \theta_{in}$. Similarly, the sum of the weight arm angle, Φ , and the output offset, θ_w , is the output angle, θ_4 .

We can simplify our synthesis by considering some properties of a mechanical-advantage generator. The overall mechanical advantage of the mechanism may be considered as being comprised of three components: (1) the mechanical advantage given by the ratio of the length of the input lever arm to the length of the output lever arm (a constant); (2) the effect of the change in the torque at the output brought about by the weight moving through the gravitational field (a function of Φ only); and (3) the mechanical advantage of the four-bar mechanism (a function of θ_2). Notice that the mechanical advantage function is independent of the scale and orientation of the linkage. The angle that the ground link makes with the horizontal, χ , can be set arbitrarily without changing the functional relationship between input and the output link motion. If all links of the four-bar are rotated by χ the mechanical advantage of the four-bar remains the same. The mechanical advantage due to the moving weight remains the same if the offset angles are adjusted to maintain the same start angles (relative to gravity) for β and Φ . We

take advantage of this fact by deriving the synthesis equations for the non-rotated case ($\chi = 0$) and allowing the synthesized linkage to be rotated as desired. This is shown in Fig. 2-3. Our linkage can be scaled arbitrarily, so we define the dimensionless parameters L_n to be non-dimensional link lengths given by:

$$L_n = \frac{l_n}{l_1}, n = 1 \dots 4 \quad (2.3)$$

Therefore, for our synthesis, L_1 is set to unity without loss of generality. Once a linkage with acceptable geometric and force properties has been synthesized, the actual scale is set by the designer with a free choice of l_1 .

2.1.2 Four-Link Weighted-Coupler-Link Case

The schematic diagram for the weighted-coupler case is shown in Fig. 2-4. Again we know one linkage parameter, l_{in} , and we know the desired resistance curve, $R(\beta)$. We have the same eight design parameters as in the previous section. Here the sum of the weight arm angle, Φ , and the output offset, θ_w , gives the coupler angle, θ_3 .

Unlike the weighted-grounded-link case, however, the scale and rotation cannot be changed arbitrarily. The weighted-coupler case resembles a path-generator linkage in this way. The similarities of the weighted-grounded-link case and the weighted-coupler link case to function-generators and path-generators will be explored in greater detail in Chapters 3 and 4. Subsection 2.2.2 below shows that our inability to separate rotation and scale allows us to theoretically match a greater number of precision points than for the weighted-grounded-link case.

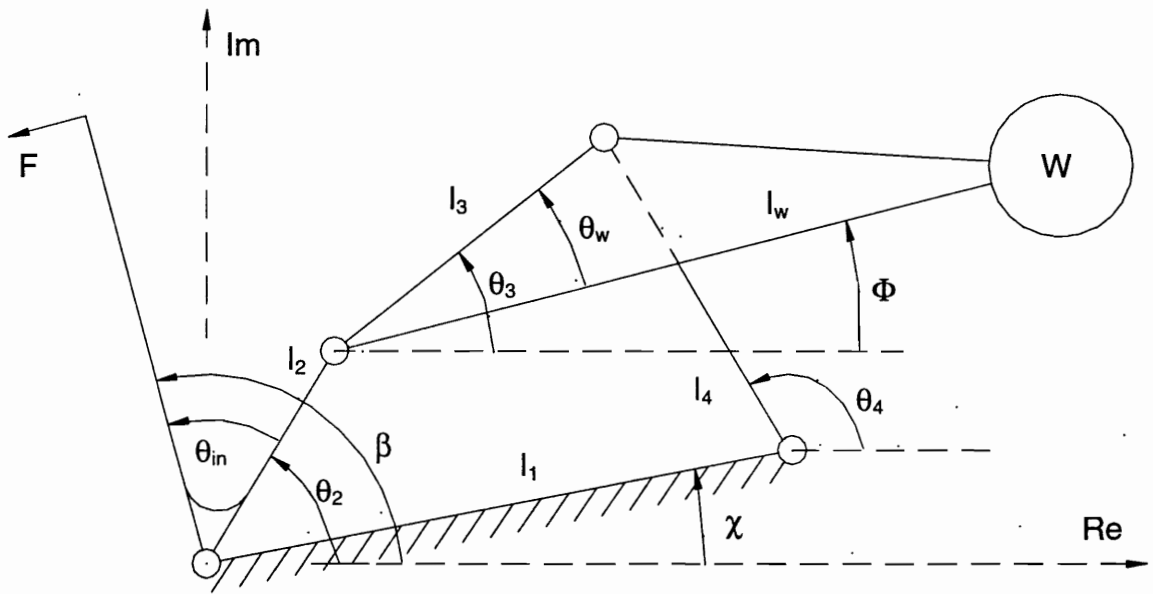


Figure 2-4, Standard Weighted-Coupler Model

2.1.3 Strength Data Issues

Strength data is gathered at a series of discrete points. Usually a strain gage or load cell is used to measure the static force exerted by the user. This produces a good estimate of the force exerted during motion, since all Nautilus strength training equipment is designed for slow-speed movements. It has been suggested that the use of a dynamic tests might result in data which is more true to the application in exercise equipment. However, once dynamic effects become significant in the exercise, no simple machine can tailor resistance to the user's strength. Also, dynamic tests have never yielded repeatable data in practice. Ongoing investigations may overcome these problems.

The strength tests result in a set of discrete data points, which is not sufficient for our purposes. Because we intend to match an integrated constraint at each position, we must choose between either a polynomial fit to the data or some point to point method of integration. For a point to point method, one choice would be to integrate a cubic spline that has been fit to the data. However, we choose a polynomial fit with least squared error. This type of fit has four advantages over a cubic spline fit:

1. Exercise physiology indicates that true strength curves are continuous and relatively smooth (Lieber, 1992). A low degree least-square-polynomial curve fit has the advantage of naturally eliminating some experimental noise that might exist.
2. A polynomial fit is continuously, rather than piecewise, integrable over the angular range.
3. Least-square polynomial fits can be applied to multiple-valued data. This is significant because multiple data sets can be combined to give a fit with greater statistical accuracy.
4. Statistical analysis can be performed on a least-squares curve fit. The statistical significance of the coefficient of the highest degree term can be found using an F distribution (Hogg and Ledolter, 1992). Usually the polynomials we use are of sufficiently low degree that this is not an issue.

The matrix method is one approach to implementing a least-square polynomial curve fit. Let \underline{x} be the column vector of abscissa points for the data, and \underline{y} be the column vector of ordinate points for the data. Next, define

$$X = \begin{bmatrix} \underline{x}^0 & \underline{x}^1 & \cdots & \underline{x}^n \end{bmatrix}. \quad (2.4)$$

In this expression the exponentiation is performed by element, and n is defined to be the degree of the polynomial. The vector of coefficients, \underline{b} , who's polynomial minimizes the sum of the square of the error between the data ordinates and the function, is

$$\underline{b} = \left(X^T X \right)^{-1} \cdot X \underline{y}. \quad (2.5)$$

2.2 Number of Mathematical Solutions

This section examines the governing mathematical equations for both the weighted-grounded-link and the weighted-coupler cases. This will allow us to determine the limiting numbers of precision points for which we can synthesize. This is similar to the general work in Sandor and Erdman (1984, pp. 133-135), and to Huang and Roth (1990).

2.2.1 Four-Link Weighted-Grounded-Link Case

We begin with the loop-closure equations for position and velocity for the weighted-grounded-link mechanism shown in Fig. 2-1

$$L_2 e^{i\theta_2} + L_3 e^{i\theta_3} = 1 + L_4 e^{i\theta_4}, \quad (2.6)$$

and
$$i\omega_2 L_2 e^{i\theta_2} + i\omega_3 L_3 e^{i\theta_3} = i\omega_4 L_4 e^{i\theta_4}. \quad (2.7)$$

We know from virtual work (for the static mechanism with massless links) that

$$F \cdot l_{in} \cdot \omega_2 - W \cdot v_y^w = 0, \quad (2.8)$$

where v_y^w is the y component of the velocity of the weight. Substituting in for v_y^w in terms of the output link rotation gives

$$F \cdot l_{in} \cdot \omega_2 - W \cdot l_w \cdot \omega_4 \cdot \cos(\Phi) = 0. \quad (2.9)$$

Isolating F/W , which is the definition of the resistance function, we have

$$R = \frac{l_w \cdot \omega_4 \cdot \cos(\Phi)}{l_{in} \cdot \omega_2}, \quad (2.10a)$$

or

$$\frac{\omega_4}{\omega_2} = \frac{R \cdot l_{in}}{l_w \cdot \cos(\Phi)}. \quad (2.10b)$$

Dividing Eq. (2.9) through by ω_2 and substituting the result into Eq. (2.12) gives

$$iL_2 e^{i\theta_2} + i\Gamma_3 L_3 e^{i\theta_3} = i \frac{L_4 \cdot R \cdot l_{in}}{l_w \cdot \cos(\Phi)} e^{i\theta_4}, \quad (2.11)$$

where $\Gamma_n \equiv \omega_n / \omega_2$. Therefore, the equations that govern the mechanical-advantage generator shown in Fig. 2-1 are

$$L_2 e^{i(\beta - \theta_{in})} + L_3 e^{i\theta_3} = 1 + L_4 e^{i\theta_4}, \quad (2.12a)$$

$$iL_2 e^{i(\beta - \theta_{in})} + i\Gamma_3 L_3 e^{i\theta_3} = i \frac{L_4 \cdot R \cdot l_{in}}{l_w \cdot \cos(\theta_4 - \theta_w)} e^{i\theta_4}. \quad (2.12b)$$

These represent four scalar equations at each precision point (two real and two imaginary). For each value of β , we know a corresponding value of R from the strength curve data. Therefore, there are six unknown scalar design parameters: L_2 , L_3 , L_4 , θ_{in} , θ_w , and l_w . There are three unknown variables which are functions of β : θ_3 , θ_4 and Γ_3 . At

each precision point, we will add four new scalar equations, but only three new scalar unknowns (the variables which are functions of theta).

The excess of unknowns over equations is reduced with the addition of precision points. We conclude that the number of degrees of freedom in the solution decreases with the addition of precision points. The results of this analysis are summarized in Table 2.1. Recall that the number of free parameters that we actually have available is increased by two, because our ability to scale and rotate the resulting linkage has not been included in this analysis.

Table 2.1, Number of Possible Solutions for the Weighted-Grounded-Link Case

Number of precision pts. in R	Number of scalar equations	Number of scalar unknowns	Max number of free parameter choices	Number of solutions
1	4	9	5	$(\infty)^5$
2	8	12	4	$(\infty)^4$
3	12	15	3	$(\infty)^3$
4	16	18	2	$(\infty)^2$
5	20	21	1	$(\infty)^1$
6	24	24	0	Finite

(superscript numeral indicates the number of infinities or degrees of freedom)

At this point, we could use a system of 24 transcendental scalar equations with 24 unknowns for our synthesis. It is unlikely that a set of equations explicit in our design parameters exists for such a complicated system. We could use a numerical routine to find a solution, but the solution may be poorly conditioned and may yield complex values for any design parameter, for example. We choose to solve the system of equations corresponding to four precision positions. This approach leads to a closed-form solution

to the synthesis equations. It also provides the designer with a family of solutions from which to select a promising design. The method of solution employed in Chapter 3 uses four precision points in R , and one free parameter choice, l_w . The result is a locus of pivot locations representing one infinity of solutions.

2.2.2 Four-Link Weighted-Coupler-Link Case

Analysis of the weighted-coupler case shown in Fig. 2-4 is similar to the method employed above. This case differs from the previous one in that the mechanism cannot be freely scaled or rotated. Again, we begin with the loop closure equations for position and velocity

$$l_2 e^{i\theta_2} + l_3 e^{i\theta_3} = l_1 e^{i\chi} + l_4 e^{i\theta_4}, \quad (2.13)$$

and

$$i\omega_2 l_2 e^{i\theta_2} + i\omega_3 l_3 e^{i\theta_3} = i\omega_4 l_4 e^{i\theta_4}. \quad (2.14)$$

Applying virtual work (for the static mechanism with massless links) results in an equation similar to Eq. (2.10), except that for this case the location of the weight is given by

$$\vec{s}^w = l_2 e^{i\theta_2} + l_w e^{i(\theta_3 - \theta_w)}. \quad (2.15)$$

The y component of the time derivative is

$$v_y^w = \text{Im} \left(i\omega_2 l_2 e^{i\theta_2} + i\omega_3 l_w e^{i(\theta_3 - \theta_w)} \right). \quad (2.16)$$

Substituting in for v_y^w in Eq. (2.10)

$$F \cdot l_{in} \cdot \omega_2 - W \cdot \text{Im} \left(i\omega_2 l_2 e^{i\theta_2} + i\omega_3 l_w e^{i(\theta_3 - \theta_w)} \right) = 0, \quad (2.17a)$$

$$\text{or} \quad F \cdot l_{in} \cdot \omega_2 - W \cdot \omega_2 l_2 \cos(\theta_2) - W \cdot \omega_3 l_w \cos(\theta_3 - \theta_w) = 0. \quad (2.17b)$$

Isolating F/W , the definition of the resistance function we have

$$R = \frac{\omega_2 l_2 \cos(\theta_2) + \omega_3 l_w \cos(\theta_3 - \theta_w)}{l_{in} \cdot \omega_2}, \quad (2.18a)$$

$$\text{or} \quad \frac{\omega_3}{\omega_2} = \frac{R \cdot l_{in} - l_2 \cos(\theta_2)}{l_w \cos(\theta_3 - \theta_w)}. \quad (2.18b)$$

Dividing Eq. (2.16) through by ω_3 and substituting in Eq. (2.20) results in

$$il_2 e^{i\theta_2} + i \left(\frac{R \cdot l_{in} - l_2 \cos(\theta_2)}{l_w \cos(\theta_3 - \theta_w)} \right) l_3 e^{i\theta_3} = i\Gamma_4 l_4 e^{i\theta_4}. \quad (2.19)$$

The governing equations are

$$l_2 e^{i(\beta - \theta_{in})} + l_3 e^{i\theta_3} = l_1 e^{i\chi} + l_4 e^{i\theta_4}, \quad (2.20a)$$

$$il_2 e^{i(\beta - \theta_{in})} + i \left(\frac{R \cdot l_{in} - l_2 \cos(\beta - \theta_{in})}{l_w \cos(\theta_3 - \theta_w)} \right) l_3 e^{i\theta_3} = i\Gamma_4 l_4 e^{i\theta_4}. \quad (2.20b)$$

Again, we have four scalar equations at each precision point. There are eight unknown scalar design parameters: $l_1, l_2, l_3, l_4, \theta_{in}, \theta_w, \chi$ and l_w . We also have three unknown variables which are functions of β : θ_3, θ_4 and Γ_4 . Again, at each precision point we will add three new scalar unknowns. The results of the analysis are summarized in Table 2.2.

Table 2.2, Number of Possible Solutions for the Weighted-Coupler Link Case

Number of precision pts. in R	Number of scalar equations	Number of scalar unknowns	Max number of free parameter choices	Number of solutions
1	4	11	7	$(\infty)^7$
2	8	14	6	$(\infty)^6$
3	12	17	5	$(\infty)^5$
4	16	20	4	$(\infty)^4$

5	20	23	3	$(\infty)^3$
6	24	26	2	$(\infty)^2$
7	28	29	1	$(\infty)^1$
8	32	32	0	Finite

Notice that, although we have gained two precision points compared to the previous case, we have lost our two hidden free parameters: scaling and rotation. A closed-form synthesis method for this case is developed in chapter 4.

2.3 Design Constraints

The primary objective of our design problem is to closely match the strength curve with the resistance curve. A number of less quantitative design considerations, or constraints, are also imposed in the final analysis of the design. In many cases a design which has a perfectly acceptable resistance curve must be rejected due to other considerations. Seven design constraints common in the Nautilus design work are summarized below:

1. In general, the design should fit a standardized frame. Nautilus uses a number of standardized frames for their equipment. The design linkage should remain within the plane of the frame throughout the range of motion for safety considerations. The grounded pivots of the linkage should be located near convenient anchoring locations. If the linkage does not fit one of the standardized frame geometries, a new frame design will be required. This results in additional design work, additional expenses on fabrication, such as new welding fixtures, and a new item to be keep in inventory. In many cases, this would be prohibitively expensive.

2. Because the linkage-based Power Plus line is relatively new, many linkages may need to be suitable for retrofit into existing equipment. For example, an existing machine with a belt-wrapped cam might have an unacceptable number of failures due to belt wear. A linkage design would not only need to meet the specific frame already in use, it would also have to meet the existing pivot positions. If an acceptable linkage can be designed, an in-field retrofit might be possible.
3. Strength of materials issues require that the maximum axial stress within the coupler link and the bearing stresses at the ground pivot be kept at acceptable levels. Procedures for analysis of the static stresses are developed in Chapter 3 and Chapter 4.
4. The lengths of the links may be unacceptable. Links which are too short can cause interference and are difficult to machine. They might lead to dangerous pinch points if exposed. They also have higher internal stresses. Longer links (in particular in the scaleable case where the size of the linkage has been increased to avoid stress problems) are likely to violate frame constraints and require more material. Also, as the length of the link increases, so does its mass. Because our synthesis assumes massless links, this could have a negative impact on the performance of the design.
5. The load weight should be kept as low as possible within the machine throughout the range of motion. The load weight will be a significant portion of the total weight of the machine for high-end (strong) users. As the height of the load weight increases,

the center of gravity of the machine rises, making it less stable. Large vertical strokes of the weight can be dangerous if the weight is dropped from the top of the stroke.

6. Horizontal motion of the load weight does not theoretically effect the input force (no work is done). However, because some dynamic effects will come into play, large side-to-side motions of the weight are unacceptable. They affect both the accuracy of the resistance curve and the stability of the machine.
7. The geometry of the linkage may lead to clearance problems. Links of the actual linkages do not have to match the kinematic link models. They can, for example, be bent to allow clearance as long as the geometry of the pivot points remains the same. However, for any tube size, there is a maximum radius bend Nautilus can produce with its tube-bending machines.

It is difficult for a design to meet all of the design constraints and simultaneously match the desired resistance curve. Therefore, it is vitally important that the designer have maximum flexibility in selecting alternate solutions.

The approach adopted here gives the designer a number of options for arriving at an acceptable design. Our closed-form weighted-grounded-link synthesis technique is very robust, because it allows the designer to make a number of intelligent free choices while still yielding an infinite set of solutions to choose from. Should these solutions prove inadequate, the designer has an option to synthesize a weighted-coupler linkage as an alternative.

If neither of these cases is acceptable, we have other alternatives, discussed in Chapter 3. In particular, because the resistance curve has been arbitrarily nondimensionalized with respect to the weight, we can reduce the resistance curve while maintaining its shape and then synthesize again. Such a reduction is geometric. That is, the change in the design resistance curve can be accomplished by multiplying by a scalar less than one. For example suppose that the maximum a user can lift over the range of a “preacher curl” exercise is 100 pounds. If the linkage is synthesized with no reduction factor, the appropriate weight load on the output link of the machine is 100 pounds. If a reduction factor of 0.9 has been applied during the synthesis, then a weight of $100 / 0.9$ pounds should match the strength curve of the user. Note that an increase in the resistance curve (multiplication by greater than 1) is discouraged for three reasons: (1) it increases the stroke length of the output thus violating a design criteria, (2) motion through an increased stroke makes the nonlinearity of the weight angle ($\cos(\Phi)$) more pronounced, and (3) reducing the amount of weight a user can lift on a machine has a negative psychological impact.

We have concluded our preliminary investigation of this synthesis problem. We now have all of the tools required to develop our synthesis technique.

Chapter 3, Weighted-Grounded-Link Synthesis Method

3.1 Massless Links and Static Force Transfer

Before beginning to discuss our synthesis, we will examine the nature of two key assumptions. Our justification for these assumptions is based on the Nautilus equipment application. Nevertheless, it is believed that these assumptions will apply directly to many other problems, or will at least provide a good starting point for force-based linkage design.

The first assumption is that the effect of the link masses on the input force is negligible relative to the effect of the load mass. We know that the validity of this assumption depends on the exercise being performed and on the strength of the user of the machine. Certain exercises, like the seated leg press which use the large muscles of the leg and buttocks, have larger load weights. Other exercises which use the smaller muscle groups, like bicep curls, neck exercises, and wrist abduction, have lower load weights. For low-end users of these machines (users who lift small weights), link masses and inertias may be significant.

Even though our assumption may be in jeopardy, it would be difficult to account for these masses in a closed-form synthesis procedure, since the link masses depend on the as yet unknown link lengths and shapes. Our alternative is an analysis of the effect of the link masses on the static resistance curve. This analysis is developed in Chapter 5. If

the analysis reveals that the masses do have a significant negative impact on the performance, then we do have alternatives. One is equilibration of the design linkage using balancing masses.

Our second assumption is that the dynamic forces are small compared to the static forces. In the case of an exercise machine, the magnitude of the dynamic effects are controlled by the manner in which the user performs the exercise. Our assumption is validated by proper use of the exercise machine. Nautilus recommends that exercises be performed in a slow, smooth manner. Again, we can look at the validity of this assumption using an analysis performed after the fact. This analysis is developed in Chapter 5.

This assumption is extremely important in the Nautilus application because dynamic effects depend on the trajectory (time-motion relationship) of the input. This input trajectory is not well defined in the case of our application. We have little recourse for detrimental dynamic effects, because these are user dependent.

3.2 Integrating Force Constraints

In this and the following sections, we will synthesize a weighted-grounded-link four-bar by integrating the force constraints to develop a functional relationship between the input and the output. We select four precision points and invert the mechanism. The inversion of the problem is a body-guidance of the input arm through four positions. One infinity of solutions to the synthesis problem are found using standard Burmester theory.

The inverted solutions will be mapped back into non-inverted space in order to plot the Burmester curves.

We begin our examination of this method by reviewing the integration of force constraints to form position constraints. We will look at two general problems before examining the problem specific to our application.

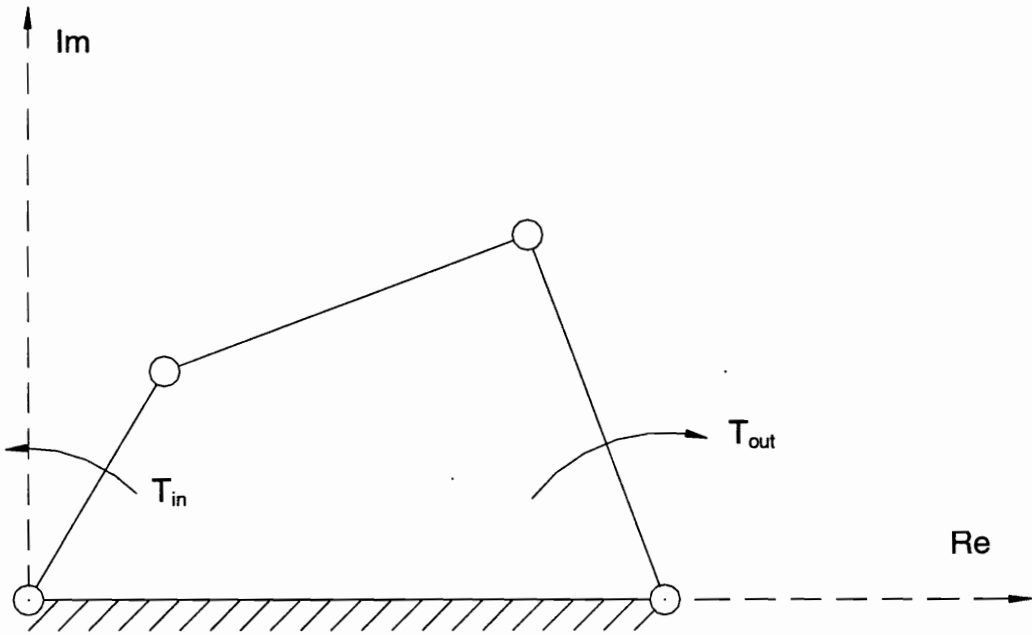


Figure 3-1, Constant Torque Resistance

3.2.1 The General Problem -- Constant Torque Resistance

A general force generating linkage problem is the one shown in Fig. 3-1. In this case, the desired applied torque, T_{in} , is a prescribed function of a constant resisting torque, T_{out} . The resistance curve is given by

$$R(\theta_2) = \frac{T_{in}(\theta_2)}{T_{out}}. \quad (3.1)$$

From virtual work we can find a relationship between T_{in} and T_{out}

$$\begin{aligned}\vec{T}_{in} \cdot \delta \vec{\theta}_2 + \vec{T}_{out} \cdot \delta \vec{\theta}_4 &= 0, \\ T_{in} \delta \theta_2 &= T_{out} \delta \theta_4.\end{aligned}\tag{3.2}$$

If the mechanism is assumed to be static at each position in the motion, then a virtual displacement is equivalent to an actual displacement. If we integrate this equation over some range of motion, from an initial position to some final position, we have

$$\int_{\theta_{2o}}^{\theta_2} T_{in} d\theta_2 = \int_{\theta_{4o}}^{\theta_4} T_{out} d\theta_4.\tag{3.3}$$

Because T_{out} is a constant, we can pull it out of the integral on the right hand side. Dividing both sides by T_{out} , and moving the constant under the integral we are left with

$$\int_{\theta_{4o}}^{\theta_4} d\theta_4 = \int_{\theta_{2o}}^{\theta_2} \frac{T_{in}}{T_{out}} d\theta_2 = \int_{\theta_{2o}}^{\theta_2} R d\theta_2.\tag{3.4}$$

If we know R as a function of θ_2 , then we can evaluate the definite integral on the right hand side after choosing a reference angle, θ_{2o} . The final result is a functional relationship between θ_4 and θ_2

$$\theta_4(\theta_2) = \int_{\theta_{2o}}^{\theta_2} R d\theta_2 + \theta_{4o} = A_R(\theta_2) + \theta_{4o},\tag{3.5}$$

where

$$A_R(\theta_2) \equiv \int_{\theta_{2o}}^{\theta_2} R d\theta_2.\tag{3.6}$$

We call A_R the *area under the resistance curve*. Assuming we know one reference angle in θ_4 corresponding to an angle in θ_2 , we can transform our force generation problem into a problem whose constraint is a functional relationship between the output and the input.

Designing a linkage to meet this constrained functional relationship is a standard problem in kinematics. It can be solved using standard synthesis techniques. The resulting linkage is called a *function generator*. It is for this reason that we call force-generating linkages whose resistance is on a grounded link a *mechanical-advantage generator*.

3.2.2 The Linear Torsion Spring Problem

This technique can be applied to other types of problems. A linkage whose resistance is provided by a linear torsional spring is shown in Fig. 3-2. If the torsional spring constant is k_T , and the unstretched angle of the spring is Ξ , then the torque on the output link is

$$T_{out} = k_T(\theta_4 - \Xi). \quad (3.7)$$

If in this case we nondimensionalize the resistance curve with respect to the torsional stiffness of the spring, $R \equiv T_{in}/k_T$, then we can use a similar process to find a relationship between θ_4 and θ_2

$$\int_{\theta_{2o}}^{\theta_2} T_{in} d\theta_2 = \int_{\theta_{4o}}^{\theta_4} k_T(\theta_4 - \Xi) d\theta_4, \quad (3.8)$$

$$\int_{\theta_{2o}}^{\theta_2} R d\theta_2 = \int_{\theta_{4o}}^{\theta_4} (\theta_4 - \Xi) d\theta_4, \quad (3.9)$$

$$A_R = \left[\frac{\theta_4^2}{2} \right]_{\theta_{4o}}^{\theta_4} - \Xi [\theta_4]_{\theta_{4o}}^{\theta_4}, \quad (3.10)$$

$$\theta_4^2 - 2\Xi\theta_4 - (2A_R + \theta_{4o}^2 - 2\Xi\theta_{4o}) = 0. \quad (3.11)$$

An explicit equation in θ_4 as a function of θ_2 can be found using the quadratic equation

$$\theta_4(\theta_2) = \Xi \pm \sqrt{\Xi^2 + \theta_{4_o}^2 - 2\Xi\theta_{4_o} + 2A_R(\theta_2)}. \quad (3.12)$$

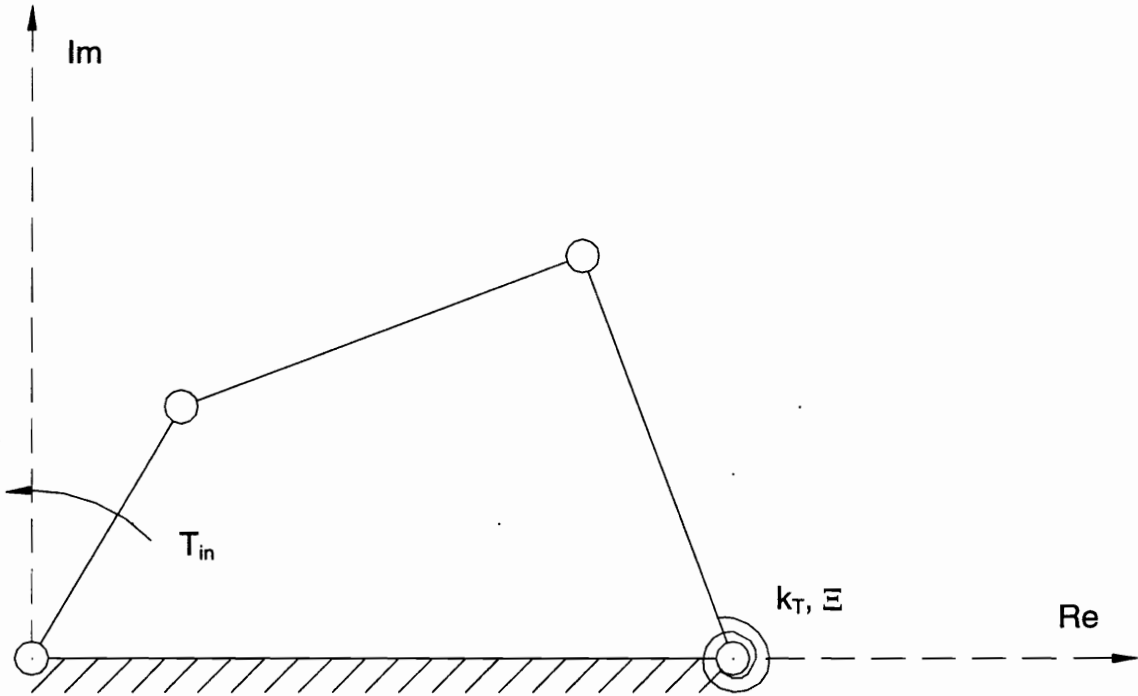


Figure 3-2, Linear Torsional Spring Resistance

The function is double valued because both positive and negative rotations of θ_4 about Ξ store energy in the spring.

3.2.3 The Load Weight Problem

Our standard synthesis problem, the weighted-grounded-link four-bar mechanism is shown in Fig. 3-3. We will use the same technique applied above to transform the problem into a function generator. To retain the maximum number of precision points, we want to constrain as few unknowns as possible along the way. From virtual work we have

$$\vec{T}_{in} \cdot \delta \vec{\beta} + \vec{W} \cdot \delta \vec{s}^w = 0. \quad (3.13)$$

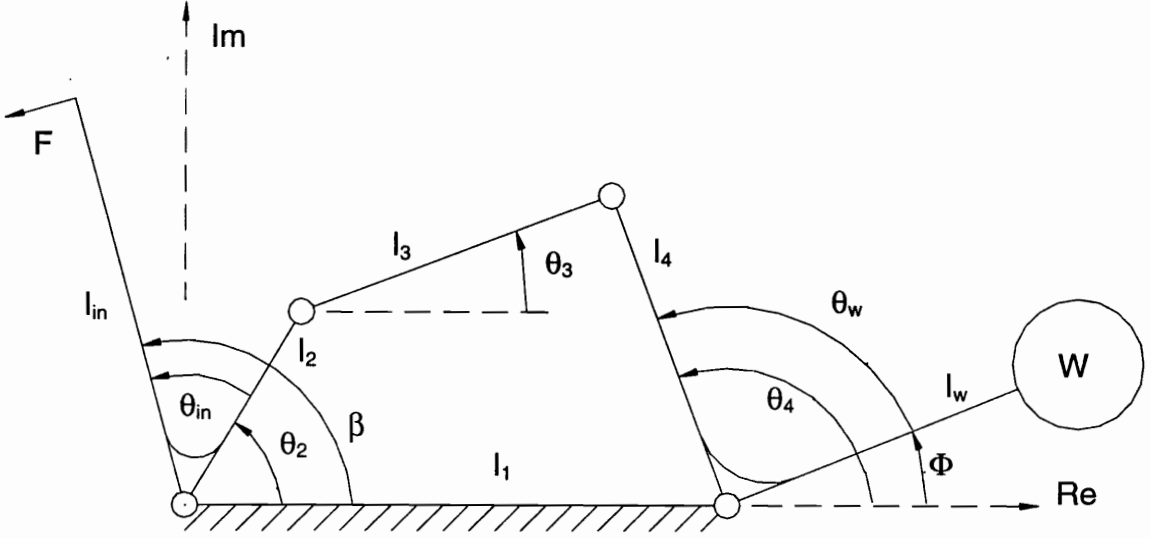


Figure 3-3, Standard Weighted-Grounded-Link Model

We make the same argument for actual verses true differentials as above. Integrating both sides

$$\int T_{in} \cdot d\beta = \int W \cdot ds_y^w. \quad (3.14)$$

From our model we have

$$s_y^w = l_w \cdot \sin(\Phi). \quad (3.15)$$

Substituting the force on the input link times its length for the input torque, and recognizing that the weight, W , is a constant, we have

$$\int Fl_{in} d\beta = W \int ds_y^w = W [s_y^w - s_{y_o}^w]. \quad (3.16)$$

Dividing through by W and recognizing that l_{in} is a constant leaves

$$l_{in} \int \left(\frac{F}{W} \right) \cdot d\beta = l_w (\sin(\Phi) - \sin(\Phi_o)), \quad (3.17)$$

$$\sin \Phi = \frac{l_{in}}{l_w} A_R + \sin \Phi_o . \quad (3.18)$$

The value for l_{in} is given. The value for A_R is known for each precision point in β . If we select values for the two parameters, l_w and Φ_o , we are left with a functional relationship between Φ and β

$$\Phi(\beta) = \sin^{-1} \left(\sin \Phi_o + \frac{l_{in}}{l_w} \cdot A_R(\beta) \right) . \quad (3.19)$$

Expecting the designer to select the length of the weight arm, l_w , and the weight reference angle, Φ_o , is not unreasonable. The designer will frequently have a range of acceptable values for these parameters based on other design constraints. A note about this equation: the inverse sine is multi-valued function. We will assume that the weight remains on the right hand side of the output pivot (i.e. Φ remains between -90° and 90°). This allows us to use the default for the inverse tangent function. We may do this without loss of generality because all solutions in which Φ remains between 90° and 270° have mirror image solutions in the other range.

Before synthesis is attempted, the designer should check to see if the total work, given by the area under the resistance curve, is feasible for the given parameters. If not, Eq. (3.19) will result in a complex number for Φ . Total work output can never exceed the work done in moving the weight from its lowest point to its highest point, as constrained by the output link length. The maximum height is reached when $\Phi = 90^\circ$.

$$\sin \Phi_{\max} = 1 \geq \frac{l_{in}}{l_w} A_R + \sin \Phi_o \quad (3.20)$$

This results in a bound on the minimum value of l_w for a given value of Φ_o . Or, alternatively, it results in a bound on the maximum value of Φ_o for a given value of l_w .

$$l_w \geq \frac{A_{R\max} \cdot l_{in}}{1 - \sin \Phi_o} \quad (3.21a)$$

$$\Phi_o \leq \sin^{-1} \left(1 - \frac{l_{in}}{l_w} A_{R\max} \right) \quad (3.21b)$$

If R is everywhere positive, $A_{R\max}$ is the value of A_R at the maximum value of β .

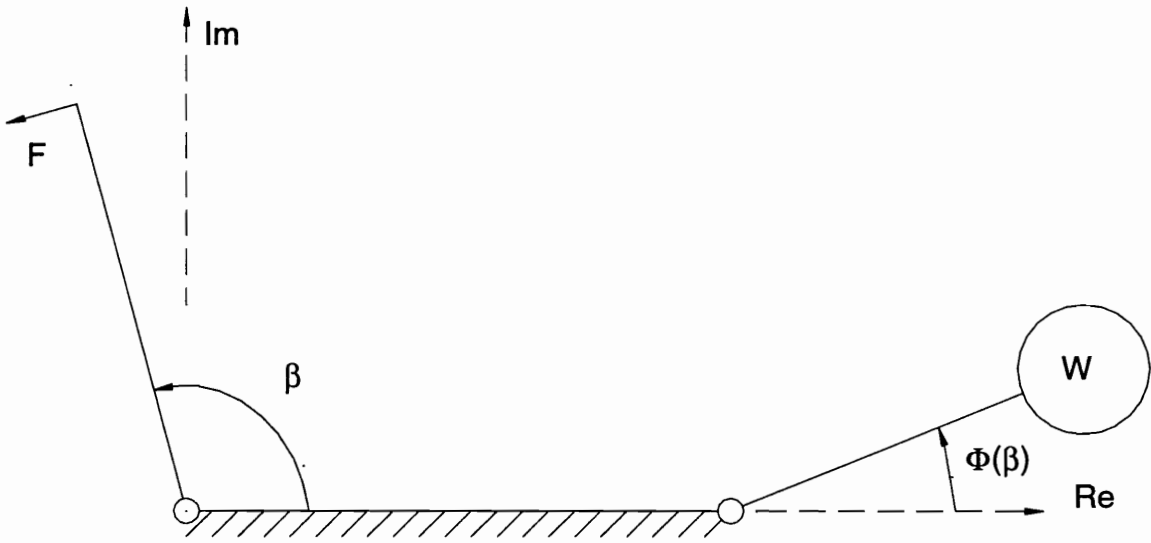


Figure 3-4, Function Generator

We have succeeded in converting the prescribed mechanical advantage synthesis problem into a standard function generation synthesis problem by developing a functional relationship between the input link and the output link. This is shown pictorially in Fig. 3-4.

3.3 Transformation to Body-Guidance Space by Inversion

Any of the function generators developed in section 3.2 can be synthesized with four precision points using Burmester theory. Although the following is applicable to all of the cases, we will examine our standard case, the weighted-grounded-link four-bar, throughout the remainder of this chapter.

Four precision point position synthesis is a well documented, standard kinematic synthesis problem (see for example, Sandor and Erdman, 1984). Burmester theory was developed to solve body-guidance type linkage synthesis problems. In order to take

advantage of this synthesis method, we must first invert our function generator. The inversion maps the function generation synthesis problem into an equivalent body guidance synthesis problem.

In the inverted frame of reference, we choose the weight arm to be the ground link. We orient the inverted mechanism such that the weight arm lies

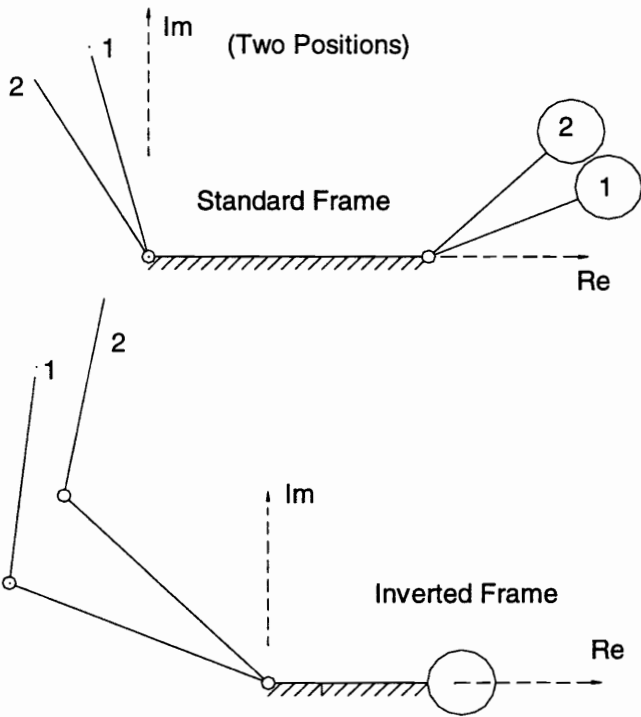


Figure 3-5, Inverted Function Generator

along the real axis, and what was the grounded output pivot becomes the origin. Figure 3-5 shows how two positions in the function generation (non-inverted) space map to the body guidance (inverted) space. Now our goal is to synthesis a linkage dyad (two link series pair) which guides a body attached to the input arm through the four precision points. Proper definition of a body guidance problem requires that we know the position vector of a point on the body at each precision point. We must also know the change in orientation of a line on the body between each precision point. The convenient point on our body is the location of what was the input grounded pivot in function generation space. The input arm is a convenient line on our body. If we define \bar{D}_n as the vector which locates the point at precision point n , and α_n as rotation of the body between precision point n and the first precision point, then

$$\bar{D}_n = L_1 e^{i(\pi - \Phi_n)} = e^{i(\pi - \Phi_n)}, n = 1 \dots 4, \quad (3.22)$$

$$\alpha_n = (\beta_n - \Phi_n) - (\beta_1 - \Phi_1), n = 1 \dots 4. \quad (3.23)$$

3.4 Four Position Body-Guidance Synthesis (Burmester Theory)

Now that the problem has been mapped to a standard, four-precision-point, Body-Guidance problem, we may apply Burmester theory. Burmester theory in linkage synthesis was first implemented on the computer by Fruedenstein at Columbia University in the 1950s (Sandor, 1993). An excellent reference on the method is the text by Sandor and Erdman (1984).

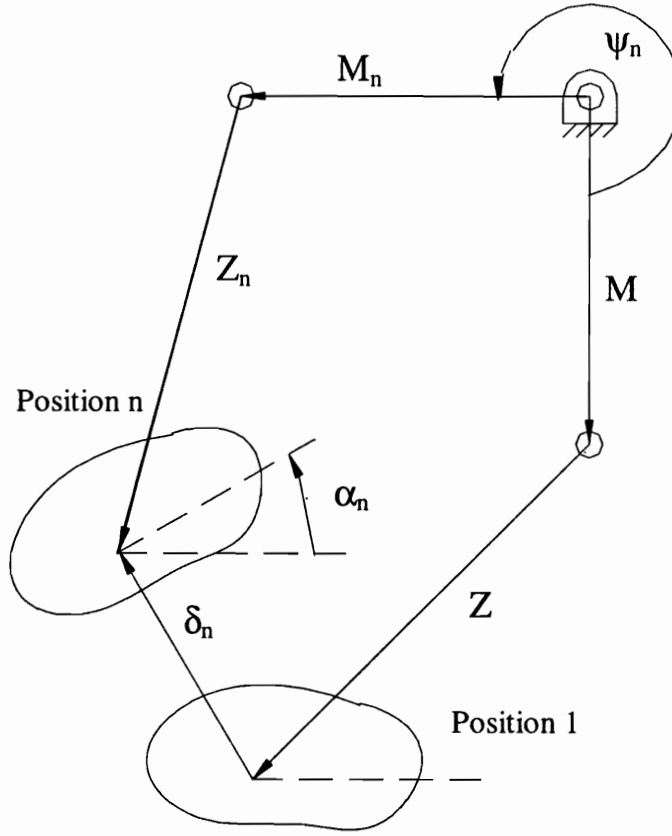


Figure 3-6, Body Guidance Solution Dyad

3.4.1 Matrix Formulation of Loop Closure

Figure 3-6 shows a standard body-guidance problem at two precision positions, n and 1. Vectors \bar{M} and \bar{Z} are a solution dyad at the first precision point. We can write a loop closure equation from position one to position n , $n = 2 \dots 4$

$$\bar{\delta}_n - \bar{Z}e^{i\alpha_n} - \bar{M}e^{i\psi_n} = -\bar{Z} - \bar{M}, \quad (3.24)$$

where $\bar{\delta}_n$ is the vector which locates our reference point with respect to its position at the first precision point. Note that the link \bar{M} undergoes pure rotation between precision points because it is attached to a grounded revolute joint. Also, \bar{Z} is attached to the body,

and so it rotates by the same amount as the body between precision points. Based on our knowledge of the body's motion

$$\bar{\delta}_n = \bar{D}_n - \bar{D}_1 = e^{i(\pi-\Phi_n)} - e^{i(\pi-\Phi_1)}. \quad (3.25)$$

It is convenient to express Eqs. (3.24) in matrix form

$$\begin{bmatrix} e^{i\psi_2} - 1 & e^{i\alpha_2} - 1 \\ e^{i\psi_3} - 1 & e^{i\alpha_3} - 1 \\ e^{i\psi_4} - 1 & e^{i\alpha_4} - 1 \end{bmatrix} \cdot \begin{bmatrix} \bar{M} \\ \bar{Z} \end{bmatrix} = \begin{bmatrix} \bar{\delta}_2 \\ \bar{\delta}_3 \\ \bar{\delta}_4 \end{bmatrix}. \quad (3.26)$$

Equation (3.26) represents a system of six scalar equations (three vector equations) with seven scalar unknowns. The seven scalar unknowns are the real and imaginary parts of \bar{M} and \bar{Z} , and $\psi_2 \dots \psi_4$. We expect that one infinity of solutions should exist (that is, the system has one mathematical degree of freedom). We can eliminate the two vector unknowns by recognizing that in order for solutions to exist, one vector equation must be linearly dependent on the other two. This can be easily shown by modifying Eq. (3.26) to the form

$$\begin{bmatrix} e^{i\psi_2} - 1 & e^{i\alpha_2} - 1 & \bar{\delta}_2 \\ e^{i\psi_3} - 1 & e^{i\alpha_3} - 1 & \bar{\delta}_3 \\ e^{i\psi_4} - 1 & e^{i\alpha_4} - 1 & \bar{\delta}_4 \end{bmatrix} \cdot \begin{bmatrix} \bar{M} \\ \bar{Z} \\ -1 \end{bmatrix} = \begin{bmatrix} 0 \\ 0 \\ 0 \end{bmatrix}. \quad (3.27)$$

If the matrix on the left hand side were invertible, then no solution could exist, because this would imply that $-1 = 0$. Therefore, the matrix must be singular. By expressing this result in terms of the determinate of the coefficient matrix, we can eliminate the vector unknowns from our equations:

$$\det \begin{bmatrix} e^{i\psi_2} - 1 & e^{i\alpha_2} - 1 & \bar{\delta}_2 \\ e^{i\psi_3} - 1 & e^{i\alpha_3} - 1 & \bar{\delta}_3 \\ e^{i\psi_4} - 1 & e^{i\alpha_4} - 1 & \bar{\delta}_4 \end{bmatrix} = 0. \quad (3.28)$$

3.4.2 Solving the Quasi-Loop-Closure Equation

If we expand the determinate in Eq. (3.28) about the first column, which contains the three remaining unknowns, we have:

$$\bar{\Delta}_2 e^{i\psi_2} + \bar{\Delta}_3 e^{i\psi_3} + \bar{\Delta}_4 e^{i\psi_4} + \bar{\Delta}_1 = 0, \quad (3.29a)$$

$$\bar{\Delta}_2 \equiv \det \begin{bmatrix} e^{i\alpha_3} - 1 & \bar{\delta}_3 \\ e^{i\alpha_4} - 1 & \bar{\delta}_4 \end{bmatrix}, \quad (3.29b)$$

$$\bar{\Delta}_3 \equiv -\det \begin{bmatrix} e^{i\alpha_2} - 1 & \bar{\delta}_2 \\ e^{i\alpha_4} - 1 & \bar{\delta}_4 \end{bmatrix}, \quad (3.29c)$$

$$\bar{\Delta}_4 \equiv \det \begin{bmatrix} e^{i\alpha_2} - 1 & \bar{\delta}_2 \\ e^{i\alpha_3} - 1 & \bar{\delta}_3 \end{bmatrix}, \quad (3.29d)$$

$$\bar{\Delta}_1 \equiv -\bar{\Delta}_2 - \bar{\Delta}_3 - \bar{\Delta}_4. \quad (3.29e)$$

We call Eq. (3.29a) a *quasi-loop-closure equation*, because it has the same mathematical form as loop closure, only with complex coefficients. The standard approach to solving this equation is presented in Sandor and Erdman (1984). Their approach is formulated in the context of a computer program which might be implemented in FORTRAN or C. We offer the following alternative approach which takes advantage of the capabilities of

current mathematical software, like MathSoft Mathcad® or Mathematica®. These packages have significantly greater ability to deal with complex vectors.

Each of the complex coefficients acts to rotate the corresponding term. If will look at them as magnitudes and rotation operations, we can combine the rotation with the existing exponent. Thus

$$\bar{\Delta}_n = \Delta_n e^{i(\arg(\bar{\Delta}_n))}, \quad (3.30)$$

and the quasi-loop-closure equation becomes

$$\Delta_2 e^{i\Omega_2} + \Delta_3 e^{i\Omega_3} + \Delta_4 e^{i\Omega_4} + \Delta_1 e^{i\Omega_1} = 0, \quad (3.31a)$$

$$\Omega_2 \equiv \psi_2 + \arg(\bar{\Delta}_2), \quad (3.31b)$$

$$\Omega_3 \equiv \psi_3 + \arg(\bar{\Delta}_3), \quad (3.31c)$$

$$\Omega_4 \equiv \psi_4 + \arg(\bar{\Delta}_4), \quad (3.31d)$$

$$\Omega_1 \equiv \arg(\bar{\Delta}_1). \quad (3.31e)$$

We have converted the quasi-loop-closure equation into an actual loop closure equation. As we index through the values of angle ψ_2 , we can solve for ψ_3 and ψ_4 using the technique described in section 1.3.1. The nonlinear transcendental nature of Eq. (3.31a) leads to a quadratic equation in one of the two unknowns. This means that for each value of ψ_2 , there are two solution dyads. The solution dyads can be found from Eq. (3.26)

$$\bar{Z} = \frac{(e^{i\psi_2} - 1)\bar{\delta}_4 - (e^{i\psi_4} - 1)\bar{\delta}_2}{(e^{i\psi_2} - 1)(e^{i\alpha_4} - 1) - (e^{i\psi_4} - 1)(e^{i\alpha_2} - 1)} \quad (3.32a)$$

$$\vec{M} = \frac{\vec{\delta}_2 - (e^{i\alpha_2} - 1)\vec{Z}}{e^{i\psi_2} - 1} \quad (3.32b)$$

3.5 Transformation to Non-Inverted Solution Space

The solution vectors \vec{M} and \vec{Z} are expressed in the inverted (body guidance) frame of reference. The real axis of the non-inverted frame is coincident with the ground link, and its origin is at the grounded pivot of the input. To express the solution vectors in the non-inverted frame requires a rotation and negation. Recall that the solution vectors are expressed at the first precision point. The non-inverted solution vectors, \vec{M}' and \vec{Z}' , are given by

$$\vec{Z}' = -\vec{Z} \cdot e^{i\Phi_1} \quad (3.33a)$$

$$\vec{M}' = -\vec{M} \cdot e^{i\Phi_1} \quad (3.33b)$$

We now have an infinite solution set of pairs \vec{M}' and \vec{Z}' , two for each value of ψ_2 . In function generator space, the coupler link vector is \vec{M}' , and its base is located by \vec{Z}' . The locus of solutions can be viewed by plotting the Burmester point pairs that correspond to the coupler pivot locations. The corresponding Burmester point pairs are given by

$$\vec{P}_1 = \vec{Z}', \quad (3.34a)$$

and

$$\vec{P}_2 = \vec{Z}' + \vec{M}', \quad (3.34b)$$

where the origin of the complex plane is the input pivot of the ground link. The output pivot of the ground link is given by (1,0).

3.6 Solution Interpretation and Analysis

A number of issues need to be clarified with respect to the synthesis method presented above. In section 3.2 we derive a functional relationship between the input and output angles. In each of the cases we assumed that the input torque is applied in a positive z sense. This is consistent with a co-rotating linkage. However, for the counter-rotating case, the input torque is applied in a negative z sense. This does not effect our synthesis method, it simply introduces a sign of minus one in the calculation of A_R . While this might seem to indicate that A_R would be negative, recall that now the linkage is rotating in the clockwise direction. Each precision point will be smaller than the previous one. When we perform the definite integration, the negative sign introduced by rotation cancels the negative sign from the torque. A_R remains positive. We expect this because a negative A_R would means that the weight is lowering during the stroke.

The solution control variable, ψ_2 , has physical meaning. In body-guidance space, it is the rotation of the fixed link in the dyad between the first and second precision point. In function-generator space, it is the change in angle of the coupler link between the first and second precision point. We will make use of this fact in selecting appropriate ranges over which to iterate (see 3.7.3 below).

Solving for solutions to the synthesis problem requires solving an intermediate loop-closure problem. Because the solutions to the loop-closure equation are the roots of a polynomial of degree two, there is no guarantee that, for any value of ψ_2 , ψ_3 and ψ_4 are

not complex. Complex values for these angles are not physically meaningful solutions. The only way to verify that a given value of ψ_2 does not give complex results is to check it and see.

The problem we are attempting to solve is a difficult one. Although our goal is to match a force curve, we are synthesizing for precision points in the integral of our constraint. We can verify that the solution linkage has a resistance curve that matches our design criteria through a static force analysis. Like all body-guidance synthesis problems, the solution to the mathematical equations produces is not guaranteed to meet the constraints we have placed on it in a physically meaningful way. Problems of this type are called *defects*.

3.6.1 Solution Defects and Rectification

Solutions to linkage synthesis problems can exhibit three major types of defects (Mabie and Reinholtz, 1987). These defects are Grashoff defect, order defect, and branch defect. Grashoff defect exists when the input link is not a crank, that is, it cannot rotate 360° without reaching a dead point. Grashoff defect only exists for applications that require a fully rotating input. Order defect exists when the guided body travels through all of the precision points, but in the wrong order (1-3-2-4, etc.). Branch defect is the most common type of defect. In a branch defective linkage, the mechanism can never go through all of the precision points. Branch defective linkages satisfy all of the mathematical equations governing the synthesis, and they can be assembled such that the linkage satisfies each individual precision point. Nevertheless, the synthesis equations do

not guarantee that the linkage with the synthesized design parameters will satisfy all of the precision points in the same physical closure. Linkages with branch defect have one or more precision points that lies in the opposite closure from the one that satisfies the first precision point.

Branch defect and order defect immediately invalidate the solution. Grashoff defect eliminates the solution if the application requires a fully rotating input crank. There is no recourse for solutions which exhibit defects; they must be discarded.

Confirmation of the existence of a defect requires only simple analysis. Position analysis of one closure of the solution at the precision points will show that at least one precision point is not reached by a branch defective linkage. Linkages with Grashoff defect will fail to assemble (see Eq. (1.12)) over some range of input angle. And, of course, order defective linkages will exhibit paths whose sequence is incorrect.

The process of removing defective solutions from the solution set is called *rectification*. There are two simple methods for rectification that require no more analysis than we have already derived. In one method, the computer that is performing the synthesis can analyze each solution as it is generated. Solutions with defects are flagged, and they are not displayed as part of the Burmester curves. This is a computationally cumbersome method. The other method is manual. The designer selects a solution linkage from the set that may or may not have defects. The computer performs an analysis of the solution, and if the solution exhibits a defect, the designer discards it

and begins again. The choice between these methods depends on the tradeoff between computational time and designer competence.

3.6.2 Analysis of the Resistance Curve

The accuracy of the fit of the resistance curve of the solution linkage to the desired curve must be checked for every potential solution. The theoretical resistance curve of the solution is found using simple static force analysis. For the weighted-grounded-link case we know that

$$R(\beta) = \frac{l_w}{l_{in}} \cdot \frac{\omega_4}{\omega_2} \cdot \cos(\Phi(\beta)), \quad (3.35)$$

as shown in section 2.2.1. Position analysis of the linkage must be performed over the range of β using the governing loop closure equation

$$L_2 e^{i(\beta - \theta_{in})} + L_3 e^{i\theta_3} = 1 + L_4 e^{i(\Phi + \theta_w)}. \quad (3.36)$$

Once the position analysis is completed, solving for the ratio ω_4 / ω_2 is a linear problem.

A form of the velocity loop-closure equivalent to what we have derived previously is

$$\begin{bmatrix} L_4 \cos(\Phi + \theta_w) & -L_3 \cos(\theta_3) \\ L_4 \sin(\Phi + \theta_w) & -L_3 \sin(\theta_3) \end{bmatrix} \cdot \begin{bmatrix} \omega_4 / \omega_2 \\ \omega_3 / \omega_2 \end{bmatrix} = \begin{bmatrix} L_2 \cos(\beta - \theta_{in}) \\ L_2 \sin(\beta - \theta_{in}) \end{bmatrix}, \quad (3.37)$$

or

$$\begin{bmatrix} \omega_4 / \omega_2 \\ \omega_3 / \omega_2 \end{bmatrix} = \begin{bmatrix} L_4 \cos(\Phi + \theta_w) & -L_3 \cos(\theta_3) \\ L_4 \sin(\Phi + \theta_w) & -L_3 \sin(\theta_3) \end{bmatrix}^{-1} \cdot \begin{bmatrix} L_2 \cos(\beta - \theta_{in}) \\ L_2 \sin(\beta - \theta_{in}) \end{bmatrix}. \quad (3.38)$$

We now have sufficient information to calculate the resistance curve of the design over the range of the user input angle.

3.6.3 Analysis of Coupler and Bearing Stress

Once a design is found that is free from defects and has an acceptable resistance curve, link forces and bearing loads should be checked. Although we cannot calculate the stresses since we do not know the cross sectional area of the links or the maximum load weight which might be applied to the weight arm, we can calculate the nondimensionalized forces which give rise to these stresses. If the nondimensionalized (with respect to W) coupler force is F_3 , then, summing moments about the fixed pivot of the input link, we have

$$R \cdot l_{in} - F_3 l_2 \sin(\theta_2 - \theta_3) = 0, \quad (3.39a)$$

or

$$F_3 = \frac{l_{in}}{l_2} \cdot \frac{1}{\sin(\theta_2 - \theta_3)} R. \quad (3.39b)$$

A positive sign for F_3 indicates tension; a negative sign for F_3 indicates compression. Notice in Eq. (3.39b) how the scale of the linkage (l_2) effects the magnitude of F_3 . In this application the lengths of the links are typically small, and the magnitude of the forces are relatively low compared to the stiffness of the members. Because of this, we need not be concerned about the coupler buckling under compression. For other applications a separate analysis would need to be performed.

The magnitudes of the nondimensionalized bearing forces, B_{in} and B_{out} , are found by summing the forces on the two grounded links

$$Rie^{i\beta} + F_3 e^{i\theta_3} + \bar{B}_{in} = 0, \quad (3.40a)$$

$$B_{in} = \sqrt{\left(R \sin(\beta) - F_3 \cos(\theta_3)\right)^2 + \left(R \cos(\beta) + F_3 \sin(\theta_3)\right)^2}, \quad (3.40b)$$

and
$$-i - F_3 e^{i\theta_3} + \vec{B}_{out} = 0, \quad (3.41a)$$

$$B_{out} = \sqrt{(F_3 \cos(\theta_3))^2 + (F_3 \sin(\theta_3) + 1)^2} \quad (3.41b)$$

If the solution linkage passes all of our litmus tests -- no defects, acceptable resistance curve, small magnitude internal forces -- then the linkage will need to be evaluated based on the more subjective criteria laid out in section 2.3. The best design will likely be a compromise between the many design criteria.

3.7 Design Tactics and Example Problem

Because of the many design constraints, a premium has been placed on giving the designer the maximum flexibility in this synthesis method. With this flexibility has come a large number of decisions the designer must make. The designer must choose four precision points, the weight arm length, the weight arm start angle, and the range of the iteration variable, ψ_2 . These choices will result in one infinity of solutions, two at each ψ_2 , to choose from. Even when the final choice of the design has been made, the designer must still decide on the scale and orientation of the solution. This flexibility for the designer is powerful, but only when the designer understands the underlying principles of the synthesis.

3.7.1 Choosing Precision Points

The ability to freely choose four precision points is the most power tool that the designer has in finding solutions with acceptable resistance curves. Because this tool is

so useful, we do not recommend an automated method like Chebyshev spacing (Mabie and Reinholtz, 1987) for selecting the precision point locations. Instead we suggest that the designer use active manipulation of the precision point spacing to try to improve the design.

Starting with a fairly even spacing is typically a good idea. The designer might try to cover areas in which the resistance curve changes shape rapidly with denser spacing. Sometimes it is useful to place precision points near the ends of the range in β , in order to enforce the total energy transfer to the weight.

If solutions seem to be exhibiting poor resistance properties over a specific region of the range, the local resistance properties can be greatly improved by placing two precision points relatively close together in the troublesome region. Of course, this limits the designer's ability to control other portions of the curve.

3.7.2 Choosing the Weight Start Angle and Arm Length

Φ_o and the corresponding value of β_o are reference angles, and may be chosen arbitrarily. The most sensible choice is to make β_o the start angle, because the designer is more likely to be able to choose a corresponding Φ_o based on other design considerations. The weight angle corresponding to an arbitrary user input angle is not as well defined by the problem.

In general the designer should choose as long a weight arm length as possible, and a start angle as near to zero as possible. A slightly negative choice is better than slightly positive one, because the weight is moving up (for always positive resistance curves), and

so will remain in the linear region for more of the motion. By selecting a longer weight arm, the designer has restricted the change in Φ to as small a value as possible, and one which is near to zero throughout its range. This makes the torque applied to the weight arm as linear as possible. Sometimes, the shape of the curve is so radical that the design can benefit from the sine function introduced by varying Φ over the range of motion. In these special cases, the weight arm should start at a more negative angle. It is almost never acceptable for the weight arm to come close to the singular positions -90° and 90° during its motion.

In many cases, the length of the weight arm is constrained to some maximum length to keep the overall machine compact for safety. In such cases the designer needs to be aware of the limiting value of Φ_o for this value of l_w , given by Eq. (3.21b). The designer should try to avoid start angles that are near this limit. Otherwise the linkage will be approaching a singular value near the top of its stroke.

3.7.3 Choosing the Solution Range

The solution range is determined by the range of values chosen for ψ_2 . If the entire locus of solutions is to be displayed, ψ_2 must vary from 0 to 360° in infinitesimal steps. The Burmester curves of the full solution set are likely to be located far away from the pivot points for some ranges of ψ_2 . Since the computer screen is scaled to map the entire set, it may be difficult to see the solutions which have the best geometric properties. Also, the full solution set will likely contain at least some values of ψ_2 for

which $\psi_{3,4}$ are complex. After making an initial scan of the full solution set, the designer should “zoom in” on those ranges of ψ_2 which have promising geometric properties.

Recall that variable ψ_2 is the change in angle of the coupler link between the first precision point and the second precision point. This physical meaning for the variable gives us some insight as to where useful ranges of ψ_2 might exist. The magnitude of ψ_2 should be on the same order of magnitude as the change in the input arm. Consider a synthesis in which the second and third precision points in β differ by less than 1° . It is conceivable that a good design would have a small value of ψ_2 , perhaps a degree or two. A solution whose ψ_2 value is on the order of 100° or -100° will rarely be useful in this case. On the other hand, if $\beta_2 - \beta_1$ is, say, 50° , a good design's coupler might rotate by $+20^\circ$ in the first part of the motion and by -20° during the last part of the motion resulting in a ψ_2 of 0° . Our argument is based on the premise that radical motions of the coupler relative to the input link are likely to be unacceptable, but that the coupler can have large, unpredictable motions over large ranges of β .

3.7.4 Avoiding Defective Regions

If the manual method of defect rectification is being used by the designer, then it is important to remember that local regions on the Burmester curves tend to have the same defects. It should also be noted that defect problems in the two solutions generated by the alternative signs of the quadratic equation in the synthesis calculations are unrelated. The two solutions might have the same defect or they might not. If a defective

design is encountered, there are three options: (1) select ψ_2 values moving away from the defect until a non-defective region is reached, (2) try the other solution for the current value of ψ_2 or (3) modify the synthesis parameters (precision point location, etc.).

3.7.5 Alternatives for Difficult Problems

Some problems are difficult by nature. The resistance curve might be radically shaped. The ground pivot locations might be constrained because the design is a retrofit to an existing machine (constraining the ground pivot locations takes away or ability to scale and rotate the solution linkage freely). The starting position of the weight might be such that the top of the weight stroke is near the singular position. These and other problems can make the synthesis methods we have developed frustrating. There are three last resort alternatives which we can turn to:

1. We can reduce the design resistance curve by a scalar multiplication which retains the curves shape, $\tilde{R} = \epsilon R$, where $\epsilon > 1$. This will result in less angular motion of the weight arm and hence a more linear problem (see 3.7.2 above). Recall that this geometric reduction will be canceled by increasing the load weight.
2. Try a weighted-coupler linkage synthesized according to the method presented in the next chapter.
3. Use a Watt six-bar or other, more complex, linkage. Elementary synthesis of Watt six-link mechanisms is discussed in Chapter 6.
4. If the resistance curve of the linkage is marginally acceptable, and all other design criteria are met, a method of post-synthesis “tweaking” is possible. In chapter 5 a

sensitivity analysis is developed. Judicious variation of parameters, to which the analysis confirms the design is most sensitive, can lead to an improved resistance curve.

Another alternative is optimization. The groundwork for an optimal synthesis method is discussed in Chapter 6.

3.7.5 Example -- Synthesis of a Compound Rowing Machine

A compound rowing machine provides a workout for a compound muscle group in the upper back. This group is usually a difficult one to target with an exercise machine. A summary of the solution and intermediate values in the synthesis are given below. The solution, as it would appear in a Mathcad program, is also included in Appendix A.

- The input link given for the design has a length of 1.018 m (40.1 in). The discrete data points for the strength curve are given in Table 3.1.
- A least-square polynomial curve fit of order three is used to determine the proper functional relationship between R and β .

$$R = 0.263\beta^3 - 1.477\beta^2 + 2.768\beta - 0.73$$

- We choose the length of the weight arm to be $l_w = 1.143$ m (45 in) and the weight start angle to be $\Phi_o = 5^\circ$. Table 3.2 summarizes the chosen precision points and the corresponding values for A_R and Φ (found by transforming the problem into a function generator).

- The known values in the matrix formulation of the Burmester problem are given in Table 3.3.
- The coefficients of the quasi-loop-closure equation are given in Table 3.4.
- One portion of the infinite solution set is shown in Fig. 3-7. The Burmester curves are for the positive closure of the quadratic equation over the range of $\psi_2 = 5.5^\circ$ to 25.5° .
- The solution we have chosen is $\psi_2 = 15.5^\circ$. We choose a scale of $l_1 = 0.203$ m (8 in) and a rotation of $\chi = 165^\circ$. The design parameters for the solution are given in Table 3.5. The solution linkage is shown in Fig. 3-8.
- Analysis shows that the linkage has good resistance curve. The internal coupler force and fixed pivot bearing loads are also acceptable. These are shown in Figs. 3-9, 3-10 and 3-11.

Table 3.1, Strength Data,
Compound Row

Input Angle, β (deg)	Strength Data, S (%)
60	85.75
65	88
70	92.5
75	96.5
80	97.25
85	98
90	98.75
95	100
100	100

Table 3.2, Precision Points

Precision Pt.	β (deg.)	A_R (deg. %)	Φ (deg.)
1	60.5	42.7	5.38
2	85	2332	26.73
3	93	3124	34.97
4	98	3623	40.59

Table 3.3, Body Motion

Precision Pt.	δ (in)	α (deg.)
2	0.102+0.356i	3.149
3	0.176+0.479i	2.915
4	0.236+0.557i	2.290

Table 3.4, Quasi-Loop-Closure Coefficients ($\times 10^{-3}$)

$\Delta_1 = 1.05 - 0.51i$
$\Delta_2 = -9.34 + 4.64i$
$\Delta_3 = 16.6 - 8.33i$
$\Delta_4 = 8.36 + 4.20i$

Table 3.5, Solution Design Parameters

$l_1 = 0.203 \text{ m (8.00 in)}$
$l_2 = 0.509 \text{ m (20.04 in)}$
$l_3 = 0.281 \text{ m (11.07 in)}$
$l_4 = 0.675 \text{ m (26.58 in)}$
$l_{in} = 1.019 \text{ m (40.10 in)}$
$l_w = 1.143 \text{ m (45.00 in)}$
$\theta_{in} = 7.27^\circ$
$\theta_w = 5.33^\circ$
$\chi = 165.00^\circ$

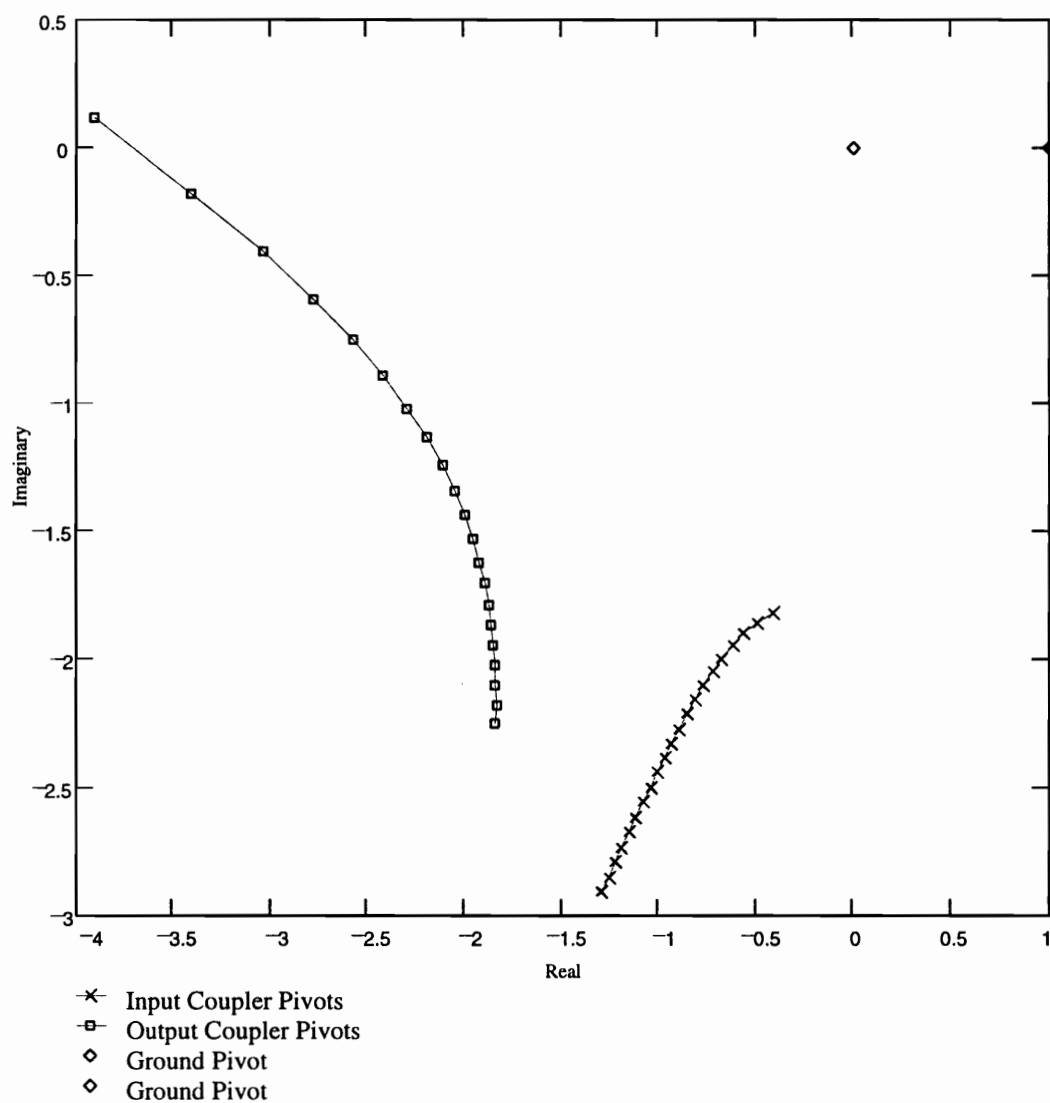


Figure 3-7, Burmester Curves

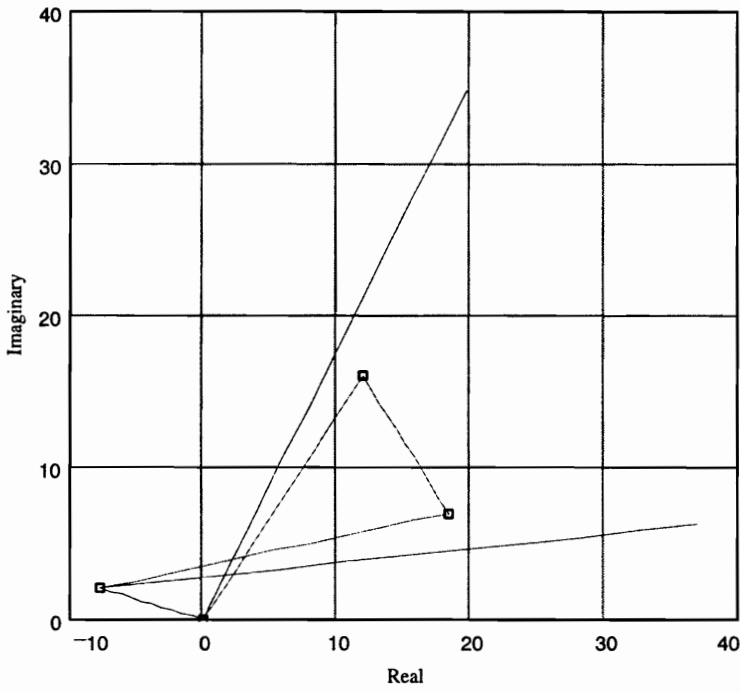


Figure 3-8, Solution Linkage

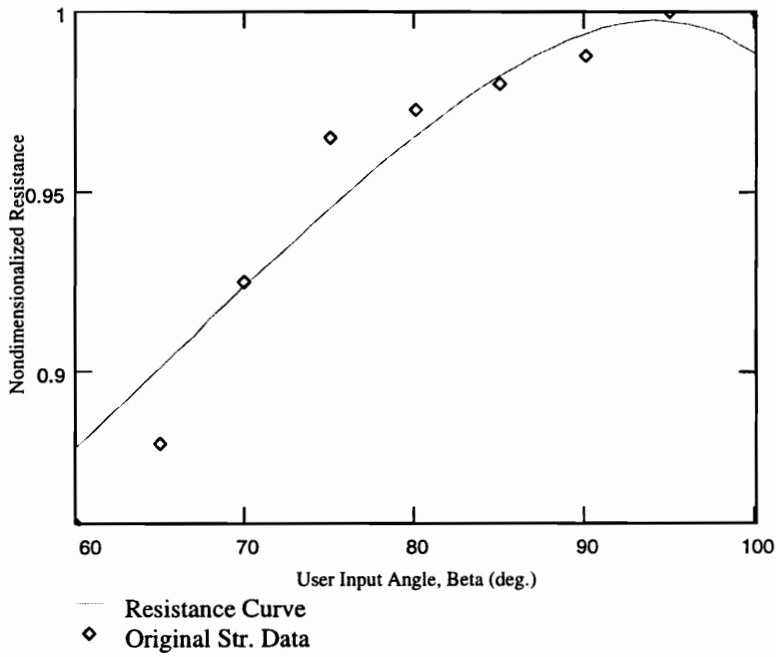


Figure 3-9, Resistance Curve of the Soln

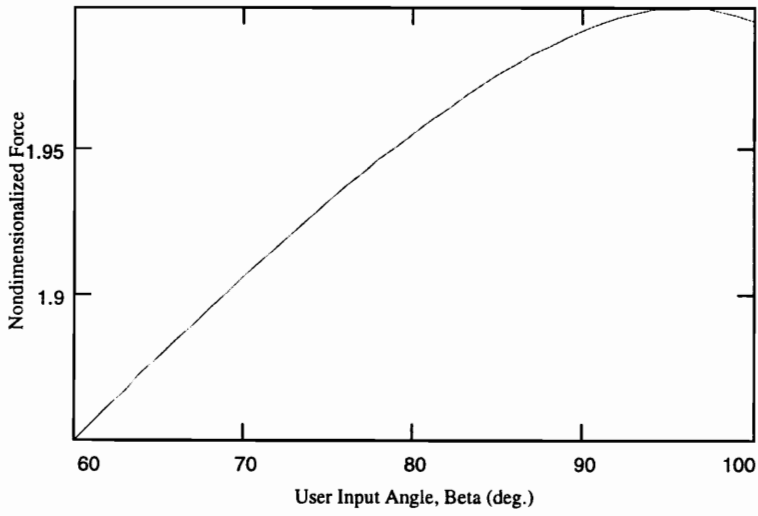


Figure 3-10, Internal Coupler Force

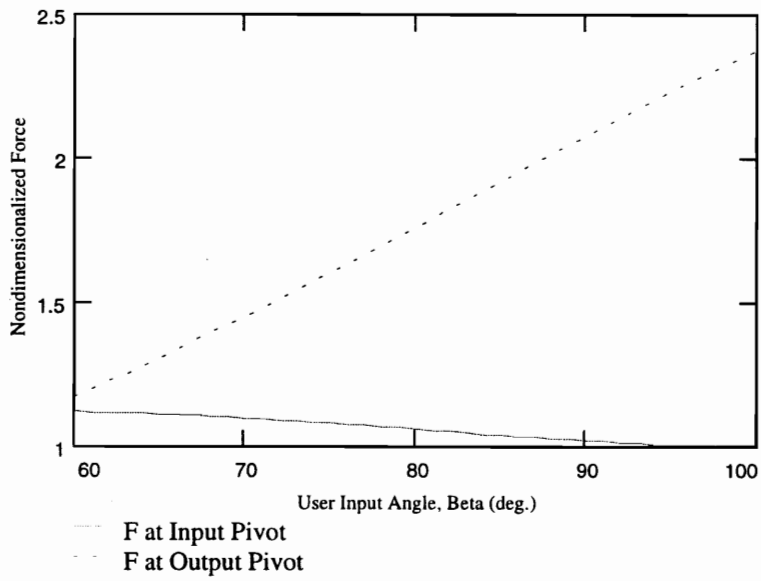


Figure 3-11, Bearing Forces

Chapter 4, Weighted-Coupler Synthesis Method

4.1 How This Problem Differs

Chapter 4, like Chapter 3, develops synthesis techniques for a class of linkages that may be useful in force-generating mechanism applications. This chapter examines four-link mechanisms whose load is located on the coupler link.

In the last chapter we saw that the synthesis of linkages whose input force is prescribed as a function of position, with the resistance provided on the grounded output link, were related to standard function generator problems. Consider qualitatively the version of the synthesis problem in which the resistance is a load weight on the coupler link. Assume that we will employ a similar method to the one employed previously. That is, we integrate the static force over the range of motion. In doing so, we are expressing the principle of conservation of energy; that the work applied to the handle will be conserved through a change in gravitational potential energy of the weight. This means that for each position of the input handle, the weight must have changed in height by a predetermined amount. Therefore, the path that the weight takes in gravitational or imaginary direction is predetermined. A standard kinematic synthesis problem is to move a point on the coupler through a path constrained in both the x and y directions. For this reason we call this type of synthesis *one-dimensionally constrained path generation*. The relationship between standard synthesis and related force generation problem is

summarized in Table 4.1. Special modifications to the standard kinematic synthesis problems, in particular, modifications in which one or more constraint has been removed, are discussed by Reinholtz, et al. (1987).

Table 4.1, Relationships Between Force Generating Synthesis and Standard Synthesis Problems

Force Generation Problem	Related Standard Synthesis Problem	How Force Generation Differs
Grounded-Link Resistance	Function Generator of Order Two (both position and first derivative constrained)	Zero-th Order Derivative Unconstrained
Coupler-Link Resistance	Path Generator	Real Axis Motion (motion normal to the gravitational direction) Unconstrained

4.2 Integrating Force Constraints

As with grounded-link resistance synthesis, we will assume that the linkage is massless with negligible dynamic effects. We will take advantage of the principle of conservation of energy by integrating the force constraints. In this case, the integrated force constraint will allow us to prescribe the motion of the coupler link through four precision positions. We will not need to invert the linkage to form a body guidance problem; our guided body will be the weight arm attached to the coupler link. One infinity of solutions to the synthesis problem will be found and displayed using standard Burmester theory.

4.2.1 The Track-Mounted Linear Tension-Compression Spring Problem

A linkage whose resistance is provided by a track-mounted linear tension-compression spring is shown in Fig. 4-1. The slider attached to the upper end of the

spring is massless. It allows the spring to slide freely in the real axis direction, meaning that forces are only developed in the imaginary direction. If the spring constant is k , the unstretched length of the spring is l_o and the coupler point to which the spring is attached is located by a vector \vec{s} , then the force on the coupler output link is

$$\vec{F}_{out} = ki(h - l_o - \text{Im}(\vec{s})). \quad (4.3)$$

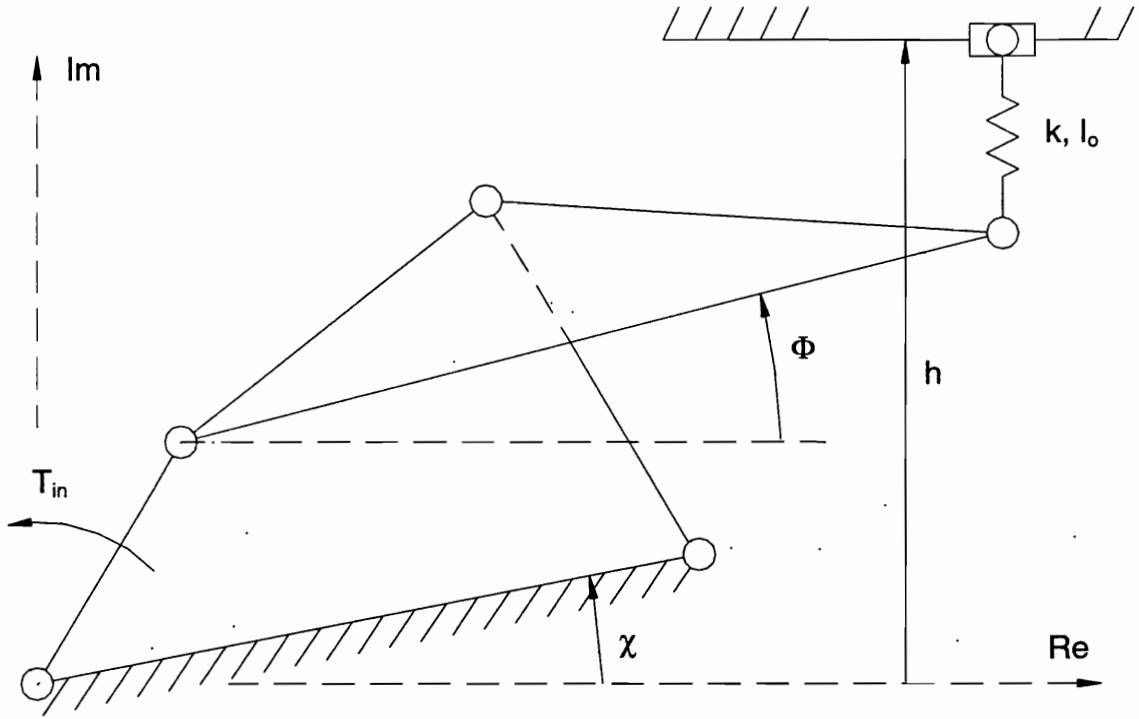


Figure 4-1, Track-Mounted Linear Spring Resistance

Defining s_y to be the imaginary part of \vec{s} , and applying virtual work

$$\vec{T}_{in} \cdot \delta \vec{\theta}_2 + ik(h - l_o - s_y) \cdot \delta \vec{s} = 0, \quad (4.3a)$$

$$T_{in} \delta \theta_2 + k(h - l_o - s_y) \delta s_y = 0. \quad (4.3b)$$

Suppose that in this case the resistance curve is nondimensionalized with respect to k , then recalling that the system is static and integrating, we have

$$\int_{\theta_{2o}}^{\theta_2} T_{in} d\theta_2 + \int_{s_{yo}}^{s_y} k(h - l_o - s_y) ds_y = 0, \quad (4.4a)$$

$$\int_{\theta_{2o}}^{\theta_2} \frac{T_{in}}{k} d\theta_2 + [(h - l_o)s_y]_{s_{yo}}^{s_y} - \left[\frac{s_y^2}{2} \right]_{s_{yo}}^{s_y} = 0, \quad (4.4b)$$

$$A_R + (h - l_o)s_y - (h - l_o)s_{yo} - \frac{s_y^2}{2} + \frac{s_{yo}^2}{2} = 0, \quad (4.4c)$$

$$s_y^2 - 2(h - l_o)s_y - (2A_R - 2(h - l_o)s_{yo} + s_{yo}^2) = 0. \quad (4.4d)$$

We can solve for the motion of the pivot in the imaginary direction using the quadratic equation

$$s_y = (h - l_o) \pm \sqrt{(h - l_o)^2 + s_{yo}^2 - 2(h - l_o)s_{yo} + 2A_R(\theta_2)} \quad (4.5)$$

This function is double valued for the same reason that the torsional spring displacement in section 3.2.2 was double valued. The spring can store energy through either tension or compression. Taking our knowledge of the location of the spring attachment point into account

$$s_y = l_2 \sin(\theta_2) + l_w \sin(\Phi), \quad (4.6a)$$

or

$$\Phi = \sin^{-1} \left(\frac{s_y - l_2 \sin(\theta_2)}{l_w} \right), \quad (4.6b)$$

and

$$\Phi_o = \sin^{-1} \left(\frac{s_{yo} - l_2 \sin(\theta_{2o})}{l_w} \right). \quad (4.6c)$$

If the coupler link is to be a body guided through space, then we have established the change in its orientation between precision points. Recognizing that $L_2 e^{i\theta_2}$, the end of link 2, locates a point on the body, we could synthesize a linkage at four precision points using Burmester theory.

4.2.2 The Load Weight Problem

Consider our standard synthesis problem shown in Fig. 4-2, the weighted-coupler four-bar mechanism. As usual, we apply virtual work

$$\vec{T}_{in} \cdot \delta \vec{\beta} + \vec{W} \cdot \delta \vec{s}^w = 0, \quad (4.7a)$$

$$\int T_{in} \cdot d\beta = \int W \cdot ds_y^w. \quad (4.7b)$$

The previous steps are identical to those in Section 3.2.3. Here they begin to differ, because

$$s_y^w = L_2 \sin(\beta - \theta_{in}) + l_w \cdot \sin(\Phi). \quad (4.8)$$

Once again,

$$\int_{\beta_o}^{\beta} F l_{in} d\beta = W \int_{s_{y_o}^w}^{s_y^w} ds_y^w = W [s_y^w - s_{y_o}^w]. \quad (4.9)$$

However,

$$l_{in} \int_{\beta_o}^{\beta} \left(\frac{F}{W} \right) \cdot d\beta = l_w (\sin(\Phi) - \sin(\Phi_o)) + L_2 (\sin(\beta - \theta_{in}) - \sin(\beta_o - \theta_{in})), \quad (4.10a)$$

$$\sin \Phi = \frac{l_{in}}{l_w} A_R + \sin \Phi_o + \frac{l_2}{l_w} (\sin(\beta - \theta_{in}) - \sin(\beta_o - \theta_{in})), \quad (4.10b)$$

$$\Phi(\beta) = \sin^{-1} \left(\sin \Phi_o + \frac{l_{in}}{l_w} \cdot A_R(\beta) + \frac{l_2}{l_w} [\sin(\beta - \theta_{in}) - \sin(\beta_o - \theta_{in})] \right). \quad (4.10c)$$

We have established a relationship that is a function of the user input angle, β . This can be used to calculate changes in orientation of the coupler link between precision points.

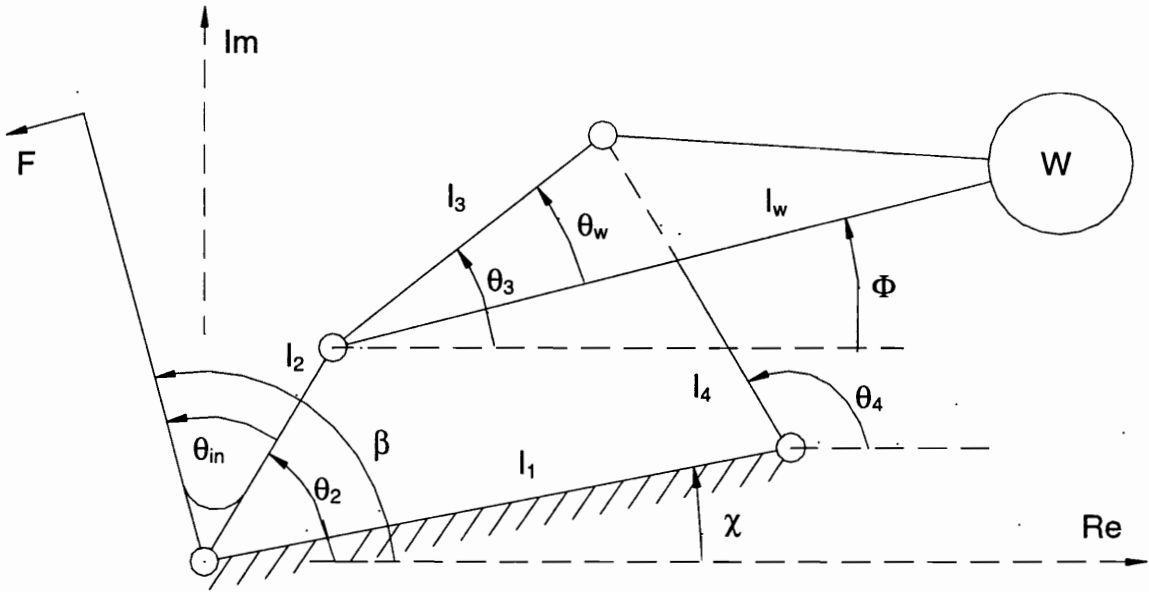


Figure 4-2, Standard Weighted-Coupler Model

Again we stipulate that the default value of the inverse sine be used without loss of generality, because of the nature of mirrored solution pairs.

Notice that this equation has more unknowns than the analogous equation for the weighted-grounded link case given by Eq. (3.19). To solve the explicit equation in Φ , the designer must make three free-parameter choices, namely, l_2 , l_w , and θ_{in} . Notice also that the free-parameter choices here accomplish the same physical purpose as the choice of l_w in the analogous weighted-grounded-link problem. Along with Φ_o , these choices exactly locate the weight in the real-imaginary plane at the reference input angle. For this reason, the weighted-coupler case may be less powerful than the weighted-grounded-link case. In

the weighted coupler case two additional up-front parameter choices are required to accomplish the same task.

Certain values of the free-parameters that the designer is choosing could result in complex results for Φ at a precision point. This occurs when the linkage is incapable of raising the load weight sufficiently high to provide the requisite energy storage given by the area under the resistance curve. An analysis of the bounds placed on each of the parameters by the others would be useful for the designer. The development of this analysis is similar to the one presented in Chapter 3. Here the analysis is complicated by the additional variables and by the interaction between the area under the resistance curve and sine of the input angle terms. In the weighted-grounded-link case we could be sure that critical value occurred when A_R reached its maximum. Here the bounds must be checked over the full range of β . To ensure real valued Φ

$$\sin(\Phi)_{\max} = 1 \geq \frac{l_{in}}{l_w} A_R + \sin \Phi_o + \frac{l_2}{l_w} (\sin(\beta - \theta_{in}) - \sin(\beta_o - \theta_{in})). \quad (4.11)$$

The expression can be used to bound l_w , l_2 , and Φ_o in terms of the other selections.

$$l_w \geq \max_{\beta} \left\{ \frac{1}{1 - \sin(\Phi)} \left[l_2 (\sin(\beta - \theta_{in}) - \sin(\beta_o - \theta_{in})) + l_{in} A_R \right] \right\}, \quad (4.12a)$$

$$l_2 \leq \min_{\beta} \left\{ \frac{l_w \left(1 - \frac{l_{in}}{l_w} A_R - \sin \Phi_o \right)}{(\sin(\beta - \theta_{in}) - \sin(\beta_o - \theta_{in}))} \right\}, \quad (4.12b)$$

$$\Phi_o \leq \min_{\beta} \left\{ \sin^{-1} \left[1 - \frac{l_{in}}{l_w} A_R - \frac{l_2}{l_w} (\sin(\beta - \theta_{in}) - \sin(\beta_o - \theta_{in})) \right] \right\}, \quad (4.12c)$$

In view of the requirement that these bounds be evaluated over the range of β , we suggest an alternative. Rather than evaluating these expressions, the designer can select values for the control variables, and then check the values of Φ that result from equation (4.10c). If any of the values of Φ are found to be complex, then one or more of the variables could be adjusted in light of the above bounds (Φ_o or l_2 decreased, l_w increased) until the values of Φ are all real numbers.

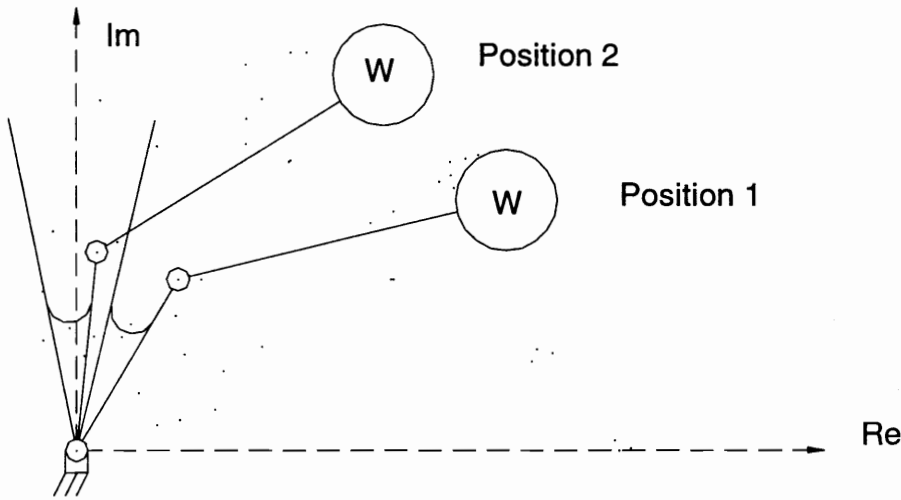


Figure 4-3, Resulting Body-Guidance Problem

We have succeeded in converting the one-dimensionally constrained path generation problem into a standard body guidance problem. We know the motion of one point on the body (coupler link) and the change in orientation of the body as a function of the input angle, as seen in Fig. 4-3.

4.3 Four Position Body-Guidance Synthesis (Burmester Theory)

Burmester synthesis is applicable to each of the cases examined above. This section is presented from the perspective of synthesis for a weight loaded coupler. In Section 4.2.3 we derived an expression for the rotation of the coupler link as a function of the user input angle. Combined with the knowledge of the motion of the input side pivot on the coupler link, this is the essential information for a Burmester-based synthesis of the linkage. Unlike the weighted-ground-link case, no inversion is necessary.

A point is located on the body by

$$\vec{D}_n = l_2 e^{i(\beta_n - \theta_{in})}. \quad (4.13)$$

Knowledge of the motion of this point is important because it forms on leg of our loop-closure equation between the n^{th} precision point and precision point 1. Recall from Chapter 3, and in particular from Fig. 3-6, that we require six known variables to solve for one infinity of linkages which satisfy four precision points exactly. We need the three vectors that locate the point of interest at the second, third and fourth precision points with respect to the first precision point

$$\vec{\delta}_n = \vec{D}_n - \vec{D}_1 = l_2 e^{(-\theta_{in})} (e^{\beta_n} - e^{\beta_1}), n = 2 \dots 4. \quad (4.14)$$

We also need the change in orientation between the same precision points

$$\alpha_n = \Phi_n - \Phi_1, n = 2 \dots 4. \quad (4.15)$$

The synthesis using Burmester theory is exactly the same for this case as it was for the weighted-ground-link case. Equations (3.26) through (3.32) are invoked to solve for two values for \bar{Z} and \bar{M} for each value of ψ_2 .

Because in this case the mechanism was not inverted, the solution vectors do not need to be mapped back from an inverted reference frame. Let \bar{P}_1 through \bar{P}_4 be the vectors which locate the four pivot points (starting with the grounded input pivot, and progressing clock-wise around the linkage) for each solution at the first precision point. Table 4.2 gives the relationship between the solution vectors and the pivot points. A plot of these four points gives a graphical display of the solution. In particular, points \bar{P}_3 and \bar{P}_4 , which are functions of ψ_2 , are the Burmester point pair.

Table 4.2, Solution Pivot Locations in the Real-Imaginary Plane

Pivot	\bar{P}_1	\bar{P}_2	\bar{P}_3	\bar{P}_4
Location	origin (0+0i)	$l_2 e^{i(\beta_1 - \theta_{in})}$	$\bar{P}_2 - \bar{Z}$	$\bar{P}_3 - \bar{M}$

4.4 Solution Interpretation and Analysis

Most of the restrictions associated with the weighted-grounded-link case also apply to this synthesis. The synthesis is derived for a co-rotating linkage. Counter-rotating linkages can be designed by introducing a negative sign in the virtual work relationship which is then negated by the fact that the precision points occur in a decreasing order. Two solutions for the guiding dyad can be found for each precision point because the governing synthesis equation is of degree two. For some values of ψ_2

there is no acceptable physical solution to the synthesis because the solution to the quasi-loop-closure equation is complex. Real valued solutions can have Grashoff, order and branch defects which make them unacceptable.

As before, solutions which match all precision points are not guaranteed to be useful. Between the precision points the linkage is likely to deviate from the desired function. This deviation is intensified because the fundamental design criteria, force generation, is a function of the derivative of the position curve used in the synthesis. Even linkages that pass this strict requirement can be made unacceptable by their internal forces and bearing loads.

One design consideration of note has changed. The physical interpretation of the solution control variable, ψ_2 , is no longer related to the coupler rotation. Because in this case no inversion was necessary to establish a body-guidance problem, ψ_2 is still associated with rotation about a grounded pivot, as shown in Fig. 3-6. In this synthesis, ψ_2 is the change in θ_4 between the first and second precision point.

4.4.1 Analysis of Resistance Curve

Once a solution has been found on the Burmester curves that has good geometric properties, and no defects, the theoretical resistance curve of the solution linkage must be calculated. We used virtual work in section 2.2.2 to develop an expression for the resistance curve for this case

$$R(\beta) = \frac{l_2}{l_{in}} \cos(\beta - \theta_{in}) + \frac{\omega_3}{\omega_2} \cdot \frac{l_w}{l_{in}} \cos(\theta_3 - \theta_w). \quad (4.16)$$

The force analysis requires prior position (θ_3) and the velocity (ω_3/ω_2) analysis to be performed on the linkage. Position and velocity ratios are found as a function of input position by loop-closure

$$l_2 e^{i(\beta - \theta_{in})} + l_3 e^{i\theta_3} = l_1 e^{i\chi} + l_4 e^{i(\Phi + \theta_w)}, \quad (4.17)$$

and

$$\begin{bmatrix} \omega_4 / \omega_2 \\ \omega_3 / \omega_2 \end{bmatrix} = \begin{bmatrix} l_4 \cos(\Phi + \theta_w) & -l_3 \cos(\theta_3) \\ l_4 \sin(\Phi + \theta_w) & -l_3 \sin(\theta_3) \end{bmatrix}^{-1} \cdot \begin{bmatrix} l_2 \cos(\beta - \theta_{in}) \\ l_2 \sin(\beta - \theta_{in}) \end{bmatrix}, \quad (4.18)$$

as has been shown previously. Calculation of the resistance curve of the design over the range of the input angle is performed by the computer. Evaluation as to whether the fit of the curve is acceptable is the responsibility of the designer. This differs from optimal synthesis in which the computer is both the calculator and the evaluator.

4.4.2 Analysis of Grounded-Link and Bearing Stress

The final critical check of our synthesized linkage is the magnitude of the forces developed within the mechanism. This is the final check of the solution linkage. For a more detailed analysis, the accuracy of our assumptions would need to be verified based on procedures laid out in Chapter 5. The designer could also evaluate the impact of assembly tolerancing on the design's performance. This analysis is also laid out in the same chapter. However, we consider these analyses to be post-processing issues, whereas the analysis of forces is an integral and required part of a good synthesis package. Complete stress analysis relies on the designers knowledge of the shapes and cross-sectional area of the links, and on the likely applied loads. Our analysis provides the

designer with the key element to the stress analysis, an evaluation of nondimensionalized forces which give rise to the stresses. Unlike the weighted-grounded-link case, it is the grounded output link which is a two force member, not the coupler. Because of this, the bearing force at the output and the internal force in link 4 are the same. They are found based on static sum of the moments on the coupler link about the input-side coupler pivot

$$F_4 l_3 \sin(\theta_3 + \theta_4) + l_w \cos(\Phi) = 0, \quad (4.19a)$$

or

$$F_4 = \frac{l_w}{l_3} \cdot \frac{\cos(\theta_3 - \theta_w)}{\sin(\theta_3 + \theta_4)}, \quad (4.19b)$$

and

$$B_{out} = \left| \frac{l_w}{l_3} \cdot \frac{\cos(\theta_3 - \theta_w)}{\sin(\theta_3 + \theta_4)} \right|. \quad (4.19c)$$

Following standard notation, a positive sign for F_4 indicates tension. As before, the size of the linkage (l_w/l_3) effects the stresses. But this time, the designer has no ability to adjust the linkage scale directly.

The nondimensionalized bearing forces at the input is found by summing forces on link three to determine the force at the input-side coupler pivot, and then summing forces on link two to find the force of interest

$$\vec{F}_2 - i - F_4 e^{i\theta_4} = 0, \quad (4.20a)$$

$$i \operatorname{Re}^{i\beta} + \vec{B}_{in} - \vec{F}_2 = 0, \quad (4.20b)$$

$$\vec{B}_{in} = i + F_4 e^{i\theta_4} - i \operatorname{Re}^{i\beta} \quad (4.20c)$$

$$B_{in} = \sqrt{(F_4 \cos(\theta_4) + \operatorname{Re} \sin(\beta))^2 + (1 - \operatorname{Re} \cos(\beta) + F_4 \sin(\theta_4))^2} \quad (4.20d)$$

This concludes the techniques of closed-form synthesis developed to design planar four-link mechanisms for force generation. In the next section, we will present an example of the techniques developed in this chapter applied to the synthesis of a weighted-coupler-link force-generating linkage. The chapters following this will present some important post-processing analyses, some alternative linkages and synthesis methods, a summary of the work completed to date, and some suggestions for further research.

4.5 Example Problem

An example mechanism is synthesized to meet the input force requirements specified below. The solution as it would appear in a Mathcad program, is also included in Appendix B.

- The input link given for the design has a length of 0.889 m (35 in). The discrete strength data points are given in Table 4.3.
- A least-square polynomial curve fit of order three is used to determine a functional relationship between R and β .

$$R = 3.265\beta^3 - 12.826\beta^2 + 16.58\beta - 6.072$$

- We choose the length $l_w = 0.889$ m (35 in), $l_2 = 0.254$ m (10 in), the weight start angle to be $\Phi_o = -15^\circ$, and the input offset angle $\theta_{in} = 55^\circ$. Table 4.4 summarizes the

chosen precision points and the corresponding values for A_R and Φ which allow us to complete body-guidance synthesis.

- The known values in the matrix formulation of the Burmester problem are given in Table 4.5.
- The coefficients of the quasi-loop-closure equation are given in Table 4.6.
- One portion of the infinite solution set is shown in Fig. 4-4. The Burmester curves are for the negative closure of the quadratic equation over the range of $\psi_2 = -1.25^\circ$ through -15° .
- The solution we have chosen is $\psi_2 = -2.5^\circ$. The design parameters for the solution are given in Table 4.7. The solution linkage is shown in Fig. 4-5.
- Analysis shows that the linkage has good resistance curve. The internal coupler force and fixed pivot bearing loads are also acceptable. These are shown in Figs. 4-6, 4-7 and 4-8.

Table 4.3, Strength Data

Input Angle, β (deg)	Strength Data, S (%)
50	80
52	85
54	90
56	93
58	95
60	98
62	99
64	99.5
66	100

Table 4.4, Precision Points

Precision Pt.	β (deg.)	A_R (deg. %)	Φ (deg.)
1	50.5	40.34	-14.73
2	52	165.4	-13.88
3	58	711.8	-10.05
4	65	1400	-5.11

Table 4.5, Body Motion

Precision Pt.	δ (in)	α (deg.)
2	0.017+0.261i	0.849
3	0.017+1.308i	4.684
4	-0.121+2.521i	9.625

Table 4.6, Quasi-Loop-Closure Coefficients ($\times 10^{-3}$)

$\Delta_1 = 13-3i$
$\Delta_2 = -7+i$
$\Delta_3 = 2-0.42i$
$\Delta_4 = -9+2i$

Table 4.7, Solution Design Parameters

$l_1 = 0.0734$ m (2.89 in)
$l_2 = 0.254$ m (10.0 in)
$l_3 = 0.328$ m (12.9 in)
$l_4 = 0.0457$ m (1.80 in)
$l_{in} = 0.889$ m (35 in)
$l_w = 0.889$ m (35 in)
$\theta_{in} = 55^\circ$
$\theta_w = -160.6^\circ$
$\chi = -116.6^\circ$

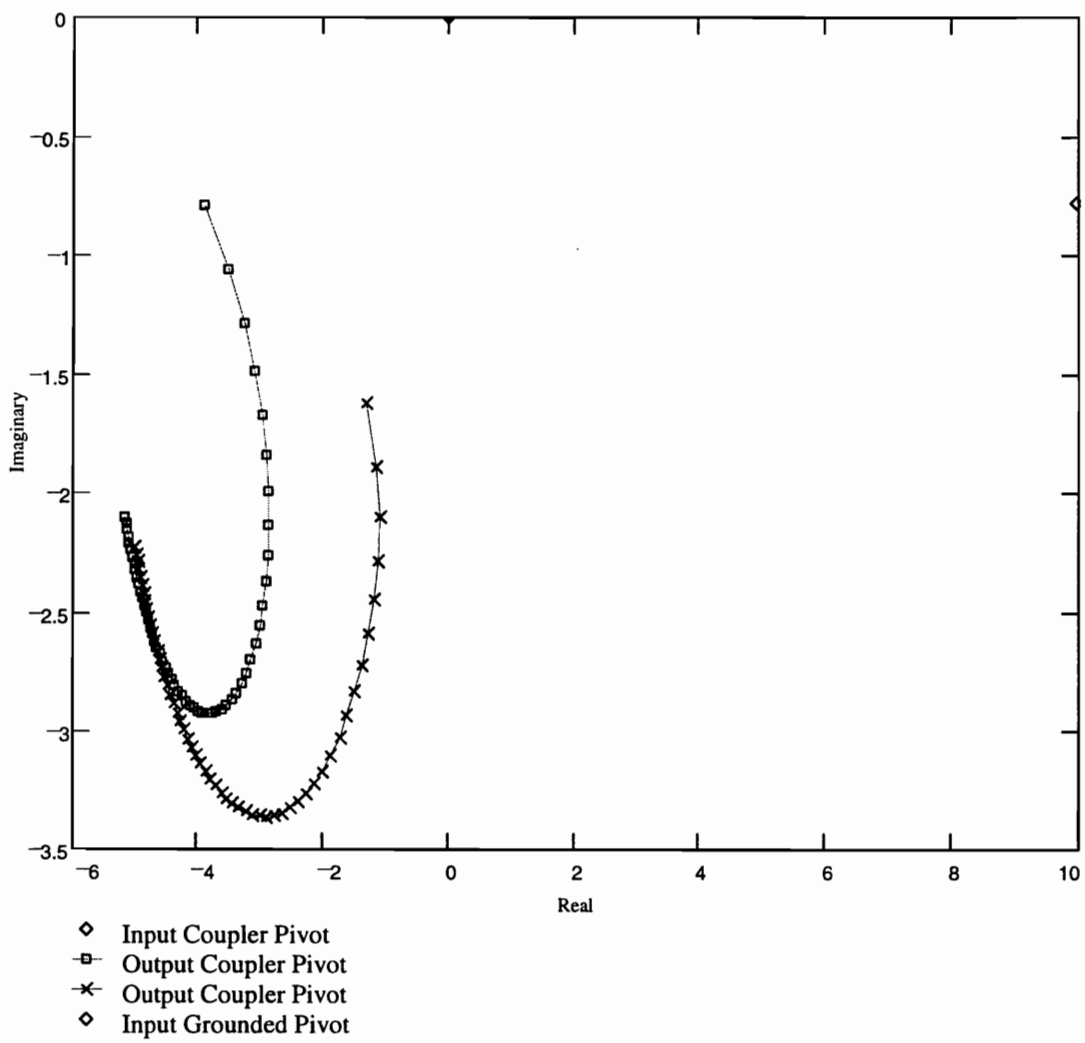


Figure 4-4, Burmester Curves

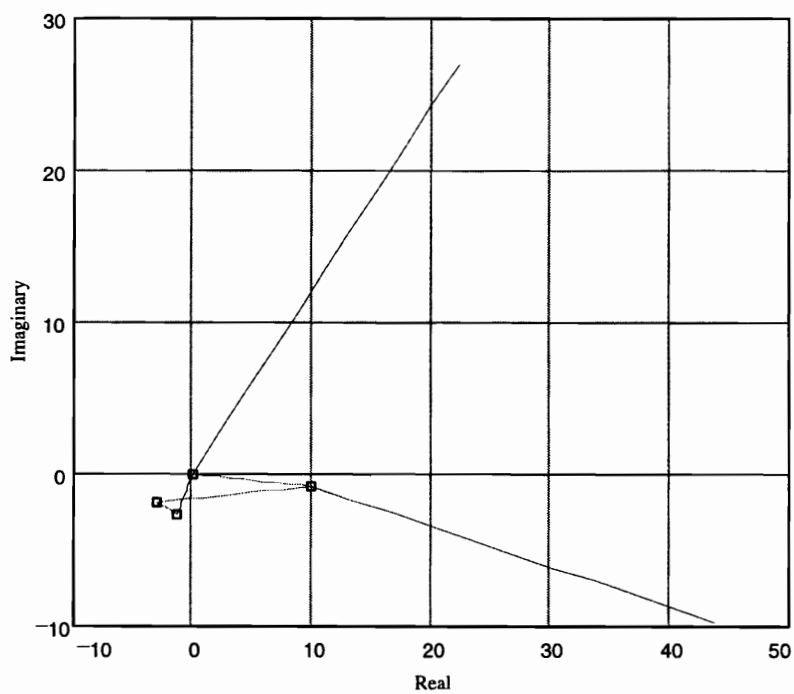


Figure 4-5, Solution Linkage

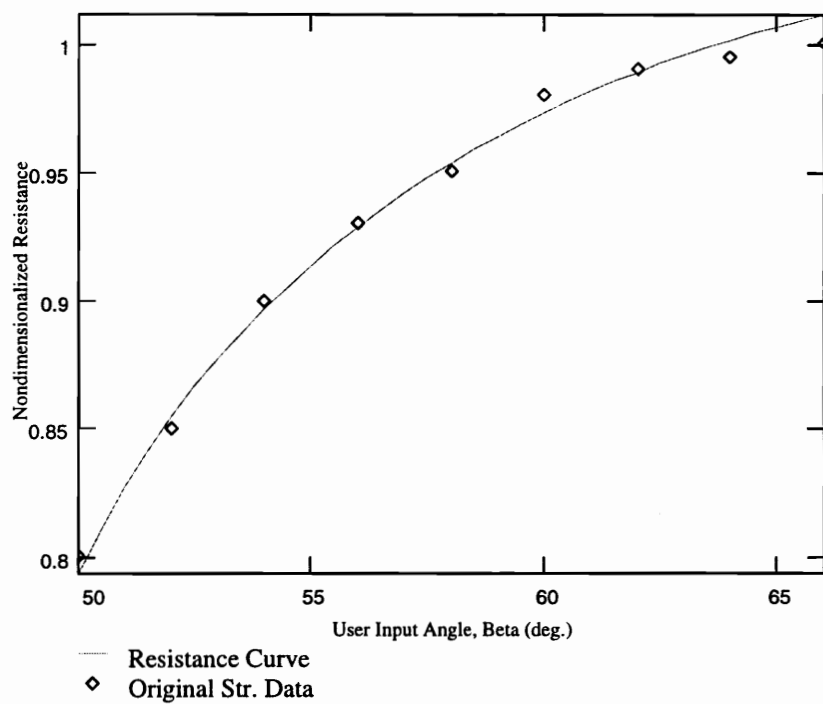


Figure 4-6, Resistance Curve of the Soln

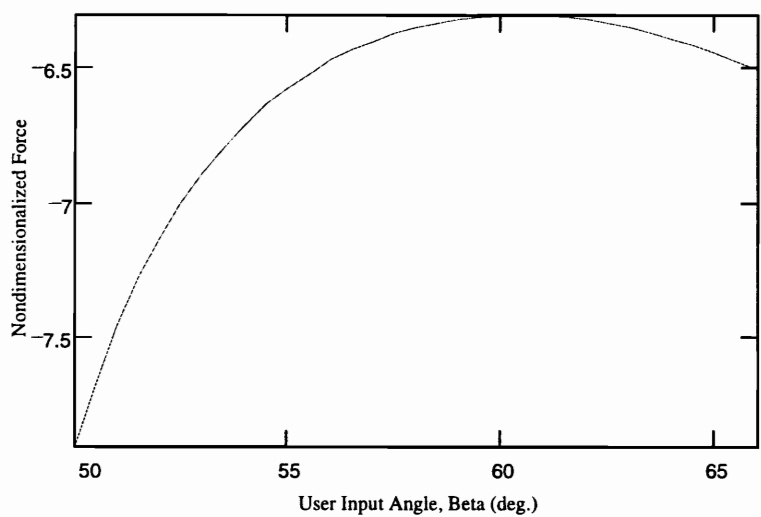


Figure 4-7, Internal Coupler Force

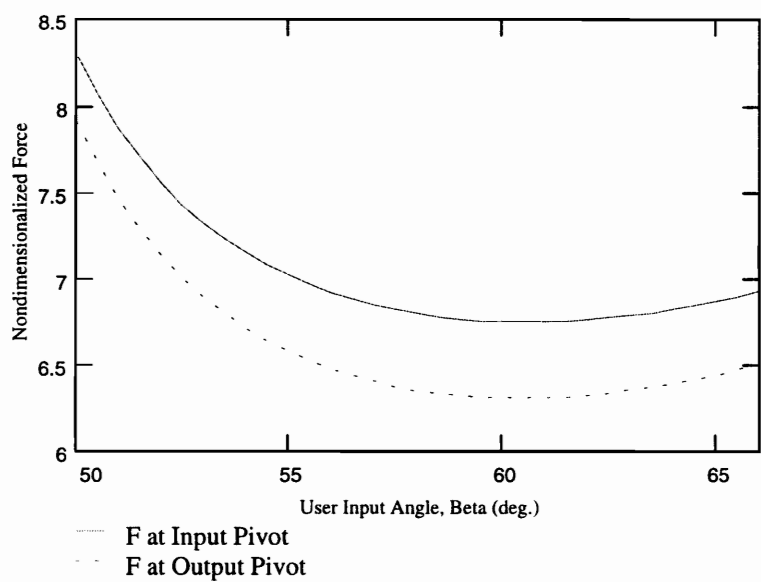


Figure 4-8, Bearing Forces

Chapter 5, Post Processing: Sensitivity and Force Analysis

5.1 Applications of Sensitivity Analysis

In the previous chapters we have considered the motivation for synthesizing force generating linkages, and have developed closed-form synthesis methods. Our synthesis methods were based on the assumption that the links are approximately massless, and that the dynamic forces are small compared to the static forces. In this chapter, we develop analysis techniques that will allow us to determine the sensitivity of our solution to design parameter variation, verify the validity of our assumptions, and possibly even improve upon our design.

Following synthesis, an analysis can be performed to evaluate the sensitivity of the design to parameter variation. This analysis will enable us to evaluate the sensitivity of the design to manufacturing tolerances, and give us the ability to “tweak” our design. We will see in Chapter 6 that this sensitivity analysis can also be useful as part of an optimal synthesis approach.

The sensitivity of the linkage to design parameter variations will be expressed in the form of influence coefficients. An influence coefficient is the partial derivatives of the output with respect to a design parameter. In our case, the output of interest is the resistance curve of the linkage. Therefore, the influence coefficient, κ is given by

$$\kappa_q = \frac{\partial R}{\partial q}, \quad (5.1)$$

where q is one of the eight design parameters, l_2 , l_3 , l_4 , l_1 , θ_{in} , θ_w , l_w or χ . The change in the resistance curve due to a small parameter change is

$$\Delta R \approx \kappa_q \Delta q. \quad (5.2)$$

Influence coefficients can also be applied to concurrent changes in multiple parameters

$$\Delta R \approx \sum_i \kappa_{q_i} \Delta q_i + \sum_j \sum_i \kappa_{q_i q_j} \Delta q_i \Delta q_j, \quad (5.3a)$$

or, ignoring higher order paired terms

$$\Delta R \approx \sum_i \kappa_{q_i} \Delta q_i. \quad (5.3b)$$

For the problem at hand, influence coefficients can be calculated using closed-form equations. The shape of the influence coefficient function, evaluated over the range of the input angle, β , can be a useful design tool. It gives the designer valuable information about how changes in the design variables impact the resistance curve.

In order to properly evaluate the influence coefficients, we must first decide how the partial derivatives are to be taken. For our application, the length of the input link and the range of the user input motion are given. Therefore it is essential that changes in the parameters not effect the user input angle, β .

$$\frac{\partial \beta}{\partial q} = 0 \quad (5.4)$$

Also, the input arm length, l_{in} will not be allowed to vary. Imagine that the user input arm is fixed in space, and then image how a change in one design parameter, holding all others constant, will effect the shape of the linkage. Note that only changes in one parameter, θ_{in} , will effect θ_2 , because β is not allowed to vary. We can also see this from the definition of θ_2

$$\frac{\partial \theta_2}{\partial \theta_{in}} = \frac{\partial}{\partial \theta_{in}} (\beta - \theta_{in}) = -1. \quad (5.5)$$

It should also be apparent that changes in l_w and θ_w will effect none of the four-bar linkage angles, although they will certainly effect the resistance curve.

$$\frac{\partial \theta_3}{\partial \theta_w} = \frac{\partial \theta_4}{\partial \theta_w} = \frac{\partial \theta_3}{\partial l_w} = \frac{\partial \theta_4}{\partial l_w} = 0 \quad (5.6)$$

It seems likely that changes in the other five parameters will effect θ_3 and θ_4 as well as effecting the resistance curve directly.

The partial derivative of the resistance curve should be a function of the partial derivatives of the link lengths, angular velocity ratios and angles. The angular velocity ratios are in turn functions of the link lengths and the linkage angles. Finally, the linkage angles are functions of the link lengths and the input angle as given by loop-closure. The particulars of these computations are provided in full detail in Appendix C. Appendices D and E show closed-form Mathcad computations of the influence coefficients for the weighted-grounded-link case and the weighted-coupler-link case, respectively.

Influence coefficients have long been used in statistical analysis of the error generated in mechanisms. Dhande, in particular, has been a proponent of this approach (Dhande and Chakraborty, 1973, Dhande, 1974, Dhande and Chakraborty, 1975, Dhande and Chakraborty, 1978, and Mallik and Dhande, 1987). The tolerance or uncertainty of a manufactured variable generally has a statistical meaning (typically three standard deviations on the normal curve). Based on this, we can apply an uncertainty analysis to our linkage, using influence coefficients. The basic law of propagation of uncertainty is given by the following equation (Beckwith and Marangoni, 1990)

$$U_R = \sqrt{\sum_i (U_i \kappa_i)^2}, \quad (5.7)$$

where U is the (statistical) uncertainty in the parameter. The number of standard deviations implicit in the uncertainty must be the same for all variables. Using this type of analysis, we can place statistical bounds on the error in the resistance curve due, for example, to manufacturing tolerances.

Sensitivity analysis can also be used as a tool in design. Recall that our closed-form synthesis method is only able to satisfy constraints in the integrated resistance curve at four precision points. It is conceivable that, for a given problem, none of the synthesized linkages (those that satisfy exactly four precision points) will produce an acceptable resistance curve. There may be a linkage nearby, one that does not satisfy four precision points, that does have an acceptable resistance curve. We can use our sensitivity analysis to find linkages which are near a solution linkage that have improved

properties. In particular, the influence coefficients that we have calculated clearly demonstrate which parameters have the greatest local impact. If there is a problem in one small section of the range of motion, then the parameter whose influence coefficient is maximum in that range can be “tweaked” slightly to improve the design.

The process we have just discussed is really a manual form of optimization. The designer assesses the error in the design, chooses a variable to change, and then changes the variable and evaluates the results. This gives an indication of how the influence coefficients might be valuable in an optimization routine.

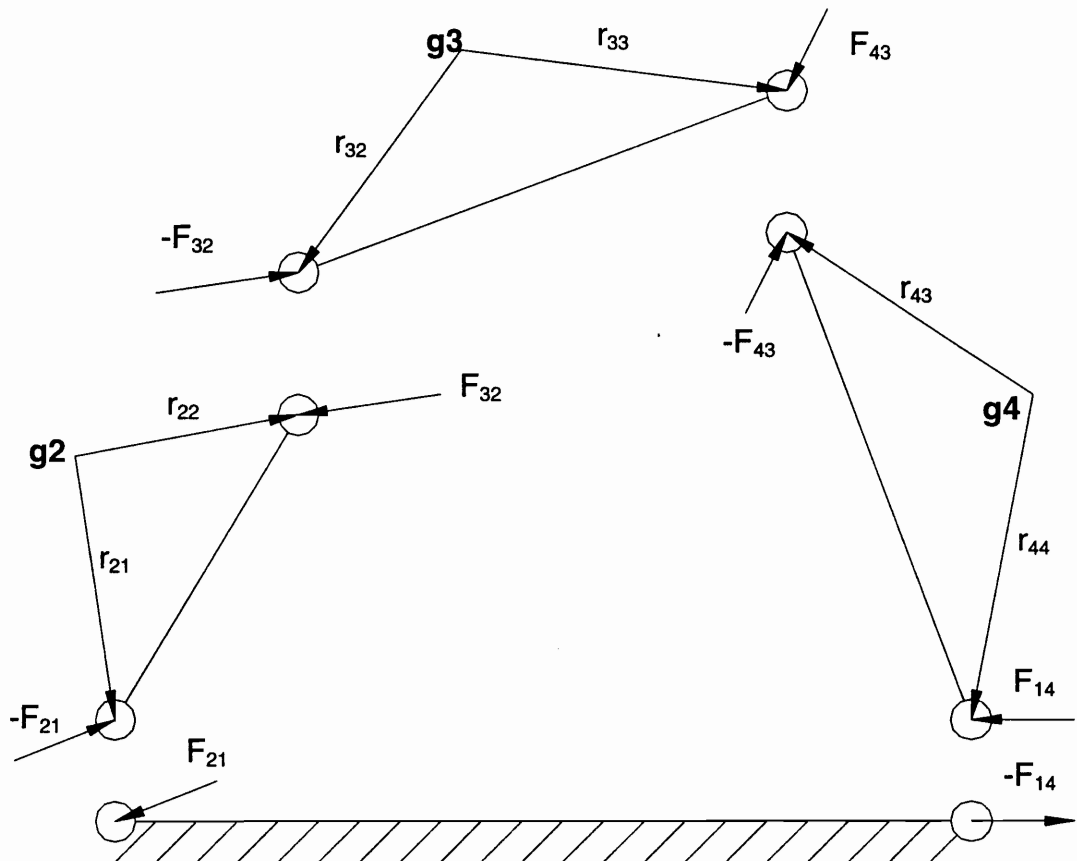


Figure 5-1, Free Body Diagram, Mabie and Reinholtz (1987), p. 414

5.2 Extended Force Analysis

Critical to our synthesis were two assumptions: the assumption of massless links, and the assumption of negligible dynamic forces. Using the techniques developed below, the validity of the assumptions for a given linkage can be examined. In this section we develop post-synthesis methods for examining the effects of link masses and of dynamic forces.

5.2.1 Static Effect of Massed Links

To determine the static effect of link masses, we will ignore for a moment the effect of the load mass, and then add its effect in afterwards using the principle of superposition. Consider the static free-body diagram of the linkage shown in Fig. 5-1. The static force analysis of this linkage is performed using the matrix method from Mabie and Reinholtz (1987, pp. 413-418). The matrix relationship between the vector of input torque and pivot bearing forces and the vector of applied static forces is given by

$$\begin{bmatrix}
-1 & 0 & 1 & 0 & 0 & 0 & 0 & 0 & 0 \\
0 & -1 & 0 & 1 & 0 & 0 & 0 & 0 & 0 \\
r_{21y} & -r_{21x} & -r_{22y} & r_{22x} & 0 & 0 & 0 & 0 & 1 \\
0 & 0 & -1 & 0 & 1 & 0 & 0 & 0 & 0 \\
0 & 0 & 0 & -1 & 0 & 1 & 0 & 0 & 0 \\
0 & 0 & r_{32y} & -r_{32x} & -r_{33y} & r_{33x} & 0 & 0 & 0 \\
0 & 0 & 0 & 0 & -1 & 0 & 1 & 0 & 0 \\
0 & 0 & 0 & 0 & 0 & -1 & 0 & 1 & 0 \\
0 & 0 & 0 & 0 & r_{43y} & -r_{43x} & -r_{44y} & r_{44x} & 0
\end{bmatrix}
\begin{bmatrix}
F_{21x} \\
F_{21y} \\
F_{32x} \\
F_{32y} \\
F_{43x} \\
F_{43y} \\
F_{14x} \\
F_{14y} \\
T^M_{in}
\end{bmatrix}
=
\begin{bmatrix}
0 \\
-m_2 g \\
0 \\
0 \\
-m_3 g \\
0 \\
0 \\
-m_4 g \\
0
\end{bmatrix}, \quad (5.8)$$

where: \vec{r}_{nm} locates the m^{th} pivot (grounded input pivot is number one; counting clockwise around the linkage) from the n^{th} link's center of mass; F_{ij} is the joint force between link i and link j , acting on link j ; m_k is the mass of link k ; T^M_{in} is the input torque required to hold the linkage at a static position in the presence of massed links. We are interested only in the effect of the link masses on the applied force

$$F^M_{in} = \frac{T^M_{in}}{l_{in}}. \quad (5.9)$$

This can be calculated directly for each position in the linkage

$$F^M_{in} = \begin{bmatrix} 0 \\ 0 \\ 0 \\ 0 \\ 0 \\ 0 \\ 0 \\ 0 \\ \frac{1}{l_{in}} \end{bmatrix}^T \left(\begin{bmatrix} -1 & 0 & 1 & 0 & 0 & 0 & 0 & 0 & 0 \\ 0 & -1 & 0 & 1 & 0 & 0 & 0 & 0 & 0 \\ r_{21y} & -r_{21x} & -r_{22y} & r_{22x} & 0 & 0 & 0 & 0 & 1 \\ 0 & 0 & -1 & 0 & 1 & 0 & 0 & 0 & 0 \\ 0 & 0 & 0 & -1 & 0 & 1 & 0 & 0 & 0 \\ 0 & 0 & r_{32y} & -r_{32x} & -r_{33y} & r_{33x} & 0 & 0 & 0 \\ 0 & 0 & 0 & 0 & -1 & 0 & 1 & 0 & 0 \\ 0 & 0 & 0 & 0 & 0 & -1 & 0 & 1 & 0 \\ 0 & 0 & 0 & 0 & r_{43y} & -r_{43x} & -r_{44y} & r_{44x} & 0 \end{bmatrix}^{-1} \begin{bmatrix} 0 \\ -m_2 g \\ 0 \\ 0 \\ -m_3 g \\ 0 \\ 0 \\ -m_4 g \\ 0 \end{bmatrix} \right) \quad (5.10)$$

We have a closed-form expression for the applied force required to balance the static effect of the link masses at each position in the linkage motion. Plots of these forces as a function of input link motion may be sufficient to reach our goal, evaluation of the massless link assumption. The designer may instead wish to see the effect directly on the (dimensionalized) resistance curve of the machine. Clearly, the relative effect of the link masses will be maximized when the load weight is minimum. We suggest calculating the effect on the resistance curve at both the maximum and minimum load weights for the machine

$$R^M_{\Delta \min} = R + \frac{F^M_{in}}{W_{\max}} \quad (5.11a)$$

$$R^M_{\Delta \max} = R + \frac{F^M_{in}}{W_{\min}} \quad (5.11b)$$

A sample of these calculations for the weighted-grounded-link design is presented in Appendix F. The linkage analyzed is the example from chapter 3.

If the mass of the links has a significant effect on the design's resistance curve, we can design an equilibration system which counters the effect of the link masses. This can be accomplished by either selectively adding mass to the linkage, or by designing a sub-unit mechanism (see Chapter 1).

A situation of particular importance occurs when the required force at the handle, to balance the static effect of the link masses, is negative. This means that if the load weight is removed, and no force is applied to the handle, the mass of the links will cause the linkage to rotate, bring the weight arm up. This may be a dangerous situation in our application. In such a case the linkage will certainly have to be equilibrated.

5.2.2 Dynamic Effects and Trajectory Selection

For our application the design linkage is clearly not static while in operation, and our assumption of static operation may put our final design in jeopardy. In the application to strength exercise equipment we had no recourse because the input trajectory (time dependent motion of the input) is unknown for our application. For other applications in which the input trajectory is well defined, we could have synthesized using optimization techniques taking into account the dynamics of the linkage. If the design is synthesized using the techniques presented in Chapters 3 and 4, then it is advisable to investigate possible dynamic effects on the design performance.

In our application the input trajectory is unknown. In order to investigate the dynamic performance of a design linkage, we must assume a time dependent function for the input motion. There are a number of possible trajectories we could assume. For example, assume that for the proper motion in a given exercise, the stroke should take t_c seconds to complete. Further, let us assume that it is useful for the motion to be broken into f parts over the time interval. Perhaps during the first fraction $(1/f)$ of the motion the input handle undergoes a constant angular acceleration, α , starting from rest, and during the last fraction it undergoes an equal and opposite angular acceleration bringing the handle to rest at precisely the final position in the motion. Based on these assumptions, the angular velocity of the input link must be

$$\omega_2 = \int_0^t \alpha_2 dt = \begin{cases} \int_0^t \alpha dt, & 0 \leq t \leq t_c/f \\ \int_0^{t_c/f} \alpha dt, & t_c/f \leq t \leq t_c \left(1 - \frac{1}{f}\right), \\ \int_0^{t_c/f} \alpha dt + \int_{t_c(1-1/f)}^t -\alpha dt, & t_c \left(1 - \frac{1}{f}\right) \leq t \leq t_c \end{cases} \quad (5.12a)$$

or

$$\omega_2 = \begin{cases} \alpha \cdot t, & 0 \leq t \leq t_c/f \\ \frac{\alpha \cdot t_c}{f}, & t_c/f \leq t \leq t_c \left(1 - \frac{1}{f}\right), \\ \alpha \cdot (t_c - t), & t_c \left(1 - \frac{1}{f}\right) \leq t \leq t_c \end{cases} \quad (5.12b)$$

The angle of the handle is

$$\beta - \beta_o = \int_0^t \omega_2 dt = \begin{cases} \int_0^t \alpha \cdot t dt, & 0 \leq t \leq \frac{t_c}{f} \\ \int_0^{\frac{t_c}{f}} \alpha \cdot t dt + \int_{\frac{t_c}{f}}^t \frac{\alpha \cdot t_c}{f} dt, & \frac{t_c}{f} \leq t \leq t_c \left(1 - \frac{1}{f}\right) \\ \int_0^{\frac{t_c}{f}} \alpha \cdot t dt + \int_{\frac{t_c}{f}}^{t_c \left(1 - \frac{1}{f}\right)} \frac{\alpha \cdot t_c}{f} dt + \int_{t_c \left(1 - \frac{1}{f}\right)}^t \alpha \cdot (t_c - t) dt, & t_c \left(1 - \frac{1}{f}\right) \leq t \leq t_c \end{cases} \quad (5.13a)$$

$$\text{or } \beta = \begin{cases} \frac{\alpha \cdot t^2}{2} + \beta_o, & 0 \leq t \leq \frac{t_c}{f} \\ \frac{1}{2} \alpha_c \left(\frac{-t_c + 2ft}{f^2} \right) + \beta_o, & \frac{t_c}{f} \leq t \leq t_c \left(1 - \frac{1}{f}\right) \\ \frac{-\alpha}{2} t^2 + \alpha t_c \cdot t - \left(\alpha t_c^2 \frac{1 - f + \frac{f^2}{2}}{f^2} \right) + \beta_o, & t_c \left(1 - \frac{1}{f}\right) \leq t \leq t_c \end{cases} \quad (5.13b)$$

But at $t = t_c$, β must equal β_f . Therefore

$$\alpha t_c^2 \frac{f - 1}{f^2} + \beta_o = \beta_f. \quad (5.14)$$

This gives the following expression for the constant angular acceleration in terms of the range of the link motion, the total time, and the fraction of time during the acceleration and deceleration

$$\alpha = \frac{(\beta_f - \beta_o) f^2}{(f - 1) t_c^2}. \quad (5.15)$$

We will use this type of trajectory as an example in calculating dynamic effects. A more complete analysis for this application would require laboratory investigation of typical trajectories for the intended exercise.

After position analysis has been applied to our design linkage at each position in the input, we can evaluate the angular velocities of the coupler and output links using the linear velocity analysis derived previously

$$\begin{bmatrix} \omega_4 \\ \omega_3 \end{bmatrix} = \begin{bmatrix} l_4 \cos(\theta_4) & -l_3 \cos(\theta_3) \\ l_4 \sin(\theta_4) & -l_3 \sin(\theta_3) \end{bmatrix}^{-1} \cdot \begin{bmatrix} l_2 \cos(\theta_2) \\ l_2 \sin(\theta_2) \end{bmatrix} \cdot \omega_2. \quad (5.16)$$

In a similar fashion, beginning with Eq. (1.15) in chapter 1, we can derive relationships for the angular accelerations of these links

$$\begin{bmatrix} -\omega_2^2 l_2 \cos(\theta_2) - \alpha_2 l_2 \sin(\theta_2) - \omega_3^2 l_3 \cos(\theta_3) - \alpha_3 l_3 \sin(\theta_3) \\ -\omega_2^2 l_2 \sin(\theta_2) + \alpha_2 l_2 \cos(\theta_2) - \omega_3^2 l_3 \sin(\theta_3) + \alpha_3 l_3 \cos(\theta_3) \end{bmatrix} = \begin{bmatrix} -\omega_4^2 l_4 \cos(\theta_4) - \alpha_4 l_4 \sin(\theta_4) \\ -\omega_4^2 l_4 \sin(\theta_4) + \alpha_4 l_4 \cos(\theta_4) \end{bmatrix} \quad (5.17a)$$

$$\begin{bmatrix} -l_4 \sin(\theta_4) & l_3 \sin(\theta_3) \\ l_4 \cos(\theta_4) & -l_3 \cos(\theta_3) \end{bmatrix} \cdot \begin{bmatrix} \alpha_4 \\ \alpha_3 \end{bmatrix} = \begin{bmatrix} l_4 \cos(\theta_4) & -l_3 \cos(\theta_3) \\ l_4 \sin(\theta_4) & -l_3 \sin(\theta_3) \end{bmatrix} \cdot \begin{bmatrix} \omega_4^2 \\ \omega_3^2 \end{bmatrix} + \begin{bmatrix} -l_2 \cos(\theta_2) \\ -l_2 \sin(\theta_2) \end{bmatrix} \omega_2^2 + \begin{bmatrix} -l_2 \sin(\theta_2) \\ l_2 \cos(\theta_2) \end{bmatrix} \alpha_2 \quad (5.17b)$$

$$\begin{bmatrix} \alpha_4 \\ \alpha_3 \end{bmatrix} = \begin{bmatrix} -l_4 \sin(\theta_4) & l_3 \sin(\theta_3) \\ l_4 \cos(\theta_4) & -l_3 \cos(\theta_3) \end{bmatrix}^{-1} \cdot \left(\begin{bmatrix} l_4 \cos(\theta_4) & -l_3 \cos(\theta_3) \\ l_4 \sin(\theta_4) & -l_3 \sin(\theta_3) \end{bmatrix} \cdot \begin{bmatrix} \omega_4^2 \\ \omega_3^2 \end{bmatrix} + \begin{bmatrix} -l_2 \cos(\theta_2) \\ -l_2 \sin(\theta_2) \end{bmatrix} \omega_2^2 + \begin{bmatrix} -l_2 \sin(\theta_2) \\ l_2 \cos(\theta_2) \end{bmatrix} \alpha_2 \right) \quad (5.17c)$$

We now have the complete velocity and acceleration for the linkage as a function of time.

We will derive the dynamic effects for the weighted-grounded-link case as an example, with the trajectory, velocity and acceleration analyses derived above. Because the load weight will effect the location of the center of mass of the output link, we must either rederive the matrix equations for the modified center of mass, or make use of the matrices derived in the previous section and account for the effect of the load weight

using superposition. Following the second alternative, we begin by only examining the dynamic resistance curve for the link masses. We use the matrix formulation derived above the only difference being an augmentation of the applied force vector to account for the dynamic “inertial forces”

$$\text{Left Hand Side of Eq. (5.8)} = \begin{bmatrix} -m_2 a_{g2x} \\ -m_2 g - m_2 a_{g2y} \\ -I_2 \alpha_2 \\ -m_3 a_{g3x} \\ -m_3 g - m_3 a_{g3y} \\ -I_3 \alpha_3 \\ -m_4 a_{g4x} \\ -m_4 g - m_4 a_{g4y} \\ -I_4 \alpha_4 \end{bmatrix} \quad (5.18)$$

This expression can be evaluated for the input torque. Then the resistance curve for the link masses is

$$R^{DM} = \frac{T^{DM}_{in}}{l_{in} W}. \quad (5.19)$$

The superscript D indicates that the quantity under consideration involves dynamic effects; the superscript M indicates that only the link masses are being considered.

For the weighted-grounded-link case, the acceleration of the load weight is given by the second time derivative of its position vector (superscript w indicates the vector involves the load weight)

$$\vec{a}^w = \frac{d}{dt} \left(\frac{d}{dt} l_w e^{i(\theta_4 - \theta_w)} \right) = l_w (-\omega_4^2 + i\alpha_4) e^{i(\theta_4 - \theta_w)}. \quad (5.20)$$

The equivalent “inertial force” is given by $-(W/g) \vec{a}^w$. Applying virtual work to the mechanism we have

$$-\left(\frac{W}{g}\right) \vec{a}^w \cdot \vec{v}^w + \vec{W} \cdot \vec{v}^w + \vec{T}^{DW}_{in} \cdot \vec{\omega}_2 = 0, \quad (5.21a)$$

$$\left(\frac{W}{g}\right) \left(l_w (\omega_4^2 - i\alpha_4) e^{i(\Phi)} \right) \cdot (l_w i \omega_4 e^{i\Phi}) - W l_w \omega_4 \cos(\Phi) + F^{DW} l_{in} \omega_2 = 0, \quad (5.21b)$$

$$\left(\frac{W l_w^2 \alpha_4 \omega_4}{g} \right) + W l_w \omega_4 \cos(\Phi) = F^{DW} l_{in} \omega_2, \quad (5.21c)$$

$$R^{DW} = \frac{F^D}{W} = \frac{l_w \omega_4}{l_{in} \omega_2} \left(\frac{l_w \alpha_4}{g} + \cos(\Phi) \right), \quad (5.21d)$$

where the superscript W indicates that the quantity is being considered includes only the effect of the load weight. Applying superposition to obtain the total dynamic resistance curve gives

$$R^D = \frac{l_w \omega_4}{l_{in} \omega_2} \left(\frac{l_w \alpha_4}{g} + \cos(\Phi) \right) + \frac{T^{DM}_{in}}{l_{in} W}. \quad (5.22)$$

We have now established the effect which the dynamics of the motion will have on the resistance curve of the machine for some assumed trajectory. Part of Appendix F is devoted to calculating the dynamic effects on the same linkage examined in the section above.

Chapter 6, Other Synthesis Cases

6.1 Enumeration of Cases

In this chapter we will examine some interesting types of force-generating linkages and an alternative method for synthesizing them. We will look at some very strange linkages with multiple types of resistance applied at multiple points. These linkages are not particularly useful in our specific application of strength exercise equipment. Yet, coupled with the added mathematical complexity, they have additional design parameters. This makes them candidates for some more sophisticated applications requiring a greater number of precision points to be met. We will also look at the Watt Six-Bar linkage, an important case. We will see that we already have the tools to synthesize linkages of this type. Finally we will turn our attention to synthesis by optimization. This extremely powerful method seems to be where the future of synthesis for force generation lies. This chapter offers an overview of the breadth of mechanisms and techniques available for force generation in linkage design.

6.1.1 Four-Link Mechanism with Multiple Weight Locations

In chapter 3 we examined force-generating four-bars whose resistance was provided by a load weight on the grounded link. In chapter 4 we examined force-generating four-bars whose resistance was provided by a load weight on the coupler link. What about four-bars with a load weight on both the coupler and grounded links? What

about four-bars with load weights on all three moving links? Such multiply weighted linkages is the topic of this section. Figure 6-1 shows a four-bar linkage with a load weight on each of the moving links. Adding load weights to multiple links complicates our synthesis. The justification for doing this is the addition of more possible precision points.

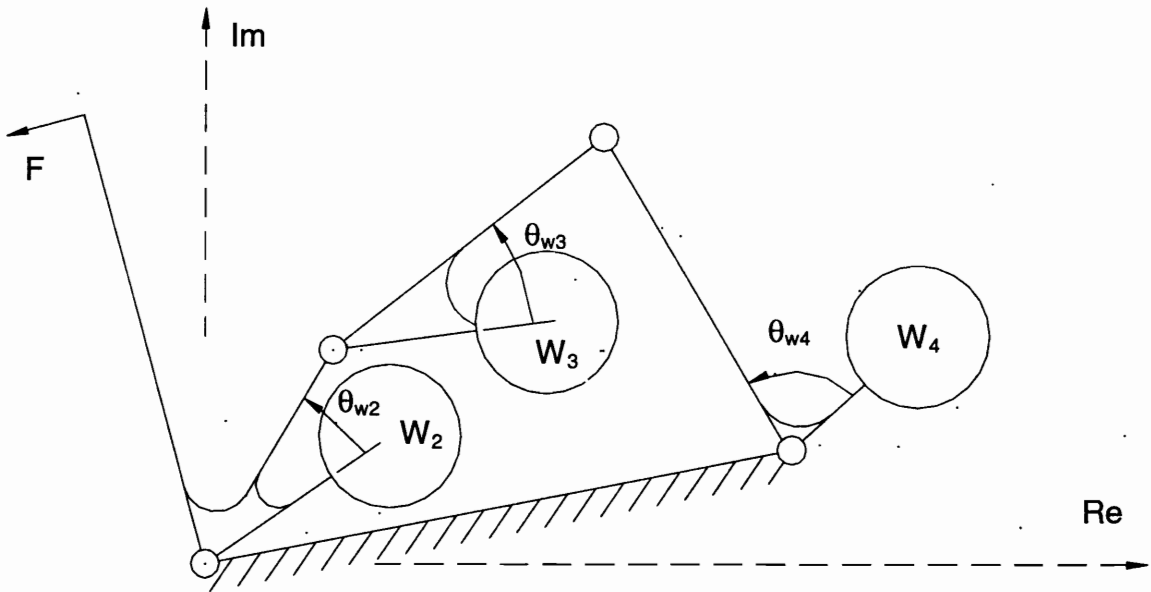


Figure 6-1, Triple-Weighted Four-Bar Linkage

To prove that the number of achievable precision points has increased, we will perform an analysis like those in section 2.2. Two of the three governing equations for this linkage will come from loop-closure, the other equation will come from virtual work. The loop-closure equations for position and velocity are

$$l_2 e^{i(\beta - \theta_{in})} + l_3 e^{i\theta_3} = l_1 e^{i\alpha} + l_4 e^{i\theta_4}, \quad (6.1)$$

and

$$i\omega_2 l_2 e^{i(\beta - \theta_{in})} + i\omega_3 l_3 e^{i\theta_3} = i\omega_4 l_4 e^{i\theta_4}. \quad (6.2)$$

Applying virtual work to the static mechanism

$$\vec{T}_{in} \cdot \delta \vec{\beta} + \vec{W}_2 \cdot \delta \vec{s}^{w2} + \vec{W}_3 \cdot \delta \vec{s}^{w3} + \vec{W}_4 \cdot \delta \vec{s}^{w4} = 0, \quad (6.3a)$$

$$Fl_{in}\omega_2 - W_2 l_{w2} \omega_2 \cos(\beta - \theta_{in} - \theta_{w2}) + \dots \\ - W_3 (l_2 \omega_2 \cos(\beta - \theta_{in}) + l_{w3} \omega_3 \cos(\theta_3 - \theta_{w3})) - W_4 l_{w4} \omega_4 \cos(\theta_4 - \theta_{w4}) = 0, \quad (6.3b)$$

OR

$$F = W_2 \frac{l_{w2}}{l_{in}} \cos(\beta - \theta_{in} - \theta_{w2}) + \dots \\ W_3 \left(\frac{l_2}{l_{in}} \cos(\beta - \theta_{in}) + \frac{l_{w3}}{l_{in}} \Gamma_3 \cos(\theta_3 - \theta_{w3}) \right) + W_4 \frac{l_{w4}}{l_{in}} \Gamma_4 \cos(\theta_4 - \theta_{w4}), \quad (6.3c)$$

where $\Gamma_n \equiv \omega_n / \omega_2$. If we define the nondimensional resistance curve to be $R \equiv F / W_4$,

and the nondimensional load weights to be $\tilde{W} \equiv W_n / W_4$, then we have

$$R = \tilde{W}_2 \frac{l_{w2}}{l_{in}} \cos(\beta - \theta_{in} - \theta_{w2}) + \dots \\ \tilde{W}_3 \left(\frac{l_2}{l_{in}} \cos(\beta - \theta_{in}) + \frac{l_{w3}}{l_{in}} \Gamma_3 \cos(\theta_3 - \theta_{w3}) \right) + \frac{l_{w4}}{l_{in}} \Gamma_4 \cos(\theta_4 - \theta_{w4}) \quad (6.4)$$

The force-generation of this linkage obeys 5 scalar equations at each precision point:

vector position equation $l_2 e^{i(\beta - \theta_{in})} + l_3 e^{i\theta_3} = l_1 e^{i\chi} + l_4 e^{i\theta_4}, \quad (6.5a)$

vector velocity equation $l_2 e^{i(\beta - \theta_{in})} + \Gamma_3 l_3 e^{i\theta_3} = \Gamma_4 l_4 e^{i\theta_4}, \quad (6.5b)$

scalar force equation $R = \tilde{W}_2 \frac{l_{w2}}{l_{in}} \cos(\beta - \theta_{in} - \theta_{w2}) + \dots \\ \tilde{W}_3 \left(\frac{l_2}{l_{in}} \cos(\beta - \theta_{in}) + \frac{l_{w3}}{l_{in}} \Gamma_3 \cos(\theta_3 - \theta_{w3}) \right) + \frac{l_{w4}}{l_{in}} \Gamma_4 \cos(\theta_4 - \theta_{w4}) \quad (6.5c)$

There are three knowns: β , R , and l_{in} . There unknown design parameters: θ_{in} , θ_{w2} , θ_{w3} ,

θ_{w4} , l_{w2} , l_{w3} , l_{w4} , l_1 , l_2 , l_3 , l_4 , χ , \tilde{W}_2 , and \tilde{W}_3 . There are four additional unknown variables

for every precision point: $\Gamma_3, \Gamma_4, \theta_3, \theta_4$. We start at the first precision point with 5 scalar equations and 18 unknowns. With each additional precision point we add 5 equations, but only 4 unknowns. Therefore, our mathematical analysis shows that the design is not constrained to a finite number of solutions until 14 precision points are reached. It should therefore be possible to synthesize triple-weighted four-bar linkages to match an input force curve more precisely.

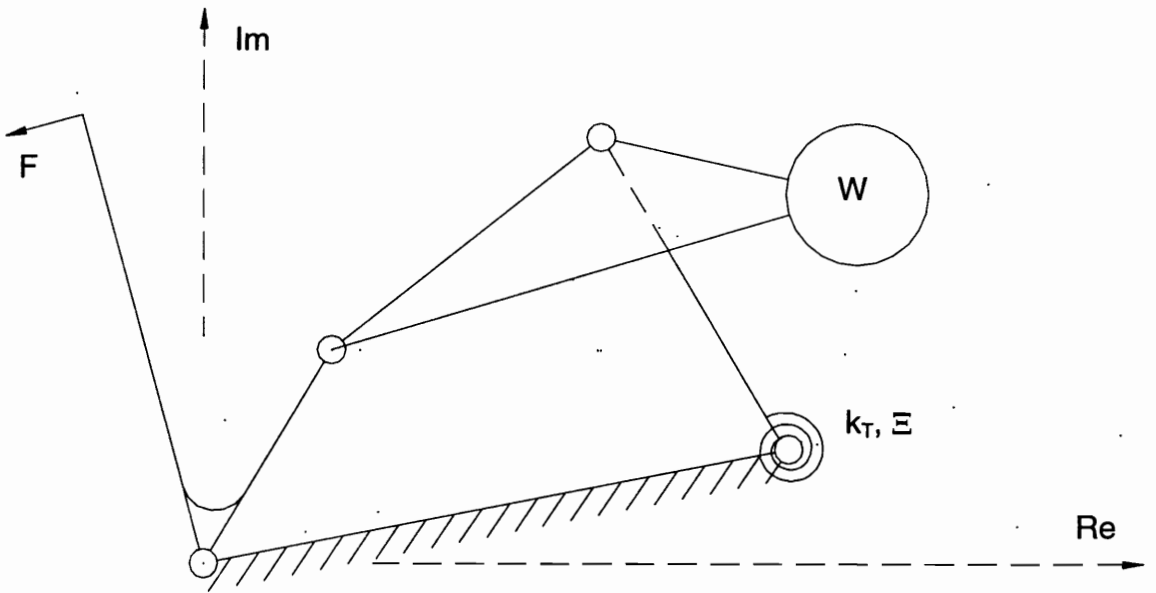


Figure 6-2, Four-Bar Linkage with Multiple Resistance Types

Two important points about the above linkage must be made. First, the closed-form synthesis methods are probably intractable for problems of this complexity. We must either choose a large number of free parameters to reduce the problem to a manageable size for developing closed-form equations or attempt to solve a large system of simultaneous transcendental equations. The designer can usually make use of a few

carefully selected free parameters to improve the chances of developing good solutions. Assigning a large number of free parameters simply to generate closed-form solutions is counterproductive. The best method for synthesizing a linkage of this type is probably either optimization or some other numerical approach. Second, designs of this type will not be useful for the Nautilus application. It is unreasonable to ask the user to determine the proper weights to be placed at each location based on decimal ratios found in the synthesis.

6.1.2 Four-Link Mechanism with Multiple Resistance Types

Chapters 3 and 4 addressed the synthesis for load weight resistance and also presented a partial development for constant torque and spring resistance. It is also possible to intermix a variety of resistance types in one linkage. Let us examine, as an example, the weighted-coupler, grounded-torsional-spring linkage shown in Fig. 6-2. The loop closure equations are the same as those for the previous case, Eq. (6.5a) and Eq. (6.5b). Derivation of the governing force equation starts with virtual work

$$\vec{T}_{in} \cdot \delta \vec{\beta} + \vec{W} \cdot \delta \vec{s}^w + \vec{F}_s \cdot \delta \vec{\theta}_4 = 0, \quad (6.6a)$$

$$Fl_{in} \omega_2 - W(l_2 \omega_2 \cos(\beta - \theta_2) + l_w \omega_3 \cos(\theta_3 - \theta_w)) + k_T(\Xi - \theta_4) \omega_4 = 0, \quad (6.6b)$$

$$Fl_{in} = W(l_2 \cos(\beta - \theta_2) + l_w \Gamma_3 \cos(\theta_3 - \theta_w)) + k_T(\theta_4 - \Xi) \Gamma_4, \quad (6.6c)$$

where k_T is the torsional spring constant, and Ξ is the unstretched spring angle. If the nondimensionalized resistance curve, R , is given by Fl_{in} / k_T , then we have the following governing equation:

$$R = \tilde{W} \left(\frac{l_2}{l_{in}} \cos(\beta - \theta_2) + \frac{l_w}{l_{in}} \Gamma_3 \cos(\theta_3 - \theta_w) \right) + (\theta_4 - \Xi) \Gamma_4, \quad (6.7a)$$

where

$$\tilde{W} \equiv \frac{W \cdot l_{in}}{k_T}. \quad (6.7b)$$

In this case our knowns are β , R , l_{in} , and k_T . Our unknown parameters are Ξ , θ_{in} , θ_w , l_w , l_l , l_2 , l_3 , l_4 , χ , and \tilde{W} . Again, we have five equations at each precision point, and each precision point introduces four new unknowns: Γ_3 , Γ_4 , θ_3 , θ_4 . The governing mathematical equations limit this mechanism to a maximum of 10 precision points.

This linkage also might be useful where an application calls for extremely accurate matching of the resistance curve. As with the previous linkage, more sophisticated synthesis methods need to be brought to bear to make full use of this design.

6.1.3 Two-Degree-of-Freedom Five-Bar Under Gravity Load

Planar mobility or number of degrees of freedom is one of the very first topics addressed in most elementary kinematics texts. Mabie and Reinholtz (1987); for example, deal with this topic on page 11 of the introductory chapter to their text. Students of kinematics quickly realize that a four-link closed-loop chain connected by revolute joints is a single degree of freedom mechanism called a four-bar linkage. Additional links can be added to form single-degree-of-freedom mechanisms if they have multiple loops. But a five-link single-closed-loop chain is shown to be a two-degree-of-freedom mechanism. In this section we will show how a weighted five-bar linkage can be used as a single-input force-generating mechanism.

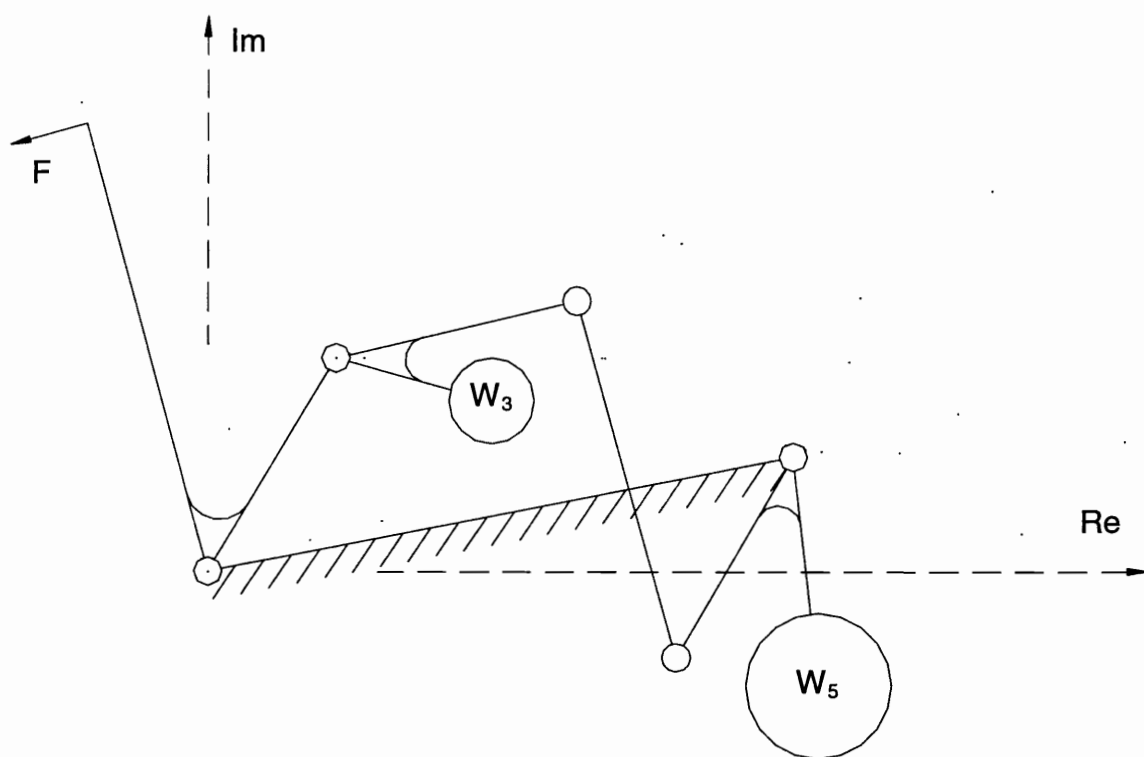


Figure 6-3, Double-Weighted Five-Bar Linkage

The planar five-bar mechanism, shown in Fig. 6-3, can also be used to generate a prescribed, nonlinear, input force. Of course the mechanism isn't truly single-degree-of-freedom in the kinematic sense. Yet, under the influence of gravity the linkage will sag to seek a minimal gravitational potential energy configuration. Analysis at each point in the motion of the input link could be performed by an iterative process. For each point in the input motion, the input link could be treated as static. The rest of the links now comprise a four-bar linkage that could be analyzed completely by allowing one link angle to vary and applying our standard four-bar position analysis. The potential energy of the linkage could be calculated at each position, and the minimum would indicate the final closure

position for the linkage. For synthesizing mechanisms like this one, we suggest that an optimization routine be used for the synthesis with a numerical solution for the resistance curve.

Mechanisms like the one shown in Fig. 6-3 might be useful in applications where the input force changes dramatically over the range of motion. Qualitatively, if W_5 is the larger of the two load weights, then it will tend not to move very much initially and so link 5 will appear to be fixed for much of the motion. If link 5 is approximately fixed, then the remaining four links will move much like a four-bar mechanism. When the remaining four links reach a position such that the approximate four-bar linkage is at a dead point in its motion, then link 5 will be forced into motion. The result is a sudden large increase in the required applied force.

6.2 A Special Case -- The Watt Six-Bar Linkage

Any number of links can be included in a kinematic chain to form complicated force generating mechanisms. There are also other possible joints, such as prismatic, and the resulting linkages could be spatial as well as planar, as discussed by Huang and Roth (1994). In this section we turn our attention to a particularly important multi-link, multi-loop, planar chain, the Watt six-bar linkage. As we will see, we have already developed the tools required to synthesize a mechanism of this type. This mechanism is also important to our specific application in exercise equipment.

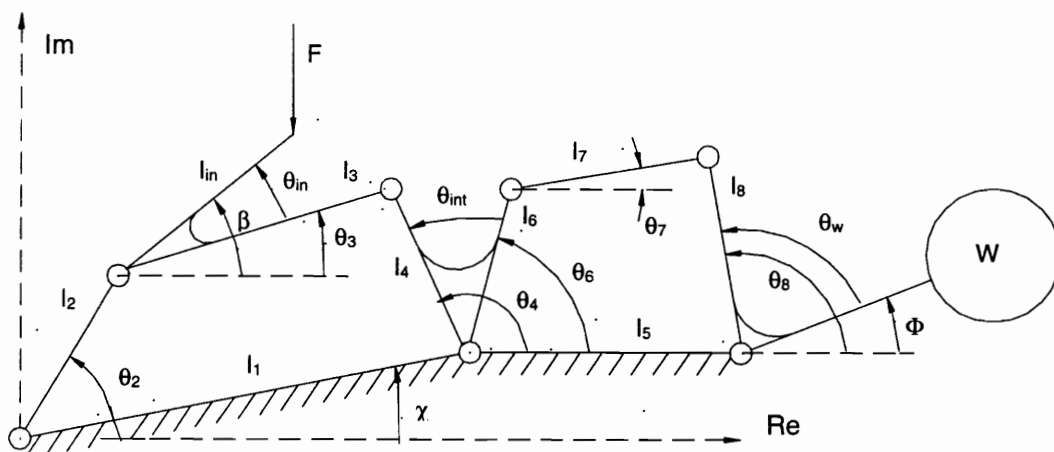


Figure 6-4, Watt Six-Bar, Body Guidance, Mechanical Adv. Generator

6.2.1 As a Series Body-Guidance, Mechanical Advantage Generator

The technique we have developed for four-bar synthesis assumed that the input force would be applied to the grounded link of our four-bar mechanism. This seems reasonable for many exercises which target a single joint: bicep curls (elbow), tricep extension (elbow), leg extension (knee), leg curls (knee), bench press (shoulders), etc. But, many exercises require more complicated path motion. These include abdominal crunch (spine), squats (knees and hips), leg press (knees and hips) etc. If the path for the exercise motion is known, then a body-guidance four-bar linkage can be synthesized to match the path of the exercise using the same techniques we have already developed. Then, if the applied force (strength curve) is known, then one of the grounded links of the body-guidance four-bar can be used as the input link to a force generating four-bar linkage.

This series chain of two four-bar linkages form a special kind of linkage called a Watt six-bar linkage. A series body guidance, mechanical advantage generator chain is shown in Fig. 6-4. The body-guidance linkage is synthesized without regard for the force transmission properties that it will exhibit. It simply matches the motion of the exercise. The second linkage is used to develop the required resistance function. The body-guidance linkage is synthesized first, using Burmester theory, or some other synthesis technique. The second step is to modify the desired resistance curve R , generated as a result of the force transmission properties of the body-guidance four-bar. Suppose we call the torque on link 4 required to keep the mechanism in a static position T_{out} . By virtual work

$$T_{out}\omega_4 + \vec{F} \cdot \vec{v}_{in} = 0, \quad (6.8a)$$

or

$$T_{out} = \frac{-\vec{F} \cdot \vec{v}_{in}}{\omega_4}, \quad (6.8b)$$

and

$$\frac{T_{out}}{W} = \frac{-\frac{\vec{F}}{|\vec{F}|} \cdot \vec{v}_{in}}{\omega_4} R. \quad (6.8c)$$

We must also determine a transformation between the input angle to the first four-bar and the input angle to the second four-bar using loop-closure position analysis of the first four-bar. Once we have these expressions, then we can synthesize the force-generating four-bar by recognizing the equivalent variables in the new problem. These variable changes are summarized in Table 6.1. The synthesis method is exactly the same as laid out in Chapter 3. We have considered the case in which the second linkage is a

mechanical advantage generator. The second linkage can also be designed as a weighted-coupler-link four-bar in a completely analogous way.

Table 6.1, Change of Variables for Synthesis

Variable from ch. 3	R	β	θ_{in}	χ	l_1	l_2	l_3	l_4	l_{in}
New variable	$\frac{\vec{F} \cdot \vec{v}_{in}}{ \vec{F} }$ R evaluated as $\frac{\omega_4 \cdot l_4}{\omega_4 \cdot l_4}$ a function of θ_4	θ_4	θ_{int}	χ_2	l_5	l_6	l_7	l_8	l_4

It is worth noting that the second linkage in this chain may be freely scaled and rotated as long as these rotations are absorbed into the offset angles at the input and output.

6.2.2 As a Double Force Generator

Another important possibility for a Watt six-bar linkage is the series double function generator. In this linkage, the first of the series four-bars is a mechanical advantage generator, and the second is either a mechanical advantage generator, or a weighted-coupler four-bar. These linkages are shown in Fig. 6-5 and Fig. 6-6 respectively. Unlike the previous case, both linkages are synthesized to deal directly with force transfer issues. This linkage is particularly useful in circumstances where the synthesized four-bars (as found by methods in chapters 3 and 4) are unable to accurately follow a specified resistance curve. A number of problems may cause our previous techniques to be inadequate. The resistance curve could be too radical and could exhibit

too many points of inflection. In this case we want to smooth the resistance curve with the first linkage. The required resistance could develop forces that are too large for the output weight arm or start angle, or it could result in internal forces which are too large. In these cases we want the first linkage to reduce the resistance curve. Recognizing an intermediate goal (smoothing, reducing, etc.) for the resistance curve, we can prescribe a torque on link 4 of the first linkage. If we call this nondimensionalized torque curve T_{out}/W , then we can develop a function-generation problem for the synthesis of the first linkage

$$-T_{out}\delta\theta_4 + Fl_{in}\delta\beta = 0 \quad (6.9a)$$

$$T_{out}(\theta_4 - \theta_{4_o}) = \int_{\beta_o}^{\beta} Fl_{in}\delta\beta \quad (6.9b)$$

$$\theta_4 = \frac{l_{in}A_R}{\left(T_{out}/W\right)} + \theta_{4_o} \quad (6.9c)$$

We now have a standard function generator between the input and output of the first linkage. The first linkage can be synthesized for four positions using the Burmester theory developed in chapter 3. After the linkage has been synthesized, a change in variables analogous to that described for the body guidance, mechanical advantage generator above, can be used to transform the synthesis of the second linkage into one of our standard problems.

This technique could be applied to a third series mechanical advantage generator (an eight-bar), in the same way. In fact, the process of adding series four-bar mechanisms can go on indefinitely. But obviously this has practical limits.

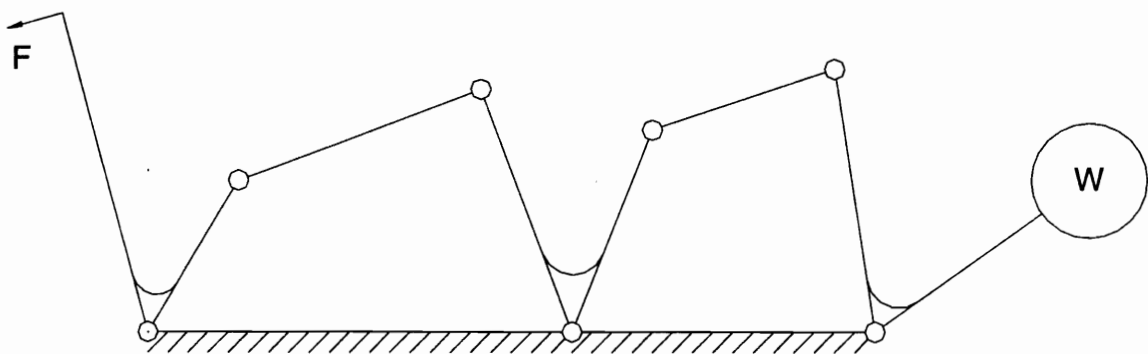


Figure 6-5, Watt Six-Bar Linkage, Double Mechanical Advantage Generator

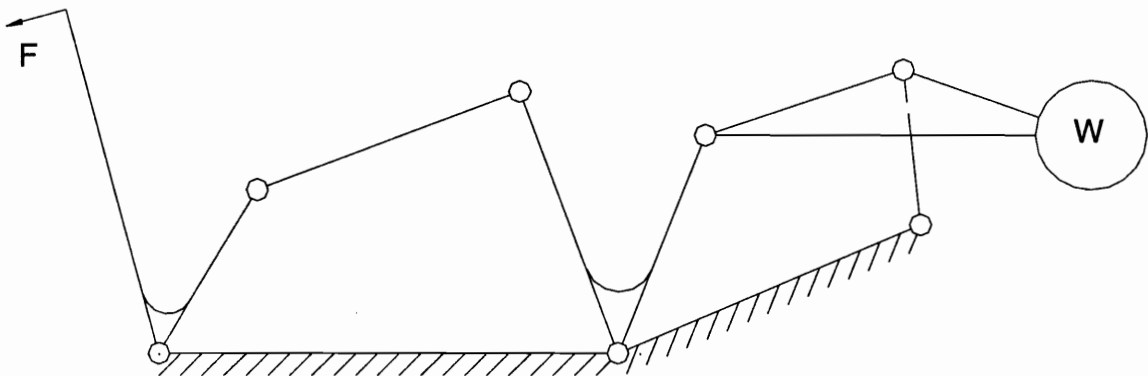


Figure 6-6, Watt Six-Bar Linkage, Mechanical Advantage Generator, Weighted-Coupler

6.3 Ground Work for Optimization

Optimization is a very powerful synthesis technique. An excellent introductory reference for optimization is Reinholtz (1983). Rather than deriving closed form synthesis equations, optimization relies on simple closed-form or numerical analysis. Optimization can be used to search for solutions that meet prespecified design objective and constraint requirements. This differs from standard numerical techniques, which solve the governing equations at specified precision points and generate one solution. Multiple iterations of the analysis allow the computer to evaluate each design and search for the optimal.

6.3.1 Development of a Cost Function

The first step to the optimization process is to develop a cost function used to judge competing designs. For the cost function in force-generating linkages we suggest the sum of the square of the error between the desired resistance curve and the resistance curve of the current design. The sum is evaluated at many points between the maximum and minimum value of the user input motion

$$V = \sum_{\beta} (R(\beta) - R_{desired}(\beta))^2 . \quad (6.10)$$

Squaring the error assures that negative and positive error are penalized equally, as well as penalizing a small range of large error more than a large range of small error. Notice that we have said nothing about requiring that the resistance curve be analyzed for

massless links, nor for static forces. Optimization allows us to synthesize many mechanisms that would be difficult in closed form. Some salient advantages of optimization-based design are listed below:

1. Synthesis of mechanisms with massed links is possible. We suggest that a constant, the mass per unit length of the kinematic link vector, be used.
2. Synthesis for dynamic forces is possible. This is particularly important for applications with well defined input trajectories. Dynamic motion synthesis also allows us to introduce new types of resistance components, dashpots, for example.
3. Synthesis for more complex linkages and multiple resistance applications.

In addition to using the cost function to fit the desired resistance curve, we could also penalize linkages for high manufacturing cost, or for excessively long links, for example. Many optimization algorithms enforce additional constraints through the use of penalty functions.

6.3.2 Penalty Functions

Penalty functions can be used to enforce inequality constraints for example. Typically a penalty function is zero for designs which do not violate the constraint and is a large value for designs which violate the constraint (sufficiently large such that a design which violates the constraint will never be optimal). The penalty function is added to the base cost function to find the total cost function of a design. For our specific application we anticipate that penalty functions might be used to enforce the following six inequality constraints on the design linkage:

1. The moving pivots of the linkage must remain within the frame of the machine throughout the range of input motion. The constraint is enforced as a minimum and maximum on the real and imaginary components of each moving pivot for each β analyzed.
2. The load weight must remain above the intended floor for the machine. The constraint is enforced as a minimum value for the imaginary component of the vector locating the weight at each value of β .
3. The grounded pivot must remain within a set distance of the frame of the machine for manufacturing. The constraint is enforced by calculating the minimum distance between each grounded pivot and the frame, and comparing this to a maximum allowable value.
4. Link lengths cannot be either too long or too short. A maximum and minimum bound is placed on each link length.
5. The maximum height of the weight should not destabilize the machine. At the maximum height of the weight, the total center of mass of the linkage system is calculated and compared to a maximum.
6. The bearing and internal forces cannot exceed a preset value. The maximum over the range of β is calculated and compared to a maximum. Alternatively, the cross section of the links and maximum load weight could be design variables, and the actual stresses compared to a maximum.

These inequality constraints should be implemented such that the total cost function increases as the amount the constraint is violated increases. For example,

$$P = \begin{cases} 0 & c < 0 \\ 1e8 \cdot c & c \geq 0 \end{cases} \quad (6.11a)$$

where $c \equiv x - x_{\text{constraint}}$ for a maximum on x (6.11b)

and $c \equiv x_{\text{constraint}} - x$ for a minimum on x (6.11c)

The slope beyond the enforcement of the penalty function allows the convergence method to evaluate which direction in design parameter space will rectify the inequality constraint.

6.3.3 Convergence Methods

Synthesis by optimization is an iterative method. Starting with some initial design, chosen by the designer or at random, the cost function is evaluated. Then a direction in design space (the design parameters are being treated as a vector which indicates the current design in the space of all designs) is chosen based on either a pattern move or the gradient of the cost function. The gradient of the cost function (in the absence of penalty functions) would be

$$\vec{\nabla} V = \vec{\nabla} \sum_{\beta} (R(\beta) - R_{\text{desired}}(\beta))^2, \quad (6.12a)$$

$$\vec{\nabla} V = \sum_{\beta} \vec{\nabla} (R(\beta) - R_{\text{desired}}(\beta))^2 = \sum_{\beta} 2(R(\beta) - R_{\text{desired}}(\beta)) \vec{\nabla} (R(\beta)). \quad (6.12b)$$

The direction of the gradient is the key here, because it determines the direction in design space which most decreases the cost. A step to the next design begins the next step in the iteration.

A drawback to optimization is our inability to guarantee that a given design is a global minimum in the design space. The biggest advantage is its ability to deal with very complicated systems and multiple constraints. Optimization seems to be the best direction for further research into the synthesis of force generating mechanisms.

Chapter 7, Conclusions and Recommendations

7.1 Summary

This thesis has presented the full derivation of a technique for synthesizing force-generating four-link mechanisms. The kernel of the work is the use of an integrated virtual work relation to develop position constraints from force constraints. This synthesis technique is an efficient closed-form method for any application which requires prescribed input forces without corresponding output positions. The specific applicability of the work is demonstrated through frequent reference to the design of weighted linkages for strength exercise equipment.

The content of this thesis is not simply a mathematical derivation. Because of the strong motivation for this work from a corporate sponsor, this thesis presents a framework for a total design package. Above all else, the closed-form synthesis techniques developed emphasize flexibility. Although resistance curves (the nondimensional ratio of the input force or torque to some characteristic value of the load over the range of input motion) are the dominant quantitative constraint on the design, we recognize that numerous qualitative constraints are also of great importance. We have discussed four significant ways in which the designer is given the needed flexibility to meet qualitative and quantitative constraints: (1) Burmester theory is used to generate infinite solution sets that maximize the available solution choices; (2) emphasis is placed

on making free parameter choices only when such choices would be intuitive to the designer; (3) separate analyses (for resistance curve, internal forces, static effect of massed links, dynamic effects, sensitivity to manufacturing tolerances) allow the design to assess the quality of many aspects of the solution; and (4) numerous design alternatives are provided including geometric reduction of the resistance curve, alternative linkages (weighted-coupler four-bar, Watt six-bar), and manual optimization using sensitivity analysis.

7.2 Further Research

This research has lead to numerous avenues for further research. Some of the more intriguing are outlined below.

1. Strength curve and physiologic measurement techniques could be improved. The raw data for the strength curve for many exercises is usually either meager or relies on the intuition of experts. In particular, simple techniques for measuring dynamic, rather than static, strength curves could be useful.
2. Closed-form synthesis techniques for complex force-generating linkages could be developed. Such techniques should emphasize synthesis for the maximum number of precision points with the minimum number of free parameter selections. If too many free parameters must be chosen in order to develop closed-form equations, then the major advantage of the increased complexity will be lost. Numerical solutions might be useful on an ad hoc basis.

References

1. Bagci, C., and Rieser, G. M., 1984, "Optimum Synthesis of Function Generators Involving Derivative Constraints", *Mechanism and Machine Theory*, Vol. 19, No. 1, pp. 157-164.
2. Barker, C. R., and Shu, G.-H., 1988, "The Position Function Generation of Planar Four-Bar Mechanisms with Equal Deviation Transmission Angle Control", *Proceedings of the 20th Biennial Mechanisms Conference*, Kissimmee, FL, Sept. 25-28, pp. 271-277.
3. Beckwith, T. G., and Marangoni, R. D., 1990, "Propagation of Uncertainty", *Mechanical Measurements*, 4th ed., Addison-Wesley, Reading, MA, pp. 43-45.
4. Benedict, C. E., Matthew, G. K., and Tesar, D., 1971, "Torque Balancing of Machines by Sub-Unit Cam Systems", *Proceedings of the 2nd OSU Applied Mechanism Conference*, Oklahoma State University, Stillwater, OK, Oct. 7-8, Paper No. 15.
5. Benedict, C. E., and Tesar, D., 1970, "Optimal Torque Balancing for a Complex Stamping and Indexing Machine", ASME Paper No. 70-Mech-82.
6. Bokelberg, E. H., and Gilmore, B. J., 1990, "A Kinematic Design Methodology for Exercise/Rehabilitation Machines Using Springs and Mechanical Advantage to Provide Variable Resistance", *Proceedings of the 21st Biennial Mechanisms Conference*, Chicago, IL, Sept. 16-19, pp. 279-286.
7. Brown, R. H., and Mabie, H. H., 1971, "An Extension of the Curve-Matching Method of Velocity and Acceleration Synthesis of Four-Bar Mechanisms", *Proceedings 2nd OSU Applied Mechanism Conference*, Oklahoma State University, Stillwater, OK, October 7-8, Paper No. 3.
8. Dhande, S. G., and Chakraborty, J., 1978, "Mechanical Error Analysis of Spatial Linkages", *Journal of Mechanical Design*, Vol. 100, October, pp. 732-738.
9. Dhande, S. G., and Chakraborty, J., 1975, "Mechanical Error Analysis of Cam-Follower Systems -- A Stochastic Approach", *Proceedings of the Fourth World Congress on the Theory of Machines and Mechanisms*, University of Newcastle upon Tyne, Sept. 8-12, pp. 957-962.
10. Dhande, S. G., 1974, "Reliability Based Design of Gear Trains -- A Dynamic Programming Approach", *Design Technology Transfer presented at the Design Engineering Technical Conference*, New York, NY, October 5-9, pp. 413-422.
11. Dhande, S. G., and Chakraborty, J., 1973, "Analysis and Synthesis of Mechanical Error in Linkages -- A Stochastic Approach", *Journal of Engineering for Industry*, August, pp. 672-676.
12. Freudenstein, F., and Chen, C.-K., 1991, "Variable-Ratio Chain Drives with Noncircular Sprockets and Minimum Slack-Theory and Application", *Journal of Mechanical Design*, Vol. 113, September, pp. 253-262.
13. Freudenstein, F., 1956, "On the Maximum and Minimum Velocities and the Accelerations in Four-Link Mechanisms", *ASME Transactions*, Vol. 78, May, pp. 779-787.

14. Goodman, T. P., 1965, "Toggle Linkage Applications in Different Mechanisms", *Mechanisms, Linkages, and Mechanical Controls*, Chironis, N. P., editor, McGraw-Hill, New York, pp. 154-155.
15. Gupta, K. C., 1977, "Design of Four-Bar Function Generators with Mini-Max Transmission Angle", *Journal of Engineering for Industry*, May, pp. 360-366.
16. Gustavson, R. E., 1968, "Design of Planar Torque-Transmitting Four-Bar Linkage", ASME Paper No. 68-Mech-40.
17. Hall, Allen S., 1961, *Kinematics and Linkage Design*, Waveland Press, Prospect Heights, IL, p. 47.
18. Hamid, S., and Soni, A. H., 1971, "Design of an 'RSSR' Crank-Rocker Mechanism for Optimum Force Transmission", *Proceedings 2nd OSU Applied Mechanism Conference*, Oklahoma State University, Stillwater, OK, October 7-8, Paper No. 17.
19. Harmening, W. A., 1974, "Static Mass Balancing with a Torsion Spring and Four-Bar Linkage", ASME Paper No. 74-DET-29.
20. Harrison, J. Y., 1970, "Maximizing Human Power Output by Suitable Selection of Motion Cycle and Load", *Human Factors*, Vol. 12, No. 3, pp. 315-329.
21. Hartenberg, R. S., and Denavit, J., 1964, *Kinematic Synthesis of Linkages*, McGraw-Hill, New York.
22. Hockey, B. A., 1972, "The Minimization of the Fluctuation of Input-Shaft Torque in Plane Mechanisms", *Mechanisms and Machine Theory*, Vol. 7, pp. 335-346.
23. Huang, C., and Roth, B., 1994, "Position-Force Synthesis of Closed-Loop Linkages", *Journal of Mechanical Design*, Vol. 116, March, pp. 155-162; 1992, *Proceedings of the 22nd Biennial Mechanisms Conference*, Scottsdale, AZ, Sept. 13-16, pp. 243-251.
24. Huang, C., and Roth, B., 1990, "Dimensional Synthesis of Closed-Loop Linkages to Match Force and Position Specifications", *Proceedings of the 21st Biennial Mechanisms Conference*, Chicago, IL, Sept. 16-19, pp. 271-277.
25. Lieber, R. L., 1992, "The Production of Movement", *Skeletal Muscle Structure and Function: Implications for Rehabilitation and Sports Medicine*, Williams and Wilkins, Baltimore, MD, pp. 111-158.
26. Mabie, H. H., and Reinholtz, C. F., 1987, *Mechanisms and Dynamics of Machinery*, 4th edition, John Wiley and Sons, New York.
27. Mallik, A. K., and Dhande, S. G., 1987, "Analysis and Synthesis of Mechanical Error in Path-Generating Linkages Using a Stochastic Approach", *Mechanism and Machine Theory*, Vol. 22, No. 2, pp. 115-123.
28. Matthew, G. K., and Tesar, D., 1977, "Synthesis of Spring Parameters to Satisfy Specified Energy Levels in Planar Mechanisms" and "Synthesis of Spring Parameters to Balance General Forcing Functions in Planar Mechanisms", *Journal of Engineering for Industry*, May, pp. 341-346 and pp. 347-352.
29. Meirovitch, Leonard, 1970, *Methods of Analytical Dynamics*, McGraw-Hill, New York.
30. Midha, A., Turcic, D. A., and Bosnik, J. R., 1984, "Creativity in the Classroom -- A Collection of Case Studies in Linkage Synthesis", *Mechanism and Machine Theory*, Vol. 19, No. 1, pp. 25-44.

31. Nathan, R. H., 1985, "A Constant Force Generation Mechanism", *Journal of Mechanisms, Transmissions, and Automation in Design*, Vol. 107, December, pp. 508-512.
32. Ogawa, K., and Funabashi, H., 1969, "On the Balancing of the Fluctuating Input Torques Caused by Inertia Forces in the Crank-and-Rocker Mechanisms", *Journal of Engineering for Industry*, February, pp. 97-102.
33. Ogot, M. M., and Gilmore, B. J., 1991, "An Automated Procedure for the Maximization of the Mechanical Advantage of Planar Mechanisms", *Proceedings of the 17th Design Automation Conference*, Miami, FL, Sept 22-25, pp. 311-319.
34. Okada, T., 1986, "Optimization of Mechanisms for Force Generation by Using Pulleys and Spring", *The International Journal of Robotics Research*, Vol. 5, No. 1, Spring, pp. 77-89; 1985, *Robotics Research: The Second International Symposium*, Hanafusa, H., and Inoue, H., editors, MIT Press, Cambridge, MA, pp. 245-252.
35. Raghavan, M., and Roth, B., 1989, "On the Design of Manipulators for Applying Wrenches", *Proceedings of the IEEE International Conference on Robotics and Automation*, Vol. 1, pp. 438-443.
36. Reinholtz, C. F., Arun, V., and Williams, R. L. II, 1987, "A Reassessment of the Tasks of Kinematic Synthesis", *Proceedings of the 10th Applied Mechanisms Conference*, New Orleans, LA, Dec. 6-9.
37. Rigelman, G. A., and Kramer, S. N., 1988, "A Computer-Aided Design Technique for the Synthesis of Planar Four Bar Mechanisms Satisfying Specified Kinematic and Dynamic Conditions", *Journal of Mechanisms, Transmissions, and Automation in Design*, Vol. 110, September, pp. 263-268.
38. Roth, B., 1989, "Design and Kinematics for Force and Velocity Control of Manipulators and End-Effectors", *Robotics Science*, Brady, M., editor, The MIT Press, Cambridge, MA, pp. 459-475.
39. Sandor, G. N., 1993, "A Brief History of the First 40 Years of Modern American Kinematic Synthesis of Planar Mechanisms", *Modern Kinematics: Developments in the Last Forty Years*, Erdman, A. G., editor, John Wiley, New York, pp. 77-78.
40. Sandor, G. N., and Erdman, A. G., 1984, *Advanced Mechanism Design: Analysis and Synthesis*, Vol. 2, Prentice-Hall, New York.
41. Schaefer, R. S., and Kramer, S. N., 1979, "Selective Precision Synthesis of Planar Mechanisms Satisfying Position and Velocity Constraints", *Mechanism and Machine Theory*, Vol. 14, pp. 161-170.
42. Schneck, D. J., 1990, "Principles of Human Posture and Locomotion", *Engineering Principles of Physiologic Function*, New York University Press, New York, pp. 371-427.
43. Shooter, S. B., 1995, "Information Modeling in Mechanical Design: with Application to Cam Mechanism Design", Ph.D. Dissertation, Virginia Polytechnic Institute and State University.
44. Shoup, T. E., and Pelan, B. J., 1971, "Design of Four-Bar Mechanisms for Optimum Transmission Angle and Optimum Structural Error", *Proceedings 2nd OSU Applied*

- Mechanism Conference*, Oklahoma State University, Stillwater, OK, October 7-8, Paper No. 4.
45. Starr, P. J., 1974, "Dynamic Synthesis of Linkages: An Emerging Field", ASME Paper No. 74-DET-64.
 46. Tao, D. C., 1964, "Design of a Four-Bar Linkage for the Transmission of Torque", *Applied Linkage Synthesis*, Addison-Wesley Co., Reading, MA, pp. 61-63.
 47. Thompson, C. W., 1973, *Manual of Structural Kinesiology*, 7th ed., C. V. Mosby Co., St. Louis.
 48. Tidwell, P. H., 1995, "Wrapping Cam Mechanisms", Ph.D. Dissertation, Virginia Polytechnic Institute and State University.
 49. Tidwell, P. H., Bandukwala, N., Dhande, S. G., Reinholtz, C. F., and Webb, G, 1994, "Synthesis of Wrapping Cams", *Journal of Mechanical Design*, Vol. 116, June, pp. 634-638.
 50. Tidwell, P. H., Bandukwala, N., Dhande, S. G., Reinholtz, C. F., and Webb, G, 1992, "Synthesis of Wrapping Cams", *Proceedings of the 22nd Biennial Mechanisms Conference*, Scottsdale, AZ, Sept. 13-16, pp. 337-343.
 51. Urion, K. D., 1971, "Linkage Mechanism Matches the Path and Velocity of a Rotating Machine", *Proceedings 2nd OSU Applied Mechanism Conference*, Stillwater, OK, October 7-8, paper no. 8.
 52. Wu, F., and Lankarani, H. M., 1992, "A New Parameter for Transmission Quality and Output Sensitivity Analysis of Mechanisms", *Proceedings of the 22nd Biennial Mechanisms Conference*, Scottsdale, AZ, Sept. 13-16, pp. 103-109.
 53. Yong, L. D., and Zhen, H., 1989, "Input Torque Balancing of Linkages", *Mechanism and Machine Theory*, Vol. 24, No. 2, pp. 99-103.

Appendix A, Weighted-Grounded-Link Synthesis Program

This appendix contains a MathSoft Mathcad® version 5.0 program. The program synthesizes weighted-grounded-link four-link mechanisms by the method developed in Chapter 3. The design synthesized is summarized as an example at the end of that chapter. Textual comments are in **boldface**.

Weighted-Grounded-Link Four-Bar Synthesis

Mathcad model by: R. R. Soper, M. T. Scardina, P. H. Tidwell, C. F. Reinholtz

Created on MathSoft Mathcad version 5

Problem Setup

degree := 3 The degree of the polynomial fit to the input strength curve data

Strength Curve Data:

$$x := \begin{bmatrix} 60 \\ 65 \\ 70 \\ 75 \\ 80 \\ 85 \\ 90 \\ 95 \\ 100 \end{bmatrix} \cdot \text{deg} \qquad y := \begin{bmatrix} 85.75 \\ 88 \\ 92.5 \\ 96.5 \\ 97.25 \\ 98 \\ 98.75 \\ 100 \\ 100 \end{bmatrix} \cdot \%$$

Discrete Data Points. A polynomial of degree "degree" will be fit to the data in order to develop a functional relationship

$$\begin{aligned} \theta_{\min} &:= \min(x) & \theta_{\min} &= 60 \cdot \text{deg} \\ \theta_{\max} &:= \max(x) & \theta_{\max} &= 100 \cdot \text{deg} \end{aligned}$$

These are the extents of the input data points. They are used as integration limits below.

$$\begin{aligned} N &:= \text{length}(x) & N &= 9 \\ m &:= 0..N - 1 \end{aligned}$$

Setting up matrix operations

Curve Fitting

(Matrix Least Squares method, using the pseudo-inverse)

$k := 1 \dots \text{degree}$
 $X_{m,0} := 1$

$X^{<k>} := \overrightarrow{(x^k)}$
Fills the k^{th} column with the vectorized values of x^k .

$b := (X^T \cdot X)^{-1} \cdot (X^T \cdot y)$
LEAST SQUARE POLYNOMIAL COEFFICIENTS

$b = \begin{bmatrix} -0.73 \\ 2.768 \\ -1.477 \\ 0.263 \end{bmatrix}$
 $S(\beta) := b_0 + \sum_k b_k \cdot \beta^k$
The nondimensional strength curve function

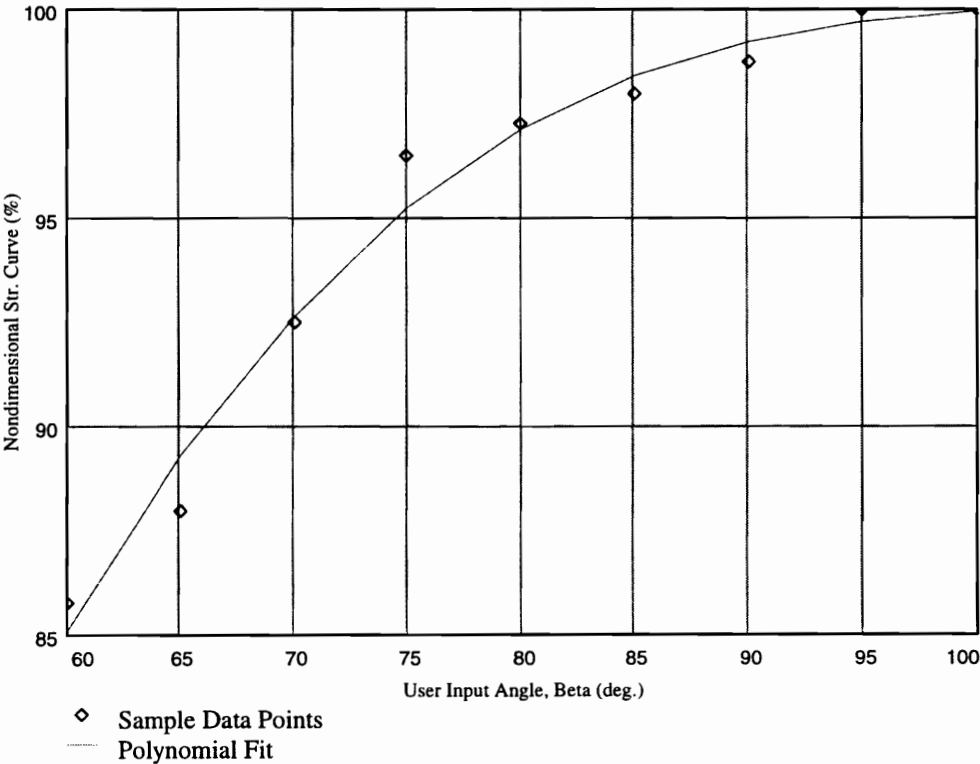


Figure A-1, Strength Curve Data

Input start angle and precision point locations:

$$\beta := \begin{bmatrix} \theta_{\min} \\ 60.5\text{-deg} \\ 85\text{-deg} \\ 93\text{-deg} \\ 98\text{-deg} \\ \theta_{\max} \end{bmatrix} \qquad \beta = \begin{bmatrix} 60 \\ 60.5 \\ 85 \\ 93 \\ 98 \\ 100 \end{bmatrix} \cdot \text{deg}$$

β_0 is the handle start angle. $\beta_1 - \beta_4$ are four "Precision Points" in the handle angle.

$q := 1..5$

$S(\beta_q)$
0.856
0.984
0.996
0.999
0.999

$$A_{R_q} := \int_{\beta_0}^{\beta_q} S(\beta) \, d\beta \qquad A_R = \begin{bmatrix} 0 \\ 42.665 \\ 2.332 \cdot 10^3 \\ 3.124 \cdot 10^3 \\ 3.623 \cdot 10^3 \\ 3.823 \cdot 10^3 \end{bmatrix} \cdot \text{deg} \cdot \%$$

A_R is the area under the strength curve for the values of β given above. This is a nondimensional measure of the input work.

Knowns: $l_{in} := 40.1$ The length of the handle.

Free parameter choices: $l_w := 45$ The length of the weight stack lever arm and the start angle for the weight stack.
 $\Phi_0 := 5\text{-deg}$

Synthesis Section

$$\Phi_q := \text{asin} \left(\frac{l_{in}}{l_w} \cdot A_{R_q} + \sin(\Phi_0) \right) \qquad \Phi = \begin{bmatrix} 5 \\ 5.382 \\ 26.732 \\ 34.966 \\ 40.592 \\ 42.98 \end{bmatrix} \cdot \text{deg}$$

Transformation to a four position body guidance problem:

$n := 2..4$ 'n' is the number of the precision points.

$$\delta_n := e^{i \cdot (180 \cdot \text{deg} - \Phi_n)} - e^{i \cdot (180 \cdot \text{deg} - \Phi_1)}$$

δ is a vector (complex valued).

$$\delta_n$$

0.102+ 0.356j
0.176+ 0.479j
0.236+ 0.557j

$$\alpha_n := \beta_n - \beta_1 + \Phi_1 - \Phi_n$$

α is the relative rotation of an imaginary body between precision points.

$$\frac{\alpha_n}{\text{deg}}$$

3.149
2.915
2.29

QUASI-LOOP-CLOSURE EQUATION

$$\Delta_2 := \begin{bmatrix} e^{i \cdot \alpha_3} - 1 & \delta_3 \\ e^{i \cdot \alpha_4} - 1 & \delta_4 \end{bmatrix}$$

$\Delta_2 = -0.009 + 0.005j$

$$\Delta_3 := - \begin{bmatrix} e^{i \cdot \alpha_2} - 1 & \delta_2 \\ e^{i \cdot \alpha_4} - 1 & \delta_4 \end{bmatrix}$$

$\Delta_3 = 0.017 - 0.008j$

$$\Delta_4 := \begin{bmatrix} e^{i \cdot \alpha_2} - 1 & \delta_2 \\ e^{i \cdot \alpha_3} - 1 & \delta_3 \end{bmatrix}$$

$\Delta_4 = -0.008 + 0.004j$

$$\Delta_1 := -\Delta_2 - \Delta_3 - \Delta_4$$

$\Delta_1 = 0.001 - 5.134 \cdot 10^{-4} j$

Δ 's are complex valued vector coefficients in an equation resembling loop closure in ψ .

Choose a range for iteration:

$\psi_2 := 5.5 \cdot \text{deg}, 6.5 \cdot \text{deg} \dots 25.5 \cdot \text{deg}$ **Iterating on ψ_2 yields a solution set of all four bar linkages which achieve the precision point values given above.**

Possible values of ψ_2 are 0 to 360 degrees. Each value will yield two solutions for the problem, a forward- and cross-closure solution. The second solutions may be viewed by changing the sign of the quadratic equation below.

Solving the quasi-loop closure problem:

$$\Omega_1 := \arg(\Delta_1) \quad \Omega_2(\psi_2) := \psi_2 + \arg(\Delta_2)$$

$$r1 := - \left(\text{Re}(\Delta_1)^2 + \text{Im}(\Delta_1)^2 \right)^{.5} \quad r2 := \left(\text{Re}(\Delta_2)^2 + \text{Im}(\Delta_2)^2 \right)^{.5}$$

$$r3 := \left(\text{Re}(\Delta_3)^2 + \text{Im}(\Delta_3)^2 \right)^{.5} \quad r4 := - \left(\text{Re}(\Delta_4)^2 + \text{Im}(\Delta_4)^2 \right)^{.5}$$

$$A(\psi_2) := r3^2 - r1^2 - r2^2 - r4^2 + 2 \cdot r1 \cdot r2 \cdot \cos(\Omega_2(\psi_2) - \Omega_1) + 2 \cdot r1 \cdot r4 - 2 \cdot r2 \cdot r4 \cdot \cos(\Omega_2(\psi_2) - \Omega_1)$$

$$B(\psi_2) := 4 \cdot r2 \cdot r4 \cdot \sin(\Omega_2(\psi_2) - \Omega_1)$$

$$C(\psi_2) := r3^2 - r1^2 - r2^2 - r4^2 + 2 \cdot r1 \cdot r2 \cdot \cos(\Omega_2(\psi_2) - \Omega_1) - 2 \cdot r1 \cdot r4 + 2 \cdot r2 \cdot r4 \cdot \cos(\Omega_2(\psi_2) - \Omega_1)$$

$$t(\psi_2) := \frac{-B(\psi_2) + \sqrt{B(\psi_2)^2 - 4 \cdot A(\psi_2) \cdot C(\psi_2)}}{2 \cdot A(\psi_2)}$$

SOLUTION SWITCHING:
Changing the sign on the quadratic equation here will result in the second set of solutions.

$$\Omega_4(\psi_2) := 2 \cdot \text{atan}\left(t(\psi_2)\right) + \Omega_1 \quad \psi_4(\psi_2) := \Omega_4(\psi_2) - \arg(\Delta_2)$$

$$T(\psi_2) := \frac{e^{i \cdot \psi_4(\psi_2)} - 1}{e^{i \cdot \psi_2} - 1}$$

$$Z(\psi_2) := \frac{\delta_4 - T(\psi_2) \cdot \delta_2}{\left[e^{i \cdot \alpha_4} - 1 - T(\psi_2) \cdot \left(e^{i \cdot \alpha_2} - 1 \right) \right]}$$

$$M(\psi_2) := \frac{\delta_2 - \left(e^{i \cdot \alpha_2} - 1 \right) \cdot Z(\psi_2)}{e^{i \cdot \psi_2} - 1}$$

SOLUTION DYAD Vectors **Z** and **M** are the solution links to the body guidance problem. In body-guidance space, link **Z** is the "rotating" link and link **M** is the "fixed" link.

Solutions to the function generation (mechanical advantage) synthesis problem are obtained by re-inverting the mechanism.

$$Z_{\text{prime}}(\psi_2) := -Z(\psi_2) \cdot e^{i \cdot \Phi_1}$$

$$M_{\text{prime}}(\psi_2) := -M(\psi_2) \cdot e^{i \cdot \Phi_1}$$

Links 2 and 3 correspond to links Z_{prime} and M_{prime} respectively.

$$L_2(\psi_2) := \left(\text{Re}(Z(\psi_2))^2 + \text{Im}(Z(\psi_2))^2 \right)^{.5}$$

$$L_3(\psi_2) := \left(\text{Re}(M(\psi_2))^2 + \text{Im}(M(\psi_2))^2 \right)^{.5}$$

$$\theta_2(\psi_2) := \arg(Z_{\text{prime}}(\psi_2))$$

$$\theta_3(\psi_2) := \arg(M_{\text{prime}}(\psi_2))$$

3. Further research could pursue a full development of the synthesis of force-generating mechanisms using optimization techniques. Force-generating linkage synthesis by optimization techniques would allow linkages of increased complexity to be synthesized. Such linkages would be extremely useful in applications which demand very accurate matching of a prescribed resistance curve, or allow additional constraints to be met.
4. The force-generating mechanisms examined in this thesis represent special sub-categories of standard kinematic synthesis problems, like those discussed in Reinholtz, et al. (1987). Further investigation may uncover other important applications that would benefit from a complete development of sub-category synthesis techniques.

BURMESTER POINT PAIRS

$$\begin{aligned}
 X1(\psi_2) &:= L_2(\psi_2) \cdot \cos(\theta_2(\psi_2)) & X2(\psi_2) &:= L_2(\psi_2) \cdot \cos(\theta_2(\psi_2)) + L_3(\psi_2) \cdot \cos(\theta_3(\psi_2)) \\
 Y1(\psi_2) &:= L_2(\psi_2) \cdot \sin(\theta_2(\psi_2)) & Y2(\psi_2) &:= L_2(\psi_2) \cdot \sin(\theta_2(\psi_2)) + L_3(\psi_2) \cdot \sin(\theta_3(\psi_2))
 \end{aligned}$$

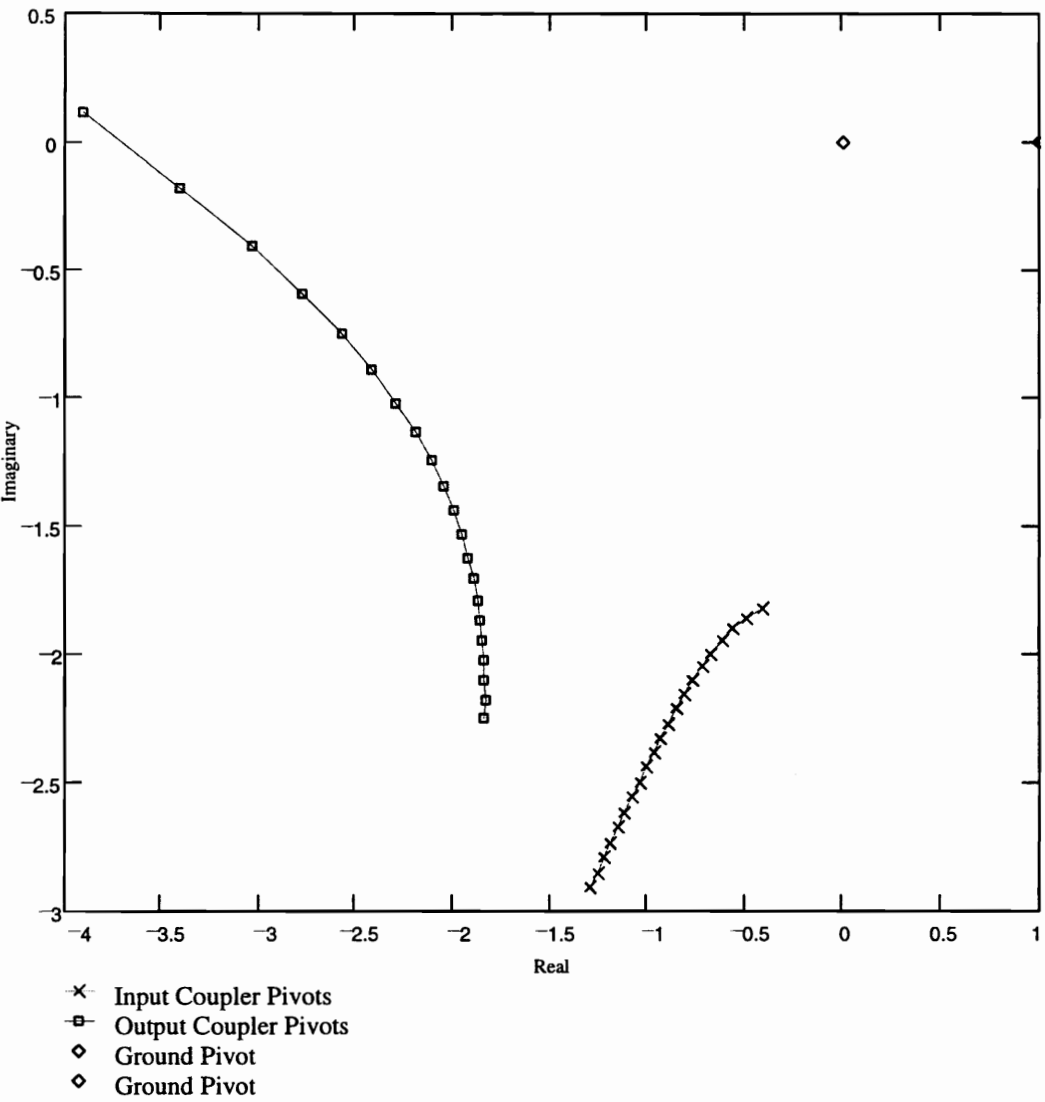


Figure A-2, Burmester Curves

CHOOSING THE SOLUTION

Choose a solution: $\psi_2 := 15.5 \cdot \text{deg}$

Choose a rotation for the ground link: $\chi := 165 \cdot \text{deg}$

Select the scale for the design: $l_1 := 8$

$$L_1 := 1 \quad l_2 := L_2(\psi_2) \cdot l_1 \quad l_3 := L_3(\psi_2) \cdot l_1$$

$$\theta_{in} := \beta_1 - \theta_2(\psi_2) - \chi \quad \theta_4 := \arg\left(l_2 \cdot e^{i \cdot \theta_2(\psi_2)} + l_3 \cdot e^{i \cdot \theta_3(\psi_2)} - l_1\right)$$

$$\theta_w := \theta_4 - \Phi_1 + \chi$$

$$l_4 := \sqrt{\text{Re}\left(l_2 \cdot e^{i \cdot \theta_2(\psi_2)} + l_3 \cdot e^{i \cdot \theta_3(\psi_2)} - l_1\right)^2 + \text{Im}\left(l_2 \cdot e^{i \cdot \theta_2(\psi_2)} + l_3 \cdot e^{i \cdot \theta_3(\psi_2)} - l_1\right)^2}$$

THE SOLUTION DESIGN PARAMETERS Fixed links and angles for the scaled solution

$$l_1 = 8 \quad l_{in} = 40.1 \quad \theta_{in} = 7.268 \cdot \text{deg} \quad \chi = 165 \cdot \text{deg}$$

$$l_2 = 20.042 \quad l_w = 45 \quad \theta_w = 5.332 \cdot \text{deg}$$

$$l_3 = 11.073$$

$$l_4 = 26.577$$

Analysis Section

Now the solution fourbar linkage is plotted:

$$\begin{pmatrix} x_1 \\ y_1 \end{pmatrix} := \begin{pmatrix} 0 \\ 0 \end{pmatrix} \quad \begin{pmatrix} x_2 \\ y_2 \end{pmatrix} := \begin{pmatrix} l_2 \cdot \cos(\theta_2(\psi_2) + \chi) \\ l_2 \cdot \sin(\theta_2(\psi_2) + \chi) \end{pmatrix} \quad \begin{pmatrix} x_4 \\ y_4 \end{pmatrix} := \begin{pmatrix} l_1 \cdot \cos(\chi) \\ l_1 \cdot \sin(\chi) \end{pmatrix} \quad \begin{pmatrix} x_{in} \\ y_{in} \end{pmatrix} := \begin{pmatrix} l_{in} \cdot \cos(\beta_1) \\ l_{in} \cdot \sin(\beta_1) \end{pmatrix}$$

$$\begin{pmatrix} x_3 \\ y_3 \end{pmatrix} := \begin{pmatrix} x_2 + l_3 \cdot \cos(\theta_3(\psi_2) + \chi) \\ y_2 + l_3 \cdot \sin(\theta_3(\psi_2) + \chi) \end{pmatrix} \quad \begin{pmatrix} x_{out} \\ y_{out} \end{pmatrix} := \begin{pmatrix} l_1 \cdot \cos(\chi) + l_w \cdot \cos(\Phi_1) \\ l_w \cdot \sin(\Phi_1) + l_1 \cdot \sin(\chi) \end{pmatrix}$$

$$m_1 := \frac{y_2 - y_1}{x_2 - x_1} \quad m_2 := \frac{y_3 - y_2}{x_3 - x_2} \quad m_3 := \frac{y_4 - y_3}{x_4 - x_3}$$

$$m_4 := \frac{y_1 - y_4}{x_1 - x_4} \quad m_{in} := \frac{y_{in} - y_1}{x_{in} - x_1} \quad m_{out} := \frac{y_{out} - y_4}{x_{out} - x_4}$$

$$step1 := \frac{x_2 - x_1}{10} \quad step2 := \frac{x_3 - x_2}{10} \quad step3 := \frac{x_4 - x_3}{10}$$

$$step4 := \frac{x_1 - x_4}{10} \quad stepin := \frac{x_{in} - x_1}{10} \quad stepout := \frac{x_{out} - x_4}{10}$$

$$rangea := x_1, x_1 + step1 .. x_2 \quad rangec := x_3, x_3 + step3 .. x_4 \quad rangee := x_1, x_1 + stepin .. x_{in}$$

$$rangeb := x_2, x_2 + step2 .. x_3 \quad ranged := x_4, x_4 + step4 .. x_1 \quad rangef := x_4, x_4 + stepout .. x_{out}$$

$$drawlinka(rangea) := m_1 \cdot (rangea - x_1) + y_1 \quad drawlinkc(rangec) := m_3 \cdot (rangec - x_3) + y_3$$

$$drawlinkb(rangeb) := m_2 \cdot (rangeb - x_2) + y_2 \quad drawlinkd(ranged) := m_4 \cdot (ranged - x_4) + y_4$$

$$drawlinke(rangee) := m_{in} \cdot (rangee - x_1) + y_1$$

$$drawlinkf(rangef) := m_{out} \cdot (rangef - x_4) + y_4$$

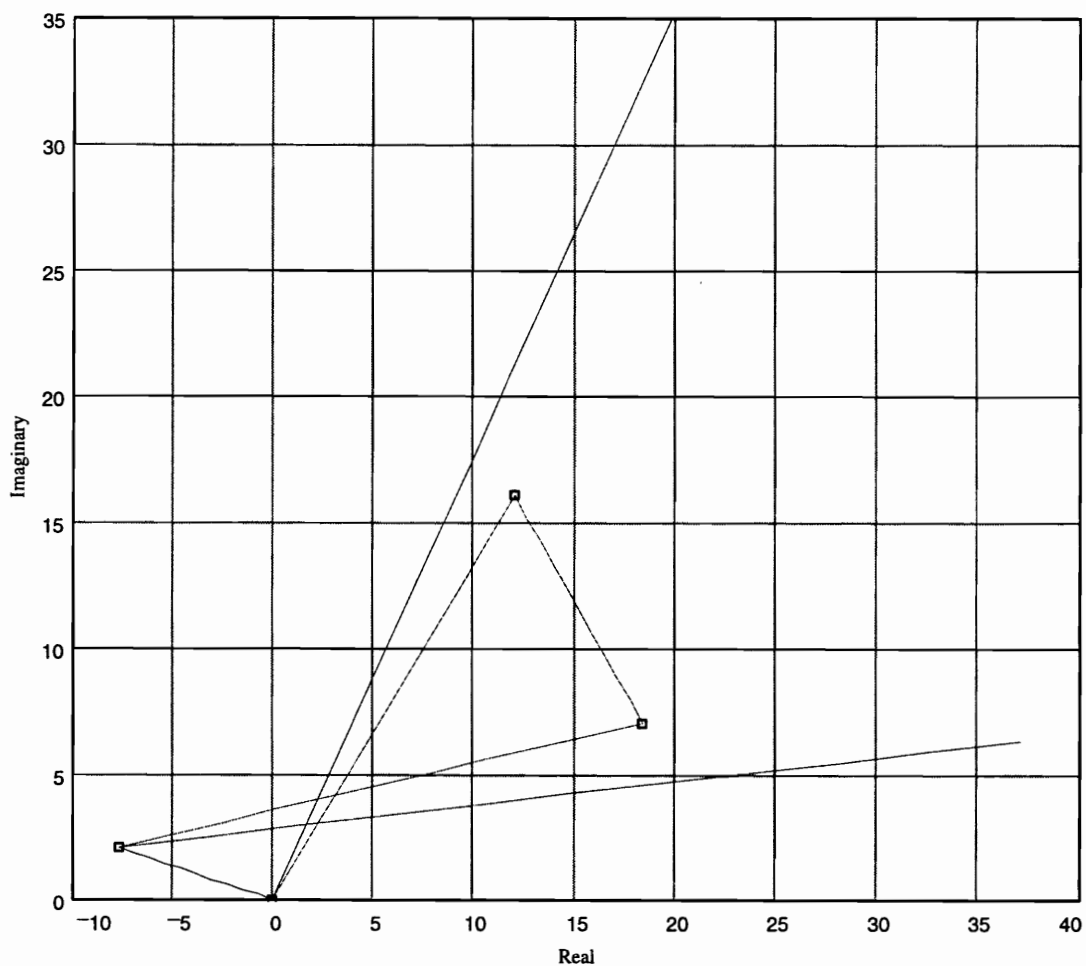


Figure A-3, Solution Linkage

Force analysis

$\xi := 1$

Indicate Closure $\xi = +1$ or -1 (the quadratic equation has two solutions, a "+" root and a "-" root)

$g := 1..4$ $b_0 := \beta_0$ $b_g := \beta_g$ $p_g := \Phi_g$ $Y1_m := y_m$ $Y2_m := x_m$ **Retaining precision point values**

$k := 0, 1..40$ $\beta_k := b_0 + k \cdot \text{deg}$ $\theta_{2_k} := \beta_k - \theta_{in}$ **Iterating**

$$E_{3_k} := 2 \cdot l_2 \cdot l_3 \cdot \sin(\theta_{2_k}) - 2 \cdot l_3 \cdot l_1 \cdot \sin(\chi) \quad F_{3_k} := 2 \cdot l_2 \cdot l_3 \cdot \cos(\theta_{2_k}) - 2 \cdot l_3 \cdot l_1 \cdot \cos(\chi)$$

$$G_{3_k} := l_2^2 + l_3^2 + l_1^2 - l_4^2 - 2 \cdot l_2 \cdot l_1 \cdot \cos(\chi) \cdot \cos(\theta_{2_k}) - 2 \cdot l_2 \cdot l_1 \cdot \sin(\chi) \cdot \sin(\theta_{2_k})$$

$$N_{3_k} := -E_{3_k} + \xi \cdot \sqrt{(E_{3_k})^2 + (F_{3_k})^2 - (G_{3_k})^2} \quad \theta_{3_k} := 2 \cdot \text{atan}\left(\frac{N_{3_k}}{G_{3_k} - F_{3_k}}\right)$$

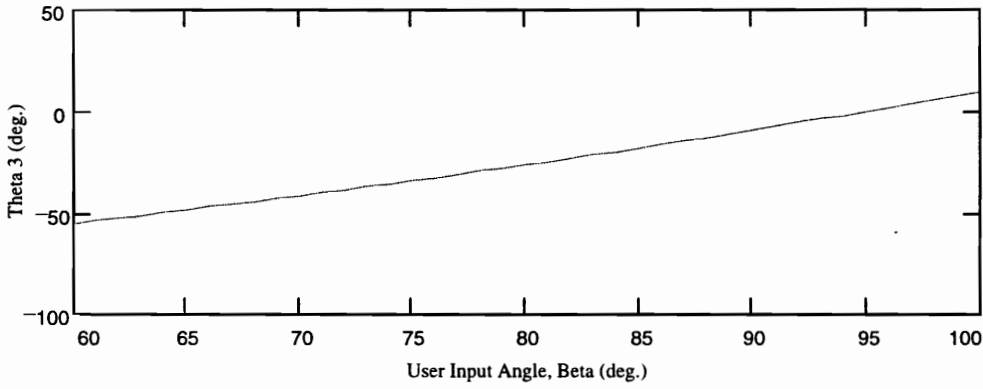


Figure A-4, Theta 3 vs. Beta

$$E_{4_k} := -2 \cdot l_2 \cdot l_4 \cdot \sin(\theta_{2_k}) + 2 \cdot l_4 \cdot l_1 \cdot \sin(\chi) \quad F_{4_k} := -2 \cdot l_2 \cdot l_4 \cdot \cos(\theta_{2_k}) + 2 \cdot l_4 \cdot l_1 \cdot \cos(\chi)$$

$$G_{4_k} := l_2^2 + l_4^2 + l_1^2 - l_3^2 - 2 \cdot l_2 \cdot l_1 \cdot \cos(\chi) \cdot \cos(\theta_{2_k}) - 2 \cdot l_2 \cdot l_1 \cdot \sin(\chi) \cdot \sin(\theta_{2_k})$$

$$N_{4_k} := -E_{4_k} + \xi \cdot \sqrt{(E_{4_k})^2 + (F_{4_k})^2 - (G_{4_k})^2} \quad \theta_{4_k} := 2 \cdot \text{atan}\left(\frac{N_{4_k}}{G_{4_k} - F_{4_k}}\right)$$

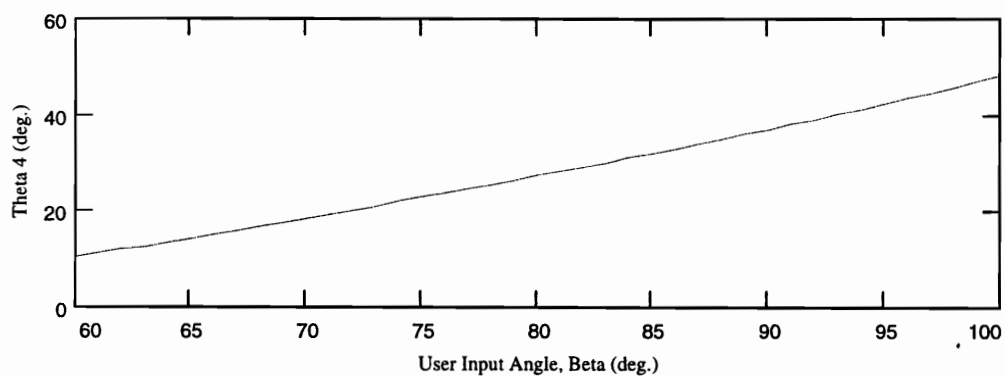


Figure A-5, Theta 4 vs. Beta

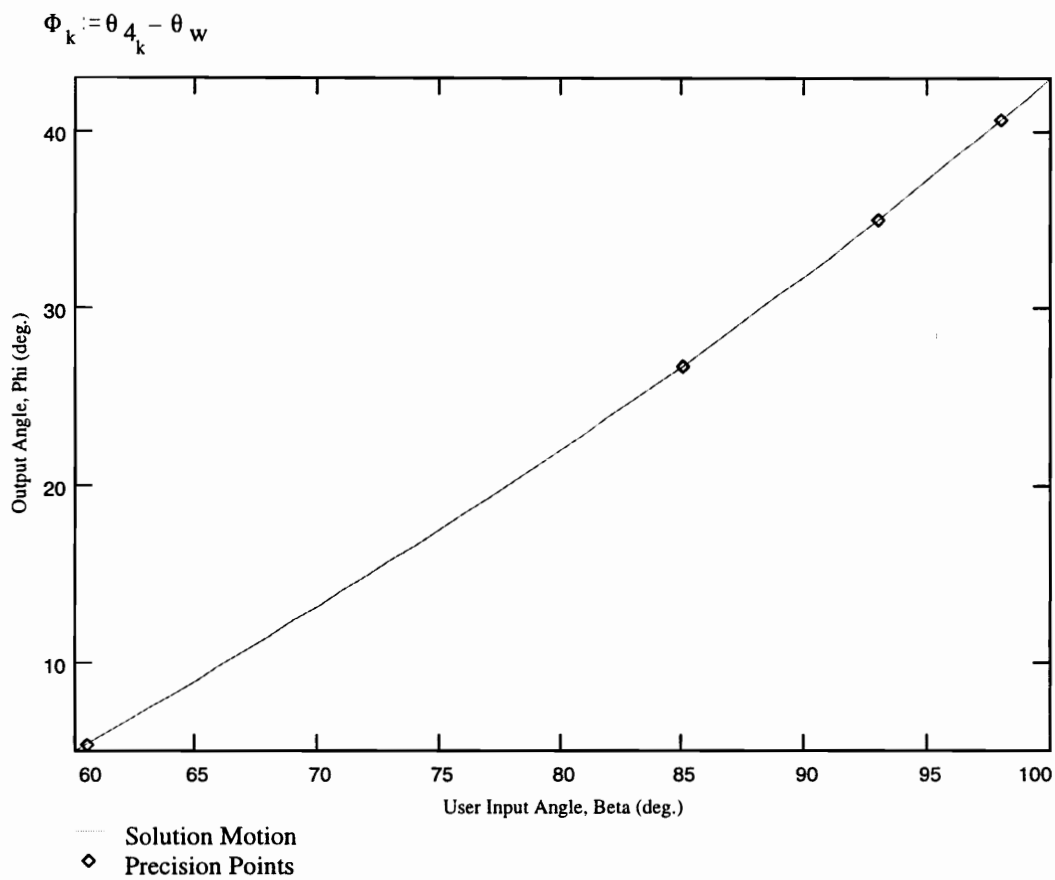


Figure A-6, Function Generation

Calculate Resistance Curve, Internal Coupler Force and Pivot Bearing Forces

$$\begin{pmatrix} \Gamma_{4_k} \\ \Gamma_{3_k} \end{pmatrix} := \begin{pmatrix} l_4 \cdot \cos(\theta_{4_k}) & -l_3 \cdot \cos(\theta_{3_k}) \\ l_4 \cdot \sin(\theta_{4_k}) & -l_3 \cdot \sin(\theta_{3_k}) \end{pmatrix}^{-1} \cdot \begin{pmatrix} l_2 \cdot \cos(\theta_{2_k}) \\ l_2 \cdot \sin(\theta_{2_k}) \end{pmatrix} \quad R_k := \frac{l_w}{l_{in}} \cdot \Gamma_{4_k} \cdot \cos(\Phi_k)$$

$$F_{3_k} := \frac{l_{in}}{l_2} \cdot \frac{R_k}{\sin(\theta_{2_k} - \theta_{3_k})}$$

$$Bin_k := \sqrt{\left(R_k \cdot \sin(\beta_k) - F_{3_k} \cdot \cos(\theta_{3_k})\right)^2 + \left(R_k \cdot \cos(\beta_k) + F_{3_k} \cdot \sin(\theta_{3_k})\right)^2}$$

$$Bout_k := \sqrt{\left(F_{3_k} \cdot \cos(\theta_{3_k})\right)^2 + \left(F_{3_k} \cdot \sin(\theta_{3_k}) + 1\right)^2}$$

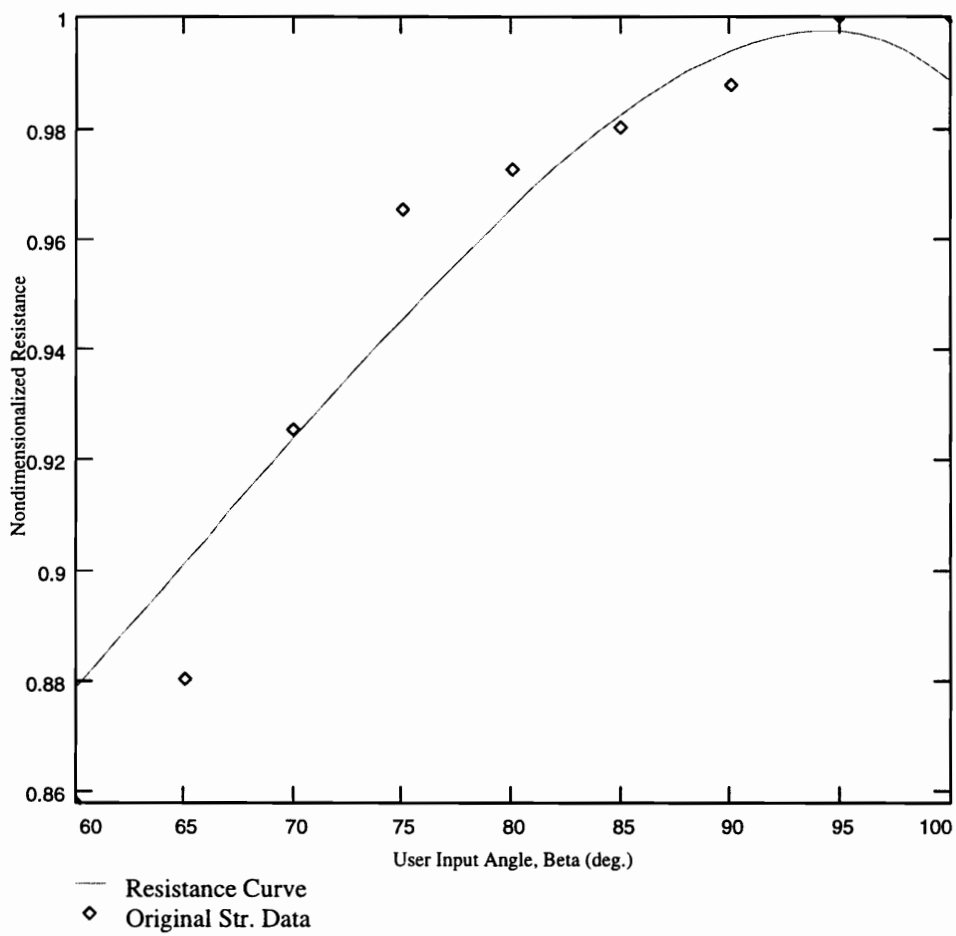


Figure A-7, Resistance Curve of the Soln

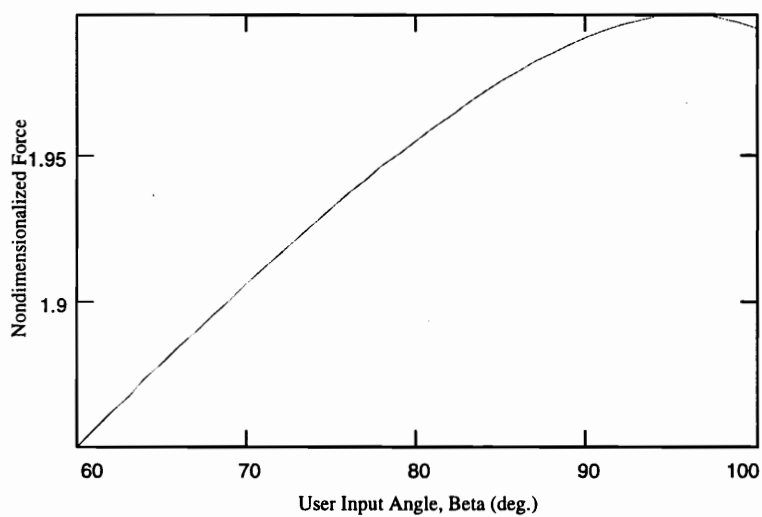


Figure A-8, Internal Coupler Force

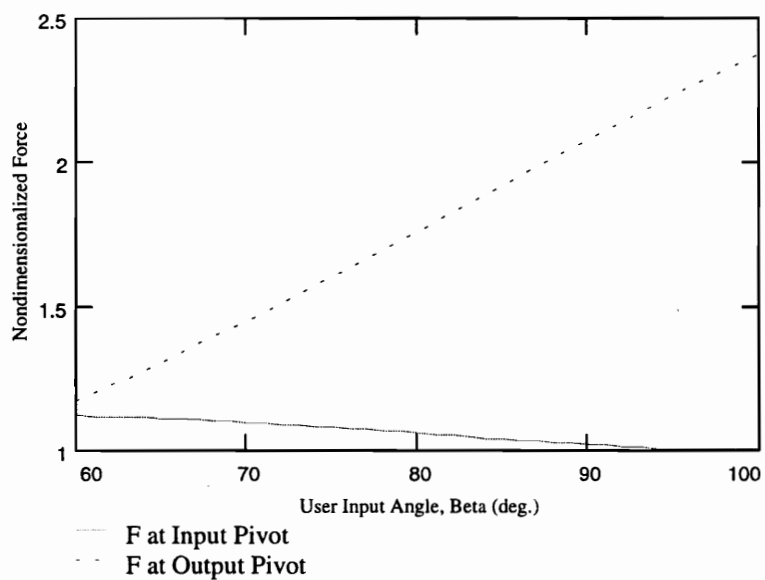


Figure A-9, Bearing Forces

Appendix B, Weighted-Coupler Synthesis Program

This appendix contains a MathSoft Mathcad® version 5.0 program. The program synthesizes weighted-coupler four-link mechanisms by the method developed in Chapter 4. The design synthesized is summarized as an example at the end of that chapter. Textual comments are in **boldface**.

Weighted-Coupler-Link Four-Bar Synthesis

Mathcad model by: R. R. Soper

Created on MathSoft Mathcad version 5

Problem Setup

degree := 3 The degree of the polynomial fit to the input strength curve data

Strength Curve Data:

$x := \begin{bmatrix} 50 \\ 52 \\ 54 \\ 56 \\ 58 \\ 60 \\ 62 \\ 64 \\ 66 \end{bmatrix} \cdot \text{deg}$	$y := \begin{bmatrix} 80 \\ 85 \\ 90 \\ 93 \\ 95 \\ 98 \\ 99 \\ 99.5 \\ 100 \end{bmatrix} \cdot \%$
--	---

Discrete Data Points. A polynomial of degree "degree" will be fit to the data in order to develop a functional relationship

$\theta_{\min} := \min(x)$	$\theta_{\min} = 50 \cdot \text{deg}$
$\theta_{\max} := \max(x)$	$\theta_{\max} = 66 \cdot \text{deg}$

These are the extents of the input data points. They are used as integration limits below.

$N := \text{length}(x)$	$N = 9$
-------------------------	---------

$m := 0..N - 1$

Setting up matrix operations

Curve Fitting

(Matrix Least Squares method, using the pseudo-inverse)

$k := 1 \dots \text{degree}$

$X_{m,0} := 1$

$X^{<k>} := \overrightarrow{(x^k)}$

Fills the k^{th} column with the vectorized values of x^k .

$b := (X^T \cdot X)^{-1} \cdot (X^T \cdot y)$

LEAST SQUARE POLYNOMIAL COEFFICIENTS

$$b = \begin{bmatrix} -6.072 \\ 16.58 \\ -12.826 \\ 3.265 \end{bmatrix}$$

$$S(\beta) := b_0 + \sum_k b_k \cdot \beta^k$$

The nondimensional strength curve function

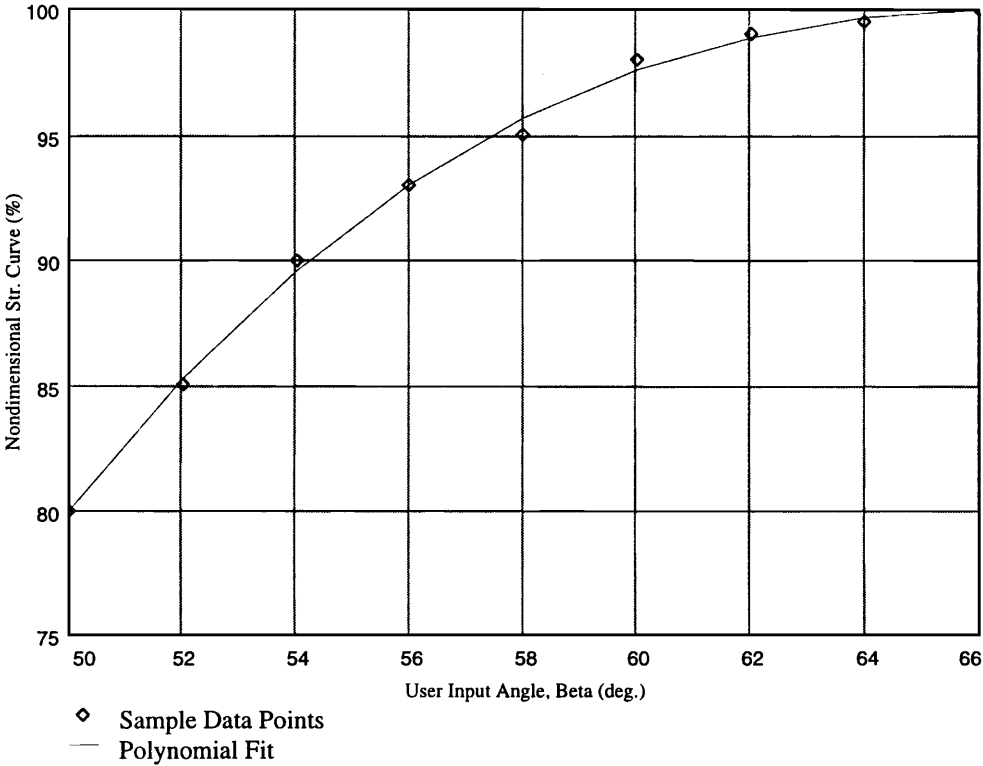


Figure B-1, Strength Curve Data

Input start angle and precision point locations:

$$\beta := \begin{bmatrix} \theta_{\min} \\ 50.5\text{-deg} \\ 52\text{-deg} \\ 58\text{-deg} \\ 65\text{-deg} \\ \theta_{\max} \end{bmatrix}$$

$$\beta = \begin{bmatrix} 50 \\ 50.5 \\ 52 \\ 58 \\ 65 \\ 66 \end{bmatrix} \cdot \text{deg}$$

β_0 is the handle start angle. $\beta_1 - \beta_4$ are four "Precision Points" in the handle angle.

$$q := 1..5$$

$S(\beta_q)$
0.814
0.852
0.956
0.999
1

$$A_{R_q} := \int_{\beta_0}^{\beta_q} S(\beta) d\beta$$

$$A_R = \begin{bmatrix} 0 \\ 40.341 \\ 165.379 \\ 711.781 \\ 1.4 \cdot 10^3 \\ 1.5 \cdot 10^3 \end{bmatrix} \cdot \text{deg} \cdot \%$$

A_R is the area under the strength curve for the values of β given above. This is a nondimensional measure of the input work.

Knowns: $l_{in} := 35$ The length of the handle.

Free parameter choices:

$l_w := 35$ $\Phi_0 := -15\text{-deg}$

$\theta_{in} := 55\text{-deg}$ $l_2 := 10$

The length of the weight stack lever arm, input link length, input offset angle and the start angle for the weight stack.

Synthesis Section

$$\Phi_q := \text{asin} \left[\frac{l_{in}}{l_w} \cdot A_{R_q} + \sin(\Phi_0) + \frac{l_2}{l_w} \cdot (\sin(\beta_0 - \theta_{in}) - \sin(\beta_q - \theta_{in})) \right]$$

$$\Phi = \begin{bmatrix} -15 \\ -14.73 \\ -13.881 \\ -10.046 \\ -5.105 \\ -4.384 \end{bmatrix} \cdot \text{deg}$$

The four position body guidance problem:

n := 2..4 'n' is the number of the precision points.

$$\delta_n := l_2 \cdot e^{i \cdot (-\theta_{in})} \cdot (e^{i \cdot \beta_n} - e^{i \cdot \beta_1})$$

δ is a vector (complex valued).

δ_n
0.017+ 0.261j
0.017+ 1.308j
-0.121+ 2.521j

$$\alpha_n := \Phi_n - \Phi_1$$

α_n
deg
0.849
4.684
9.625

α is the relative rotation of an imaginary body between precision points.

QUASI-LOOP-CLOSURE EQUATION

$$\Delta_2 := \left[\begin{bmatrix} e^{i \cdot \alpha_3} - 1 & \delta_3 \\ e^{i \cdot \alpha_4} - 1 & \delta_4 \end{bmatrix} \right]$$

$$\Delta_2 = 0.013 - 0.003j$$

$$\Delta_3 := \left[\begin{bmatrix} e^{i \cdot \alpha_2} - 1 & \delta_2 \\ e^{i \cdot \alpha_4} - 1 & \delta_4 \end{bmatrix} \right]$$

$$\Delta_3 = -0.007 + 0.001j$$

Δ 's are complex valued vector coefficients in an equation resembling loop closure in ψ .

$$\Delta_4 := \left[\begin{array}{cc} i \cdot \alpha_2 - 1 & \delta_2 \\ e & \end{array} \right] \quad \Delta_4 = 0.002 - 4.157 \cdot 10^{-4} j$$

$$\Delta_1 := -\Delta_2 - \Delta_3 - \Delta_4 \quad \Delta_1 = -0.009 + 0.002j$$

Choose a range for iteration:

$\psi_2 := -1.25\text{-deg}, -1.5\text{-deg} \dots 15\text{-deg}$ **Iterating on ψ_2 yields a solution set of all four bar linkages which achieve the precision point values given above.**

Possible values of ψ_2 are 0 to 360 degrees. Each value will yield two solutions for the problem, a forward- and cross-closure solution. The second solutions may be viewed by changing the sign of the quadratic equation below.

Solving the quasi-loop closure problem:

$$\Omega_1 := \arg(\Delta_1) \quad \Omega_2(\psi_2) := \psi_2 + \arg(\Delta_2)$$

$$r1 := -\left(\text{Re}(\Delta_1)^2 + \text{Im}(\Delta_1)^2\right)^{.5} \quad r2 := \left(\text{Re}(\Delta_2)^2 + \text{Im}(\Delta_2)^2\right)^{.5}$$

$$r3 := \left(\text{Re}(\Delta_3)^2 + \text{Im}(\Delta_3)^2\right)^{.5} \quad r4 := -\left(\text{Re}(\Delta_4)^2 + \text{Im}(\Delta_4)^2\right)^{.5}$$

$$A(\psi_2) := r3^2 - r1^2 - r2^2 - r4^2 + 2 \cdot r1 \cdot r2 \cdot \cos(\Omega_2(\psi_2) - \Omega_1) + 2 \cdot r1 \cdot r4 - 2 \cdot r2 \cdot r4 \cdot \cos(\Omega_2(\psi_2) - \Omega_1)$$

$$B(\psi_2) := 4 \cdot r2 \cdot r4 \cdot \sin(\Omega_2(\psi_2) - \Omega_1)$$

$$C(\psi_2) := r3^2 - r1^2 - r2^2 - r4^2 + 2 \cdot r1 \cdot r2 \cdot \cos(\Omega_2(\psi_2) - \Omega_1) - 2 \cdot r1 \cdot r4 + 2 \cdot r2 \cdot r4 \cdot \cos(\Omega_2(\psi_2) - \Omega_1)$$

$$t(\psi_2) := \frac{-B(\psi_2) - \sqrt{B(\psi_2)^2 - 4 \cdot A(\psi_2) \cdot C(\psi_2)}}{2 \cdot A(\psi_2)}$$

SOLUTION SWITCHING:
Changing the sign on the quadratic equation here will result in the second set of solutions.

$$\Omega_4(\psi_2) := 2 \cdot \text{atan}(t(\psi_2)) + \Omega_1 \quad \psi_4(\psi_2) := \Omega_4(\psi_2) - \arg(\Delta_2)$$

$$T(\psi_2) := \frac{e^{i \cdot \psi_4(\psi_2)} - 1}{e^{i \cdot \psi_2} - 1}$$

$$Z(\psi_2) := \frac{\delta_4 - T(\psi_2) \cdot \delta_2}{\left[e^{i \cdot \alpha_4} - 1 - T(\psi_2) \cdot (e^{i \cdot \alpha_2} - 1) \right]}$$

$$M(\psi_2) := \frac{\delta_2 - (e^{i \cdot \alpha_2} - 1) \cdot Z(\psi_2)}{e^{i \cdot \psi_2} - 1}$$

SOLUTION DYAD Vectors **Z** and **M** are the solution links to the body guidance problem. In body-guidance space, link **Z** is the "rotating" link and link **M** is the "fixed" link.

$$Z_{\text{prime}}(\psi_2) := -Z(\psi_2)$$

$$M_{\text{prime}}(\psi_2) := -M(\psi_2)$$

Links 3 and 4 correspond to links Zprime and Mprime respectively.

$$I_3(\psi_2) := \left(\text{Re}(Z(\psi_2))^2 + \text{Im}(Z(\psi_2))^2 \right)^{.5}$$

$$I_4(\psi_2) := \left(\text{Re}(M(\psi_2))^2 + \text{Im}(M(\psi_2))^2 \right)^{.5}$$

BURMESTER POINT PAIRS

$$P1 := l_2 \cdot e^{i \cdot (\beta_1 - \theta_{in})} \qquad P2(\psi_2) := P1 + Zprime(\psi_2) \qquad P3(\psi_2) := P2(\psi_2) + Mprime(\psi_2)$$

$$l_1(\psi_2) := \left(\text{Re}(P3(\psi_2))^2 + \text{Im}(P3(\psi_2))^2 \right)^{.5} \qquad \chi(\psi_2) := \text{arg}(P3(\psi_2))$$

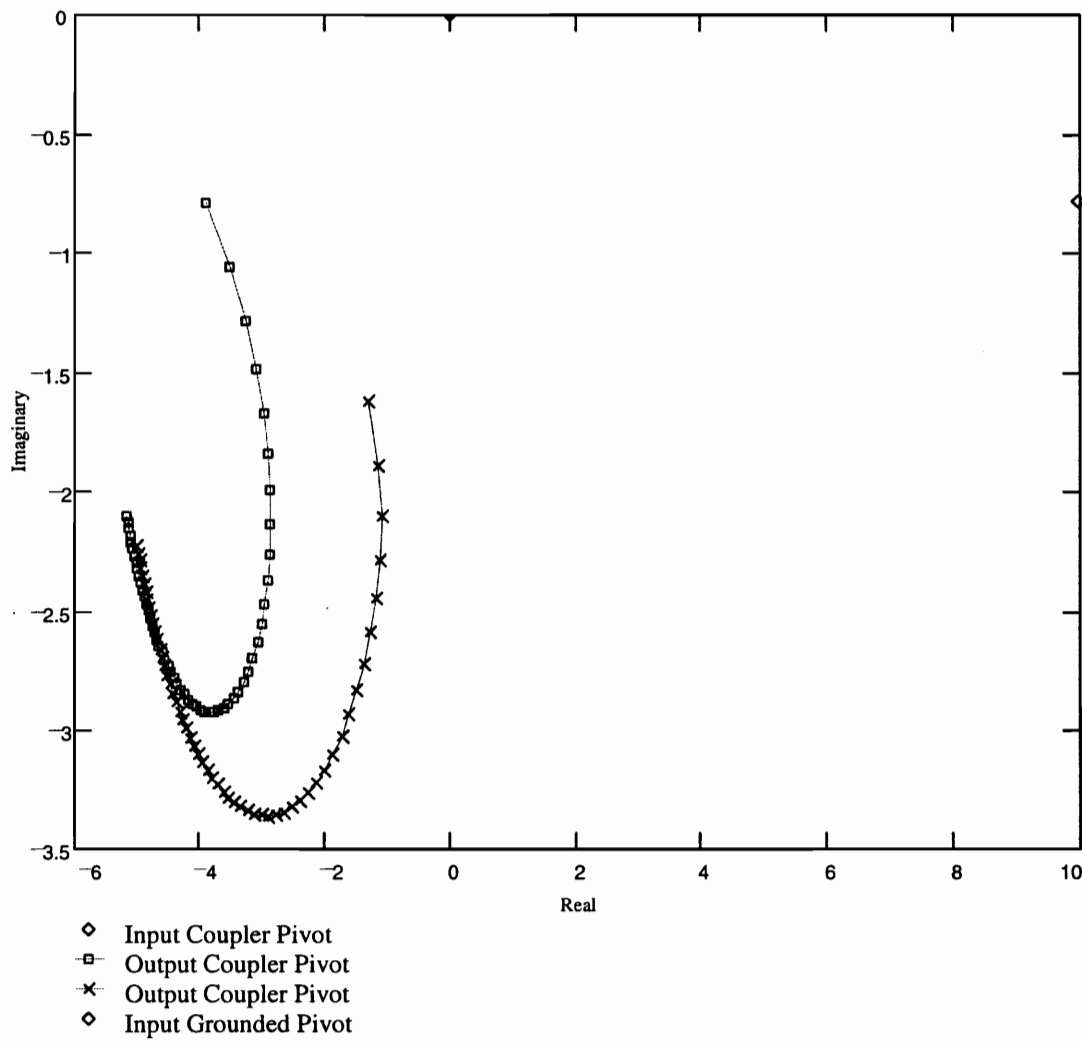


Figure B-2, Burmester Curves

CHOOSING THE SOLUTION

Choose a solution: $\psi_2 := -2.5 \cdot \text{deg}$

$$l_1 := l_1(\psi_2) \quad l_3 := l_3(\psi_2) \quad l_4 := l_4(\psi_2) \quad \chi := \chi(\psi_2)$$

$$\theta_w := \arg(\text{Zprime}(\psi_2)) - \Phi_1$$

THE SOLUTION DESIGN PARAMETERS Fixed links and angles for the solution

$$l_1 = 2.893 \quad l_{in} = 35 \quad \theta_{in} = 55 \cdot \text{deg} \quad \chi = -116.302 \cdot \text{deg}$$

$$l_2 = 10 \quad l_w = 35 \quad \theta_w = -160.567 \cdot \text{deg}$$

$$l_3 = 12.926$$

$$l_4 = 1.795$$

Analysis Section

Now the solution fourbar linkage is plotted:

$$\begin{pmatrix} x_1 \\ y_1 \end{pmatrix} := \begin{pmatrix} 0 \\ 0 \end{pmatrix} \quad \begin{pmatrix} x_2 \\ y_2 \end{pmatrix} := \begin{pmatrix} \text{Re}(P1) \\ \text{Im}(P1) \end{pmatrix} \quad \begin{pmatrix} x_3 \\ y_3 \end{pmatrix} := \begin{pmatrix} \text{Re}(P2(\psi_2)) \\ \text{Im}(P2(\psi_2)) \end{pmatrix} \quad \begin{pmatrix} x_4 \\ y_4 \end{pmatrix} := \begin{pmatrix} \text{Re}(P3(\psi_2)) \\ \text{Im}(P3(\psi_2)) \end{pmatrix}$$

$$\begin{pmatrix} x_{in} \\ y_{in} \end{pmatrix} := \begin{pmatrix} l_{in} \cdot \cos(\beta_1) \\ l_{in} \cdot \sin(\beta_1) \end{pmatrix} \quad \begin{pmatrix} x_{out} \\ y_{out} \end{pmatrix} := \begin{pmatrix} l_2 \cdot \cos(\beta_1 - \theta_{in}) + l_w \cdot \cos(\Phi_1) \\ l_2 \cdot \sin(\beta_1 - \theta_{in}) + l_w \cdot \sin(\Phi_1) \end{pmatrix}$$

$$m_1 := \frac{y_2 - y_1}{x_2 - x_1} \quad m_2 := \frac{y_3 - y_2}{x_3 - x_2} \quad m_3 := \frac{y_4 - y_3}{x_4 - x_3} \quad m_4 := \frac{y_1 - y_4}{x_1 - x_4} \quad m_{in} := \frac{y_{in} - y_1}{x_{in} - x_1}$$

$$m_{out} := \frac{y_{out} - y_2}{x_{out} - x_2} \quad \text{step1} := \frac{x_2 - x_1}{10} \quad \text{step2} := \frac{x_3 - x_2}{10} \quad \text{step3} := \frac{x_4 - x_3}{10}$$

$$\text{step4} := \frac{x_1 - x_4}{10} \quad \text{stepin} := \frac{x_{in} - x_1}{10} \quad \text{stepout} := \frac{x_{out} - x_2}{10}$$

$$\text{rangea} := x_1, x_1 + \text{step1} .. x_2 \quad \text{rangee} := x_3, x_3 + \text{step3} .. x_4 \quad \text{rangee} := x_1, x_1 + \text{stepin} .. x_{in}$$

$$\text{rangeb} := x_2, x_2 + \text{step2} .. x_3 \quad \text{ranged} := x_4, x_4 + \text{step4} .. x_1 \quad \text{rangee} := x_2, x_2 + \text{stepout} .. x_{out}$$

$$\text{drawlinka}(\text{rangea}) := m_1 \cdot (\text{rangea} - x_1) + y_1 \quad \text{drawlinkc}(\text{rangee}) := m_3 \cdot (\text{rangee} - x_3) + y_3$$

$$\text{drawlinkb}(\text{rangeb}) := m_2 \cdot (\text{rangeb} - x_2) + y_2 \quad \text{drawlinkd}(\text{ranged}) := m_4 \cdot (\text{ranged} - x_4) + y_4$$

$$\text{drawlinke}(\text{rangee}) := m_{in} \cdot (\text{rangee} - x_1) + y_1$$

$$\text{drawlinkf}(\text{rangee}) := m_{out} \cdot (\text{rangee} - x_2) + y_2$$

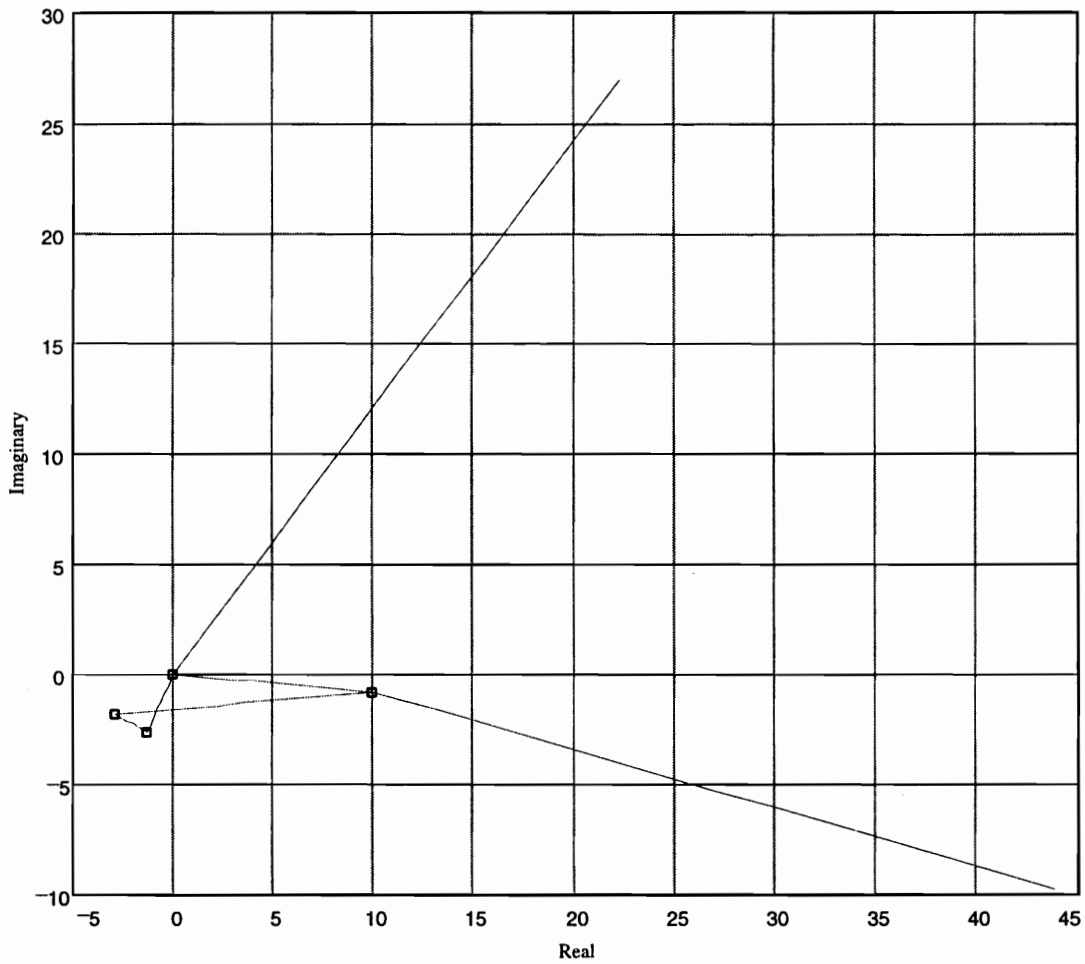


Figure B-3, Solution Linkage

Force analysis

$\xi := -1$

Indicate Closure $\xi = +1$ or -1 (the quadratic equation has two solutions, a "+" root and a "-" root)

$g := 1..4$ $b_0 := \beta_0$ $b_g := \beta_g$ $p_g := \Phi_g$ $Y1_m := y_m$ $Y2_m := x_m$ **Retaining precision point values**

$k := 0, 1..32$ $\beta_k := b_0 + \frac{k}{2} \cdot \text{deg}$ $\theta_{2_k} := \beta_k - \theta_{in}$ **Iterating**

$$E_{3_k} := 2 \cdot l_2 \cdot l_3 \cdot \sin(\theta_{2_k}) - 2 \cdot l_3 \cdot l_1 \cdot \sin(\chi) \quad F_{3_k} := 2 \cdot l_2 \cdot l_3 \cdot \cos(\theta_{2_k}) - 2 \cdot l_3 \cdot l_1 \cdot \cos(\chi)$$

$$G_{3_k} := l_2^2 + l_3^2 + l_1^2 - l_4^2 - 2 \cdot l_2 \cdot l_1 \cdot \cos(\chi) \cdot \cos(\theta_{2_k}) - 2 \cdot l_2 \cdot l_1 \cdot \sin(\chi) \cdot \sin(\theta_{2_k})$$

$$N_{3_k} := -E_{3_k} + \xi \cdot \sqrt{(E_{3_k})^2 + (F_{3_k})^2 - (G_{3_k})^2} \quad \theta_{3_k} := 2 \cdot \text{atan} \left(\frac{N_{3_k}}{G_{3_k} - F_{3_k}} \right)$$

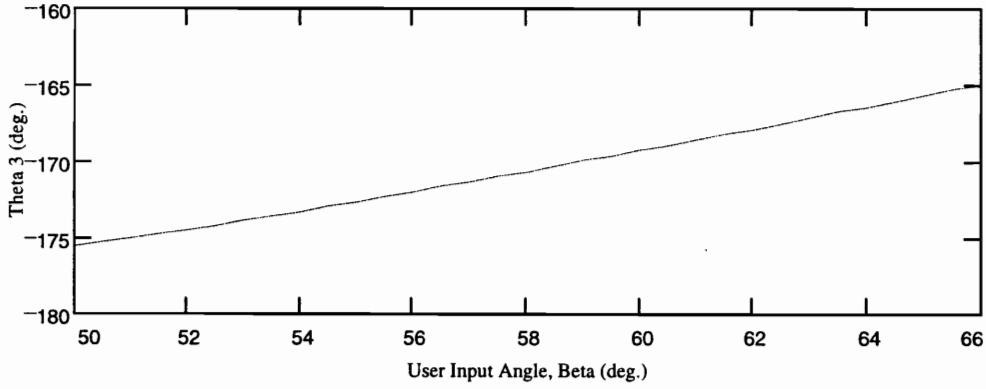


Figure B-4, Theta 3 vs. Beta

$$E_{4_k} := -2 \cdot l_2 \cdot l_4 \cdot \sin(\theta_{2_k}) + 2 \cdot l_4 \cdot l_1 \cdot \sin(\chi) \quad F_{4_k} := -2 \cdot l_2 \cdot l_4 \cdot \cos(\theta_{2_k}) + 2 \cdot l_4 \cdot l_1 \cdot \cos(\chi)$$

$$G_{4_k} := l_2^2 + l_4^2 + l_1^2 - l_3^2 - 2 \cdot l_2 \cdot l_1 \cdot \cos(\chi) \cdot \cos(\theta_{2_k}) - 2 \cdot l_2 \cdot l_1 \cdot \sin(\chi) \cdot \sin(\theta_{2_k})$$

$$N_{4_k} := -E_{4_k} + -\xi \cdot \sqrt{(E_{4_k})^2 + (F_{4_k})^2 - (G_{4_k})^2} \quad \theta_{4_k} := 2 \cdot \text{atan} \left(\frac{N_{4_k}}{G_{4_k} - F_{4_k}} \right)$$

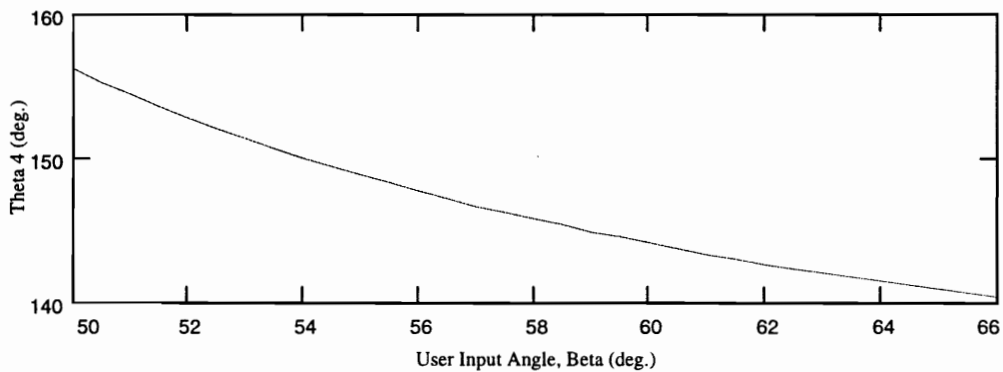


Figure B-5, Theta 4 vs. Beta

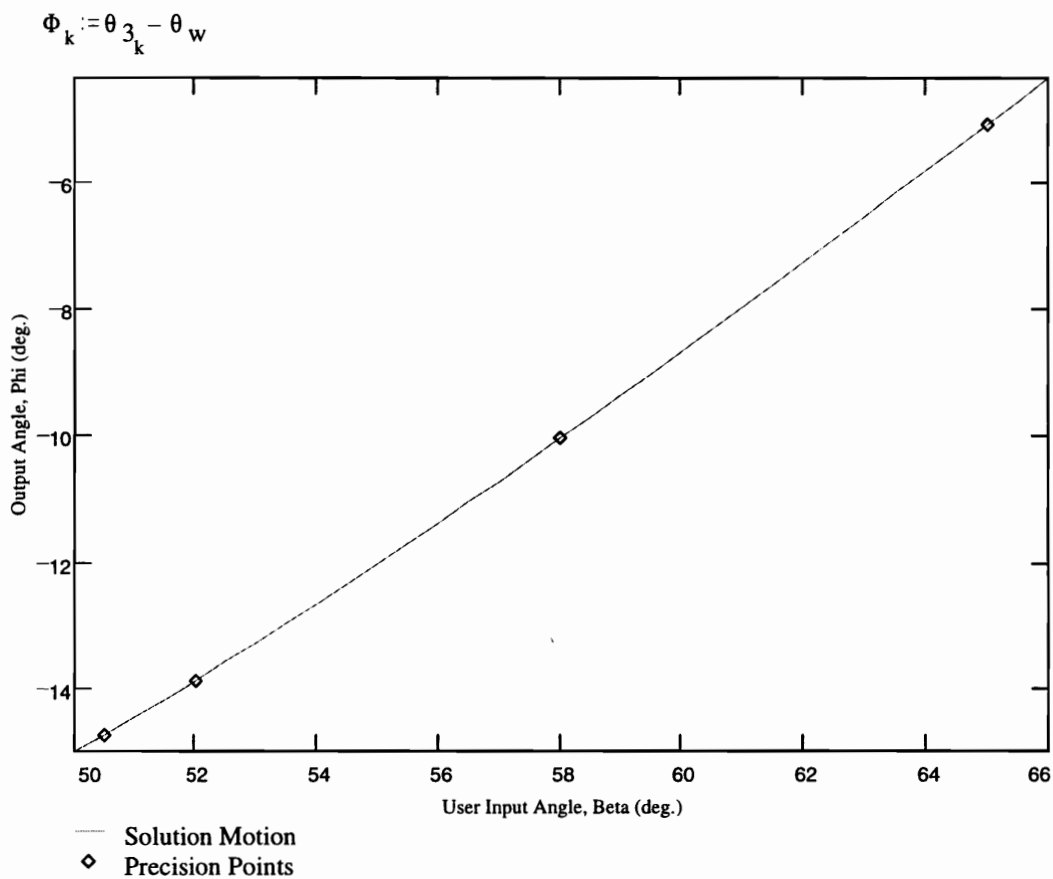


Figure B-6, Output Angle vs. Beta

Calculate Resistance Curve, Internal Coupler Force and Pivot Bearing Forces

$$\begin{pmatrix} \Gamma_{4_k} \\ \Gamma_{3_k} \end{pmatrix} := \begin{pmatrix} l_4 \cdot \cos(\theta_{4_k}) & -l_3 \cdot \cos(\theta_{3_k}) \\ l_4 \cdot \sin(\theta_{4_k}) & -l_3 \cdot \sin(\theta_{3_k}) \end{pmatrix}^{-1} \cdot \begin{pmatrix} l_2 \cdot \cos(\theta_{2_k}) \\ l_2 \cdot \sin(\theta_{2_k}) \end{pmatrix}$$

$$R_k := \left(\frac{l_2}{l_{in}} \cdot \cos(\theta_{2_k}) \right) + \frac{l_w}{l_{in}} \cdot \Gamma_{3_k} \cdot \cos(\theta_{3_k} - \theta_w)$$

$$F_{4_k} := \frac{l_w}{l_3} \cdot \frac{\cos(\Phi_k)}{\sin(\theta_{3_k} + \theta_{4_k})} \quad \text{Bout}_k := |F_{4_k}|$$

$$\text{Bin}_k := \sqrt{\left(F_{4_k} \cdot \cos(\theta_{4_k}) + R_k \cdot \sin(\beta_k) \right)^2 + \left[\left(1 - R_k \cdot \cos(\beta_k) \right) + F_{4_k} \cdot \sin(\theta_{4_k}) \right]^2}$$

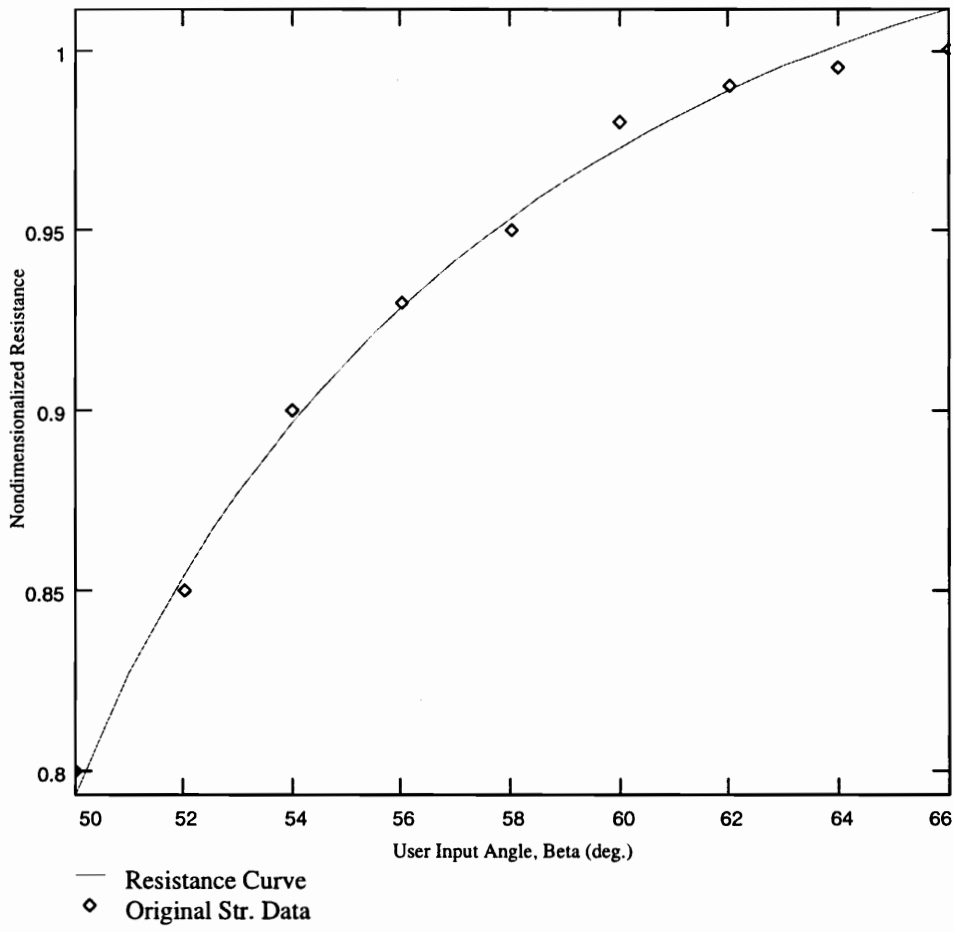


Figure B-7, Resistance Curve of the Soln

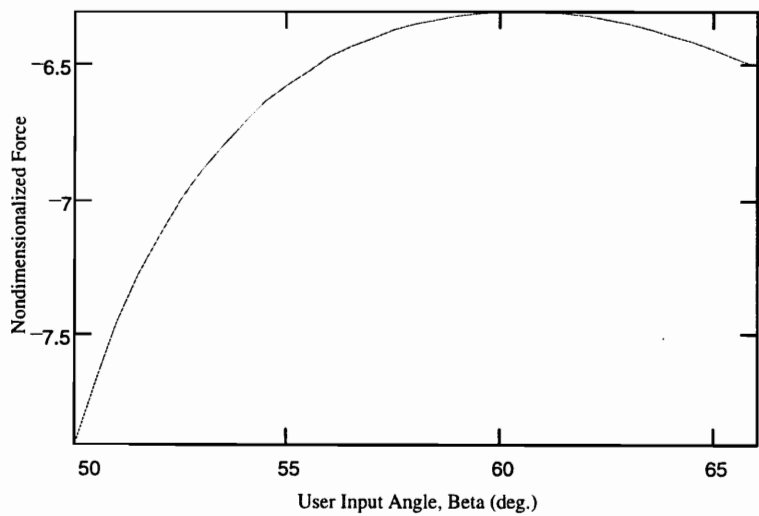


Figure B-8, Internal Coupler Force

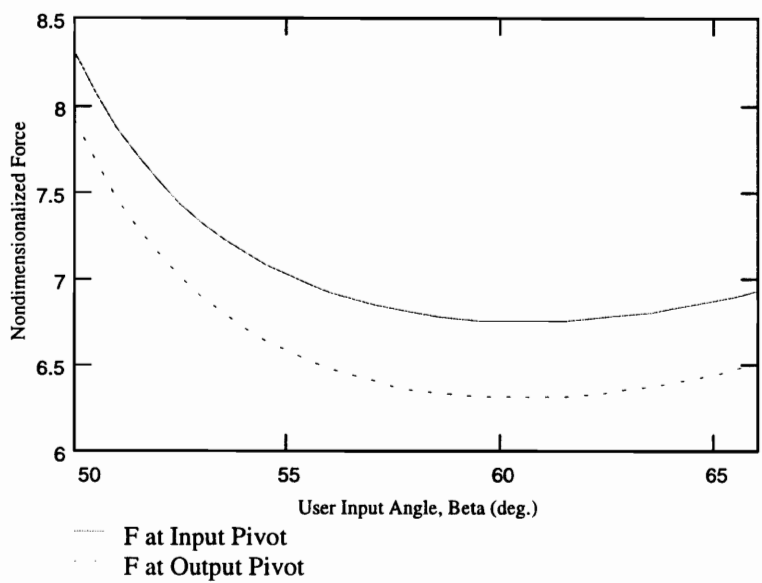


Figure B-9, Bearing Forces

Appendix C, Derivation of Influence Coefficients

This appendix summarizes the derivation of closed-form equations for the influence coefficients. The influence coefficients are the partial derivatives of the resistance curve with respect to each of the design parameters. Use of the influence coefficients for sensitivity analysis is discussed in Chapter 5. Appendices D and E are MathSoft Mathcad® programs which calculate the influence coefficients for the weighted-grounded-link case and the weighted-coupler-link case respectively.

C.1 Partial Derivatives of the Linkage Angles

C.1.1 Partial of θ_3 with Respect to the Design Parameters

Loop-closure gives us the following closed-form equations for θ_3

$$\theta_3 = 2 \tan^{-1} \left(\frac{N_3}{G_3 - F_3} \right), \quad (\text{C.1a})$$

where

$$N_3 \equiv -E_3 + \xi \sqrt{E_3^2 + F_3^2 - G_3^2}. \quad (\text{C.1b})$$

The values of E_3 , F_3 and G_3 are given in 1.3.1. They are modified here to account for rotation of the ground link, χ

$$E_3 = 2l_2l_3 \sin(\theta_2) - 2l_3l_1 \sin(\chi) \quad (\text{C.2a})$$

$$F_3 = 2l_2l_3 \cos(\theta_2) - 2l_3l_1 \cos(\chi) \quad (\text{C.2b})$$

$$G_3 = l_2^2 + l_3^2 + l_1^2 - l_4^2 - 2l_1l_2 \cos(\theta_2) \cos(\chi) - 2l_2l_1 \sin(\theta_2) \sin(\chi) \quad (C.2c)$$

The eight design parameters which can vary are $l_2, l_3, l_4, l_1, \theta_{in}, \theta_w, l_w$ and χ . Let q denote one of these design parameters, then

$$\frac{\partial}{\partial q} \theta_3 = \frac{2(G_3 - F_3)^2}{(G_3 - F_3)^2 + N_3^2} \frac{\partial}{\partial q} \left[\frac{N_3}{G_3 - F_3} \right]. \quad (C.3)$$

This is equal to

$$\frac{\partial}{\partial q} \theta_3 = H_3 \left[\frac{1}{G_3 - F_3} \left(\frac{\partial N_3}{\partial q} \right) - \frac{N_3}{(G_3 - F_3)^2} \left(\frac{\partial (G_3 - F_3)}{\partial q} \right) \right], \quad (C.4a)$$

where

$$H_3 \equiv \frac{2(G_3 - F_3)^2}{N_3^2 + (G_3 - F_3)^2}. \quad (C.4b)$$

Furthermore, define

$$I_3 \equiv \frac{\partial N_3}{\partial q} = -\frac{\partial}{\partial q} E_3 + \frac{\xi \left[E_3 \frac{\partial E_3}{\partial q} + F_3 \frac{\partial F_3}{\partial q} - G_3 \frac{\partial G_3}{\partial q} \right]}{\left[E_3^2 + F_3^2 - G_3^2 \right]^{\frac{1}{2}}}. \quad (C.5)$$

So

$$\frac{\partial}{\partial q} \theta_3 = H_3 \left[\frac{1}{G_3 - F_3} (I_3) - \frac{N_3}{(G_3 - F_3)^2} \left(\frac{\partial G_3}{\partial q} - \frac{\partial F_3}{\partial q} \right) \right]. \quad (C.6)$$

It only remains to find the partials of E_3, F_3 and G_3 with respect to each of the parameters.

With these and Eq. (C.6), we can find the partial derivative of θ_3 with respect to any parameter.

l_2 :

$$\frac{\partial E_3}{\partial l_2} = 2l_3 \sin(\theta_2) \quad (C.7a)$$

$$\frac{\partial F_3}{\partial l_2} = 2l_3 \cos(\theta_2) \quad (\text{C.7b})$$

$$\frac{\partial G_3}{\partial l_2} = 2l_2 - 2l_1 \cos(\theta_2) \cos(\chi) - 2l_1 \sin(\theta_2) \sin(\chi) \quad (\text{C.7c})$$

$$l_3: \quad \frac{\partial E_3}{\partial l_3} = 2l_2 \sin(\theta_2) - 2l_1 \sin(\chi) \quad (\text{C.8a})$$

$$\frac{\partial F_3}{\partial l_3} = 2l_2 \cos(\theta_2) - 2l_1 \cos(\chi) \quad (\text{C.8b})$$

$$\frac{\partial G_3}{\partial l_3} = 2l_3 \quad (\text{C.8c})$$

$$l_4: \quad \frac{\partial E_3}{\partial l_4} = 0 \quad (\text{C.9a})$$

$$\frac{\partial F_3}{\partial l_4} = 0 \quad (\text{C.9b})$$

$$\frac{\partial G_3}{\partial l_4} = -2l_4 \quad (\text{C.9b})$$

$$l_1: \quad \frac{\partial E_3}{\partial l_1} = -2l_3 \sin(\chi) \quad (\text{C.10a})$$

$$\frac{\partial F_3}{\partial l_1} = -2l_3 \cos(\chi) \quad (\text{C.10b})$$

$$\frac{\partial G_3}{\partial l_1} = -2l_1 - 2l_2 \cos(\theta_2) \cos(\chi) - 2l_2 \sin(\theta_2) \sin(\chi) \quad (\text{C.10c})$$

$$\theta_{in}: \quad \frac{\partial E_3}{\partial \theta_{in}} = -2l_2 l_3 \cos(\theta_2) \quad (\text{C.11a})$$

$$\frac{\partial F_3}{\partial \theta_{in}} = 2l_2 l_3 \sin(\theta_2) \quad (C.11b)$$

$$\frac{\partial G_3}{\partial \theta_{in}} = -2l_1 l_2 \sin(\theta_2) \cos(\chi) + 2l_2 l_1 \cos(\theta_2) \sin(\chi) \quad (C.11c)$$

$$\theta_w: \quad \frac{\partial E_3}{\partial \theta_w} = \frac{\partial F_3}{\partial \theta_w} = \frac{\partial G_3}{\partial \theta_w} = 0 \quad (C.12)$$

(this justifies our expectation that $\frac{\partial \theta_3}{\partial \theta_w} = 0$, see Chapter 5)

$$l_w: \quad \frac{\partial E_3}{\partial l_w} = \frac{\partial F_3}{\partial l_w} = \frac{\partial G_3}{\partial l_w} = 0 \quad (C.13)$$

(this justifies our expectation that $\frac{\partial \theta_3}{\partial l_w} = 0$, see Chapter 5)

$$\chi: \quad \frac{\partial E_3}{\partial \chi} = -2l_3 l_1 \cos(\chi) \quad (C.14a)$$

$$\frac{\partial F_3}{\partial \chi} = 2l_3 l_1 \sin(\chi) \quad (C.14b)$$

$$\frac{\partial G_3}{\partial \chi} = 2l_2 l_1 \cos(\theta_2) \sin(\chi) - 2l_2 l_1 \sin(\theta_2) \cos(\chi) \quad (C.14c)$$

C.1.2 Partial of θ_4 with Respect to the Design Parameters

The derivation here is analogous to that for θ_3 above.

$$\theta_4 = 2 \tan^{-1} \left(\frac{N_4}{G_4 - F_4} \right), \quad (C.15a)$$

$$\text{where} \quad N_4 \equiv -E_4 - \xi \sqrt{E_4^2 + F_4^2 - G_4^2}. \quad (C.15b)$$

$$E_4 = 2l_1l_4 \sin(\chi) - 2l_4l_2 \sin(\theta_2) \quad (\text{C.16a})$$

$$F_4 = 2l_1l_4 \cos(\chi) - 2l_4l_2 \cos(\theta_2) \quad (\text{C.16b})$$

$$G_4 = l_1^2 + l_4^2 + l_2^2 - l_3^2 - 2l_1l_2 \cos(\chi)\cos(\theta_2) - 2l_1l_2 \sin(\chi)\sin(\theta_2) \quad (\text{C.16c})$$

After manipulations analogous to those above, we have

$$\frac{\partial}{\partial q} \theta_4 = H_4 \left[\frac{1}{G_4 - F_4} (I_4) - \frac{N_4}{(G_4 - F_4)^2} \left(\frac{\partial G_4}{\partial q} - \frac{\partial F_4}{\partial q} \right) \right], \quad (\text{C.17a})$$

with
$$H_4 \equiv \frac{2(G_4 - F_4)^2}{N_4^2 + (G_4 - F_4)^2}, \quad (\text{C.17b})$$

and
$$I_4 \equiv \frac{\partial N_4}{\partial q} = -\frac{\partial}{\partial q} E_4 - \frac{\xi \left[E_4 \frac{\partial E_4}{\partial q} + F_4 \frac{\partial F_4}{\partial q} - G_4 \frac{\partial G_4}{\partial q} \right]}{\left[E_4^2 + F_4^2 - G_4^2 \right]^{\frac{1}{2}}}. \quad (\text{C.17c})$$

The solution to these equations also reduces to the partial derivatives of each of E_4 , F_4 , and G_4 .

$$l_2: \quad \frac{\partial E_4}{\partial l_2} = -2l_4 \sin(\theta_2) \quad (\text{C.18 a})$$

$$\frac{\partial F_4}{\partial l_2} = -2l_4 \cos(\theta_2) \quad (\text{C.18b})$$

$$\frac{\partial G_4}{\partial l_2} = 2l_2 - 2l_1 \cos(\theta_2)\cos(\chi) - 2l_1 \sin(\theta_2)\sin(\chi) \quad (\text{C.18c})$$

$$l_3: \quad \frac{\partial E_4}{\partial l_3} = 0 \quad (\text{C.19a})$$

$$\frac{\partial F_4}{\partial l_3} = 0 \quad (\text{C.19b})$$

$$\frac{\partial G_4}{\partial l_3} = -2l_3 \quad (\text{C.19c})$$

$$l_4: \quad \frac{\partial E_4}{\partial l_4} = 2l_1 \sin(\chi) - 2l_2 \sin(\theta_2) \quad (\text{C.20a})$$

$$\frac{\partial F_4}{\partial l_4} = 2l_1 \cos(\chi) - 2l_2 \cos(\theta_2) \quad (\text{C.20b})$$

$$\frac{\partial G_4}{\partial l_4} = 2l_4 \quad (\text{C.20b})$$

$$l_1: \quad \frac{\partial E_4}{\partial l_1} = 2l_4 \sin(\chi) \quad (\text{C.21a})$$

$$\frac{\partial F_4}{\partial l_1} = 2l_4 \cos(\chi) \quad (\text{C.21b})$$

$$\frac{\partial G_4}{\partial l_1} = 2l_1 - 2l_2 \cos(\theta_2) \cos(\chi) - 2l_2 \sin(\theta_2) \sin(\chi) \quad (\text{C.21c})$$

$$\theta_{in}: \quad \frac{\partial E_4}{\partial \theta_{in}} = 2l_2 l_4 \cos(\theta_2) \quad (\text{C.22a})$$

$$\frac{\partial F_4}{\partial \theta_{in}} = -2l_2 l_4 \sin(\theta_2) \quad (\text{C.22b})$$

$$\frac{\partial G_4}{\partial \theta_{in}} = -2l_1 l_2 \sin(\theta_2) \cos(\chi) + 2l_2 l_1 \cos(\theta_2) \sin(\chi) \quad (\text{C.22c})$$

$$\theta_w: \quad \frac{\partial E_4}{\partial \theta_w} = \frac{\partial F_4}{\partial \theta_w} = \frac{\partial G_4}{\partial \theta_w} = 0 \quad (\text{C.23})$$

(this justifies our expectation that $\frac{\partial \theta_4}{\partial \theta_w} = 0$, see Chapter 5)

$$l_w: \quad \frac{\partial E_4}{\partial l_w} = \frac{\partial F_4}{\partial l_w} = \frac{\partial G_4}{\partial l_w} = 0 \quad (\text{C.24})$$

(this justifies our expectation that $\frac{\partial \theta_4}{\partial l_w} = 0$, see Chapter 5)

$$\chi: \quad \frac{\partial E_4}{\partial \chi} = 2l_4l_1 \cos(\chi) \quad (\text{C.25a})$$

$$\frac{\partial F_4}{\partial \chi} = -2l_4l_1 \sin(\chi) \quad (\text{C.25b})$$

$$\frac{\partial G_4}{\partial \chi} = 2l_2l_1 \cos(\theta_2) \sin(\chi) - 2l_2l_1 \sin(\theta_2) \cos(\chi) \quad (\text{C.25c})$$

C.2 Influence Coefficients for the Weighted-Grounded-Link Case

From velocity analysis, we have that

$$\begin{bmatrix} \omega_4 / \omega_2 \\ \omega_3 / \omega_2 \end{bmatrix} = \begin{bmatrix} l_4 \cos(\theta_4) & -l_3 \cos(\theta_3) \\ l_4 \sin(\theta_4) & -l_3 \sin(\theta_3) \end{bmatrix}^{-1} \cdot \begin{bmatrix} l_2 \cos(\theta_2) \\ l_2 \sin(\theta_2) \end{bmatrix}, \quad (\text{C.26a})$$

$$\text{or} \quad \begin{bmatrix} \omega_4 / \omega_2 \\ \omega_3 / \omega_2 \end{bmatrix} = \frac{\begin{bmatrix} -l_3 \sin(\theta_3) & l_3 \cos(\theta_3) \\ -l_4 \sin(\theta_4) & l_4 \cos(\theta_4) \end{bmatrix}}{-l_3l_4 \cos(\theta_4) \sin(\theta_3) + l_3l_4 \cos(\theta_3) \sin(\theta_4)} \cdot \begin{bmatrix} l_2 \cos(\theta_2) \\ l_2 \sin(\theta_2) \end{bmatrix}. \quad (\text{C.26b})$$

Therefore, we have

$$\omega_4/\omega_2 = \frac{l_2 \sin(\theta_3) \cos(\theta_2) - \cos(\theta_3) \sin(\theta_2)}{l_4 \cos(\theta_4) \sin(\theta_3) - \cos(\theta_3) \sin(\theta_4)}. \quad (C.27)$$

From our analysis in Chapter 2, we have

$$R_g = \frac{F}{W} = \frac{l_w}{l_{in}} \cdot \frac{\omega_4}{\omega_2} \cos(\Phi), \quad (C.28)$$

where the subscript g will denote that the variable is for the weighted-grounded-link case.

Substituting in Eq. (C.27) for the angular velocity ratio

$$R_g = \frac{l_w l_2}{l_{in} l_4} \cdot \left[\frac{\sin(\theta_3) \cos(\theta_2) - \cos(\theta_3) \sin(\theta_2)}{\cos(\theta_4) \sin(\theta_3) - \cos(\theta_3) \sin(\theta_4)} \right] \cos(\theta_4 - \theta_w). \quad (C.29)$$

For simplification, we define

$$R_g = m_g \frac{n_g}{d_g}, \quad (C.30a)$$

where

$$m_g \equiv \frac{l_w l_2}{l_{in} l_4} \cos(\theta_4 - \theta_w), \quad (C.30b)$$

$$n_g \equiv \sin(\theta_3) \cos(\theta_2) - \cos(\theta_3) \sin(\theta_2), \quad (C.30c)$$

$$d_g \equiv \cos(\theta_4) \sin(\theta_3) - \cos(\theta_3) \sin(\theta_4). \quad (C.30d)$$

The influence coefficients are defined as the partial derivative of the resistance curve with respect to each of the design variables, $q = l_2, l_3, l_4, l_l, \theta_{in}, \theta_w, l_w, \chi$. Furthermore, the partial of d_g and n_g with respect to each of the design parameters will be

$$\frac{\partial d_g}{\partial q} = [\sin(\theta_4) \sin(\theta_3) + \cos(\theta_4) \cos(\theta_3)] \cdot \left(\frac{\partial \theta_3}{\partial q} - \frac{\partial \theta_4}{\partial q} \right), \quad (C.31a)$$

$$\text{and} \quad \frac{\partial n_g}{\partial q} = [\sin(\theta_3)\sin(\theta_2) + \cos(\theta_3)\cos(\theta_2)] \cdot \frac{\partial \theta_3}{\partial q}, \quad q \neq \theta_{in}, \quad (\text{C.31b})$$

$$\text{and} \quad \frac{\partial n_g}{\partial \theta_{in}} = [\sin(\theta_3)\sin(\theta_2) + \cos(\theta_3)\cos(\theta_2)] \cdot \left(1 + \frac{\partial \theta_3}{\partial \theta_{in}}\right). \quad (\text{C.31c})$$

$$l_2: \quad \frac{\partial R_g}{\partial l_2} = \frac{R_g}{l_2} + \frac{R_g}{n_g} \cdot \frac{\partial n_g}{\partial l_2} - \frac{R_g}{d_g} \cdot \frac{\partial d_g}{\partial l_2} - R_g \tan(\theta_4 - \theta_w) \frac{\partial \theta_4}{\partial l_2} \quad (\text{C.32})$$

$$l_3: \quad \frac{\partial R_g}{\partial l_3} = \frac{R_g}{n_g} \cdot \frac{\partial n_g}{\partial l_3} - \frac{R_g}{d_g} \cdot \frac{\partial d_g}{\partial l_3} - R_g \tan(\theta_4 - \theta_w) \frac{\partial \theta_4}{\partial l_3} \quad (\text{C.33})$$

$$l_4: \quad \frac{\partial R_g}{\partial l_4} = -\frac{R_g}{l_4} + \frac{R_g}{n_g} \cdot \frac{\partial n_g}{\partial l_4} - \frac{R_g}{d_g} \cdot \frac{\partial d_g}{\partial l_4} - R_g \tan(\theta_4 - \theta_w) \frac{\partial \theta_4}{\partial l_4} \quad (\text{C.34})$$

$$l_1: \quad \frac{\partial R_g}{\partial l_1} = \frac{R_g}{n_g} \cdot \frac{\partial n_g}{\partial l_1} - \frac{R_g}{d_g} \cdot \frac{\partial d_g}{\partial l_1} - R_g \tan(\theta_4 - \theta_w) \frac{\partial \theta_4}{\partial l_1} \quad (\text{C.35})$$

$$\theta_{in}: \quad \frac{\partial R_g}{\partial \theta_{in}} = \frac{R_g}{n_g} \cdot \frac{\partial n_g}{\partial \theta_{in}} - \frac{R_g}{d_g} \cdot \frac{\partial d_g}{\partial \theta_{in}} - R_g \tan(\theta_4 - \theta_w) \frac{\partial \theta_4}{\partial \theta_{in}} \quad (\text{C.36})$$

$$\theta_w: \quad \frac{\partial R_g}{\partial \theta_w} = R_g \tan(\theta_4 - \theta_w) \quad (\text{C.37})$$

$$l_w: \quad \frac{\partial R_g}{\partial l_w} = \frac{R_g}{l_w} \quad (\text{C.38})$$

$$\chi: \quad \frac{\partial R_g}{\partial \chi} = \frac{R_g}{n_g} \cdot \frac{\partial n_g}{\partial \chi} - \frac{R_g}{d_g} \cdot \frac{\partial d_g}{\partial \chi} - R_g \tan(\theta_4 - \theta_w) \frac{\partial \theta_4}{\partial \chi} \quad (\text{C.39})$$

C.3 Influence Coefficients for the Weighted-Coupler-Link Case

From Eq. (C.26) above, we have that

$$\omega_3/\omega_2 = \frac{l_2}{l_3} \left[\frac{\sin(\theta_4)\cos(\theta_2) - \cos(\theta_4)\sin(\theta_2)}{\cos(\theta_4)\sin(\theta_3) - \cos(\theta_3)\sin(\theta_4)} \right]. \quad (\text{C.40})$$

From our analysis in Chapter 2, we have

$$R_c = \frac{F}{W} = \frac{l_2}{l_{in}} \cos(\theta_2) + \frac{l_w}{l_{in}} \cdot \frac{\omega_3}{\omega_2} \cos(\Phi), \quad (\text{C.41})$$

where the subscript c will denote that the variable is for the weighted-coupler case.

Substituting in Eq. (C.40) for the angular velocity ratio

$$R_c = \frac{l_2}{l_{in}} \cos(\theta_2) + \frac{l_w l_2}{l_{in} l_3} \cdot \left[\frac{\sin(\theta_4)\cos(\theta_2) - \cos(\theta_4)\sin(\theta_2)}{\cos(\theta_4)\sin(\theta_3) - \cos(\theta_3)\sin(\theta_4)} \right] \cos(\theta_3 - \theta_w). \quad (\text{C.42})$$

For simplification, we define

$$R_c = A_c + B_c, \quad (\text{C.43a})$$

where

$$A_c \equiv \frac{l_2}{l_{in}} \cos(\theta_2), \quad (\text{C.43b})$$

$$B_c = m_c \frac{n_c}{d_c}, \quad (\text{C.43c})$$

$$m_c \equiv \frac{l_w l_2}{l_{in} l_3} \cos(\theta_3 - \theta_w), \quad (\text{C.43d})$$

$$n_c \equiv \sin(\theta_4)\cos(\theta_2) - \cos(\theta_4)\sin(\theta_2), \quad (\text{C.43e})$$

$$d_c \equiv \cos(\theta_4)\sin(\theta_3) - \cos(\theta_3)\sin(\theta_4). \quad (\text{C.43f})$$

Again, we need the partial derivative of the resistance curve with respect to each of the design variables, $q = l_2, l_3, l_4, l_1, \theta_{in}, \theta_w, l_w, \chi$. The partial of d_c and n_c with respect to each of the design parameters will be

$$\frac{\partial d_c}{\partial q} = [\sin(\theta_4)\sin(\theta_3) + \cos(\theta_4)\cos(\theta_3)] \cdot \left(\frac{\partial \theta_3}{\partial q} - \frac{\partial \theta_4}{\partial q} \right), \quad (C.44a)$$

and
$$\frac{\partial n_c}{\partial q} = [\sin(\theta_4)\sin(\theta_2) + \cos(\theta_4)\cos(\theta_2)] \cdot \frac{\partial \theta_4}{\partial q}, \quad q \neq \theta_{in}, \quad (C.44b)$$

and
$$\frac{\partial n_c}{\partial \theta_{in}} = [\sin(\theta_4)\sin(\theta_2) + \cos(\theta_4)\cos(\theta_2)] \cdot \left(1 + \frac{\partial \theta_4}{\partial \theta_{in}} \right) \quad (C.44c)$$

l_2 :
$$\frac{\partial R_c}{\partial l_2} = \frac{A_c}{l_2} + \frac{B_c}{l_2} + \frac{B_c}{n_c} \cdot \frac{\partial n_c}{\partial l_2} - \frac{B_c}{d_c} \cdot \frac{\partial d_c}{\partial l_2} - B_c \tan(\theta_3 - \theta_w) \frac{\partial \theta_3}{\partial l_2} \quad (C.45)$$

l_3 :
$$\frac{\partial R_c}{\partial l_3} = -\frac{B_c}{l_3} + \frac{B_c}{n_c} \cdot \frac{\partial n_c}{\partial l_3} - \frac{B_c}{d_c} \cdot \frac{\partial d_c}{\partial l_3} - B_c \tan(\theta_3 - \theta_w) \frac{\partial \theta_3}{\partial l_3} \quad (C.46)$$

l_4 :
$$\frac{\partial R_c}{\partial l_4} = \frac{B_c}{n_c} \cdot \frac{\partial n_c}{\partial l_4} - \frac{B_c}{d_c} \cdot \frac{\partial d_c}{\partial l_4} - B_c \tan(\theta_3 - \theta_w) \frac{\partial \theta_3}{\partial l_4} \quad (C.47)$$

l_1 :
$$\frac{\partial R_c}{\partial l_1} = \frac{B_c}{n_c} \cdot \frac{\partial n_c}{\partial l_1} - \frac{B_c}{d_c} \cdot \frac{\partial d_c}{\partial l_1} - B_c \tan(\theta_3 - \theta_w) \frac{\partial \theta_3}{\partial l_1} \quad (C.48)$$

θ_{in} :
$$\frac{\partial R_c}{\partial \theta_{in}} = A_c \tan(\theta_2) + \frac{B_c}{n_c} \cdot \frac{\partial n_c}{\partial \theta_{in}} - \frac{B_c}{d_c} \cdot \frac{\partial d_c}{\partial \theta_{in}} - B_c \tan(\theta_3 - \theta_w) \frac{\partial \theta_3}{\partial \theta_{in}} \quad (C.49)$$

θ_w :
$$\frac{\partial R_c}{\partial \theta_w} = B_c \tan(\theta_3 - \theta_w) \quad (C.50)$$

l_w :
$$\frac{\partial R_c}{\partial l_w} = \frac{B_c}{l_w} \quad (C.51)$$

$$\chi: \quad \frac{\partial R_c}{\partial \chi} = \frac{B_c}{n_c} \cdot \frac{\partial n_c}{\partial \chi} - \frac{B_c}{d_c} \cdot \frac{\partial d_c}{\partial \chi} - B_c \tan(\theta_3 - \theta_w) \frac{\partial \theta_3}{\partial \chi} \quad (\text{C.52})$$

Appendix D, Sensitivity Analysis, Weighted-Grounded-Link Case

This appendix contains a MathSoft Mathcad® version 5.0 program. It calculates the sensitivity of the weight-grounded-link linkage to variations in the design parameters. The model analyzed is the design solution from Appendix A. Textual comments are in **boldface**.

Sensitivity Analysis, Weighted-Grounded-Link Case

Created on MathSoft Mathcad version 5, by R. R. Soper

Design Parameters and Range of Motion Information

$$l_2 := 20.042 \quad l_3 := 11.073 \quad l_4 := 26.577 \quad l_1 := 8 \quad l_{in} := 40.1 \quad l_w := 45$$

$$\theta_{in} := 7.268 \text{ deg} \quad \theta_w := 5.332 \text{ deg} \quad \chi := 165 \text{ deg} \quad \xi := 1$$

$$\beta_o := 60 \text{ deg}$$

Start and Final Angle of the User Input Arm

$$\beta_f := 100 \text{ deg}$$

$$k := 0, 1 \dots 60 \quad \beta_k := \beta_o + \frac{\beta_f - \beta_o}{60} \cdot k \quad \theta_{2_k} := \beta_k - \theta_{in}$$

Analysis of the Motion of θ_3 :

$$E_{3_k} := 2 \cdot l_2 \cdot l_3 \cdot \sin(\theta_{2_k}) - 2 \cdot l_3 \cdot l_1 \cdot \sin(\chi) \quad F_{3_k} := 2 \cdot l_2 \cdot l_3 \cdot \cos(\theta_{2_k}) - 2 \cdot l_3 \cdot l_1 \cdot \cos(\chi)$$

$$G_{3_k} := l_2^2 + l_3^2 + l_1^2 - l_4^2 - 2 \cdot l_2 \cdot l_1 \cdot \cos(\chi) \cdot \cos(\theta_{2_k}) - 2 \cdot l_2 \cdot l_1 \cdot \sin(\chi) \cdot \sin(\theta_{2_k})$$

$$N_{3_k} := -E_{3_k} + \xi \cdot \sqrt{(E_{3_k})^2 + (F_{3_k})^2 - (G_{3_k})^2} \quad H_{3_k} := \frac{2 \cdot (G_{3_k} - F_{3_k})^2}{(G_{3_k} - F_{3_k})^2 + (N_{3_k})^2}$$

$$\theta_{3_k} := 2 \cdot \text{atan} \left(\frac{N_{3_k}}{G_{3_k} - F_{3_k}} \right)$$

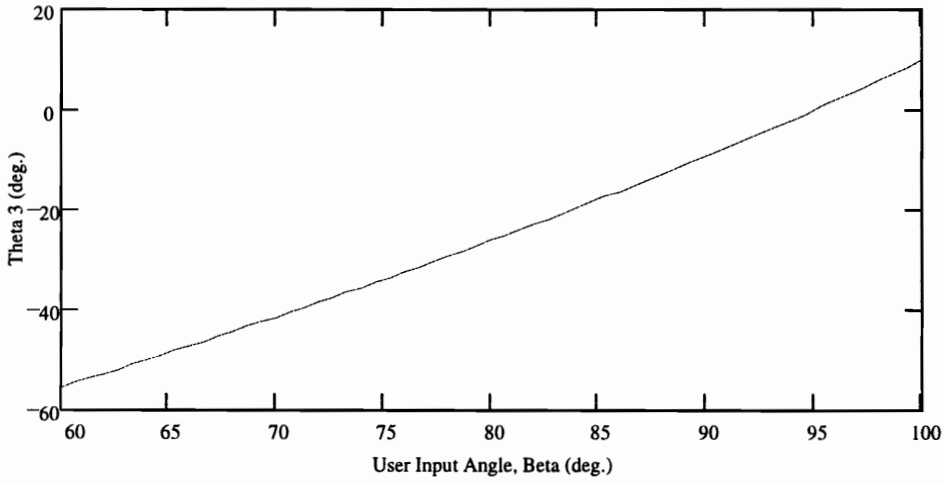


Figure D-1, Motion of Theta 3

Analysis of the Motion of θ_4 :

$$E_{4_k} := -2 \cdot l_2 \cdot l_4 \cdot \sin(\theta_{2_k}) + 2 \cdot l_4 \cdot l_1 \cdot \sin(\chi) \quad F_{4_k} := -2 \cdot l_2 \cdot l_4 \cdot \cos(\theta_{2_k}) + 2 \cdot l_4 \cdot l_1 \cdot \cos(\chi)$$

$$G_{4_k} := l_2^2 + l_4^2 + l_1^2 - l_3^2 - 2 \cdot l_2 \cdot l_1 \cdot \cos(\chi) \cdot \cos(\theta_{2_k}) - 2 \cdot l_2 \cdot l_1 \cdot \sin(\chi) \cdot \sin(\theta_{2_k})$$

$$N_{4_k} := -E_{4_k} + \sqrt{(E_{4_k})^2 + (F_{4_k})^2 - (G_{4_k})^2}$$

$$H_{4_k} := \frac{2 \cdot (G_{4_k} - F_{4_k})^2}{(G_{4_k} - F_{4_k})^2 + (N_{4_k})^2}$$

$$\theta_{4_k} := 2 \cdot \text{atan}\left(\frac{N_{4_k}}{G_{4_k} - F_{4_k}}\right)$$

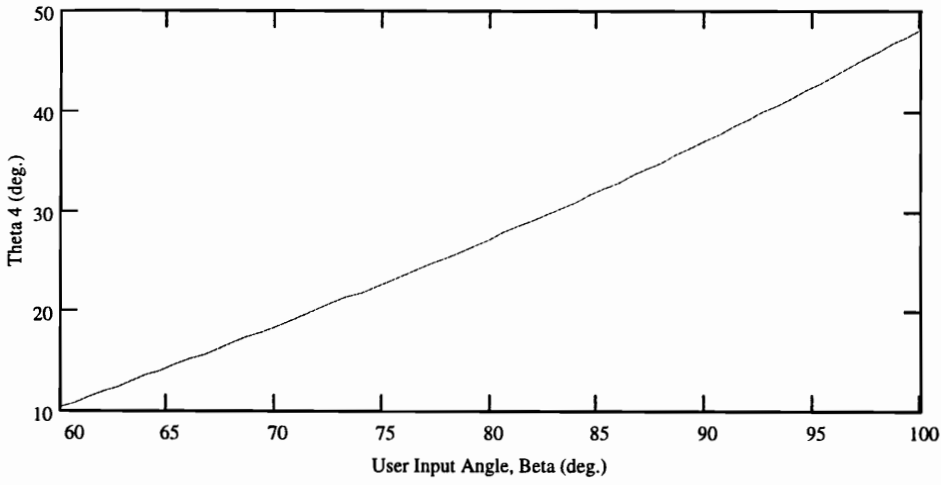


Figure D-2, Motion of Theta 4

Resistance Curve:

$$R_k = \frac{l_w \cdot l_2}{l_{in} \cdot l_4} \cdot \left(\frac{\sin(\theta_{3_k}) \cdot \cos(\theta_{2_k}) - \cos(\theta_{3_k}) \cdot \sin(\theta_{2_k})}{\cos(\theta_{4_k}) \cdot \sin(\theta_{3_k}) - \cos(\theta_{3_k}) \cdot \sin(\theta_{4_k})} \right) \cdot \cos(\theta_{4_k} - \theta_w)$$

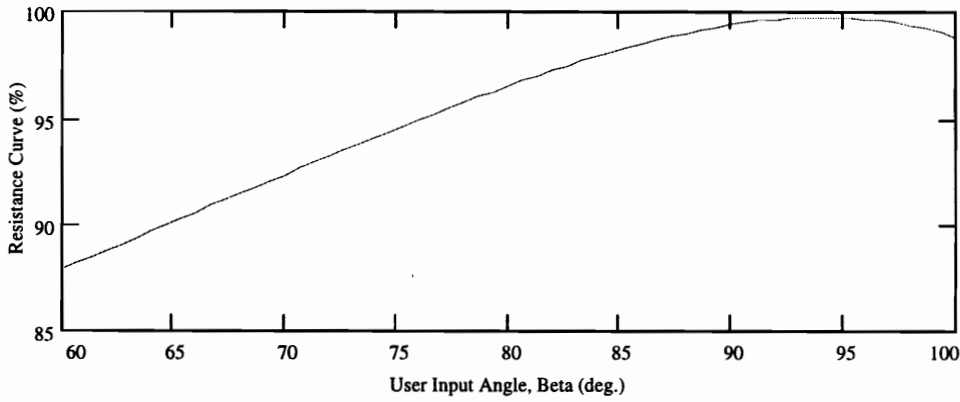


Figure D-3, Resistance Curve

Calculate Partial Derivatives of θ_3 with Respect to q

$$E3d1_k := 2 \cdot l_3 \cdot \sin(\theta_{2_k}) \quad F3d1_k := 2 \cdot l_3 \cdot \cos(\theta_{2_k})$$

$$G3d1_k := 2 \cdot l_2 - 2 \cdot l_1 \cdot \cos(\theta_{2_k}) \cdot \cos(\chi) - 2 \cdot l_1 \cdot \sin(\theta_{2_k}) \cdot \sin(\chi)$$

$$I3d1_k := -E3d1_k + \frac{\xi \cdot (E_{3_k} \cdot E3d1_k + F_{3_k} \cdot F3d1_k - G_{3_k} \cdot G3d1_k)}{\sqrt{(E_{3_k})^2 + (F_{3_k})^2 - (G_{3_k})^2}}$$

$$\theta3d1_k := H_{3_k} \cdot \left[\frac{1}{G_{3_k} - F_{3_k}} \cdot I3d1_k - \frac{N_{3_k}}{(G_{3_k} - F_{3_k})^2} \cdot (G3d1_k - F3d1_k) \right] \quad \text{Partial Derivative of } \theta_3 \text{ wrt } l_2$$

$$E3d2_k := 2 \cdot l_2 \cdot \sin(\theta_{2_k}) - 2 \cdot l_1 \cdot \sin(\chi) \quad F3d2_k := 2 \cdot l_2 \cdot \cos(\theta_{2_k}) - 2 \cdot l_1 \cdot \cos(\chi)$$

$$G3d2_k := 2 \cdot l_3 \quad I3d2_k := -E3d2_k + \frac{\xi \cdot (E_{3_k} \cdot E3d2_k + F_{3_k} \cdot F3d2_k - G_{3_k} \cdot G3d2_k)}{\sqrt{(E_{3_k})^2 + (F_{3_k})^2 - (G_{3_k})^2}}$$

$$\theta3d2_k := H_{3_k} \cdot \left[\frac{1}{G_{3_k} - F_{3_k}} \cdot I3d2_k - \frac{N_{3_k}}{(G_{3_k} - F_{3_k})^2} \cdot (G3d2_k - F3d2_k) \right] \quad \text{Partial Derivative of } \theta_3 \text{ wrt } l_3$$

$$E3d3_k := 0 \quad F3d3_k := 0 \quad G3d3_k := -2 \cdot l_4$$

$$I3d3_k := -E3d3_k + \frac{\xi \cdot (E_{3_k} \cdot E3d3_k + F_{3_k} \cdot F3d3_k - G_{3_k} \cdot G3d3_k)}{\sqrt{(E_{3_k})^2 + (F_{3_k})^2 - (G_{3_k})^2}}$$

$$\theta_{3d3_k} := H_{3_k} \cdot \left[\frac{1}{G_{3_k} - F_{3_k}} \cdot I_{3d3_k} - \frac{N_{3_k}}{(G_{3_k} - F_{3_k})^2} \cdot (G_{3d3_k} - F_{3d3_k}) \right] \quad \text{Partial Derivative of } \theta_3 \text{ wrt } I_4$$

$$\begin{aligned} E_{3d4_k} &:= -2 \cdot l_3 \cdot \sin(\chi) & F_{3d4_k} &:= -2 \cdot l_3 \cdot \cos(\chi) \\ G_{3d4_k} &:= -2 \cdot l_1 - 2 \cdot l_2 \cdot \cos(\theta_{2_k}) \cdot \cos(\chi) - 2 \cdot l_2 \cdot \sin(\theta_{2_k}) \cdot \sin(\chi) \\ I_{3d4_k} &:= -E_{3d4_k} + \frac{\xi \cdot (E_{3_k} \cdot E_{3d4_k} + F_{3_k} \cdot F_{3d4_k} - G_{3_k} \cdot G_{3d4_k})}{\sqrt{(E_{3_k})^2 + (F_{3_k})^2 - (G_{3_k})^2}} \end{aligned}$$

$$\theta_{3d4_k} := H_{3_k} \cdot \left[\frac{1}{G_{3_k} - F_{3_k}} \cdot I_{3d4_k} - \frac{N_{3_k}}{(G_{3_k} - F_{3_k})^2} \cdot (G_{3d4_k} - F_{3d4_k}) \right] \quad \text{Partial Derivative of } \theta_3 \text{ wrt } I_1$$

$$\begin{aligned} E_{3d5_k} &:= -2 \cdot l_2 \cdot l_3 \cdot \cos(\theta_{2_k}) & F_{3d5_k} &:= 2 \cdot l_2 \cdot l_3 \cdot \sin(\theta_{2_k}) \\ G_{3d5_k} &:= -2 \cdot l_1 \cdot l_2 \cdot \sin(\theta_{2_k}) \cdot \cos(\chi) + 2 \cdot l_1 \cdot l_2 \cdot \cos(\theta_{2_k}) \cdot \sin(\chi) \\ I_{3d5_k} &:= -E_{3d5_k} + \frac{\xi \cdot (E_{3_k} \cdot E_{3d5_k} + F_{3_k} \cdot F_{3d5_k} - G_{3_k} \cdot G_{3d5_k})}{\sqrt{(E_{3_k})^2 + (F_{3_k})^2 - (G_{3_k})^2}} \end{aligned}$$

$$\theta_{3d5_k} := H_{3_k} \cdot \left[\frac{1}{G_{3_k} - F_{3_k}} \cdot I_{3d5_k} - \frac{N_{3_k}}{(G_{3_k} - F_{3_k})^2} \cdot (G_{3d5_k} - F_{3d5_k}) \right] \quad \text{Partial Derivative of } \theta_3 \text{ wrt } \theta \text{ in}$$

$$\begin{aligned} E_{3d8_k} &:= -2 \cdot l_3 \cdot l_1 \cdot \cos(\chi) & F_{3d8_k} &:= 2 \cdot l_3 \cdot l_1 \cdot \sin(\chi) \\ G_{3d8_k} &:= 2 \cdot l_2 \cdot l_1 \cdot \cos(\theta_{2_k}) \cdot \sin(\chi) - 2 \cdot l_2 \cdot l_1 \cdot \sin(\theta_{2_k}) \cdot \cos(\chi) \end{aligned}$$

$$I3d8_k := -E3d8_k + \frac{\xi \cdot (E3_k \cdot E3d8_k + F3_k \cdot F3d8_k - G3_k \cdot G3d8_k)}{\sqrt{(E3_k)^2 + (F3_k)^2 - (G3_k)^2}}$$

$$\theta3d8_k := H3_k \cdot \left[\frac{1}{G3_k - F3_k} \cdot I3d8_k - \frac{N3_k}{(G3_k - F3_k)^2} \cdot (G3d8_k - F3d8_k) \right] \quad \text{Partial Derivative of } \theta3 \text{ wrt } \chi$$

Calculate Partial Derivatives of $\theta4$ with Respect to q

$$E4d1_k := -2 \cdot l4 \cdot \sin(\theta2_k) \quad F4d1_k := -2 \cdot l4 \cdot \cos(\theta2_k)$$

$$G4d1_k := 2 \cdot l2 - 2 \cdot l1 \cdot \cos(\theta2_k) \cdot \cos(\chi) - 2 \cdot l1 \cdot \sin(\theta2_k) \cdot \sin(\chi)$$

$$I4d1_k := -E4d1_k - \frac{\xi \cdot (E4_k \cdot E4d1_k + F4_k \cdot F4d1_k - G4_k \cdot G4d1_k)}{\sqrt{(E4_k)^2 + (F4_k)^2 - (G4_k)^2}}$$

$$\theta4d1_k := H4_k \cdot \left[\frac{1}{G4_k - F4_k} \cdot I4d1_k - \frac{N4_k}{(G4_k - F4_k)^2} \cdot (G4d1_k - F4d1_k) \right] \quad \text{Partial Derivative of } \theta4 \text{ wrt } l_2$$

$$E4d2_k := 0 \quad F4d2_k := 0 \quad G4d2_k := -2 \cdot l3$$

$$I4d2_k := -E4d2_k - \frac{\xi \cdot (E4_k \cdot E4d2_k + F4_k \cdot F4d2_k - G4_k \cdot G4d2_k)}{\sqrt{(E4_k)^2 + (F4_k)^2 - (G4_k)^2}}$$

$$\theta4d2_k := H4_k \cdot \left[\frac{1}{G4_k - F4_k} \cdot I4d2_k - \frac{N4_k}{(G4_k - F4_k)^2} \cdot (G4d2_k - F4d2_k) \right] \quad \text{Partial Derivative of } \theta4 \text{ wrt } l_3$$

$$E4d3_k := 2 \cdot l_1 \cdot \sin(\chi) - 2 \cdot l_2 \cdot \sin(\theta_{2_k}) \quad F4d3_k := 2 \cdot l_1 \cdot \cos(\chi) - 2 \cdot l_2 \cdot \cos(\theta_{2_k})$$

$$G4d3_k := 2 \cdot l_4 \quad I4d3_k := -E4d3_k - \frac{\xi \cdot (E_{4_k} \cdot E4d3_k + F_{4_k} \cdot F4d3_k - G_{4_k} \cdot G4d3_k)}{\sqrt{(E_{4_k})^2 + (F_{4_k})^2 - (G_{4_k})^2}}$$

$$\theta 4d3_k := H_{4_k} \cdot \left[\frac{1}{G_{4_k} - F_{4_k}} \cdot I4d3_k - \frac{N_{4_k}}{(G_{4_k} - F_{4_k})^2} \cdot (G4d3_k - F4d3_k) \right] \quad \text{Partial Derivative of } \theta 4 \text{ wrt } l_4$$

$$E4d4_k := 2 \cdot l_4 \cdot \sin(\chi) \quad F4d4_k := 2 \cdot l_4 \cdot \cos(\chi)$$

$$G4d4_k := 2 \cdot l_1 - 2 \cdot l_2 \cdot \cos(\theta_{2_k}) \cdot \cos(\chi) - 2 \cdot l_2 \cdot \sin(\theta_{2_k}) \cdot \sin(\chi)$$

$$I4d4_k := -E4d4_k - \frac{\xi \cdot (E_{4_k} \cdot E4d4_k + F_{4_k} \cdot F4d4_k - G_{4_k} \cdot G4d4_k)}{\sqrt{(E_{4_k})^2 + (F_{4_k})^2 - (G_{4_k})^2}}$$

$$\theta 4d4_k := H_{4_k} \cdot \left[\frac{1}{G_{4_k} - F_{4_k}} \cdot I4d4_k - \frac{N_{4_k}}{(G_{4_k} - F_{4_k})^2} \cdot (G4d4_k - F4d4_k) \right] \quad \text{Partial Derivative of } \theta 4 \text{ wrt } l_1$$

$$E4d5_k := 2 \cdot l_2 \cdot l_4 \cdot \cos(\theta_{2_k}) \quad F4d5_k := 2 \cdot l_2 \cdot l_4 \cdot \sin(\theta_{2_k})$$

$$G4d5_k := -2 \cdot l_1 \cdot l_2 \cdot \sin(\theta_{2_k}) \cdot \cos(\chi) + 2 \cdot l_1 \cdot l_2 \cdot \cos(\theta_{2_k}) \cdot \sin(\chi)$$

$$I4d5_k := -E4d5_k - \frac{\xi \cdot (E_{4_k} \cdot E4d5_k + F_{4_k} \cdot F4d5_k - G_{4_k} \cdot G4d5_k)}{\sqrt{(E_{4_k})^2 + (F_{4_k})^2 - (G_{4_k})^2}}$$

$$\theta 4 d 5_k = H_{4_k} \cdot \left[\frac{1}{G_{4_k} - F_{4_k}} \cdot I 4 d 5_k - \frac{N_{4_k}}{(G_{4_k} - F_{4_k})^2} \cdot (G 4 d 5_k - F 4 d 5_k) \right] \quad \text{Parital Derivative of } \theta 4 \text{ wrt } \theta \text{ in}$$

$$E 4 d 8_k := 2 \cdot l_{4_k} \cdot l_1 \cdot \cos(\chi) \quad F 4 d 8_k := -2 \cdot l_{4_k} \cdot l_1 \cdot \sin(\chi)$$

$$G 4 d 8_k := 2 \cdot l_2 \cdot l_1 \cdot \cos(\theta_{2_k}) \cdot \sin(\chi) - 2 \cdot l_2 \cdot l_1 \cdot \sin(\theta_{2_k}) \cdot \cos(\chi)$$

$$I 4 d 8_k := -E 4 d 8_k - \frac{\xi \cdot (E_{4_k} \cdot E 4 d 8_k + F_{4_k} \cdot F 4 d 8_k - G_{4_k} \cdot G 4 d 8_k)}{\sqrt{(E_{4_k})^2 + (F_{4_k})^2 - (G_{4_k})^2}}$$

$$\theta 4 d 8_k = H_{4_k} \cdot \left[\frac{1}{G_{4_k} - F_{4_k}} \cdot I 4 d 8_k - \frac{N_{4_k}}{(G_{4_k} - F_{4_k})^2} \cdot (G 4 d 8_k - F 4 d 8_k) \right] \quad \text{Parital Derivative of } \theta 4 \text{ wrt } \chi$$

Calculate Influence Coef. for Weighted-Grounded-Link Case

$$d_k := \cos(\theta_{4_k}) \cdot \sin(\theta_{3_k}) - \cos(\theta_{3_k}) \cdot \sin(\theta_{4_k}) \quad n_k := \sin(\theta_{3_k}) \cdot \cos(\theta_{2_k}) - \cos(\theta_{3_k}) \cdot \sin(\theta_{2_k})$$

Influence Coefficient: dR/dl_2

$$dd 1_k := (\sin(\theta_{4_k}) \cdot \sin(\theta_{3_k}) + \cos(\theta_{4_k}) \cdot \cos(\theta_{3_k})) \cdot (\theta 3 d 1_k - \theta 4 d 1_k)$$

$$nd 1_k := (\sin(\theta_{3_k}) \cdot \sin(\theta_{2_k}) + \cos(\theta_{3_k}) \cdot \cos(\theta_{2_k})) \cdot (\theta 3 d 1_k)$$

$$\kappa_{1_k} := \frac{R_k}{l_2} + \frac{R_k}{n_k} \cdot nd 1_k - \frac{R_k}{d_k} \cdot dd 1_k - R_k \cdot \tan(\theta_{4_k} - \theta_w) \cdot \theta 4 d 1_k$$

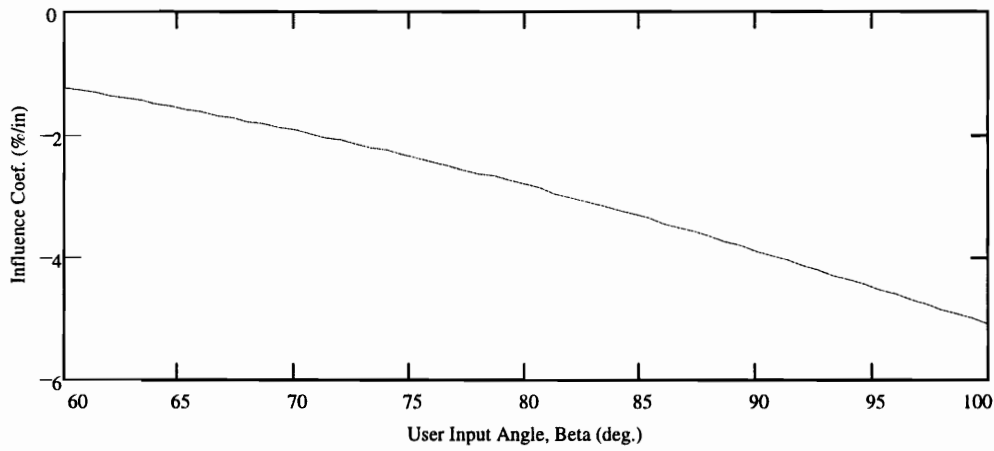


Figure D-4, Influence Coefficient, I2

Influence Coefficient: dR/dI_3

$$dd2_k := \left(\sin(\theta_{4_k}) \cdot \sin(\theta_{3_k}) + \cos(\theta_{4_k}) \cdot \cos(\theta_{3_k}) \right) \cdot (\theta_{3d2_k} - \theta_{4d2_k})$$

$$nd2_k := \left(\sin(\theta_{3_k}) \cdot \sin(\theta_{2_k}) + \cos(\theta_{3_k}) \cdot \cos(\theta_{2_k}) \right) \cdot (\theta_{3d2_k})$$

$$\kappa_{2_k} := \frac{R_k}{n_k} \cdot nd2_k - \frac{R_k}{d_k} \cdot dd2_k - R_k \cdot \tan(\theta_{4_k} - \theta_w) \cdot \theta_{4d2_k}$$

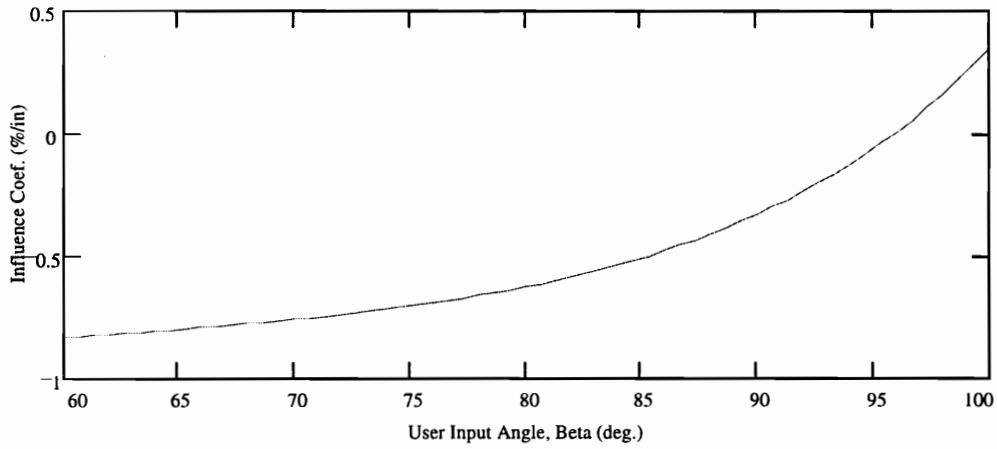


Figure D-5, Influence Coefficient, I3

Influence Coefficient: dR/dl_4

$$dd3_k := \left(\sin(\theta_{4_k}) \cdot \sin(\theta_{3_k}) + \cos(\theta_{4_k}) \cdot \cos(\theta_{3_k}) \right) \cdot (\theta_3 d3_k - \theta_4 d3_k)$$

$$nd3_k := \left(\sin(\theta_{3_k}) \cdot \sin(\theta_{2_k}) + \cos(\theta_{3_k}) \cdot \cos(\theta_{2_k}) \right) \cdot (\theta_3 d3_k)$$

$$\kappa_{3_k} := \frac{R_k}{n_k} \cdot nd3_k - \frac{R_k}{d_k} \cdot dd3_k - R_k \cdot \tan(\theta_{4_k} - \theta_w) \cdot \theta_4 d3_k - \frac{R_k}{l_4}$$

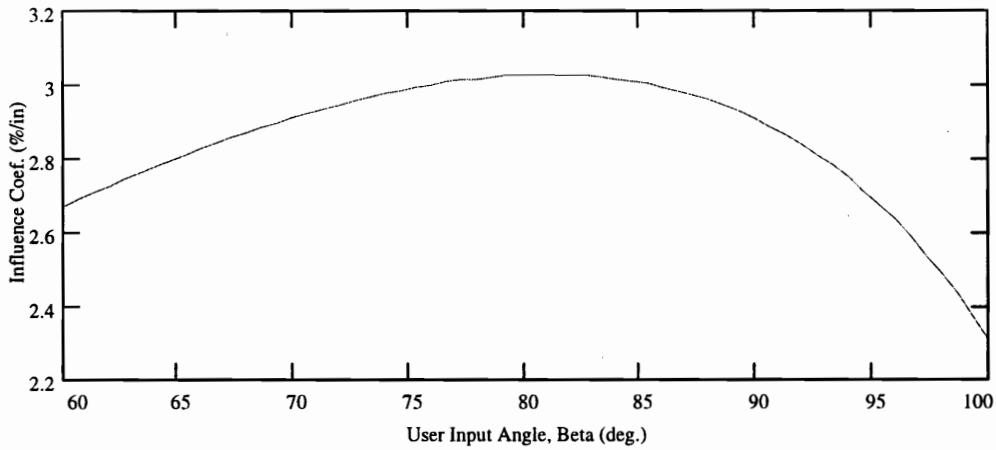


Figure D-6, Influence Coefficient, 14

Influence Coefficient: dR/dl_3

$$dd4_k := \left(\sin(\theta_{4_k}) \cdot \sin(\theta_{3_k}) + \cos(\theta_{4_k}) \cdot \cos(\theta_{3_k}) \right) \cdot (\theta_3 d4_k - \theta_4 d4_k)$$

$$nd4_k := \left(\sin(\theta_{3_k}) \cdot \sin(\theta_{2_k}) + \cos(\theta_{3_k}) \cdot \cos(\theta_{2_k}) \right) \cdot (\theta_3 d4_k)$$

$$\kappa_{4_k} := \frac{R_k}{n_k} \cdot nd4_k - \frac{R_k}{d_k} \cdot dd4_k - R_k \cdot \tan(\theta_{4_k} - \theta_w) \cdot \theta_4 d4_k$$

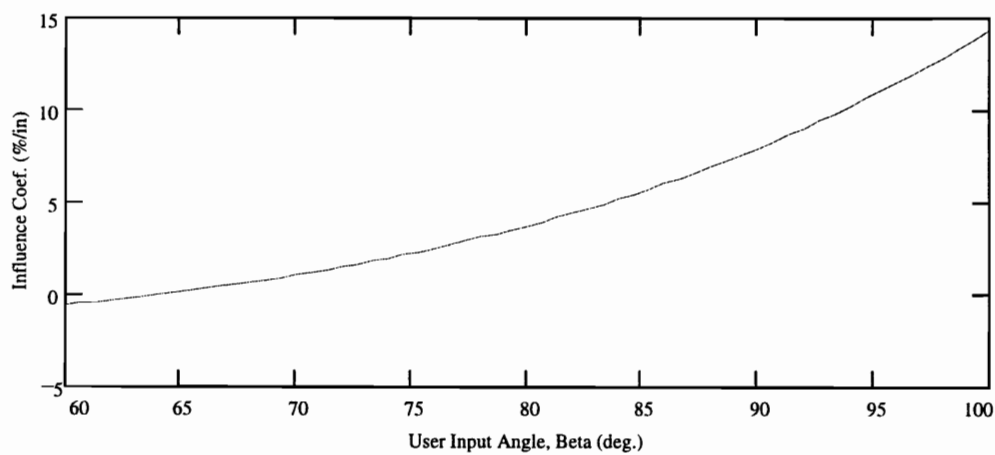


Figure D-7, Influence Coefficient, I1

Influence Coefficient: $dR/d \theta_{in}$

$$dd5_k := \left(\sin(\theta_{4_k}) \cdot \sin(\theta_{3_k}) + \cos(\theta_{4_k}) \cdot \cos(\theta_{3_k}) \right) \cdot (\theta_{3d5_k} - \theta_{4d5_k})$$

$$nd5_k := \left(\sin(\theta_{3_k}) \cdot \sin(\theta_{2_k}) + \cos(\theta_{3_k}) \cdot \cos(\theta_{2_k}) \right) \cdot (\theta_{3d5_k} + 1)$$

$$\kappa_{5_k} := \frac{R_k}{n_k} \cdot nd5_k - \frac{R_k}{d_k} \cdot dd5_k - R_k \cdot \tan(\theta_{4_k} - \theta_w) \cdot \theta_{4d5_k}$$

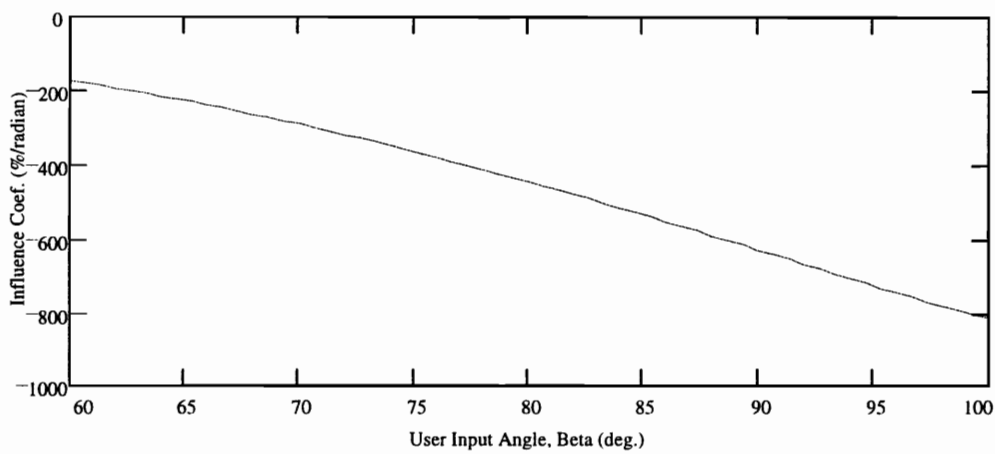


Figure D-8, I. C., theta in

Influence Coefficient: $dR/d\theta_w$ $\kappa_{6_k} := R_k \cdot \tan(\theta_{4_k} - \theta_w)$

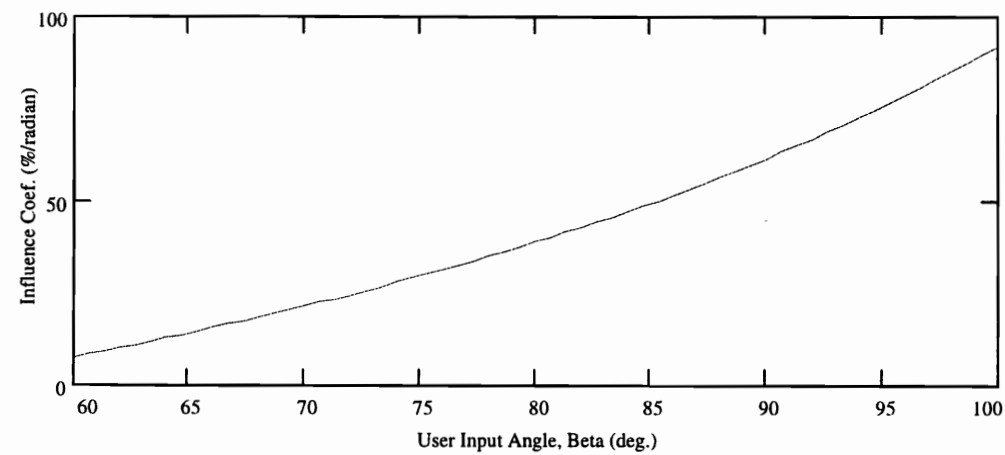


Figure D-9, I. C., θ_w

Influence Coefficient: dR/dl_w $\kappa_{7_k} := \frac{R_k}{l_w}$

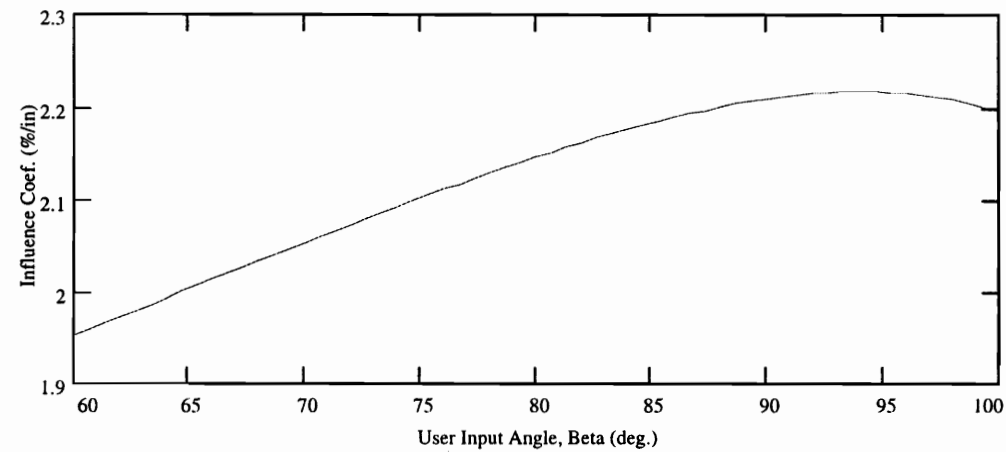


Figure D-10, Influence Coefficient, l_w

Influence Coefficient: $dR/d\chi$

$$dd\delta_k := \left(\sin(\theta_{4_k}) \cdot \sin(\theta_{3_k}) + \cos(\theta_{4_k}) \cdot \cos(\theta_{3_k}) \right) \cdot (\theta_3 d\delta_k - \theta_4 d\delta_k)$$

$$nd\delta_k := \left(\sin(\theta_{3_k}) \cdot \sin(\theta_{2_k}) + \cos(\theta_{3_k}) \cdot \cos(\theta_{2_k}) \right) \cdot (\theta_3 d\delta_k)$$

$$\kappa_{\delta_k} := \frac{R_k}{n_k} \cdot nd\delta_k - \frac{R_k}{d_k} \cdot dd\delta_k - R_k \cdot \tan(\theta_{4_k} - \theta_w) \cdot \theta_4 d\delta_k$$

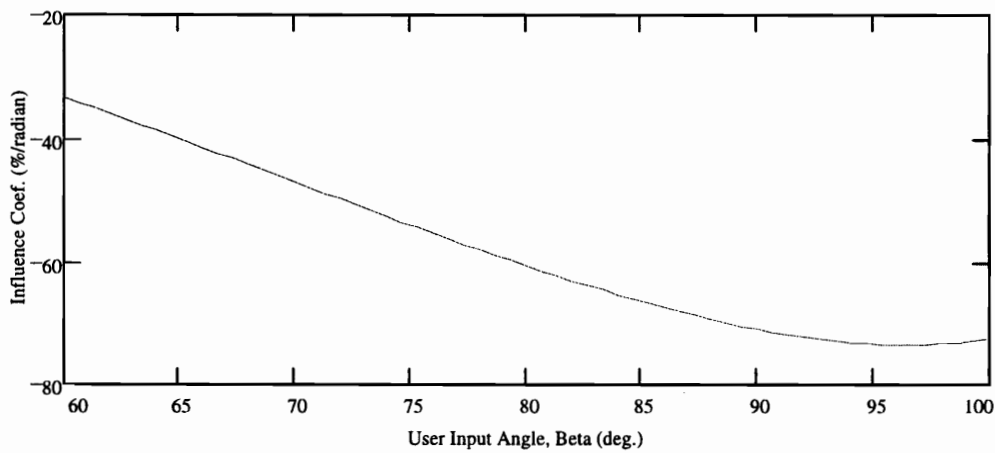


Figure D-11, Influence Coefficient, Chi

Appendix E, Sensitivity Analysis, Weighted-Coupler Case

This appendix contains a MathSoft Mathcad® version 5.0 program. It calculates the sensitivity of the weighted-coupler four-bar linkage to variations in the design parameters. The model analyzed is the design solution from Appendix B. Textual comments are in **boldface**.

Sensitivity Analysis, Weighted-Coupler-Link Case

Created on MathSoft Mathcad version 5, by R. R. Soper

Design Parameters and Range of Motion Information

$$l_2 := 20.042 \quad l_3 := 11.073 \quad l_4 := 26.577 \quad l_1 := 8 \quad l_{in} := 40.1 \quad l_w := 45$$

$$\theta_{in} := 7.268 \text{ deg} \quad \theta_w := 5.332 \text{ deg} \quad \chi := 165 \text{ deg} \quad \xi := 1$$

$$\beta_o := 60 \text{ deg}$$

Start and Final Angle of the User Input Arm

$$\beta_f := 100 \text{ deg}$$

$$k := 0, 1..60 \quad \beta_k := \beta_o + \frac{\beta_f - \beta_o}{60} \cdot k \quad \theta_{2_k} := \beta_k - \theta_{in}$$

Analysis of the Motion of θ_3 :

$$E_{3_k} := 2 \cdot l_2 \cdot l_3 \cdot \sin(\theta_{2_k}) - 2 \cdot l_3 \cdot l_1 \cdot \sin(\chi) \quad F_{3_k} := 2 \cdot l_2 \cdot l_3 \cdot \cos(\theta_{2_k}) - 2 \cdot l_3 \cdot l_1 \cdot \cos(\chi)$$

$$G_{3_k} := l_2^2 + l_3^2 + l_1^2 - l_4^2 - 2 \cdot l_2 \cdot l_1 \cdot \cos(\chi) \cdot \cos(\theta_{2_k}) - 2 \cdot l_2 \cdot l_1 \cdot \sin(\chi) \cdot \sin(\theta_{2_k})$$

$$N_{3_k} := -E_{3_k} + \xi \cdot \sqrt{(E_{3_k})^2 + (F_{3_k})^2 - (G_{3_k})^2} \quad H_{3_k} := \frac{2 \cdot (G_{3_k} - F_{3_k})^2}{(G_{3_k} - F_{3_k})^2 + (N_{3_k})^2}$$

$$\theta_{3_k} := 2 \cdot \text{atan} \left(\frac{N_{3_k}}{G_{3_k} - F_{3_k}} \right)$$

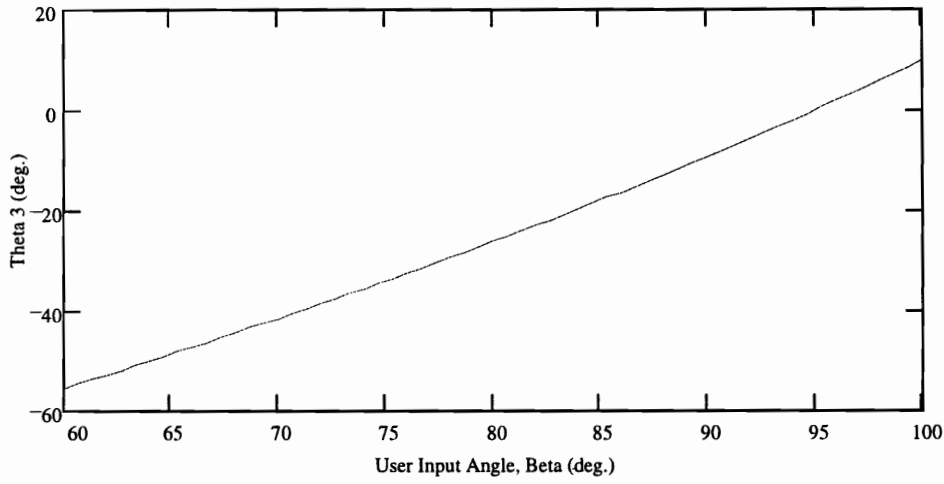


Figure E-1, Motion of Theta 3

Analysis of the Motion of θ_4 :

$$E_{4_k} := -2 \cdot l_2 \cdot l_4 \cdot \sin(\theta_{2_k}) + 2 \cdot l_4 \cdot l_1 \cdot \sin(\chi) \quad F_{4_k} := -2 \cdot l_2 \cdot l_4 \cdot \cos(\theta_{2_k}) + 2 \cdot l_4 \cdot l_1 \cdot \cos(\chi)$$

$$G_{4_k} := l_2^2 + l_4^2 + l_1^2 - l_3^2 - 2 \cdot l_2 \cdot l_1 \cdot \cos(\chi) \cdot \cos(\theta_{2_k}) - 2 \cdot l_2 \cdot l_1 \cdot \sin(\chi) \cdot \sin(\theta_{2_k})$$

$$N_{4_k} := -E_{4_k} + \xi \cdot \sqrt{(E_{4_k})^2 + (F_{4_k})^2 - (G_{4_k})^2}$$

$$H_{4_k} := \frac{2 \cdot (G_{4_k} - F_{4_k})^2}{(G_{4_k} - F_{4_k})^2 + (N_{4_k})^2}$$

$$\theta_{4_k} := 2 \cdot \text{atan}\left(\frac{N_{4_k}}{G_{4_k} - F_{4_k}}\right)$$

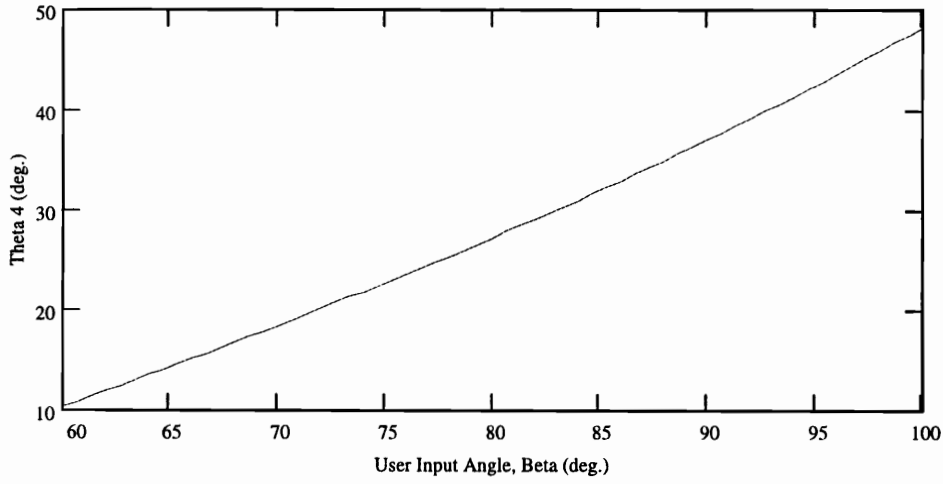


Figure E-2, Motion of Theta 4

Resistance Curve:
$$A_k := \frac{l_2}{l_{in}} \cdot \cos(\theta_{2_k})$$

$$B_k := \frac{l_w \cdot l_2}{l_{in} \cdot l_3} \cdot \left(\frac{\sin(\theta_{4_k}) \cdot \cos(\theta_{2_k}) - \cos(\theta_{4_k}) \cdot \sin(\theta_{2_k})}{\cos(\theta_{4_k}) \cdot \sin(\theta_{3_k}) - \cos(\theta_{3_k}) \cdot \sin(\theta_{4_k})} \right) \cdot \cos(\theta_{3_k} - \theta_w) \quad R_k := A_k + B_k$$

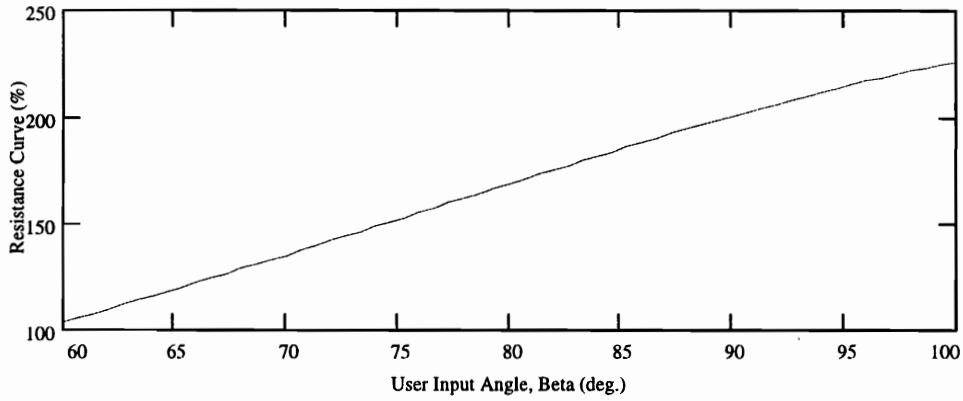


Figure E-3, Resistance Curve

Calculate Partial Derivatives of θ_3 with Respect to q

$$E3d1_k := 2 \cdot l_3 \cdot \sin(\theta_{2_k}) \quad F3d1_k := 2 \cdot l_3 \cdot \cos(\theta_{2_k})$$

$$G3d1_k := 2 \cdot l_2 - 2 \cdot l_1 \cdot \cos(\theta_{2_k}) \cdot \cos(\chi) - 2 \cdot l_1 \cdot \sin(\theta_{2_k}) \cdot \sin(\chi)$$

$$I3d1_k := -E3d1_k + \frac{\xi \cdot (E_{3_k} \cdot E3d1_k + F_{3_k} \cdot F3d1_k - G_{3_k} \cdot G3d1_k)}{\sqrt{(E_{3_k})^2 + (F_{3_k})^2 - (G_{3_k})^2}}$$

$$\theta3d1_k := H_{3_k} \cdot \left[\frac{1}{G_{3_k} - F_{3_k}} \cdot I3d1_k - \frac{N_{3_k}}{(G_{3_k} - F_{3_k})^2} \cdot (G3d1_k - F3d1_k) \right] \quad \text{Partial Derivative of } \theta_3 \text{ wrt } l_2$$

$$E3d2_k := 2 \cdot l_2 \cdot \sin(\theta_{2_k}) - 2 \cdot l_1 \cdot \sin(\chi) \quad F3d2_k := 2 \cdot l_2 \cdot \cos(\theta_{2_k}) - 2 \cdot l_1 \cdot \cos(\chi)$$

$$G3d2_k := 2 \cdot l_3 \quad I3d2_k := -E3d2_k + \frac{\xi \cdot (E_{3_k} \cdot E3d2_k + F_{3_k} \cdot F3d2_k - G_{3_k} \cdot G3d2_k)}{\sqrt{(E_{3_k})^2 + (F_{3_k})^2 - (G_{3_k})^2}}$$

$$\theta3d2_k := H_{3_k} \cdot \left[\frac{1}{G_{3_k} - F_{3_k}} \cdot I3d2_k - \frac{N_{3_k}}{(G_{3_k} - F_{3_k})^2} \cdot (G3d2_k - F3d2_k) \right] \quad \text{Partial Derivative of } \theta_3 \text{ wrt } l_3$$

$$E3d3_k := 0 \quad F3d3_k := 0 \quad G3d3_k := -2 \cdot l_4$$

$$I3d3_k := -E3d3_k + \frac{\xi \cdot (E_{3_k} \cdot E3d3_k + F_{3_k} \cdot F3d3_k - G_{3_k} \cdot G3d3_k)}{\sqrt{(E_{3_k})^2 + (F_{3_k})^2 - (G_{3_k})^2}}$$

$$\theta 3d3_k := H_{3_k} \cdot \left[\frac{1}{G_{3_k} - F_{3_k}} \cdot I3d3_k - \frac{N_{3_k}}{(G_{3_k} - F_{3_k})^2} \cdot (G3d3_k - F3d3_k) \right] \quad \text{Partial Derivative of } \theta 3 \text{ wrt } l_4$$

$$E3d4_k := -2 \cdot l_3 \cdot \sin(\chi) \quad F3d4_k := -2 \cdot l_3 \cdot \cos(\chi)$$

$$G3d4_k := -2 \cdot l_1 - 2 \cdot l_2 \cdot \cos(\theta_{2_k}) \cdot \cos(\chi) - 2 \cdot l_2 \cdot \sin(\theta_{2_k}) \cdot \sin(\chi)$$

$$I3d4_k := -E3d4_k + \frac{\xi \cdot (E_{3_k} \cdot E3d4_k + F_{3_k} \cdot F3d4_k - G_{3_k} \cdot G3d4_k)}{\sqrt{(E_{3_k})^2 + (F_{3_k})^2 - (G_{3_k})^2}}$$

$$\theta 3d4_k := H_{3_k} \cdot \left[\frac{1}{G_{3_k} - F_{3_k}} \cdot I3d4_k - \frac{N_{3_k}}{(G_{3_k} - F_{3_k})^2} \cdot (G3d4_k - F3d4_k) \right] \quad \text{Partial Derivative of } \theta 3 \text{ wrt } l_1$$

$$E3d5_k := -2 \cdot l_2 \cdot l_3 \cdot \cos(\theta_{2_k}) \quad F3d5_k := 2 \cdot l_2 \cdot l_3 \cdot \sin(\theta_{2_k})$$

$$G3d5_k := -2 \cdot l_1 \cdot l_2 \cdot \sin(\theta_{2_k}) \cdot \cos(\chi) + 2 \cdot l_1 \cdot l_2 \cdot \cos(\theta_{2_k}) \cdot \sin(\chi)$$

$$I3d5_k := -E3d5_k + \frac{\xi \cdot (E_{3_k} \cdot E3d5_k + F_{3_k} \cdot F3d5_k - G_{3_k} \cdot G3d5_k)}{\sqrt{(E_{3_k})^2 + (F_{3_k})^2 - (G_{3_k})^2}}$$

$$\theta 3d5_k := H_{3_k} \cdot \left[\frac{1}{G_{3_k} - F_{3_k}} \cdot I3d5_k - \frac{N_{3_k}}{(G_{3_k} - F_{3_k})^2} \cdot (G3d5_k - F3d5_k) \right] \quad \text{Partial Derivative of } \theta 3 \text{ wrt } \theta \text{ in}$$

$$E3d8_k := -2 \cdot l_3 \cdot l_1 \cdot \cos(\chi) \quad F3d8_k := 2 \cdot l_3 \cdot l_1 \cdot \sin(\chi)$$

$$G3d8_k := 2 \cdot l_2 \cdot l_1 \cdot \cos(\theta_{2_k}) \cdot \sin(\chi) - 2 \cdot l_2 \cdot l_1 \cdot \sin(\theta_{2_k}) \cdot \cos(\chi)$$

$$I3d8_k := -E3d8_k + \frac{\xi \cdot (E_{3_k} \cdot E3d8_k + F_{3_k} \cdot F3d8_k - G_{3_k} \cdot G3d8_k)}{\sqrt{(E_{3_k})^2 + (F_{3_k})^2 - (G_{3_k})^2}}$$

$$\theta3d8_k := H_{3_k} \cdot \left[\frac{1}{G_{3_k} - F_{3_k}} \cdot I3d8_k - \frac{N_{3_k}}{(G_{3_k} - F_{3_k})^2} \cdot (G3d8_k - F3d8_k) \right] \quad \text{Partial Derivative of } \theta3 \text{ wrt } \chi$$

Calculate Partial Derivatives of $\theta4$ with Respect to q

$$E4d1_k := -2 \cdot l_4 \cdot \sin(\theta_{2_k}) \quad F4d1_k := -2 \cdot l_4 \cdot \cos(\theta_{2_k})$$

$$G4d1_k := 2 \cdot l_2 - 2 \cdot l_1 \cdot \cos(\theta_{2_k}) \cdot \cos(\chi) - 2 \cdot l_1 \cdot \sin(\theta_{2_k}) \cdot \sin(\chi)$$

$$I4d1_k := -E4d1_k - \frac{\xi \cdot (E_{4_k} \cdot E4d1_k + F_{4_k} \cdot F4d1_k - G_{4_k} \cdot G4d1_k)}{\sqrt{(E_{4_k})^2 + (F_{4_k})^2 - (G_{4_k})^2}}$$

$$\theta4d1_k := H_{4_k} \cdot \left[\frac{1}{G_{4_k} - F_{4_k}} \cdot I4d1_k - \frac{N_{4_k}}{(G_{4_k} - F_{4_k})^2} \cdot (G4d1_k - F4d1_k) \right] \quad \text{Partial Derivative of } \theta4 \text{ wrt } l_2$$

$$E4d2_k := 0 \quad F4d2_k := 0 \quad G4d2_k := -2 \cdot l_3$$

$$I4d2_k := -E4d2_k - \frac{\xi \cdot (E_{4_k} \cdot E4d2_k + F_{4_k} \cdot F4d2_k - G_{4_k} \cdot G4d2_k)}{\sqrt{(E_{4_k})^2 + (F_{4_k})^2 - (G_{4_k})^2}}$$

$$\theta4d2_k := H_{4_k} \cdot \left[\frac{1}{G_{4_k} - F_{4_k}} \cdot I4d2_k - \frac{N_{4_k}}{(G_{4_k} - F_{4_k})^2} \cdot (G4d2_k - F4d2_k) \right] \quad \text{Partial Derivative of } \theta4 \text{ wrt } l_3$$

$$E4d3_k := 2 \cdot l_1 \cdot \sin(\chi) - 2 \cdot l_2 \cdot \sin(\theta_{2_k}) \quad F4d3_k := 2 \cdot l_1 \cdot \cos(\chi) - 2 \cdot l_2 \cdot \cos(\theta_{2_k})$$

$$G4d3_k := 2 \cdot l_4 \quad I4d3_k := -E4d3_k - \frac{\xi \cdot (E_{4_k} \cdot E4d3_k + F_{4_k} \cdot F4d3_k - G_{4_k} \cdot G4d3_k)}{\sqrt{(E_{4_k})^2 + (F_{4_k})^2 - (G_{4_k})^2}}$$

$$\theta4d3_k := H_{4_k} \cdot \left[\frac{1}{G_{4_k} - F_{4_k}} \cdot I4d3_k - \frac{N_{4_k}}{(G_{4_k} - F_{4_k})^2} \cdot (G4d3_k - F4d3_k) \right] \quad \text{Partial Derivative of } \theta_4 \text{ wrt } l_4$$

$$E4d4_k := 2 \cdot l_4 \cdot \sin(\chi) \quad F4d4_k := 2 \cdot l_4 \cdot \cos(\chi)$$

$$G4d4_k := 2 \cdot l_1 - 2 \cdot l_2 \cdot \cos(\theta_{2_k}) \cdot \cos(\chi) - 2 \cdot l_2 \cdot \sin(\theta_{2_k}) \cdot \sin(\chi)$$

$$I4d4_k := -E4d4_k - \frac{\xi \cdot (E_{4_k} \cdot E4d4_k + F_{4_k} \cdot F4d4_k - G_{4_k} \cdot G4d4_k)}{\sqrt{(E_{4_k})^2 + (F_{4_k})^2 - (G_{4_k})^2}}$$

$$\theta4d4_k := H_{4_k} \cdot \left[\frac{1}{G_{4_k} - F_{4_k}} \cdot I4d4_k - \frac{N_{4_k}}{(G_{4_k} - F_{4_k})^2} \cdot (G4d4_k - F4d4_k) \right] \quad \text{Partial Derivative of } \theta_4 \text{ wrt } l_1$$

$$E4d5_k := 2 \cdot l_2 \cdot l_4 \cdot \cos(\theta_{2_k}) \quad F4d5_k := 2 \cdot l_2 \cdot l_4 \cdot \sin(\theta_{2_k})$$

$$G4d5_k := -2 \cdot l_1 \cdot l_2 \cdot \sin(\theta_{2_k}) \cdot \cos(\chi) + 2 \cdot l_1 \cdot l_2 \cdot \cos(\theta_{2_k}) \cdot \sin(\chi)$$

$$I4d5_k := -E4d5_k - \frac{\xi \cdot (E_{4_k} \cdot E4d5_k + F_{4_k} \cdot F4d5_k - G_{4_k} \cdot G4d5_k)}{\sqrt{(E_{4_k})^2 + (F_{4_k})^2 - (G_{4_k})^2}}$$

$$\theta_{4d5_k} := H_{4_k} \cdot \left[\frac{1}{G_{4_k} - F_{4_k}} \cdot I_{4d5_k} - \frac{N_{4_k}}{(G_{4_k} - F_{4_k})^2} \cdot (G_{4d5_k} - F_{4d5_k}) \right] \quad \text{Parital Derivative of } \theta_4 \text{ wrt } \theta \text{ in}$$

$$E_{4d8_k} := 2 \cdot l_{4_k} \cdot l_1 \cdot \cos(\chi) \quad F_{4d8_k} := -2 \cdot l_{4_k} \cdot l_1 \cdot \sin(\chi)$$

$$G_{4d8_k} := 2 \cdot l_2 \cdot l_1 \cdot \cos(\theta_{2_k}) \cdot \sin(\chi) - 2 \cdot l_2 \cdot l_1 \cdot \sin(\theta_{2_k}) \cdot \cos(\chi)$$

$$I_{4d8_k} := -E_{4d8_k} - \frac{\xi \cdot (E_{4_k} \cdot E_{4d8_k} + F_{4_k} \cdot F_{4d8_k} - G_{4_k} \cdot G_{4d8_k})}{\sqrt{(E_{4_k})^2 + (F_{4_k})^2 - (G_{4_k})^2}}$$

$$\theta_{4d8_k} := H_{4_k} \cdot \left[\frac{1}{G_{4_k} - F_{4_k}} \cdot I_{4d8_k} - \frac{N_{4_k}}{(G_{4_k} - F_{4_k})^2} \cdot (G_{4d8_k} - F_{4d8_k}) \right] \quad \text{Parital Derivative of } \theta_4 \text{ wrt } \chi$$

Calculate Influence Coef. for Weighted-Coupler-Link Case

$$d_k := \cos(\theta_{4_k}) \cdot \sin(\theta_{3_k}) - \cos(\theta_{3_k}) \cdot \sin(\theta_{4_k}) \quad n_k := \sin(\theta_{4_k}) \cdot \cos(\theta_{2_k}) - \cos(\theta_{4_k}) \cdot \sin(\theta_{2_k})$$

Influence Coefficient: dR/dl_2

$$dd1_k := (\sin(\theta_{4_k}) \cdot \sin(\theta_{3_k}) + \cos(\theta_{4_k}) \cdot \cos(\theta_{3_k})) \cdot (\theta_{3d1_k} - \theta_{4d1_k})$$

$$nd1_k := (\sin(\theta_{4_k}) \cdot \sin(\theta_{2_k}) + \cos(\theta_{4_k}) \cdot \cos(\theta_{2_k})) \cdot (\theta_{4d1_k})$$

$$\kappa_{1_k} := \frac{R_k}{l_2} + \frac{B_k}{n_k} \cdot nd1_k - \frac{B_k}{d_k} \cdot dd1_k - R_k \cdot \tan(\theta_{3_k} - \theta_w) \cdot \theta_{3d1_k}$$

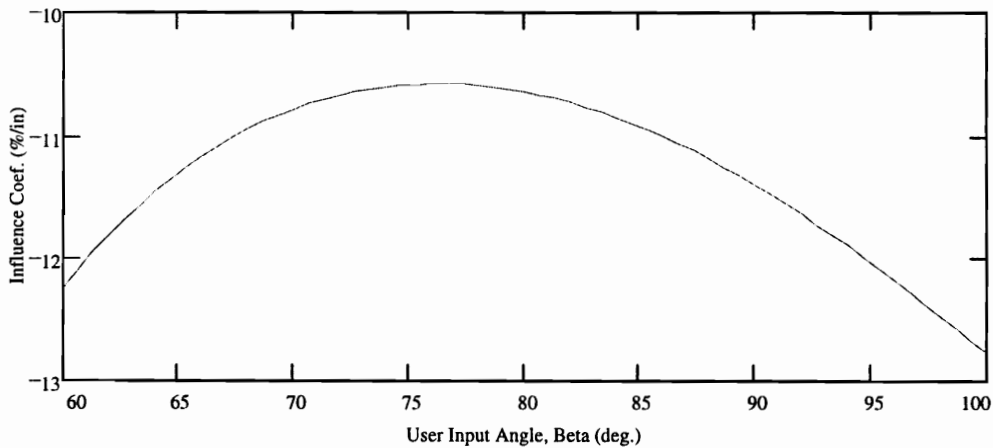


Figure E-4, Influence Coefficient, I2

Influence Coefficient: dR/dI_3

$$dd2_k := \left(\sin(\theta_{4_k}) \cdot \sin(\theta_{3_k}) + \cos(\theta_{4_k}) \cdot \cos(\theta_{3_k}) \right) \cdot (\theta_{3d2_k} - \theta_{4d2_k})$$

$$nd2_k := \left(\sin(\theta_{4_k}) \cdot \sin(\theta_{2_k}) + \cos(\theta_{4_k}) \cdot \cos(\theta_{2_k}) \right) \cdot (\theta_{4d2_k})$$

$$\kappa_{2_k} := \frac{B_k}{n_k} \cdot nd2_k - \frac{B_k}{d_k} \cdot dd2_k - B_k \cdot \tan(\theta_{3_k} - \theta_w) \cdot \theta_{3d2_k} - \frac{B_k}{l_3}$$

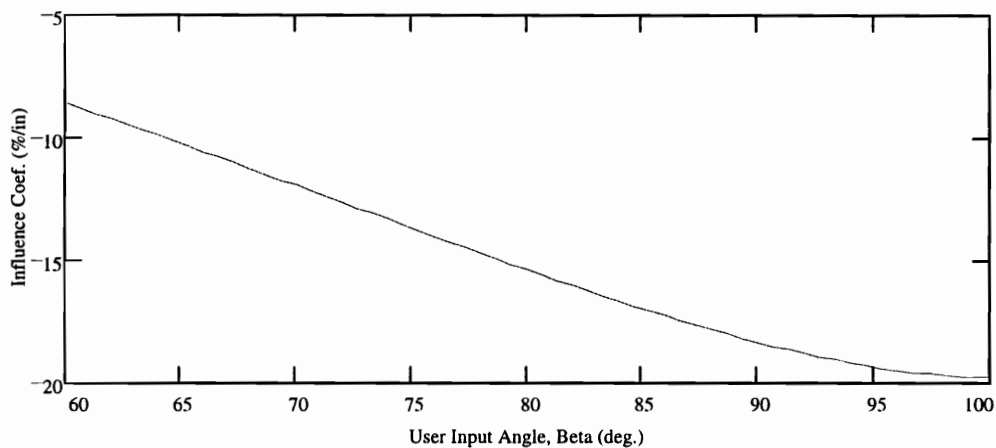


Figure E-5, Influence Coefficient, I3

Influence Coefficient: dR/dl_4

$$dd3_k := \left(\sin(\theta_{4_k}) \cdot \sin(\theta_{3_k}) + \cos(\theta_{4_k}) \cdot \cos(\theta_{3_k}) \right) \cdot (\theta_{3d3_k} - \theta_{4d3_k})$$

$$nd3_k := \left(\sin(\theta_{4_k}) \cdot \sin(\theta_{2_k}) + \cos(\theta_{4_k}) \cdot \cos(\theta_{2_k}) \right) \cdot (\theta_{4d3_k})$$

$$\kappa_{3_k} := \frac{B_k}{n_k} \cdot nd3_k - \frac{B_k}{d_k} \cdot dd3_k - B_k \cdot \tan(\theta_{3_k} - \theta_w) \cdot \theta_{3d3_k}$$

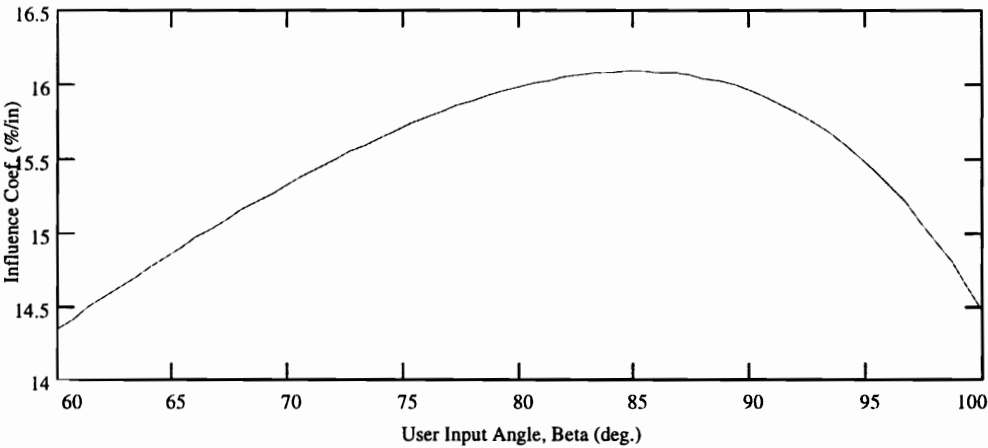


Figure E-6, Influence Coefficient, I_4

Influence Coefficient: dR/dl_3

$$dd4_k := \left(\sin(\theta_{4_k}) \cdot \sin(\theta_{3_k}) + \cos(\theta_{4_k}) \cdot \cos(\theta_{3_k}) \right) \cdot (\theta_{3d4_k} - \theta_{4d4_k})$$

$$nd4_k := \left(\sin(\theta_{4_k}) \cdot \sin(\theta_{2_k}) + \cos(\theta_{4_k}) \cdot \cos(\theta_{2_k}) \right) \cdot (\theta_{4d4_k})$$

$$\kappa_{4_k} := \frac{B_k}{n_k} \cdot nd4_k - \frac{B_k}{d_k} \cdot dd4_k - B_k \cdot \tan(\theta_{3_k} - \theta_w) \cdot \theta_{3d4_k}$$

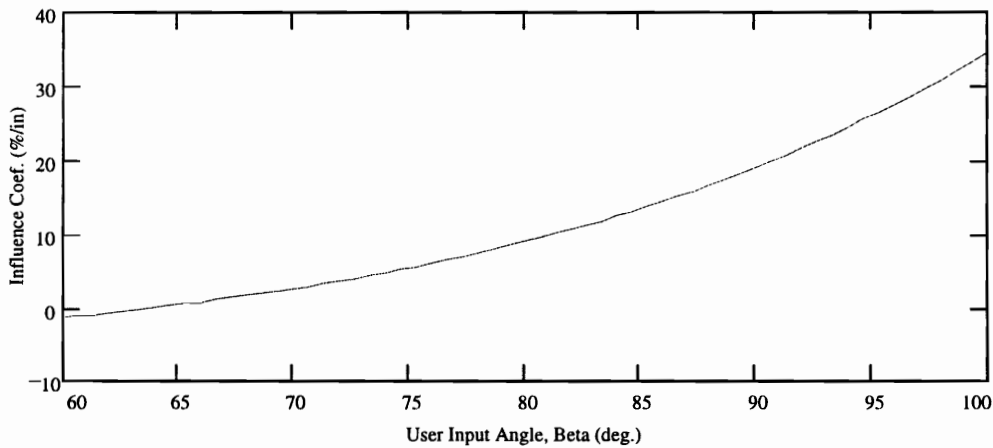


Figure E-7, Influence Coefficient, I1

Influence Coefficient: $dR/d \theta_{in}$

$$dd5_k := \left(\sin(\theta_{4_k}) \cdot \sin(\theta_{3_k}) + \cos(\theta_{4_k}) \cdot \cos(\theta_{3_k}) \right) \cdot (\theta_{3d5_k} - \theta_{4d5_k})$$

$$nd5_k := \left(\sin(\theta_{4_k}) \cdot \sin(\theta_{2_k}) + \cos(\theta_{4_k}) \cdot \cos(\theta_{2_k}) \right) \cdot (\theta_{4d5_k} + 1)$$

$$\kappa_{5_k} := \frac{B_k}{n_k} \cdot nd5_k - \frac{B_k}{d_k} \cdot dd5_k - B_k \cdot \tan(\theta_{3_k} - \theta_w) \cdot \theta_{3d5_k} + A_k \cdot \tan(\theta_{2_k})$$

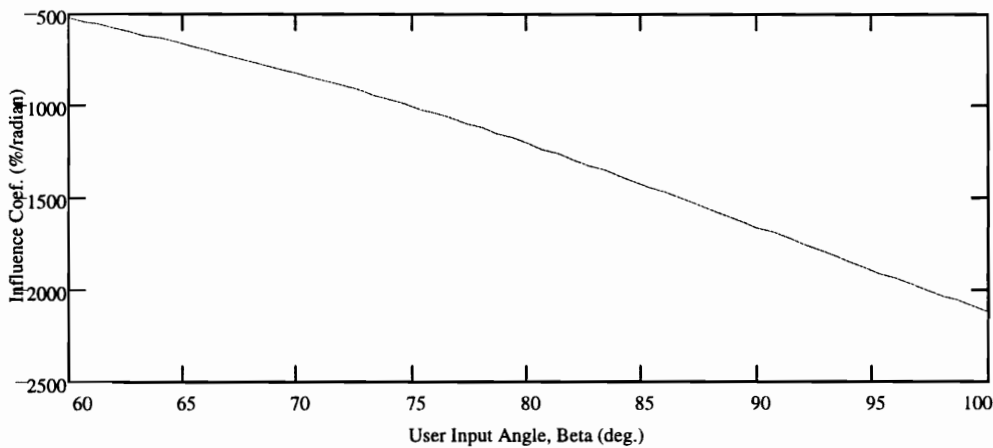


Figure E-8, I. C., θ_{in}

Influence Coefficient: $dR/d\theta_w$ $\kappa_6 := B_k \cdot \tan(\theta_{3k} - \theta_w)$

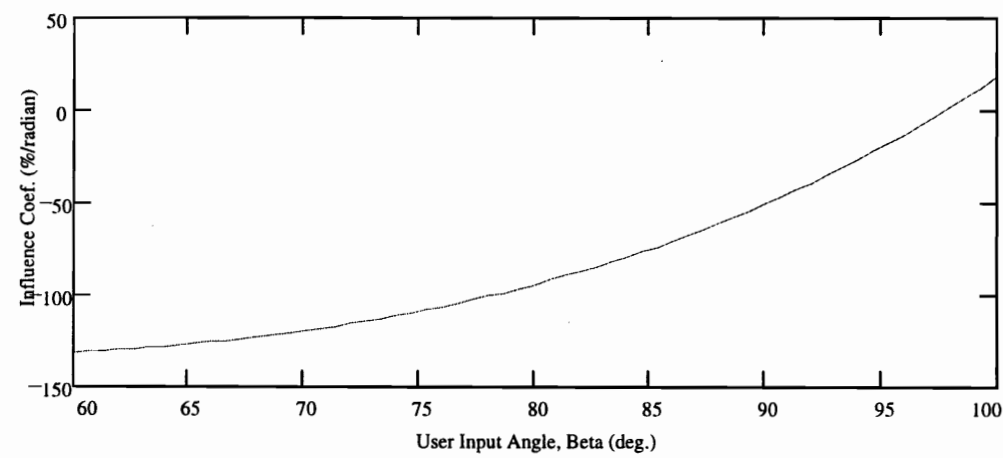


Figure E-9, I. C., θ_w

Influence Coefficient: dR/dl_w $\kappa_7 := \frac{B_k}{l_w}$

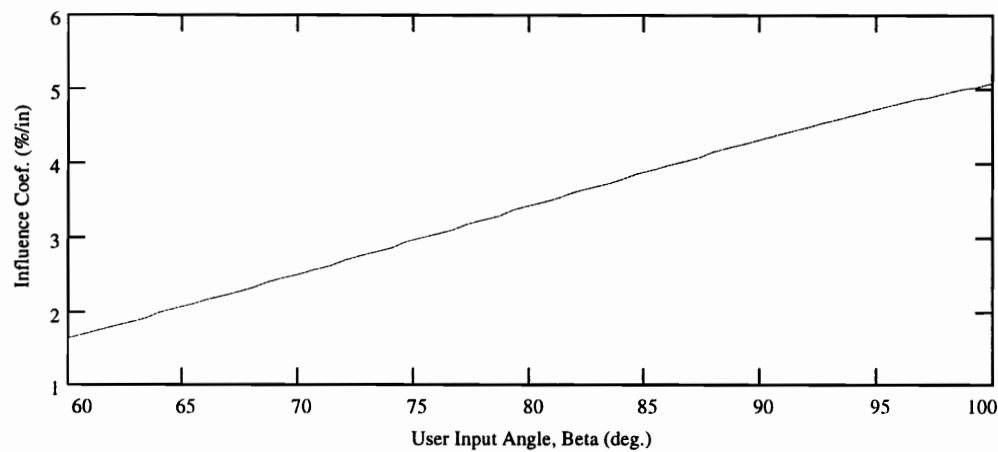


Figure E-10, Influence Coefficient, l_w

Influence Coefficient: $dR/d\chi$

$$dd8_k := \left(\sin(\theta_{4_k}) \cdot \sin(\theta_{3_k}) + \cos(\theta_{4_k}) \cdot \cos(\theta_{3_k}) \right) \cdot (\theta_{3d8_k} - \theta_{4d8_k})$$

$$nd8_k := \left(\sin(\theta_{4_k}) \cdot \sin(\theta_{2_k}) + \cos(\theta_{4_k}) \cdot \cos(\theta_{2_k}) \right) \cdot (\theta_{4d8_k})$$

$$\kappa_{8_k} := \frac{B_k}{n_k} \cdot nd8_k - \frac{B_k}{d_k} \cdot dd8_k - B_k \cdot \tan(\theta_{3_k} - \theta_w) \cdot \theta_{3d8_k}$$

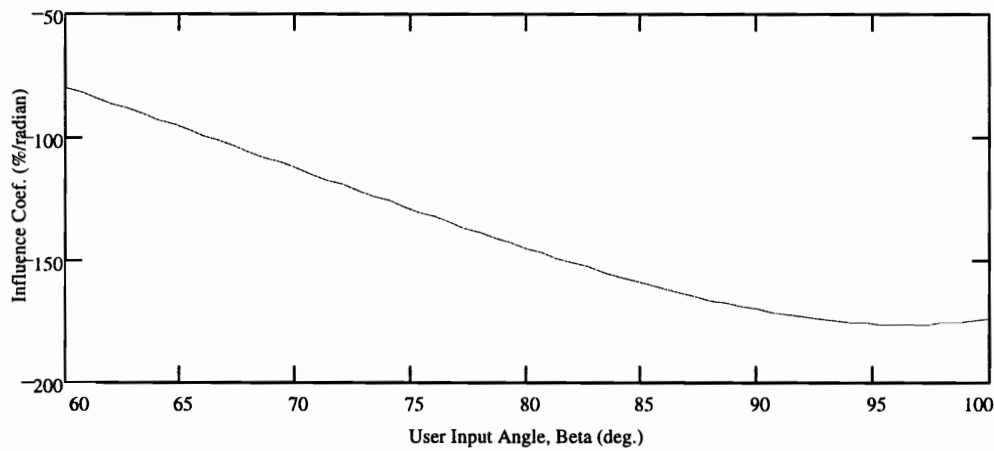


Figure E-11, Influence Coefficient, Chi

Appendix F, Post-Processing: Analysis Programs

This appendix contains a MathSoft Mathcad® version 5.0 program. It performs a linkage analysis to verify the assumptions in the synthesis method. The analysis is performed on the weighted-grounded-link design from Appendix A as an example. Textual comments are in **boldface**.

Static Force Analysis: Effect of Link Masses

Mathcad model By R. R. Soper, C. Marcuson, C.
Stillings, E.K. Ko, Sanjay Dhande, and C. F. Reinholtz

DATA INPUT

(lengths in inches, angles in degrees)

$$l_1 := 8 \quad l_2 := 20.042 \quad l_3 := 11.073 \quad l_4 := 26.577 \quad l_{in} := 40.1$$

$$\theta_{in} := 7.268 \text{ deg} \quad l_w := 45 \quad \theta_w := 5.332 \text{ deg} \quad \chi := 165 \text{ deg}$$

$$d := 40 \quad \text{Number of data points over the range of } \beta$$

$$\xi := 1 \quad \text{Indicate closure, } \xi = +1 \text{ or } -1$$

$$\beta_{min} := 60 \text{ deg} \quad \beta_{max} := 100 \text{ deg} \quad \text{Range of Motion}$$

$$loc_1 := \frac{l_2}{2} \quad \text{Distance between the grounded input pivot and the cg of } l_2$$

$$loc_2 := \frac{l_3}{2} \quad \text{Distance between coupler pivot on the input side and the cg of } l_3$$

$$loc_3 := \frac{l_4}{2} \quad \text{Distance between the grounded output pivot and the cg of } l_4$$

$$\phi_{21} := 0 \text{ deg} \quad \text{Angle about grounded input pivot which locates the cg of } l_2 \text{ with respect to } l_2 \text{'s kinematic vector}$$

$$\phi_{32} := 0 \text{ deg} \quad \text{Angle about input side pivot which locates the cg of } l_3 \text{ with respect to } l_3 \text{'s kinematic vector}$$

$$\phi_{44} := 0 \text{ deg} \quad \text{Angle about grounded output pivot which locates the cg of } l_4 \text{ with respect to } l_4 \text{'s kinematic vector}$$

$w_2 := 10$ **Weight of l_2 (in pounds)**

$w_3 := 10$ **Weight of l_3 (in pounds)**

$w_4 := 10$ **Weight of l_4 (in pounds)**

$W_{\max} := 300$ **Maximum load weight used on the weight arm (in pounds)**

$W_{\min} := 30$ **Minimum load weight used on the weight arm (in pounds)**

CALCULATIONS

$k := 0..d$

$$\beta_k := \beta_{\min} + \frac{\beta_{\max} - \beta_{\min}}{d} \cdot k$$

Standard Position Analysis

$$\theta_{2_k} := \beta_k - \theta_{\text{in}}$$

$$E_{3_k} := 2 \cdot l_2 \cdot l_3 \cdot \sin(\theta_{2_k}) - 2 \cdot l_3 \cdot l_1 \cdot \sin(\chi) \quad F_{3_k} := 2 \cdot l_2 \cdot l_3 \cdot \cos(\theta_{2_k}) - 2 \cdot l_3 \cdot l_1 \cdot \cos(\chi)$$

$$G_{3_k} := l_2^2 + l_3^2 + l_1^2 - l_4^2 - 2 \cdot l_2 \cdot l_1 \cdot \cos(\chi) \cdot \cos(\theta_{2_k}) - 2 \cdot l_2 \cdot l_1 \cdot \sin(\chi) \cdot \sin(\theta_{2_k})$$

$$N_{3_k} := -E_{3_k} + \xi \cdot \sqrt{(E_{3_k})^2 + (F_{3_k})^2 - (G_{3_k})^2} \quad \theta_{3_k} := 2 \cdot \text{atan} \left(\frac{N_{3_k}}{G_{3_k} - F_{3_k}} \right)$$

$$E_{4_k} := -2 \cdot l_2 \cdot l_4 \cdot \sin(\theta_{2_k}) + 2 \cdot l_4 \cdot l_1 \cdot \sin(\chi) \quad F_{4_k} := -2 \cdot l_2 \cdot l_4 \cdot \cos(\theta_{2_k}) + 2 \cdot l_4 \cdot l_1 \cdot \cos(\chi)$$

$$G_{4_k} := l_2^2 + l_4^2 + l_1^2 - l_3^2 - 2 \cdot l_2 \cdot l_1 \cdot \cos(\chi) \cdot \cos(\theta_{2_k}) - 2 \cdot l_2 \cdot l_1 \cdot \sin(\chi) \cdot \sin(\theta_{2_k})$$

$$N_{4_k} := -E_{4_k} + -\xi \cdot \sqrt{(E_{4_k})^2 + (F_{4_k})^2 - (G_{4_k})^2} \quad \theta_{4_k} := 2 \cdot \text{atan} \left(\frac{N_{4_k}}{G_{4_k} - F_{4_k}} \right)$$

Moving vectors which locate the pivots with respect to the centers of mass

$$\begin{aligned} r_{21_k} &:= -l_{oc1} \cdot e^{i \cdot (\theta_{2k} + \phi_{21})} & r_{22_k} &:= l_2 \cdot e^{i \cdot \theta_{2k}} + r_{21_k} \\ r_{32_k} &:= -l_{oc2} \cdot e^{i \cdot (\theta_{3k} + \phi_{32})} & r_{33_k} &:= l_3 \cdot e^{i \cdot \theta_{3k}} + r_{32_k} \\ r_{44_k} &:= -l_{oc3} \cdot e^{i \cdot (\theta_{4k} + \phi_{44})} & r_{43_k} &:= l_4 \cdot e^{i \cdot \theta_{4k}} + r_{44_k} \end{aligned}$$

Matrix Method to solve for bearing forces and input torque

$$A(k) := \begin{bmatrix} 1 & 0 & -1 & 0 & 0 & 0 & 0 & 0 & 0 \\ 0 & 1 & 0 & -1 & 0 & 0 & 0 & 0 & 0 \\ \text{Im}(r_{21_k}) & -\text{Re}(r_{21_k}) & -\text{Im}(r_{22_k}) & \text{Re}(r_{22_k}) & 0 & 0 & 0 & 0 & 1 \\ 0 & 0 & 1 & 0 & -1 & 0 & 0 & 0 & 0 \\ 0 & 0 & 0 & 1 & 0 & -1 & 0 & 0 & 0 \\ 0 & 0 & \text{Im}(r_{32_k}) & -\text{Re}(r_{32_k}) & -\text{Im}(r_{33_k}) & \text{Re}(r_{33_k}) & 0 & 0 & 0 \\ 0 & 0 & 0 & 0 & 1 & 0 & 1 & 0 & 0 \\ 0 & 0 & 0 & 0 & 0 & 1 & 0 & 1 & 0 \\ 0 & 0 & 0 & 0 & \text{Im}(r_{43_k}) & -\text{Re}(r_{43_k}) & \text{Im}(r_{44_k}) & -\text{Re}(r_{44_k}) & 0 \end{bmatrix}$$

$$B := \begin{bmatrix} 0 \\ -w_2 \\ 0 \\ 0 \\ -w_3 \\ 0 \\ 0 \\ -w_4 \\ 0 \end{bmatrix}$$

$$C(k) := (A(k))^{-1} \cdot B$$

$$T_k := C(k)_8$$

Effective torque on input link due to link masses

$$\Delta F_k := \frac{T_k}{l_{in}}$$

Normal force at end of input handle due to link masses

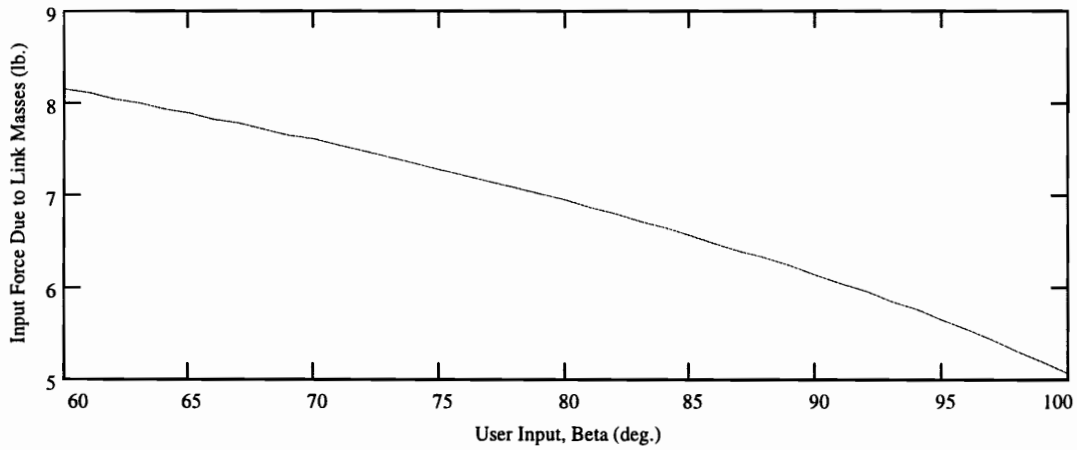


Figure F-1, Change in Input Force

Calculate the Resistance Curve

$$\begin{pmatrix} \Gamma_{4_k} \\ \Gamma_{3_k} \end{pmatrix} := \begin{pmatrix} l_4 \cdot \cos(\theta_{4_k}) & -l_3 \cdot \cos(\theta_{3_k}) \\ l_4 \cdot \sin(\theta_{4_k}) & -l_3 \cdot \sin(\theta_{3_k}) \end{pmatrix}^{-1} \cdot \begin{pmatrix} l_2 \cdot \cos(\theta_{2_k}) \\ l_2 \cdot \sin(\theta_{2_k}) \end{pmatrix} \quad R_k := \frac{l_w}{l_{in}} \cdot \Gamma_{4_k} \cdot \cos(\theta_{4_k} - \theta_w)$$

$$\Delta R_{\max_k} := \frac{\Delta F_k}{W_{\min}} \quad \Delta R_{\min_k} := \frac{\Delta F_k}{W_{\max}} \quad \text{The change in the resistance curve due to the link masses}$$

$$R_{\max_k} := R_k + \Delta R_{\max_k}$$

$$R_{\min_k} := R_k + \Delta R_{\min_k}$$

**Actual resistance curves
including effects of link
masses and load weight**

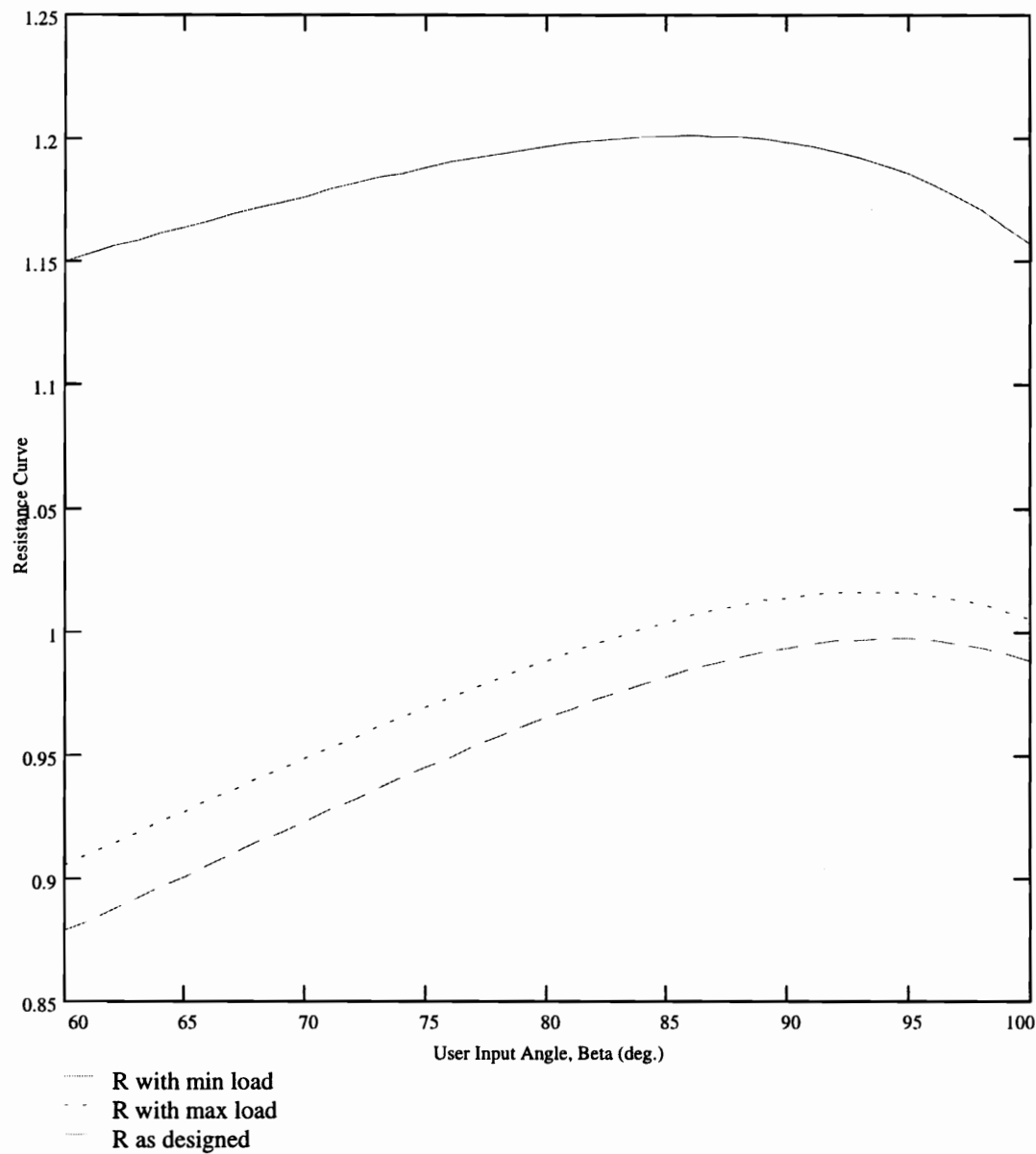


Figure F-2, R with Effect of Link Masses

Dynamic Force Analysis

Mathcad model By R. R. Soper

Establish the probable input trajectory

$$t_c := 4$$

$$f := 5$$

The motion time and
number of time segments

Calculations

$$j := 1, 2, \dots, 50 \cdot f \quad t_j := \frac{t_c}{50 \cdot f} \cdot j \quad \alpha := \frac{(\beta_{\max} - \beta_{\min}) \cdot f^2}{(f - 1) \cdot t_c^2} \quad \frac{\alpha}{\text{deg}} = 15.625$$

Constant angular
acceleration and
deceleration of the
first and f^{th} time
segments

$$L := 1, 2, \dots, 50 \quad \text{(Phase 1)}$$

$$\alpha_{2_L} := \alpha \quad \omega_{2_L} := \alpha \cdot t_L \quad \beta_L := \frac{\alpha \cdot (t_L)^2}{2} + \beta_{\min}$$

$$M := 50, 51, \dots, (f - 1) \cdot 50 \quad \text{(Phase 2)}$$

$$\alpha_{2_M} := 0 \quad \omega_{2_M} := \frac{\alpha \cdot t_c}{f} \quad \beta_M := \frac{1}{2} \cdot \alpha \cdot t_c \cdot \frac{2 \cdot t_M \cdot f - t_c}{f^2} + \beta_{\min}$$

Input trajectory over the three
significant phases: acceleration,
stable and deceleration phases

$$N := (f - 1) \cdot 50, (f - 1) \cdot 50 + 1, \dots, 50 \cdot f \quad \text{(Phase 3)}$$

$$\alpha_{2_N} := -\alpha \quad \omega_{2_N} := \alpha \cdot (t_c - t_N) \quad \beta_N := \frac{-\alpha \cdot (t_N)^2}{2} + \alpha \cdot t_c \cdot t_N - \alpha \cdot t_c^2 \cdot \frac{1 - f + \frac{f^2}{2}}{f^2} + \beta_{\min}$$

**Resulting
Assumed
Trajectory**

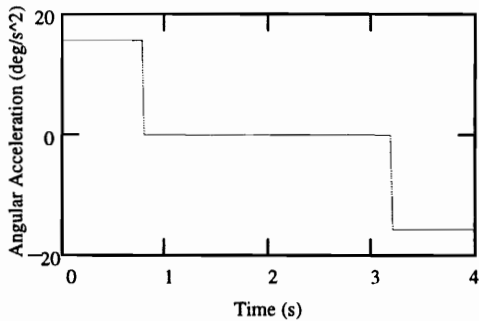


Fig. F-3a, Input Acceleration Trajectory

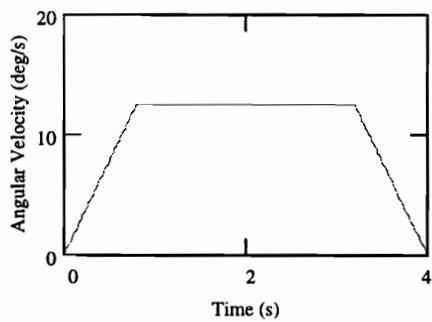


Fig. F-3b, Input Velocity Trajectory

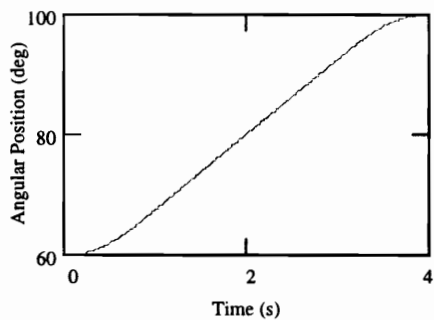


Fig. F-3c, Input Position Trajectory

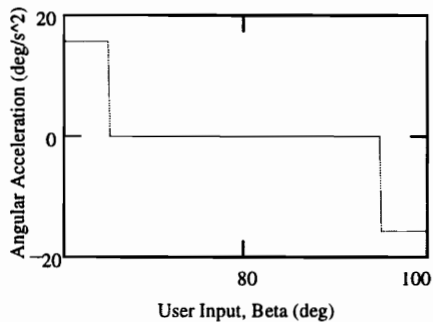


Fig. F-4a, Acceleration vs. Position

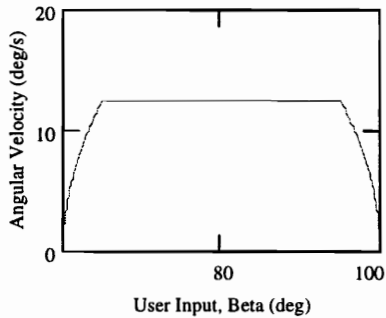


Fig. F-4b, Velocity vs. Position

Standard Position Analysis

$$\theta_{2_j} := \beta_j - \theta_{in}$$

$$E_{3_j} := 2 \cdot l_2 \cdot l_3 \cdot \sin(\theta_{2_j}) - 2 \cdot l_3 \cdot l_1 \cdot \sin(\chi) \quad F_{3_j} := 2 \cdot l_2 \cdot l_3 \cdot \cos(\theta_{2_j}) - 2 \cdot l_3 \cdot l_1 \cdot \cos(\chi)$$

$$G_{3_j} := l_2^2 + l_3^2 + l_1^2 - l_4^2 - 2 \cdot l_2 \cdot l_1 \cdot \cos(\chi) \cdot \cos(\theta_{2_j}) - 2 \cdot l_2 \cdot l_1 \cdot \sin(\chi) \cdot \sin(\theta_{2_j})$$

$$N_{3_j} := -E_{3_j} + \xi \cdot \sqrt{(E_{3_j})^2 + (F_{3_j})^2 - (G_{3_j})^2} \quad \theta_{3_j} := 2 \cdot \text{atan}\left(\frac{N_{3_j}}{G_{3_j} - F_{3_j}}\right)$$

$$E_{4_j} := -2 \cdot l_2 \cdot l_4 \cdot \sin(\theta_{2_j}) + 2 \cdot l_4 \cdot l_1 \cdot \sin(\chi) \quad F_{4_j} := -2 \cdot l_2 \cdot l_4 \cdot \cos(\theta_{2_j}) + 2 \cdot l_4 \cdot l_1 \cdot \cos(\chi)$$

$$G_{4_j} := l_2^2 + l_4^2 + l_1^2 - l_3^2 - 2 \cdot l_2 \cdot l_1 \cdot \cos(\chi) \cdot \cos(\theta_{2_j}) - 2 \cdot l_2 \cdot l_1 \cdot \sin(\chi) \cdot \sin(\theta_{2_j})$$

$$N_{4_j} := -E_{4_j} - \xi \cdot \sqrt{(E_{4_j})^2 + (F_{4_j})^2 - (G_{4_j})^2} \quad \theta_{4_j} := 2 \cdot \text{atan}\left(\frac{N_{4_j}}{G_{4_j} - F_{4_j}}\right)$$

Velocity and Acceleration Analysis

$$\begin{pmatrix} \omega_{4_j} \\ \omega_{3_j} \end{pmatrix} := \begin{pmatrix} l_4 \cdot \cos(\theta_{4_j}) & -l_3 \cdot \cos(\theta_{3_j}) \\ l_4 \cdot \sin(\theta_{4_j}) & -l_3 \cdot \sin(\theta_{3_j}) \end{pmatrix}^{-1} \cdot \begin{pmatrix} l_2 \cdot \cos(\theta_{2_j}) \\ l_2 \cdot \sin(\theta_{2_j}) \end{pmatrix} \cdot \omega_{2_j}$$

$$\begin{pmatrix} \alpha_{4_j} \\ \alpha_{3_j} \end{pmatrix} := \begin{pmatrix} -l_4 \cdot \sin(\theta_{4_j}) & l_3 \cdot \sin(\theta_{3_j}) \\ l_4 \cdot \cos(\theta_{4_j}) & -l_3 \cdot \cos(\theta_{3_j}) \end{pmatrix}^{-1} \cdot \left[\begin{pmatrix} l_4 \cdot \cos(\theta_{4_j}) & -l_3 \cdot \cos(\theta_{3_j}) \\ l_4 \cdot \sin(\theta_{4_j}) & -l_3 \cdot \sin(\theta_{3_j}) \end{pmatrix} \cdot \begin{bmatrix} (\omega_{4_j})^2 \\ (\omega_{3_j})^2 \end{bmatrix} \dots \right. \\ \left. + \begin{pmatrix} -l_2 \cdot \cos(\theta_{2_j}) \\ -l_2 \cdot \sin(\theta_{2_j}) \end{pmatrix} \cdot (\omega_{2_j})^2 + \begin{pmatrix} -l_2 \cdot \sin(\theta_{2_j}) \\ l_2 \cdot \cos(\theta_{2_j}) \end{pmatrix} \cdot \alpha_{2_j} \right]$$

Moving vectors which locate the pivots with respect to the centers of mass

$$r_{21_j} := -l_{oc\ 1} \cdot e^{i \cdot (\theta_{2_j} + \phi_{21})}$$

$$r_{22_j} := l_2 \cdot e^{i \cdot \theta_{2_j}} + r_{21_j}$$

$$r_{32_j} := -l_{oc\ 2} \cdot e^{i \cdot (\theta_{3_j} + \phi_{32})}$$

$$r_{33_j} := l_3 \cdot e^{i \cdot \theta_{3_j}} + r_{32_j}$$

$$r_{44_j} := -l_{oc\ 3} \cdot e^{i \cdot (\theta_{4_j} + \phi_{44})}$$

$$r_{43_j} := l_4 \cdot e^{i \cdot \theta_{4_j}} + r_{44_j}$$

Accelerations of the link cgs

$$a_{g2_j} := \left[\left(\omega_{2_j} \right)^2 - i \cdot \alpha_{2_j} \right] \cdot r_{21_j}$$

$$a_{g3_j} := \left[\left(\omega_{3_j} \right)^2 - i \cdot \alpha_{3_j} \right] \cdot r_{32_j} + l_2 \cdot e^{i \cdot \theta_{2_j}} \cdot \left[- \left(\omega_{2_j} \right)^2 + i \cdot \alpha_{2_j} \right]$$

$$a_{g4_j} := \left[\left(\omega_{4_j} \right)^2 - i \cdot \alpha_{4_j} \right] \cdot r_{44_j}$$

$$I_2 := \frac{1}{12} \cdot \frac{w_2}{386.09} \cdot l_2^2$$

$$I_3 := \frac{1}{12} \cdot \frac{w_3}{386.09} \cdot l_3^2$$

$$I_4 := \frac{1}{12} \cdot \frac{w_3}{386.09} \cdot l_4^2$$

Calculate mass moment of inertia for the links. This assumes $I = 1/12$ (mass) (kinematic length)². If true inertias are known, they can be assigned here.

Calculate the dynamic effects of the link masses

$$A(j) := \begin{bmatrix} 1 & 0 & -1 & 0 & 0 & 0 & 0 & 0 & 0 \\ 0 & 1 & 0 & -1 & 0 & 0 & 0 & 0 & 0 \\ \text{Im}(r_{21_j}) & -\text{Re}(r_{21_j}) & -\text{Im}(r_{22_j}) & \text{Re}(r_{22_j}) & 0 & 0 & 0 & 0 & 1 \\ 0 & 0 & 1 & 0 & -1 & 0 & 0 & 0 & 0 \\ 0 & 0 & 0 & 1 & 0 & -1 & 0 & 0 & 0 \\ 0 & 0 & \text{Im}(r_{32_j}) & -\text{Re}(r_{32_j}) & -\text{Im}(r_{33_j}) & \text{Re}(r_{33_j}) & 0 & 0 & 0 \\ 0 & 0 & 0 & 0 & 1 & 0 & 1 & 0 & 0 \\ 0 & 0 & 0 & 0 & 0 & 1 & 0 & 1 & 0 \\ 0 & 0 & 0 & 0 & \text{Im}(r_{43_j}) & -\text{Re}(r_{43_j}) & \text{Im}(r_{44_j}) & -\text{Re}(r_{44_j}) & 0 \end{bmatrix}$$

$$B(j) := \begin{bmatrix} -\frac{w_2}{386.09} \cdot \text{Re}(a_{g2_j}) \\ -w_2 - \frac{w_2}{386.09} \cdot \text{Im}(a_{g2_j}) \\ -I_2 \cdot \alpha_2 \\ -\frac{w_3}{386.09} \cdot \text{Re}(a_{g3_j}) \\ -w_3 - \frac{w_3}{386.09} \cdot \text{Im}(a_{g3_j}) \\ -I_3 \cdot \alpha_3 \\ -\frac{w_4}{386.09} \cdot \text{Re}(a_{g4_j}) \\ -w_4 - \frac{w_4}{386.09} \cdot \text{Im}(a_{g4_j}) \\ -I_4 \cdot \alpha_4 \end{bmatrix}$$

$$C(j) := (A(j))^{-1} \cdot B(j)$$

$$T_{Dm_j} := C(j)_8$$

Effective torque on input link due to dynamic link mass effects

Resistance Curve as Designed

$$R_j := \frac{l_w}{l_{in}} \cdot \frac{\omega_{4_j}}{\omega_{2_j}} \cdot \left(\cos \left(\theta_{4_j} - \theta_w \right) \right)$$

Resistance Curve with Dynamic Effects (superposition)

$$R_{D_j} := \frac{T_{Dm_j}}{l_{in} \cdot W_{max}} + \frac{l_w}{l_{in}} \cdot \frac{\omega_{4_j}}{\omega_{2_j}} \cdot \left(\frac{l_w \cdot \alpha_{4_j}}{386.09} + \cos \left(\theta_{4_j} - \theta_w \right) \right)$$

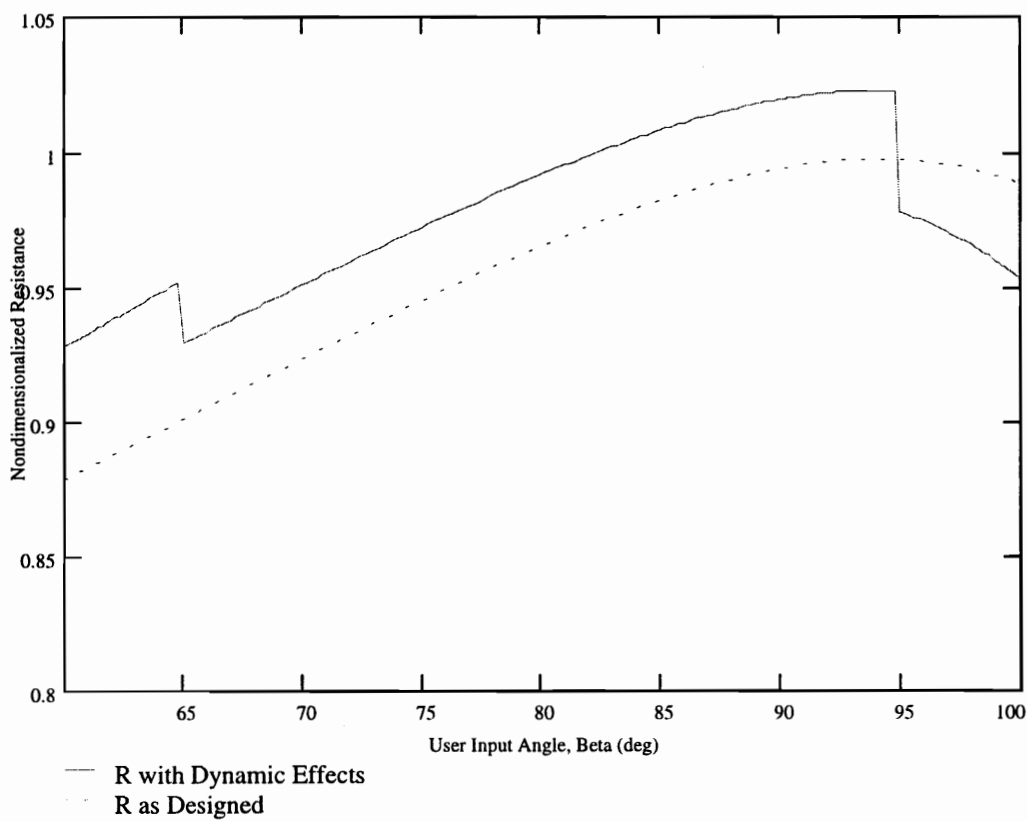


Figure F-5, R with Dynamic Effects

Vita

Robert Randall Soper was born in Fairfax Virginia on May 3, 1972. He graduated from Thomas Jefferson High School for Science and Technology in June 1990. He entered the College of Engineering at Virginia Tech in August of 1990, two days after he met his future wife, Anita Lynne Garlich (they married on August 14, 1993). He graduated, *summa cum laude*, in honors, with a BS in Mechanical Engineering and a minor in Economics in May 1994.

Randy has worked a computer support specialist for the National Institutes of Health, an administrative consultant and engineering intern for N.E.T. Federal, Inc., and a consultant for the Kollmorgen Corp., Industrial Drives Division.

Randy first became involved with force-generating linkage synthesis for Nautilus International, Inc. as an undergraduate student in a senior design course. He will begin work on his Ph.D. in the Engineering Science and Mechanics Department, Virginia Tech, in August 1995.

A handwritten signature in black ink, reading "R. Randall Soper". The signature is stylized, with the first letters of the first and last names being large and prominent. The middle name "Randall" is written in a cursive script.

R. Randall Soper